A CLINICAL AND MOLECULAR GENETIC INVESTIGATION INTO INHERITED RENAL TUBULOPATHY AND NEPHROCALCINOSIS

Dr Chris Laing MBChB MRCP

CONTENTS

SECTION II. AUTOSOMAL DOMINANT DIABETES INSIPIDUS

SECTION III. AUTOSOMAL DOMINANT RENAL FANCONI SYNDROME

SECTION IV. AUTOSOMAL DOMINANT RENAL TUBULAR ACIDOSIS

REFERENCES

ACKNOWLEDGEMENTS

I am indebted to many, without whose help I would not have been able to undertake this research. I thank them sincerely for their support, hard work, expertise, teaching and friendship.

Professor Mike Tanner and his research group in Bristol provided valuable assistance with the section on renal tubular acidosis. I would in particular like to thank Ashley Toye for providing the Band 3 constructs and Lesley Bruce for teaching me genomic sequencing and SSCP, during my time in Bristol.

In the Galton Laboratory Mari-Wyn Burley taught me the basics of laboratory science and provided invaluable oversight and technical assistance with the genotyping, sequencing and SSCP experiments described. I also thank Claire Willoughby and Rosemary Ekong for their work on the genotyping studies and for their role in overseeing the medical students William James White, Timo Heikkla and Nicole Eady, who I also thank for their great efforts.

I am indebted to Kathy Hurley for her help recruiting and characterising the large dominant AI family described in Section I. I must also thank Professor Mike Dixon and his group for their work sequencing the Enamelin gene in this family.

I thank the INSEMR U478 group for all their efforts in training me in molecular biology, cell culture and transgenics. In particular I would like to thank Marcel Blot-Chabaud, Ahmed Beggah, Stephania Puttini and Antoine-Ouvrard Pascaud.

I would like to thank the many clinicians who assisted the genetic studies by helping with patient recruitment, characterisation and sampling. They are given further credit in the main text.

I am grateful to Oliver Wrong for his enthusiasm, vast depths of knowledge and (at times daunting) intellectual rigour.

I am indebted to Frederic Jaisser, for taking me under his wing at U478 Paris and expending considerable resources on supervising a novice molecular biologist.

I am, of course, deeply indebted to my principal supervisors Sue Povey and Robert Unwin. I thank them for their encouragement, guidance, wisdom and patience. Robert Unwin has, in particular, been an invaluable mentor over the years in clinical work and in research and I am greatly indebted to him.

Finally, I would like to thank the patients and unaffected family members who agreed to participate in this research. I hope in time research of this kind will help alleviate the burden of genetic diseases such as those described in this thesis.

DECLARATION

The work described in this thesis was only possible through collaboration. Several projects were progressed in tandem. I initiated the family-based studies described in Section I-III. I, then moved to France to begin work on section IV while collaborators in London, Cambridge and Manchester undertook further laboratory work on these projects, which I helped oversee. My personal contribution and those of my collaborators is described below. I have also acknowledged work undertaken by others in the main text of the thesis.

SECTION I: THE ENAMEL RENAL SYNDROME

I collated clinical details on the ERS kindreds and (with Robert Unwin and Oliver Wrong) recruited further families via communication with their respective clinicians. I performed the linkage studies and data analysis on the initial candidate genes at the "secretory calcium-binding phosphoprotein gene cluster" -*AMBN, BMP 3, IBSP, SPP1* – as well as the genes *BGLAP* and *MGP*. I then applied to the Human genome Resource centre in Cambridge (HGMP-RC) for access to their semi-automated genotyping facilities. Andrew Dearlove, one of their researchers, performed this genotyping and provided data from which I extracted informative genotypes for the loci of the candidate genes *VDR*, *ECAC1* and *CALB1*. From this raw data I performed haplotyping and data analysis.

I recruited and sampled the large ADAI family and arranged for screening for nephrocalcinosis. Having excluded renal involvement (and ERS) I then performed genotyping and genetic linkage for the 4q locus previously implicated in ADAI by other researchers. Having confirmed this, Professor Mike Dixon's group (Department of Dental Medicine and Surgery at the University of Manchester) performed the mutation screening of the *ENAM* gene. This mutation screening was primarily undertaken by Helen M Raipur.

SECTION II: AUTOSOMAL DOMINANT DIABETES INSIPIDUS

I performed the contact tracing, sampling, DNA extraction and collated clinical data on the DI patients. I also performed clinical screening of unaffected family members, including scheduling bladder ultrasonography for them. I

performed the water deprivation testing and AVP sampling in collaboration with Faya Ahmed (research fellow in clinical biochemistry, Royal Hospital. The AVP assays were done in the laboratory of Pascale Houllier, INSERM, Paris. Genotyping was performed by myself, with further genotyping performed by James William White (medical student, UCL) and Claire Willoughby (PhD student in Human Genetics, UCL). Rosemary Ekong (research scientist, Galton Laboratory, UCL) provided further valuable assistance with genetics experiments. Data interpretation of genotypes was performed collaboratively. Sequencing on the *AVP-NPII* gene was performed commercially.

SECTION III: AUTOSOMAL DOMINANT RENAL FANCONI SYNDROME

I performed the contact tracing, sampling, DNA sampling and collation of clinical data on ADRFS patients. I also arranged for screening of unaffected family members, in collaboration with Robert Unwin, and performed the DNA extraction. Urine retinol binding protein assay was performed by Martha Lapsley, at the Department of biochemistry, St Hellier Hospital. Claire Willoughby (PhD student, Human Genetics, UCL), Timo Heikkla (medical student, UCL) and Nicole H Eady (medical student, UCL) performed the Ch15 genotyping, though I decided on the Ch15 strategy, and helped oversee their work. Interpretation of genotypes was collaborative.

SECTION IV: AUTOSOMAL DOMINANT RENAL TUBULAR ACIDOSIS

All the work described in this section was done by myself.

INTRODUCTION

In this thesis I describe research undertaken into four inherited conditions affecting renal tubular function; the enamel renal syndrome, a dominantly inherited form of diabetes insipidus, autosomal dominant renal Fanconi syndrome and autosomal dominant renal tubular acidosis. These conditions had been found in families that had been under the care of the renal unit at The Middlesex Hospital, where I was based as a clinical research fellow.

Research into these conditions progressed simultaneously, but for the purposes of clarity I have divided this thesis into four sections, each devoted to a single condition. Each section has four chapters that, in turn, describe background (including aims of the work), methods, results and conclusions for each project. As such the work is presented as four discrete projects, though there is considerable overlap in the pathologies described in each condition and the methods deployed to investigate them.

This research was started at a time when there was considerable progress in our understanding of the molecular basis of renal tubular disorders. Very detailed clinical evaluation, which had been driven by the great renal clinical physiologists such as Charles Dent and Oliver Wrong (much of it dating back to the 1950s) was being used to support familial genetic 'positional cloning' research projects. This partnering of 'new genetics' and classical applied renal physiology had led to a number of research successes, including the identification of the genes for Bartter's syndrome, Gitelman syndrome and Dent's disease. These results were extended into transgenic cell and mouse models that led to further pay-offs, not only in our understanding of the disease processes, but of basic human renal physiology and its molecular deteminants.

This area of research - the molecular genetics of renal tubular disorders – may be seen to represent an examplar of collaborative translational research. It was a great pleasure to be involved in work in this area.

In this thesis I will present my own, albeit small, contribution to the field.

SECTION I

THE ENAMEL-RENAL SYNDROME

SECTION I – CHAPTER 1

BACKGROUND

1.1 INTRODUCTION

In 1972 David MacGibbon (a dentist based in Queensland, Australia) published a case report entitled " Generalised Enamel Hypoplasia and Renal Dysfunction". In it he described two cases in which there appeared to be an association between amelogenesis imperfecta (an abnormality of dental enamel formation) and nephrocalcinosis (infrarenal calcium deposition). The phenotype appeared severe, with disfiguring dental abnormalities and serious renal manifestations including hypertension and renal failure. One of the cases suffered accelerated hypertension, multi-organ failure and death (1).

Since then a further 10 cases of this syndrome have been reported (2-9). Overall, there appears to be remarkable consistency in the phenotype, with many features apparently specific to this syndrome. It has now been named the "Enamel-Renal Syndrome". Eight cases involve sib-pairs, parents are unaffected and, in three cases, there has been consanguineous parentage. This has led us to believe that this is an inherited, autosomal recessive condition. Though this syndrome appears to be extremely rare, a similar dental phenotype is more common and it is possible that subclinical nephrocalcinosis may be present (undiagnosed) in amelogenesis imperfecta patients.

Two of the reported cases were under our care in the renal department of The Middlesex Hospital and The Eastman Dental Hospital in London. They were from a large, consanguineous family with a surviving parent and 4 unaffected sibs.

The combination of renal calcification and a dental enamel defect is of considerable interest. It might represent a systemic problem of calcium homeostasis, a developmental anomaly or be related to molecular factors that govern tissue mineralization. Though rare, determining the genetic basis of this disease might clarify molecular factors underlying nephrocalcinosis, which occurs in a number of conditions and is still poorly understood. We therefore decided to investigate the genetic basis of the enamel-renal syndrome (ERS) using our family as a starting point.

In this section I will provide background on the separate entities of amelogenesis imperfecta and nephrocalcinosis and what is known of their molecular genetics. I will then describe, in detail, the known cases of ERS. Some of this material was obtained during my research but, for the purposes of clarity, I have included these

details in this background section. I will then provide some background on the candidate genes I investigated in the genetic part of this study.

1.2 AMELOGENESIS IMPERFECTA

1.2.1 Enamel development

Early tooth formation occurs as a consequence of interactions between oral epithelium and ectomesenchyme from the neural crest. Initially dental buds are formed. Genetic defects at this stage are likely to result in complete dental agenesis. There is then a "cap stage" during which time the primary "enamel knot" is formed and this signals subsequent enamel formation during formation of the crown.

During the *secretory stage* enamel formation is initiated and the enamel *thickens*. Basal membrane, containing lamina is formed (basal lamina) and cellular differentiation then occurs. Odontoblasts secrete collagen-rich predentin matrix beneath the basal lamina. Ameloblasts form a cell layer above the basal lamina. These cells elongate, then form processes which breach the basal lamina and extend into the dentin below. The dentin begins to mineralise and at this point the ameloblasts begin to secrete enamel, forming the basis of the dentino-enamel junction. All enamel is mineralised. Unlike dentin or bone, there is no un-mineralised "pre-enamel' layer. Each secretory ameloblast then forms a "Tomes' process". This process then retreats while the ameloblast and continues to secrete enamel, forming an enamel rod that extends in length. THz follows the Tomes' process into the dentin, producing long enamel crystals. This happens in a diurnal fashion. The secretory stage then ends, the Tome's process disintegrates, and the enamel reaches full thickness.

There is then a *maturation stage* during which the enamel is hardened and textured. Ameloblasts restructure and their secretory proteins change. Kalikrein 4 (*KLK4*) and amelotin (*AMTN*) are produced. During the maturation stage a new basal lamina is formed at the base of the ameloblasts and *AMTN*, the gene of which has been recently cloned, is a major constituent of this. *KLK4* degrades the accumulated protein matrix that terminates crystal elongation. It causes the crystals to thicken as the sides of the crystals are exposed. Mineralisation thereby occurs not just at the mineralization front, but also across the entire enamel surface, and the crystals become densely packed.

In the secondary dentition it takes 3-6years for the dental enamel to reach maximal hardness. During this stage ameloblasts also modulate the surface consistency of the enamel. Ruffled or smooth enamel may be formed, depending on the tooth and location.

Even before the molecular characterisation of AI, authors were able to postulate which phase of enamel development had been disrupted by considering this developmental sequence and the physical characteristics of the abnormal enamel. Disturbance (genetic or environmental) during the *secretory* phase of enamel development will disrupt crystal elongation, resulting in abnormally thin enamel (*hypoplastic AI*). Disturbance of the *maturation* phase of enamel development results in abnormally textured or excessively soft enamel of normal thickness (*hypomaturation AI*) (10-12).

1.2.2 Amelogenesis imperfecta: definition, epidemiology and classification

Developmental defects in enamel formation may be caused by a wide variety of insults. These include chromosomal aneuploidy, generalized developmental syndromes, metabolic or endocrine disease, systemic ill health and chemical insults. The term *amelogenesis imperfecta* (AI) is usually used in reference to inherited dental enamel defects that are *not* part of a more generalised syndrome affecting other tissues (13-16).

Perhaps the greatest contribution to the clinical characterization of AI has been made by CJ Witkop, a dentist based in Minnesota, USA. In 1971 he proposed a formal definition of AI as "*a group of disfiguring hereditary conditions which affect the clinical appearance of enamel of all or nearly all the teeth, which occur in kindreds such that all the individuals in the kindred show essentially the same defect and which are unassociated with known morphologic or biochemical changes elsewhere in the body*" (17). That all affected individuals in the same kindred showed "essentially the same defect" would be later disproven, but this was otherwise an enduring representation of AI as a clinical entity distinct from more generalised developmental diseases. More recently, as it has appeared that multi-system defects may arise from a common genetic cause, this separation of AI from more generalized defects has also been challenged.

The incidence of AI appears to vary, though this may be related to epidemiological method. In 1957 Witkop oversaw a review of the dentition of 96,471 children in Michigan USA. He personally examined all enamel abnormalities not related to

caries. He excluded isolated familial cases as he felt an environmental insult could not be excluded in such cases. For the remainder of enamel defects in which there appeared to be a pattern of inheritance he found a prevalence of 1 in 14,000 (18). Backman and Holmgren surveyed 56,663 children in Sweden and found a prevalence of 1 in 718, however Sundell and Valentin performed a subsequent study on 425,000 children in central Sweden and found a prevalence of 1 in 4,000. The Backman group reported on patients in the Vasterbotten region of Sweden which has a very stable population and the likelihood of founder effects is greater (19,20).

There is a great deal of variation in AI phenotype. This has made classification difficult and as a consequence multiple classifications have emerged over the years. These have generally concentrated on the clinical findings, with mode of inheritance constituting a secondary classification. The first categorization was attempted in 1938, but it was not until 1945 that Weinmann et al divided AI into hypoplastic and hypoclacified (hypomaturation equivalent) types.

Witkop subsequently proposed a classification of AI, subdividing it into hypoplastic, hypocalcified and hypomaturation types, with further sub classification according to inheritance and particular clinical features (e.g. "snow-capped teeth") (18, 21-27).

Over the years multiple modifications of this classification were offered by a number of authors, but perhaps the most widely accepted is Witkop's 1988 classification (Table 1) (28). More recently a more structured approach according to genetic location, mutation, biochemical outcome, mode of inheritance and phenotype has been proposed (29). This may be enduring in the longer term but, unfortunately, much of this mechanistic data is currently unavailable and Witkop's more clinical classification continues to dominate.

The large epidemiological studies have shown that the hypoplastic types are more common, with commonest mode of inheritance being autosomal dominant. Unfortunately the diversity of phenotypes and their severity, even within individuals likely to share a gene defect (i.e. within families), has confounded genetic studies.

Type I hypoplastic
IA - hypoplastic, pitted, autosomal dominant
IB – hypoplastic, local, autosomal dominant
IC – hypoplastic, local autosomal recessive
ID – hypoplastic, smooth autosomal dominant
IE – hypoplastic, smooth, X-linked dominant
IF hypoplastic, rough, autosomal dominant
IG – enamel agenesis, autosomal recessive
Type II hypomaturation
IIA – hypomaturation, pigmented, autosomal recessive
IIB - hypomaturation, X-linked recessive
IIC – snow capped teeth, X-linked recessive
IID – hypomaturation, autosomal dominant
Type III Hypocalcified
IIIA – hypocalcified, autosomal dominant
IIIB – hypocalcified, autosomal recessive
Type IV - hypomaturation – hypoplastic with taurodontism
IVA – hypomaturation, hypoplastic with taurodontism, autosomal dominant
IVB – hypoplastic-hypomaturation with taurodontism, autosomal dominant

Table 1. The Witkop classification of amelogenesis imperfecta (1988).

1.2.3 Key molecules in amelogenesis

At the onset of this research it was felt that the three most important proteins in enamel formation were amelogenin, ameloblastin and tuftelin.

Amelogenin is the principal enamel matrix protein and constitutes 80-90% of enamel protein. It has a 16 amino acid signal peptide and is secreted mainly as a 175 amino acid protein (molecular weight is 25KDa), though isoforms exist. It is secreted by ameloblasts and then assembled into 20nm nanospheres, which may act as scaffolding for ordered crystal spacing and growth. Amelogenin is expressed from genes on the X and Y-chromosomes - *AMELX* and *AMELY* – though 90% is transcribed from *AMELX* (Xp22.3). During the maturation phase amelogenin is almost completely removed from the enamel, allowing dense packing and mineralization of the enamel crystallites (30-33).

Ameloblastin is a tooth specific glycoprotein and is the second most abundant enamel matrix protein. High levels appear at the secretory stage, but are diminished at the maturation stage. Its expression is different from amelogenin as it is expressed primarily at the enamel surface layer (33-35). The ameloblastin gene *AMBN* resides at 4q. It encodes a sequence of 422 amino acids corresponding to a protein of 45kD (37-39).

Tuftelin is also found in developing and mature enamel (40). More recently it has also been found in a range of other tissues. The Tuftelin gene TUFT1 encodes it. This gene was mapped, by immunofluorescence and in situ hybridization, to 1q21 in 1994. It was formally cloned and characterised in 2001, *TUFT1* encodes a 390 amino acid protein with a molecular mass of 44.3kDa (41-44).

1.2.4 X-linked amelogenesis imperfecta (OMIM 300391)

AMELX mutations have been shown to cause X-linked AI (OMIM 300391). Thus far 15 mutations have been described and have included deletion, mis-sense and nonsense mutations. These result in both *hypoplastic* and *hypomaturation* AI phenotypes. Not unexpectedly, the male phenotype is more severe and results in a near complete loss of dental enamel resulting in a brown discolouration and excessive wear. Lyonisation occurs in females, with alternate inactivation of the normal and defective X chromosome in the ameloblasts. As a consequence there are usually alternating vertical bands of normal and defective enamel.

The first AI mutation to be described was a 5Kb deletion extending from exon 3 to exon 7, resulting in the loss of all but two of the amino acids beyond the signal peptide. This caused a *hypomaturation* defect with evidence of *hypoplasia* in affected males. Four signal peptide mutations have been described. These usually terminate protein translation and result in a severe *hypoplastic* AI, with thin, smooth enamel. Four N-terminus Amelogenin mutations have been described. A single nucleotide substitution in exon 5 and a stop codon insertion resulted and a truncation of the protein product to 36 amino acids. This resulted in a *hypomaturation* phenotype with variable hypoplasia.

Figure 1. X-linked amelogenesis imperfecta due to a C-Terminus mutation in *AMELX*. The image on the left is the more severe male phenotype. On the right is the female phenotype with vertical grooves of abnormal enamel due to lyonisation. (Wright 2006)

Figure 2. X-linked amelogenesis imperfecta due to a signal peptide mutation. This is a hypoplastic mutation. The tooth colour is normal but the teeth are small. The X-ray demonstrates profound enamel thinning. (Wright 2006)

Five N-terminus mis-sense mutations causing single amino acid substitutions resulted in a hypomaturation defect with brown enamel discolouration. One of these mutations, P70T, has been shown to result in reduced effect of MMP20 (amelogenin proteinase) at the proteinase specific cleavage site, causing reduced amelogenin processing. Four mutations have been shown to truncate the amelogenin C-terminus by insertion of a premature stop codon. These mutations all result in a hypoplastic defect, with thin, smooth enamel. All but two of the latter mutations had been described at the time that I started this research (45-55).

1.2.5 Autosomal dominant and recessive amelogenesis imperfecta (OMIM 104500)

Unsurprisingly, the genetic basis of autosomal AI has proved harder to elucidate. At the time of starting this research the molecular basis of autosomal AI was unknown. The Backman group had performed genetic linkage on three families with autosomal dominant, local hypoplastic AI. A genome-wide search using microsatellite markers showed evidence of linkage to the long arm of chromosome 4q, between the markers D4S392 and D4S395. They then performed linkage analysis on a further 17 kindreds with 5 different clinical forms of autosomal dominant AI. Admixture tests with the marker D4S2456 supported heterogeneity with an odds ratio of 78:1. Only families with the local, hypoplastic phenotype showed linkage to this locus. This group performed further mapping on the 4q locus using radiation hybrid mapping and yeast artificial chromosome sequence tagged site-content mapping. They narrowed the AI 4q locus to a physical distance of 4Mb. Interestingly the affected individuals shared haplotypes at this locus, suggesting common ancestry. When the ameloblastin gene was mapped to this region it appeared a very strong candidate gene for AI, however mutation screening in 20 families did not reveal any segregation of genetic variants with AI disease. At that time, no other strong candidate genes had been mapped to this region (56-58).

There have been considerable developments in the genetic basis of autosomal AI since I began my research, including our own contribution, which I will describe. I will provide a complete update on more recent developments in the conclusions section of this chapter.

1.3 NEPHROCALCINOSIS

1.3.1 Definition and classification of nephrocalcinosis

Nephrocalcinosis is a generalized increase in the calcium content of the kidney. The inclusion of "generalized" in this definition is significant. There are several renal pathologies that lead to localised calcific scarring (such as renal infarction or previous renal abscess) but the term would not normally be used for these conditions. Oliver Wrong and Terry Feest reported on the largest series of adult nephrocalcinosis patients (nearly 400). They subdivided nephrocalcinosis anatomically and according to the scale of calcium deposition.

Cortical nephrocalcinosis occurs in the renal cortex. This is far less common and accounts for around 2% of human nephrocalcinosis, usually due to scarring, glomerular pathologies. *Medullary nephrocalcinosis* constitutes the remaining 98% of human disease, is closely related to calcium nephrolithiasis and is overwhelmingly associated with hypercalciuria. The scale of the nephrocalcinosis may be *chemical, microscopic* and *macroscopic*. *Chemical nephrocalcinosis* is increased calcium content of renal tubular epithelial cells. In *microscopic nephrocalcinosis* calcium is precipitated in crystalline form, usually as calcium oxalate or phosphate. In renal biopsy or in post-mortem histological sections of the kidney these deposits may be seen adherent to the renal tubular epithelium or in the tubulointerstitium. Very often there will be intense tubulointerstitial inflammation. This inflammatory change is more diffuse and prominent than that seen in calcium crystal deposition and is probably caused by chemical nephrocalcinosis. In chronic nephrocalcinosis, there may be tubulo-interstitial scarring and gross distortion of the tubular architecture. These findings are common to most causes of medullary nephrocalcinosis and hence histopathology does not discriminate between these.

Macroscopic nephrocalcinosis occurs when calcium crystal deposition has been so extensive that it is visible to the naked eye (at surgery or post-mortem) or radiologically (59-62).

1.3.2 Diagnosis of nephrocalcinosis

Nephrocalcinosis is usually diagnosed radiologically. There may have been an anticipation of this diagnosis which has led to the radiological test, but very often nephrocalcinosis will have been found in patients having renal imaging for less specific indications (loin, pain, haematuria, nephrolithiasis). The traditional

diagnostic test was the plain radiograph of kidneys, ureters and bladder (KUB). The exposure of these films is adjusted to maximize detection of calcified material such as stones and can demonstrate nephrocalcinosis if it is extensive. Renal ultrasound delivers less radiation than conventional x-ray and is more sensitive in detecting nephrocalcinosis. It is operator dependant and areas of increased echogenicity (such as papillary cysts) can be mistaken for nephrocalcinosis by the less experienced operator.

Computed tomography is currently the most sensitive technique for detecting renal calcium deposition. It also, by use of contrast, may more readily discriminate between true parenchymal calcium deposition and calyceal stones that have not yet detached from tubular epithelium. The downside of this test is cost and radiation exposure. Newer CT techniques have developed for looking at total calcium loading in, for example, myocardium and these may have some application is diagnosing nephrocalcinosis earlier.

As stated earlier, nephrocalcinosis may also be diagnosed by examination of renal tissue after renal biopsy or at post-mortem. Biopsy sections may miss infrarenal calcium deposits in which case the biopsy will generally show tubulointerstitial nephritis (59-62).

1.3.3 Cortical nephrocalcinosis

Cortical nephrocalcinosis is an apparently secondary phenomenon. It occurs in pathologies which cause cortical scarring. Such causes included acute cortical necrosis following severe haemorrhage, haemolytic uraemic syndrome, chronic pyelonephritis, acute and chronic glomerulonephritis, acute rejection episodes in renal transplants and surgical trauma. Benign nodular cortical nephrocalcinosis is an apparently rare and benign form (59-62).

1.3.4 Medullary nephrocalcinosis

This is by far the commonest form of nephrocalcinosis. Usually small nodules of calcification first appear in the renal pyramids, which subsequently coalesce. This process will often occur in tandem with tubulointersitial scarring and calcium oxalate or phosphate nephrolithiasis. The pattern of calcium deposition (histologically or macroscopically) is generally not cause-specific (59-62).

Figure 3. Medullary nephrocalcinosis on plain abdominal x-ray

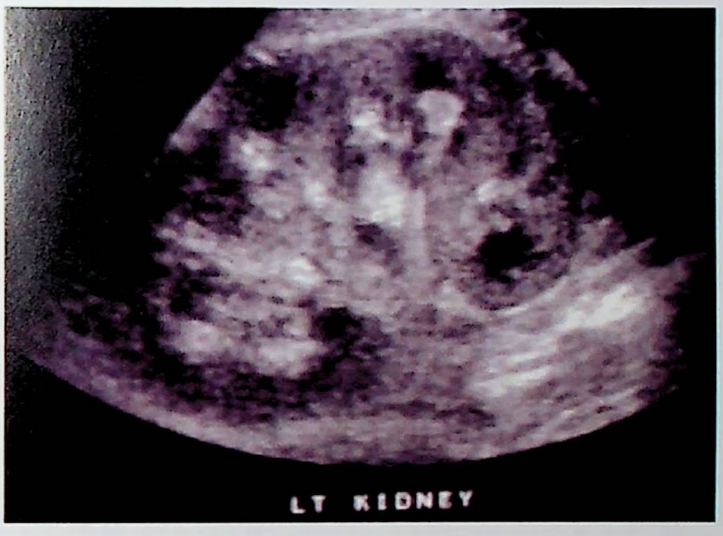

Figure 4. Medullary nephrocalcinosis on ultrasound

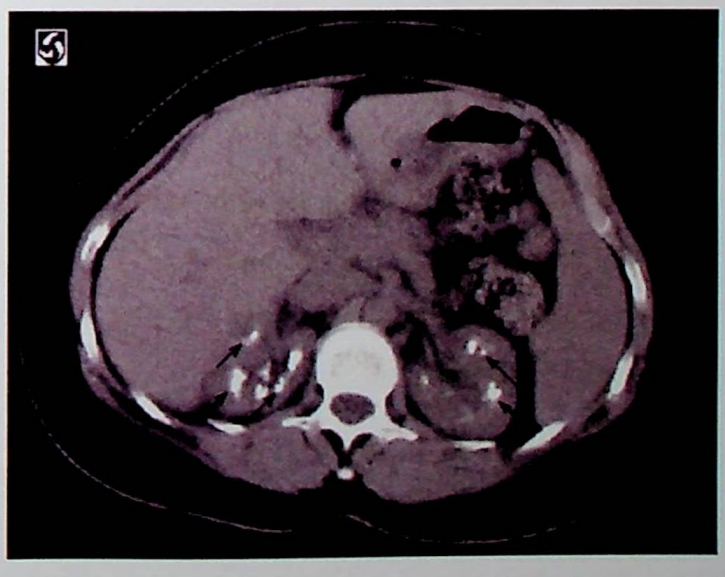

Figure 5. Medullary nephrocalcinosis on computed tomography

Some causes of nephrocalcinosis have specific features. For example in papillary necrosis due to analgesic nephropathy whole papillae may be calcified, while in medullary sponge kidney the nephrocalcinosis is characteristically very sharply defined.

Hypercalcaemia is an important cause of nephrocalcinosis. It has been postulated that an increased calcium content of the blood supply to the tubulointerstitium may result in accumulation of calcium within the renal tubular epithelium or interstitium (39,40). It is worth bearing in mind, however, that most hypercalcaemic patients will be hypercalciuric, and this may be the critical factor, particularly as nephrocalcinosis occurs in other hypercalciuric, non-hypercalcaemic states. *Primary hyperparathyroidism* is the commonest cause of both hypercalcaemia and nephrocalcinosis in adults (32% in the Wrong and Feest series). Nephrocalcinosis only affects a minority of hyperparathyroid patients (around 22%) however the sheer prevalence of primary hyperparathyroidism means that it still emerges as the commonest cause of nephrocalcinosis. Other reported causes of hypercalcaemic nephrocalcinosis include mil-alkali syndrome (due to calcium carbonate antacid remedies), malignancy, sarcoidosis and William's syndrome (idiopathic infantile hypercalcaemia) (59, 64-66).

Distal renal tubular acidosis (dRTA) is the second commonest cause of nephrocalcinosis. Data from two large series would suggest that between 70 and 80% of dRTA patients have radiological evidence of nephrocalcinosis. It appears that it is present in all forms of dRTA – autosomal dominant and recessive and due to mutations in SLC4A1, H^+-ATPase and carbonic anhydrase. It also occurs in acquired forms due to autoimmune disease such as Sjogren's syndrome and has occurred in iatrogenic carbonic anhydrase deficiency, due to the administration of acetazolamide for glaucoma. A major factor in the development of nephrocalcinosis in dRTA is hypercalciuria. This is a function of increased bone buffering and will be seen in other chronic acidotic states. Other factors leading to calcium precipitation are a relatively alkaline urine and hypocitraturia (59, 67,68).

dRTA will be discussed in depth in Section IV of this thesis, so I will not discuss it further in this section.

Hypervitaminosis D is an important cause of hypercalcaemic nephrocalcinosis. It has been reported in excess self-administration of vitamin D supplements. Vitamin D therapy is widely used in the treatment of X-linked hypophosphataemic rickets;

often in combination with phosphate, and iatrogenic nephrocalcinosis has been widely reported in this scenario. Vitamin D therapy has also caused iatrogenic nephrocalcinosis when used in the treatment of idiopathic and post-parathyroidectomy hypoparathyroidism, X-linked hypophosphataemic rickets, vitamin D-dependant rickets and familial benign hypocalciuric hypercalcaemia. Interestingly, significant hypercalcaemia has not been demonstrated in a number of cases, raising the question of whether vitamin D excess may promote infrarenal calcium deposition *per se*, regardless of its effect on serum calcium levels (59,63,69-71).

Idiopathic hypercalciuria has an as yet undetermined genetic basis, probably due to genetic heterogeneity. It is more commonly associated with calcium oxalate and phosphate nephrolithiasis but has been associated with nephrocalcinosis. In Wrong and Feest's series it constituted only 6% of nephrocalcinosis cases. Hypercalciuric nephrocalcinosis may also be associated with steroid excess (endogenous or iatrogenic) and prolonged immobilisation (59,72,73).

Dent's disease was accurately defined in 1990 by Wrong et al as "... a familial proximal renal tubular syndrome with low-molecular weight proteinuria, hypercalciuria, nephrocalcinosis, metabolic bone disease, progressive renal failure and a marked male predominance". Charles Dent had described the first case in London a generation earlier and the authors gave it the eponym "Dent's Disease". Similar syndromes were reported in North America as "X-linked recessive nephrolithiasis with renal failure", in Japan as " low molecular weight proteinuria with hypercalciuria and nephrocalcinosis" and in France and Italy as "X-linked recessive hypophosphataemic rickets with hypercalciuria". It soon became apparent that these were the same syndrome and shared a common genetic defect – inactivating mutations in the voltage-gated chloride channel CLC-5, encoded by the gene CLCN5 at the locus Xp11.22.

The Dent's phenotype is of low molecular weight proteinuria (often detected by detection of urinary retinol binding protein or b2-microglobulin) glycosuria, aminoaciduria and phosphaturia. There is often profound hypercalciuria. 75% of patients have nephrocalcinosis and 50% have nephrolithiasis with either calcium oxalate or phosphate stones. 66% of patients develop renal failure, many of these progressing to end-stage renal failure. The cause of renal failure is unclear, but there is a clearly a factor other than nephrocalcinosis (which is usually more benign) or ureteric obstruction from nephrolithiasis. It appears that proximal tubular disease

confers a greater risk of renal failure than distal tubular disease, and it is possible that some LMW proteins may be nephrotoxic. Rickets occurs in around 255 of affected males, and is likely to be a result of hyperphosphaturia.

CLC-5 is expressed primarily in the subapical endosomes of the proximal tubule, medullary thick ascending limb and type A intercalated cells of the cortical collecting duct. It is co-expressed with the H^+-ATPase that acidifies the endosomal lumen, and it is likely that this facilitates the processing of adsorbed proteins. This is the likely mechanism for tubular proteinuria. Targeted disruption of CLCN5 in mice appears to impair endosomal function of the proximal renal tubular epithelium.

PTH is a low molecular weight protein excreted in the urine. It has been hypothesized that failure of proximal PTH adsorption increases distal tubular delivery, PTH receptor activation, phosphaturia and vitamin D activation (74-83).

Primary hyperoxaluria is due to increased systemic oxalate synthesis. It has two forms, glycolic (type 1) and glyceric (type 2), and both may cause medullary nephrocalcinosis. Secondary hyperoxaluria may occur in small bowel resection or bypass, intestinal disease and ethylene glycol poisoning. The high urinary oxalate content leads to calcium oxalate crystal deposition and nephrocalcinosis (84-90).

Medullary sponge kidney (MSK) is a developmental abnormality in which the renal collecting ducts are ectatic. The calcium lies, on the whole, within the ectatic ducts rather than in the tubulointerstitium. This can be difficult to determine on ultrasound or plain radiological films. A pain radiological or computed tomography pyelogram is necessary to confirm the anatomical abnormality. MSK is associated with hemi-hypertrophy. It is also associated with hypercalciuria and renal tubular acidosis, though it is not clear if this is a secondary phenomenon, due to tubular damage (91-95).

Familial magnesium losing nephropathy has a number of forms. *Gitelman's syndrome* is associated with renal magnesium wasting, hypokalaemia and hypocalciuria. It is associated with mutations in the gene encoding the thiazide-sensitive Na-Cl co-transporter (11q23) (68). *Hypomagnesaemia type 2 (HOMG2)* is a condition of isolated renal magnesium wasting. In its autosomal dominant form, it is associated with mutations in the gene encoding the Na-K-ATPase, expressed in the distal convoluted tubule. A recessive form has not yet been characterized genetically. *Hypomagnesaemia type 2 (HOMG 2)* is another isolated magnesium-losing nephropathy and is the only familial magnesium losing nephropathy

associated with nephrocalcinosis. It is due to mutations in the claudin-16 gene, CLDN 16, at locus 3q27. Claudin 16 is a tight junction protein that facilitates the passive, para-cellular reabsorption of magnesium and calcium in the thick ascending limb of the loop of Henle. There is symptomatic hypocalcaemia and the profound hypercalciuria results in nephrolithiasis and nephrocalcinosis (69,70). Renal failure is not uncommon. *Hypomagnesaemia type 1 (HOMG 1)* is a form of intestinal wasting not associated with nephrocalcinosis (96).

Neonatal nephrocalcinosis has been recognized as a significant clinical problem in preterm children suffering neonatal respiratory distress syndrome. Incidence has been quoted at between 27 and 64 % of children requiring intensive care therapy. Multiple aetiologies have been proposed but the administration of relatively high doses of intravenous loop diuretic for prolonged periods (to reduce total lung water) has clearly been a factor. The latter increase urinary calcium and phosphate excretion. Other, potentially contributing, factors are relative hypercalcaemia in the neonatal period, a more alkaline urine composition due to underdevelopment of urinary acidification, hyper-alimentation and a high incidence of acute tubular necrosis (from systemic illness) that may potentiate tubular calcium deposition (97-100).

Fanconi syndrome is a condition of generalized proximal tubular dysfunction characterized by glycosuria, aminoaciduria, low molecular weight proteinuria, phosphaturia and excessive potassium wasting. Dent's disease is a form of Fanconi syndrome as is the renal dysfunction seen in Wilson's disease, cystinosis, tyrosinaemia, glycogen storage disease and idiopathic renal Fanconi syndrome (73). Nephrocalcinosis has been demonstrated in all of these forms of Fanconi syndrome, usually in the context of hypercalciuria (101,102). Section III of this thesis concerns an investigation into autosomal dominant renal Fanconi syndrome, and I will deal in more detail with this condition, and Fanconi syndrome in general, in this chapter.

1.3.5 Clinical features and complications of nephrocalcinosis

Nephrocalcinosis may be asymptomatic and subclinical. Patients may complain of mild loin pains or haematuria. Urinary tract infections are common and will present with frequency, dysuria, loin pain and fevers. Occasionally medullary deposits may extrude into the pelvicalyceal system and present with renal colic. In nephrocalcinosis there is intense tubulointerstitial inflammation, thus tubular dysfunction may be a *complication* of raised intracellular calcium levels and calcium

deposition as well as a *cause* of nephrocalcinosis (as in Fanconi syndrome). Patients with nephrocalcinosis often, therefore, have a tubular concentrating defect (nephrogenic diabetes insipidus), and will complain of polyuria and polydipsia. *Secondary* dRTA, again as a consequence of medullary (and hence tubular) damage is also recognized and may lead to a vicious cycle of progressive nephrocalcinosis, tubular damage, worsening acidification capacity and further nephrocalcinosis. Hypertension is recognized but less common, as many nephrocalcinosis-causing diseases lead to sodium wasting. Renal failure is uncommon in conditions not associated with generalized proximal tubular dysfunction (such as Dent's disease and idiopathic renal Fanconi syndrome) and if present is usually mild (59, 103).

I.3.6 Systemic calcium and phosphate homeostasis

A stable extracellular calcium concentration is essential for normal neuromuscular function. Of the measured plasma calcium 45% is ionised, 15% is complexed to anions such as citrate and 40% is reversibly bound to plasma proteins.

The gastrointestinal tract only absorbs a fraction of ingested calcium. The size of this fraction is under hormonal control, and subject to large variation. Renal calcium homeostasis is described in the next section. 99% of total body calcium is contained within bone where it is deposited as hydroxyapatite. Parathyroid hormone (PTH) production is controlled by ECF calcium concentration, which is directly 'sensed' by the calcium sensing receptor (CaR) in the parathyroid tissue.

As ECF calcium falls, PTH rises and this stimulates calcium and phosphate resorption from bone and (via increased activation of vitamin D) calcium and phosphate reabsorption from the gut. This might lead to an increase in plasma phosphate, however this is offset by PTH-mediated reduction on proximal tubular phosphate reabsorption. Often the latter mechanism not only maintains normal plasma phosphate, but also reduces it below the normal range. PTH also increases calcium reabsorption in the distal convoluted tubule (DCT).

The para-follicular cells of the thyroid gland secrete calcitonin. It reduces bone resorption of calcium in response to increased plasma calcium concentration in the thyroid blood flow (104,105).

1.3.7 Renal handling of calcium, phosphate and oxalate

Of calcium passing through the glomerulus 40% is protein bound, mainly to albumin, and hence not available for filtration. The remainder is constituted by "free" ionized calcium and calcium complexed to phosphate, citrate and other anions. Around 65% of filtered calcium is reabsorbed in the proximal tubule, paracellularly, driven by the lumen-positive potential difference in the pars recta of the proximal tubule. Urinary and serum calcium concentrations are probably "sensed" in the proximal tubule by the apical calcium sensing receptor (CaR). High concentrations limit PTH stimulated vitamin D production.

A further 20-25% of calcium reabsorption occurs in the thick ascending limb (TAL) of the loop of Henle. This is paracellular and driven by a positive transtubular voltage, in turn generated by luminal NaCl reabsorption and potassium recycling. CaR senses blood Ca concentrations on the basolateral lumen, regulating NaCl transport and hence calcium reabsorption in the medullary TAL. In the cortical TAL calcium sensing reduces potassium recycling and in turn NaCl and calcium reabsorption. These mechanisms serve to facilitate the excretion of calcium in dilute urine to maintain normal serum calcium levels.

The remainder of calcium reabsorption (8-10%) occurs in the distal tubule. It is reabsorbed actively via a transtubular electrochemical gradient. This is independent of sodium reabsorption. Calcium enters the luminal epithelial cells via TRPV5, a member of the transient receptor potential channel superfamily V, (also known as ECaC1). TRPV6 (ECAC2) may serve as a further calcium channel. Following entry to the luminal epithelium it is transported across the cell by calbindin 1 (CALB1) and other calcium binding proteins. It exits through the basolateral membrane via NCX (the Na^+/Ca^{2+} exchanger and PMCA (plasma membrane Ca^{2+}-ATPase). Apical calcium entry is again regulated by CaR.

80% of plasma phosphate is filtered at the glomerulus and then extensively reabsorbed in the proximal tubule. In hypophosphataemia 100% reabsorption may occur. The apical Na/Pi co-transporter transports phosphate. Phosphate balance and PTH levels determine its expression. Extracellular fluid expansion will result in phosphaturia, as Na/P1 expression is down regulated in hypervolaemia to facilitate Na excretion. There is probably little phosphate transport in the loop of Henle, however there is some phosphate reabsorption in the collecting duct.

Oxalate is freely filtered and is actively and passively secreted by renal tubular epithelium of the proximal tubule, using anion exchangers. Recently exchangers of the SLC26 family have been found to transport oxalate in exchange for chloride (106-109).

I.4 THE ENAMEL RENAL SYNDROME

At the time of initiating this project there had been three reports of enamel renal syndrome in the literature. Having embarked on this project we were approached by a group from the Université d'Odontologie de Bordeaux, France (Isobel Normand de la Tranchade et al) who have subsequently reported a case. I was able to visit them in Bordeaux, meet their patient and they provided me with a great deal of background data on their case. After presenting an abstract of our research in Capetown, we were approached by a further group from Department of Medicine, SUNY Upstate Medical University, USA (Steve Scheinman et al). They also had a family with this syndrome.

Since then a further 3 reports of ERS have been published.

In this section I have presented the clinical data on these cases, provided from published data (with permission) and through direct communications with the relevant clinicians. I will present the clinical data on our family with ERS in the results section.

1.4.1 MacGibbon (1972)

Macgibbon published the first case report of ERS, in a brother and sister sib-pair from Queensland, Australia. The sister was referred to him aged 25 years due to delayed eruption of the permanent dentition. The deciduous teeth had erupted at the expected times; however these teeth were described as highly abnormal in appearance and were likened to "stumps" by the patient. Some of these teeth were extracted at the 9 years of age, the remainder extracted when she was 13. Initially dentures were fitted but, in her 20s, the permanent upper left canine erupted causing discomfort and she sought dental advice.

She had been diagnosed as having nephrocalcinosis at the age of 11. Her brother had been diagnosed with this condition at the age of 21 following which she and her other sibs were screened. She developed pyelonephritis at the age of 15. It seems

thereafter she developed chronic pyelonephritis and ill health becoming "invalid", requiring multiple hospitalisations. Apparently renal function had remained normal.

When she was examined -aged 25 - by the author, she appeared mentally alert. She was red-haired with fair skin. Physical examination was normal other than pigmented areas on the sun-exposed surfaces.

Dental x-rays were performed which showed 16 unerupted permanent teeth. The upper left canine had breached the mucosa. The remainder were submucosal. Coronal resorption (reabsorption of the crowns of the teeth) was also noted, resulting in "scallop" shape along the long axis of the tooth. There was no resorption at the root surfaces. "Dagger-shaped" pulp calcifications were noted in 4 teeth. The lamina dura was present around unerupted teeth. There did not appear to be any dental enamel on any of the teeth. The mandibular and maxillary bones appeared of normal structure and density.

9 teeth (thought to represent a hazard to denture-fitting) were removed. These teeth were subsequently examined. Macroscopically they were of normal size but were devoid of enamel. In some teeth it was noted that the crowns terminated in a ragged fashion perpendicular to the long axis of the tooth. Coronal resorption had, in some teeth, extended into the dental pulps. Four teeth were examined histologically by ground section and decalcification. This showed an absence of enamel. There had been extensive coronal resorption of dentine with apposition of well formed lamellar and haversian bone onto the surface of the remaining dentine. There was apical and lateral hypercementosis on all root surfaces.

The author examined the health records of her brother. He had developed high blood pressure at the age of 21 and a diagnosis of nephrocalcinosis was made radiologically. He apparently suffered from severe psoriasis and hypertension and then died at the age of 26. His autopsy findings were of coronary artery occlusion as the primary cause of death, with malignant hypertension, congestive cardiac failure and uraemia as secondary factors. This report is likely to have been based on details of the clinical history available to the pathologist as well as the post-mortem itself. Unfortunately this patient's dental record was not available, but his family stated that his teeth were similar to the affected sisters, and were extracted at an early age.

As well as the affected brother and sister there were three other siblings. They had normal teeth and had radiological screening for nephrocalcinosis, which was

negative. The mother had undergone early dental extraction but her teeth had been normal in appearance on eruption. Her five sibs and parents all had normal teeth. The father, his four siblings and parents all also normal dentition. The relationship of the mother and father of the affected individuals was non-consanguineous (1).

1.4.2 Lubinsky et al (1985)

The authors were referred a bother and sister with ERS aged 9 and 11 years. Their lower incisors had erupted at 5 to 6 months, with full sets of primary teeth at 24-30 months. These teeth were discoloured – yellowish at first, darkening later. Permanent maxillary and mandibular central incisors erupted by 7 to 8 years. These appeared highly abnormal - yellow-brown, widely spaced and with short crowns - and wore rapidly. A dentist had informed the parents that no enamel was visible on these teeth.

The authors examined the brother aged 12. Only the canines and incisors had erupted and enamel was indeed completely absent from these teeth. The crown surfaces were soft and the general consistency of dentin. Extensive wear and cracking was evident. Dental x-rays showed the other permanent teeth were present but unerupted and enamel appeared, radiographically, to be absent in these teeth also. There were large follicles around the crowns. Dagger-shaped bodies were present in the pulp chambers, probably representing pulpal calcifications. There was a rough appearance of the unerupted right mandibular crown, suggesting partial reabsorption within the alveolus.

The sister was examined aged 10 years. Only the maxillary incisors and mandibular central incisors had erupted. The crowns were similar to those of her brother. Again, radiographically, enamel appeared absent on erupted and unerupted teeth, follicles were present over the unerupted crowns and radiopaque masses were present in some pulp chambers, suggesting pulpal calcification. There was a rough appearance of the unerupted first mandibular molars, suggesting these crowns were undergoing resorption. In general the findings were remarkably similar between the two sibs.

The authors were able to perform a histological examination of an exfoliated crown from the primary right maxillary canine tooth of the sister. No enamel was detected. The dentin was normal except for isolated areas of stained and sclerotic tubules. There was also a calcified mass of tubular secondary dentin with vascular inclusions

extending from the roof of the pulpal dentin into the pulp chamber. The only calcified material on the crowns was a small globule of cementum.

Both sibs had suffered nocturnal enuresis and urinary tract infections. The brother had an intravenous pyelogram (IVP) aged 5 which showed grade I reflux into the right ureter (probably incidental). Medullary nephrocalcinosis was present which progressed on subsequent plain renal X-rays taken aged 8,11 and 14. The sister had an IVP aged 6 which showed medullary nephrocalcinosis. This appeared to have progressed by the time of a subsequent plain renal x-ray aged 9, but the progression in appearances was less than that seen in her brother.

Comprehensive metabolic profiling was performed. Serum electrolytes, urea and creatinine, pH, bicarbonate, parathormone, calcitonin, vitamin D, Ca, PO_4^{2-} and alkaline phosphatase were normal. Urinary amino acids were not present. The brother had a slightly reduced 24-hour urinary creatinine clearance at 86mg/min/1.73m^2. Calcium excretion was low in both sibs – 33mg/24hrs in the brother and 25mg/24hrs in the sister (200). Urinary Ca: Cr ration was measured before and after calcium loading (1.0g oral calcium) and there was less than the expected 2-3-fold increase in calcium excretion (0.028 to 0.037 in the brother, 0.046 to 0.061 in the sister). The administration of 40mg of oral frusemide increased calcium excretion in the brother to 129mg/24hrs, but the Ca: Cr ratio was still abnormal. Urinary concentrating ability following water deprivation testing was subnormal; the brother achieved a maximal urinary concentration of 496 mosmol/l, the sister 660 mosmol/l (800). Excretion of titrateable acid in response to acid (ammonium chloride) loading was sub-maximal, suggesting a degree of renal tubular acidosis. Urinary osteocalcin was increased on two occasions in both sibs. δ-carboxyglutamic acid was decreased. Urine excretion of citrate and oxalate was normal.

The authors performed a renal biopsy on the brother aged 11. Histological examination demonstrated focal glomerulosclerosis and peri-glomerular fibrosis with some hyalinosis of scarred glomeruli. There was widespread tubular loss with a dense infiltrate of mononuclear cells in the tubulointerstitium. One round, laminated calcific body was noted within a hyalinised glomerular tuft. Infrequent calcific deposits were noted in the tubulointerstitium. Immunofluorescence was negative. Electron microscopy showed sclerosis in 14 of 28 glomeruli with tubular atrophy and intense chronic inflammatory cell infiltration. The sister underwent renal biopsy aged

9 and the findings were similar, though the interstitial inflammation and scarring was less severe (2).

1.4.3 Hall et al (1995)

The authors presented a sib pair from non-consanguineous parents of Macedonian origin. The sister presented at 9 years to the Melbourne Royal Dental Hospital for investigation of opalescent teeth. On examination most of the primary teeth were retained, yellow-brown and extensively worn with clinically absent enamel. An exfoliated left primary central incisor was examined histologically and a diagnosis of autosomal recessive amelogenesis imperfecta (Witkop Type 1G, enamel agenesis) was made. The primary teeth were removed, the permanent central incisors were exposed surgically and resin bonding was performed for protection. Pulp necrosis subsequently developed requiring endodontic treatment. Subsequently all unerupted incisors were removed, alveolectomy and soft-tissue reduction performed and dentures fitted.

She suffered an episode of acute pyelonephritis aged 10 years. General examination appeared normal with the exception of her dentition. A micturating cysto-urethrogram showed no evidence of vesico-ureteric reflux, however medullary nephrocalcinosis was noted on plain x-ray, intravenous pyelography and computed tomography of the kidneys. Pelvic calcification was noted next to the iliac vessels. Serum urea and creatinine, vitamin D, PTH and osteocalcin levels were normal as were urine excretion of calcium, oxalate and cysteine. Renal biopsy showed focal glomerulosclerosis, periglomerular fibrosis and an interstitial infiltrate with lymphocytes and plasma cells. No calcification was seen on these biopsy sections.

This patient continued to enjoy good health with normal development and growth. Renal function remained normal. The kidneys increased proportionate to age and overall size, but the nephrocalcinosis persisted.

The elder brother was examined at the age of 14 at the same centre. There were retained, discoloured primary teeth with thin or non-existent enamel. The maxillary incisors, first molars and two left premolars had erupted and were severely worn. Gingival overgrowth was present around the incisors. A dental radiograph showed intrapulpal calcifications in the lower first permanent molars. Again dental clearance and denture fitting was required for a reasonable cosmetic result.

A third, female sib was screened and had normal dentition with no nephrocalcinosis on ultrasound.

The authors performed histological and ultrastructural studies on a permanent incisor extracted from the affected sister. Only the incisal edge of this tooth had erupted, so they were able to study enamel from both erupted and unerupted sections of tooth. For light microscopy longitudinal sections were taken with a low speed diamond saw. The surface of the enamel was examined with a scanning electron microscope. Selected areas of enamel were then prepared by the relatively novel technique of argon beam thinning and then examined with a transmission electron microscope.

Light microscopy demonstrated a thin enamel layer, which was non-existent in some areas. Maximal enamel thickness was 0.2mm (1.0-2.5mm). The enamel surface was irregular and positively birefringent (normal enamel being negatively birefringent). Scanning electron microscopy showed the surface topography of unerupted enamel to be rough in some areas with widespread ovoid tubercles. There was extensive cracking of unerupted enamel with a threadlike material bridging these cracks. The erupted enamel had smoother areas, probably caused by wear. In these smooth areas the tubercles were absent and the cracks larger.

Ultrastructural examination with transmission electron microscopy showed similar appearances of erupted and unerupted enamel. The enamel consisted of thin, ribbon-like crystals that were loosely packed and the enamel was porous. The prismatic structure seen in healthy enamel was not present (3,4).

Normand de la Tranchade et al (2002)

The authors reported on a sporadic case. A 15 year-old female presented for dental treatment, primarily for cosmetic reasons. The permanent maxillary and mandibular incisors had erupted, but all her other teeth were remnant primary teeth. These teeth were yellow and highly worn. The erupted permanent teeth were also discoloured and widely spaced. There was gingival hypertrophy. Dental x-rays showed the unerupted permanent teeth, with evidence of intracoronal resorption. There was very little enamel on either the permanent or secondary teeth and there were numerous follicular cysts.

They submitted pictures to several dentists with an interest in amelogenesis, including R. Hall (author of report 1.4.3, previous). He suggested a diagnosis of ERS. The authors performed renal ultrasound on their patient, which confirmed

numerous medullary, calcific foci. Isotopic GFR was slightly reduced at 80mls/min/1.73m^2. There was no proteinuria or haematuria. PTH, vitamin D (25 and 1,25 hydroxylated), calcium, phosphate were normal. Urine oxalate was normal and there was no aminoaciduria. 24 hour urinary calcium was significantly reduced at 1.34mmol/24hr. Urinary phosphate and citrate excretion was also reduced. The patient was not hypertensive and denied any uro-nephrological symptoms or medical history.

Extensive restorative dentistry was performed. Interestingly during this the authors noted an inclusion of hard tissue in a permanent molar. Histological analysis revealed this to be Haversian bone. The authors concluded that the crown had been resorbed and replaced by bone. They were also able to perform histological examination of a dental follicle. This showed pathological calcification, consistent with the pathological pulpal calcifications seen in the x-rays of previously reported cases. Light microscopy of extracted primary teeth confirmed the complete absence of enamel. They hypothesised that the origin of the dental phenotype may be the pathological follicle, which calcifies, undergoes fibrous transformation and is unable to initiate eruption (6).

1.4.4 1.4.5 Paula et al (2005)

The authors reported on a Brazilian male of consanguineous parentage who was referred to them for dental care at the age of 13. There was no family history of dental or renal disease, the boy was otherwise healthy and he had enjoyed normal development.

On examination of the teeth at the time of referral the deciduous molars and cuspids had been retained. The gingival tissue was enlarged. The permanent upper central incisors, lower incisors and first molars had all erupted. Deciduous and permanent teeth were yellow and had a very thin layer of enamel. The upper left incisor had a semi-lunar shaped defect. Dental x-rays showed a complete set of permanent teeth with normal root development, most of which were unerupted. It was difficult to discern any difference in density between the dentine and enamel. As in other cases coronal intra-pulpal calcifications were noted. These were needle-shaped in the incisors and round in the molars. The unerupted teeth had peri-coronal radiolucencies. The roots of the upper lateral incisors appeared delacerated while lower lateral incisors were dislocated distally.

Renal ultrasound demonstrated bilateral medullary nephrocalcinosis. Urea and electrolytes, calcium and phosphate were normal. Alkaline phosphatase was slightly elevated.

Histological examination was performed on ground sections of two exfoliated deciduous teeth. This demonstrated a complete absence of enamel. The authors then performed incisional biopsies of the pericoronal tissues of two unerupted upper cuspids. The peri-coronal follicles showed hyperplastic odontogenic ectomesenchyme with round, dysplastic calcifications. Odontogenic epithelial islands of clear cells were noted against a background of myxofibrous material. The authors diagnosed hamartomatous change (7).

1.4.6 Fu et al (2006)

Fu et al reported a case of ERS with associated hypokalaemia and metabolic alkalosis (features normally associated with Bartter's syndrome). She was an only child and, as in our family, she was from consanguineous (first cousin) parents. Her gestation was complicated by severe antenatal hydramnios requiring recurrent paracentesis. She was born at 33 weeks with normal birth weight. At 2 months she was assessed for vomiting and failure to thrive.

At this stage she had normal plasma biochemistry and renal function. Serum osmolality was normal at 280mOsm/Kg. Urine osmolality was however reduced at 150-250mOsm/kg. They then performed water deprivation testing with vasopressin (0.2U/kg i.m). She failed to concentrate urine above 300mOsmol/kg in spite of 4 hours water deprivation and vasopressin, suggesting a renal tubular urinary concentrating defect. As expected serum AVP levels were high.

She was treated for nephrogenic diabetes insipidus with thiazide diuretics. Failure to thrive persisted. At 18 months she was found to have hypercalciuria; urinary calcium/creatinine ratio (Ca: Cr) was 1.8mg:mg (0.1-0.3) and hypokalaemia, with serum potassium of 2.3mmol/l (3.5-5.0). Renin was elevated at 14.4ng/ml/h (0.3-2.9) and aldosterone was elevated at 750pg/ml (36-240). Blood pressure measurements were, however, normal. Indomethacin and spironolactone were commenced as a treatment for hypokalaemia.

She appeared to develop normally, but by the age of 12 her parent had noted discolouration of her secondary teeth. This was diagnosed as AI with thin, extensively cracked, dental enamel. Medullary nephrocalcinosis was demonstrated

on renal ultrasound. The hypokalaemia and hypercalciuria and low urine osmolality had persisted. She was found to have a mild metabolic acidosis. Renin and aldosterone levels remained high in spite of normal blood pressure. Serum calcium, serum osmolality and renal function remained normal. Urinary osmolality remained low and hypercalciuria had persisted. Urinary N-acetyl-glutamate and α1-microglobulin were normal. This, and the absence of glycosuria and aminoaciduria, suggested preserved proximal tubular function. Serum intact-parathyroid hormone level was elevated at 98.0pg/ml (normal 14-66), as was vitamin D level at 103pg/ml (20-70). Protein induced by vitamin K antagonist II (PIVAKII) was normal.

The authors surmised that these finding represented another case of ERS, but noted some features common to Bartter's Syndrome (hypokalaemia and tubular concentrating defect). They then performed mutation analysis of what they considered to be candidate genes for this syndrome – NKCC2 (type 1 Bartter's syndrome), ROMK (type 2 Bartter's syndrome), CLC-Kb (type 3 Bartter's syndrome), Barttin (type 4 Bartter's syndrome), the calcium-sensing receptor (CaSR, type 5 Bartter's syndrome) and Aquaporin 2 (AQP2) the gene associated with autosomal nephrogenic diabetes insipidus. Sequencing of all exons and exon-intron boundaries demonstrated no mutations in these genes (8).

1.4.7 Hunter et al (2007)

This group reported a further case of ERS in 2007. A Caucasian male aged 13 years was referred to the University Dental Hospital Cardiff due to a failure of eruption of the secondary dentition. He was an only child with no family history of renal or dental disease. They had access to panoramic radiographs taken when the boy was 10 years old. This showed generally aberrant eruption of the permanent teeth, the maxillary left central incisor and both mandibular central incisors being the only secondary teeth present in the mouth (figure X). Crown morphology was noted to be abnormal, particularly in the developing teeth, the density of the enamel appearing closer to that of dentine.

The child was treated at a local dental centre and had a number of modifications including composite resins of the primary teeth and a maxillary over-denture.

He was subsequently referred to the University Dental College Hospital, Cardiff at the age of 13.9 years. At this stage intraoral examination showed that the maxillary left central incisor and mandibular central incisors were still the only teeth to have erupted clinically. The retained primary and erupted teeth all demonstrated thin,

yellow enamel. A panoramic dental x-ray taken at this time showed that the roots of the permanent teeth had continued to form, but had not moved through bone in an axial fashion since the previous film.

In view of the previously reported association of AI and delayed eruption with nephrocalcinosis the patient was referred for renal ultrasound examination. This demonstrated mild, medullary nephrocalcinosis. The patient's serum creatinine was higher than expected at 112µmol/l and his estimated glomerular filtration rate (MDRD calculation) was reduced at 65ml/min. Mild proteinuria was also noted. Serum PTH and urinary calcium levels were normal.

The patient has been referred for lifelong renal surveillance. As regards his dental management the authors considered a combined surgical and orthodontic approach but it was felt ankylosis of the unerupted teeth contraindicated this. Osteotomies and distraction osteogenesis has been considered as a future treatment, but cannot be considered until growth is complete. Meanwhile he is receiving maintenance prosthodontic treatment (9).

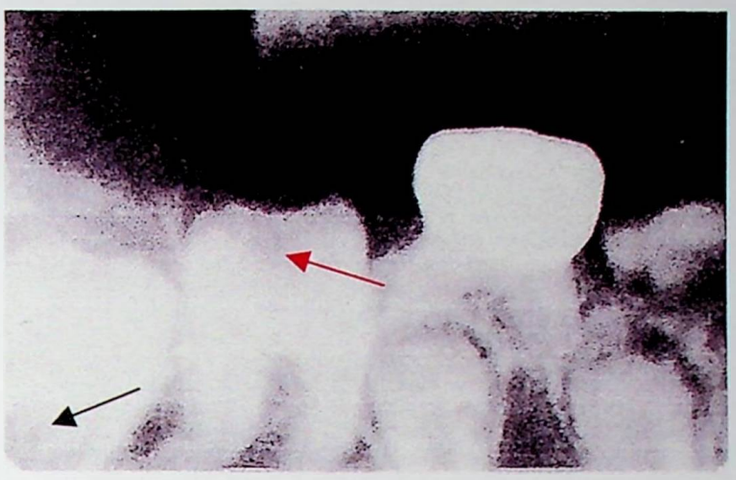

Figure 6. Dental radiograph of ERS patient. There is no enamel present on the erupted molars or unerupted teeth. There are areas of coronal resorption (red arrow) and intrapulpal calcification (black arrow). (Lubinsky et al)

Figure 7. Photograph of dentition ERS patient. There is abnormal morphology of primary and permanent dentition with thin enamel and a yellow discolouration. (Paula et al).

Figure 8. Ground section of exfoliated tooth showing an absence of enamel in ERS patient. (Paula et al).

Figure 9. Dental radiograph of ERS patient. There is widespread failure of eruption of the permanent teeth. There are intrapulpal calcifications. (Paula et al)

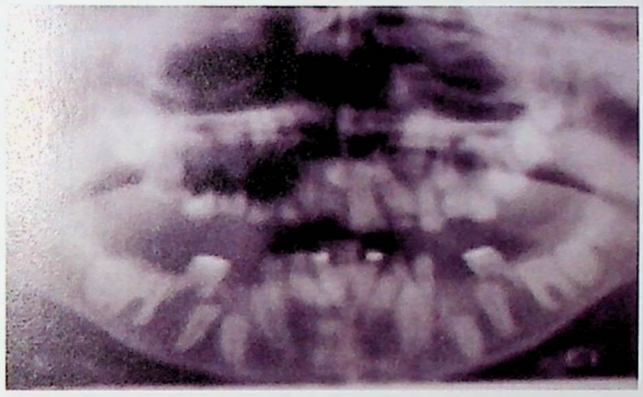

Figure 10. Oral radiograph ERS patient taken aged 13.9 years (Hunter et al)

Figure 11. Occlusal view of maxillary arch ERS patient. (Hunter et al).

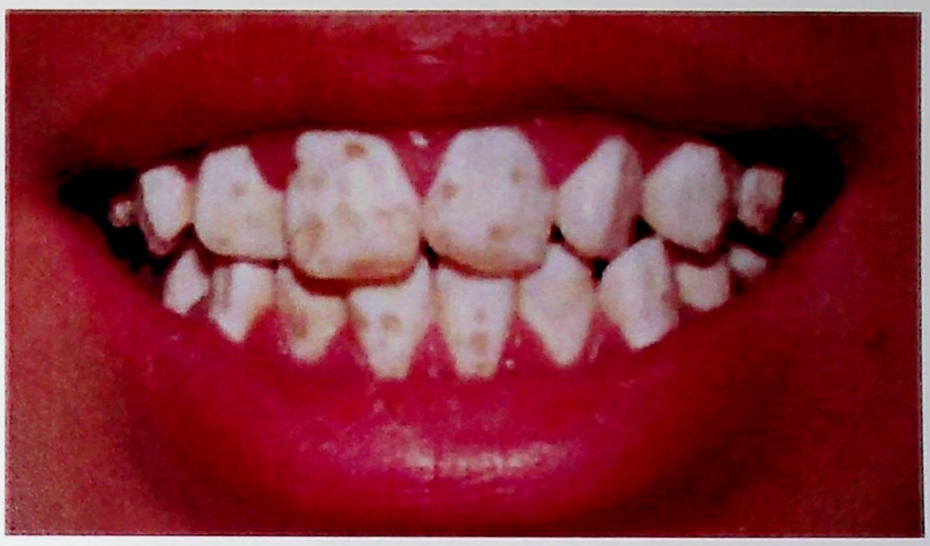

Figure 12. Photograph of dentition ERS patient. The enamel is thin with patchy discolouration due to areas of extreme thinning and visible dentin. (Jun Fu et al).

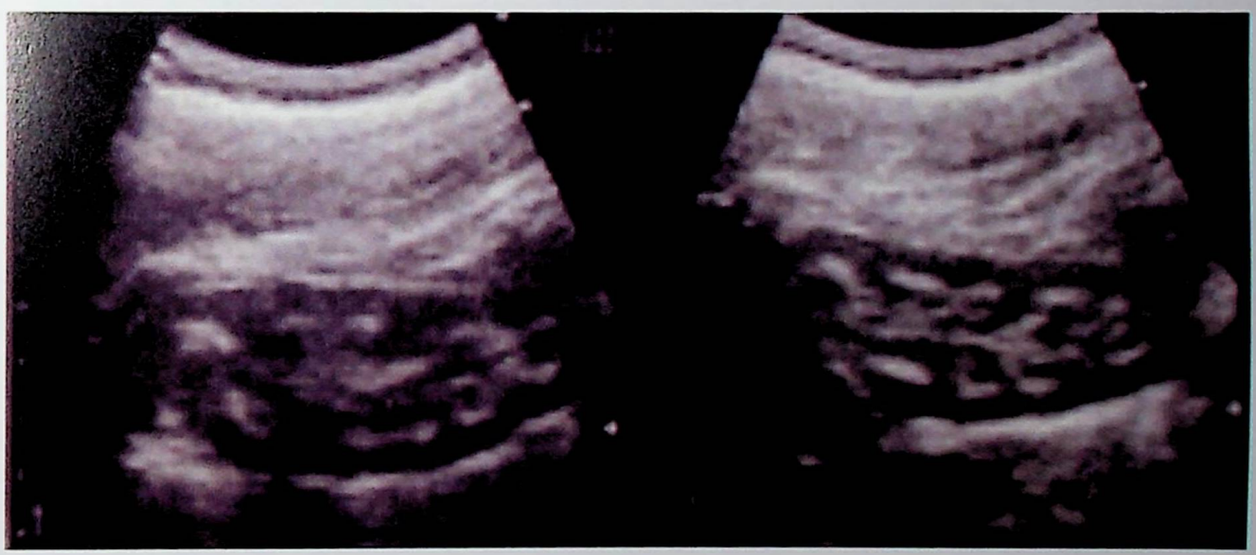

Figure 13. Renal ultrasound showing medullary nephrocalcinosis in ERS patient. (Jun Fu et al).

1.4.8. Geographical distribution of global ERS reports.

Figure 14. Location of ERS cases

1.5 CANDIDATE GENES FOR THE ENAMEL RENAL SYNDROME

Our large, consanguineous ERS kindred would potentially provide a powerful tool for examining candidate genes for this syndrome. We considered the following genes/loci to be of interest.

1.5.1 The chromosome 4 "secretory calcium-binding phosphoprotein gene cluster"

As discussed earlier (1.2.5) autosomal AI (type II) had been mapped to 4q.21 with linkage analysis at the onset of this research, however the responsible gene within this locus had not been identified. This form of AI is phenotypically similar to the type of enamel defect seen in ERS. The 4q.21 locus has been found to contain a number of genes crucial to tissue mineralization and has since been named the "secretory calcium-binding phosphoprotein gene cluster". With the exception of the amelogenin gene on the X chromosome, this locus is the principal site of genes for enamel matrix proteins (EMPs) as well as dentine and bone extracellular matrix proteins. Recently authors have found evidence that these genes originate from a common ancestor by tandem gene duplication. As such it was worth exploring whether the disease gene for ERS resided at this locus.

This locus contains the ameloblastin (*AMBN*) gene. Ameloblastin is the second most abundant enamel protein after amelogenin and has been discussed in section 1.2.3. Other genes now known to make up this cluster include dentin sialophosphoprotein (*DSPP*), dentin matrix acidic phosphoprotein 1 (*DMP1*), matrix extracellular phosphoglycoprotein (*MEPE*), bone morphogenetic protein 3 (*BMP3*), integrin binding sialoprotein (*IBSP*) and secreted phosphoprotein 1 (*SPP1*) (110,111).

SSP1 (also known as osteopontin) is expressed in bone, this expression stimulated by vitamin D. It has a role in anchoring osteoclasts to the mineral bone matrix. As well as bone it has been found in cutaneous and vascular elastic tissue. Osteopontin also functions as an immune-modulator and is expressed in macrophages, dentritic cells, neutrophils and T and B cells. It helps attract these cells to inflammatory sites and facilitates cell adhesion. SSP1 has been found in the matrix of renal stones. It is expressed in renal tissue and this expression appears to be upregulated in inflammatory renal insults (112-119).

Dentin phosphoprotein and dentin sialoprotein are the major noncollagenous components of dentin. The *DSPP* gene encodes both. Mutations in DSPP have been found to cause both dentinogenesis imperfecta and dentin dysplasia type II.

DMP1 is critical to bone mineralization and phosphate metabolism. DMP1 null mice have been found to have renal phosphate wasting and hypomineralised bone. Mutations of DMP1 have now been shown to be associated with autosomal recessive hypophosphataemia in several families. The other genes, which constitute this complex -MEPE, BMP3 and IBSP-, appear to be more specifically involved in bone, rather than dental health (120-125).

1.5.2 Bone gamma-carboxyglutamic acid protein (*BGLAP*, 1q12-q14)

BGLAP, also known as osteocalcin, is a vitamin K dependent calcium-binding protein containing gammacarboxyglutamic acid. Its function is not clear, but it is a major constituent of the noncollagenous bone matrix. It is metabolised by the liver and kidneys. Plasma levels have been found to be elevated in certain bone diseases, generating interest in it as a biomarker. Lubinsky et al had found urinary BGLAP (osteocalcin) to be elevated in both their ERS patients on two occasions. We therefore thought this gene would be worth investigating in ERS (126-133).

1.5.3 Matrix Gla protein (*MGP*, 12p13.1-p12.3)

MGP is a 10-kD vitamin K-dependent protein. It is highly expressed in kidney, heart, lung, vasculature, bone and dentin. Its expression appears to be vitamin D dependent. Mutations in MGP have been found to cause Keutel syndrome. This is an autosomal recessive condition that causes pathological tissue calcification, mid-face hypoplasia and pulmonary stenosis. Genetic variation in MGP has also been associated with increased rates of natural tooth loss (or ageing) (134-139).

1.5.4. Transient receptor potential cation channel subfamily V, member 5 (*TRPV5, ECaC1* 7q35)

TRPV5 (EcaC1) is a member of the TRPV superfamily of calcium transporters. The TRPV5 gene contains 16 exons and spans 25kb. It is expressed in the distal tubule and is the route of calcium reabsorption at that site. TRPV5 was of interest as a candidate gene in ERS due to the hypocalciuria seen in this syndrome. Further information on TPV5 function is provided in section 1.3.7 (143-145).

1.5.5 Vitamin D receptor (VDR, 12q12-q14)

VDR is an intracellular hormone receptor with wide tissue expression. When activated it alters the transcription rates for genes which cause its biological responses. The VDR gene has 11 exons and is 75kb in length.

Vitamin D has simultaneous effects on renal and intestinal phosphate and calcium handling as well as PTH. Vitamin D increases renal calcium reabsorption and calbindin expression and accelerates PTH-dependent calcium transport in the distal tubule. The distal tubule 'fine tunes' the calcium content of the urine and has the highest VDR content in the kidney. ECaC (or TRPV5) mediates vitamin D dependent calcium reabsorption and VDR binding sites have been located in the human promoter of the renal ECaC. Hypocalciuria is a key feature of ERS, so the VDR-ECaC pathway is worth considering in candidate gene selection.

VDR is expressed in developing teeth. Its regulatory role is not well understood. Vitamin D deficiency is well known to cause abnormal dental development. Enamel hypoplasia with discolouration and early wear has been shown to occur in vitamin D-dependent rickets. Interestingly vitamin D *toxicity* has also been shown to cause amelogenesis imperfecta, with a very similar phenotype to that seen in ERS.

There is a well-known association between vitamin D toxicity and nephrocalcinosis. Though this is commonly due to hypercalcaemia it has been postulated that vitamin D may affect renal parenchymal calcification more directly (146-155).

1.5.6 Calbindin 1 (*CALB1*, 8q21.3-q22.1)

The Calbindins D9K and D28K are vitamin D dependant calcium-binding proteins. They regulate cellular calcium mobilisation. The gene for Calbindin D28K (*CALB1*) was mapped to 8p12-q11.2 via Southern analysis of somatic cell hybrids and in situ hybridisation. The gene for Calbindin D9K (*CALB2*) was subsequently mapped to 16q22-q23.

Calbindin D28K has been shown, through in situ hybridisation, to be upregulated during the initiation of secretory and maturation stages of enamel mineralisation. It is also highly expressed in the kidney, where it likely plays a role in vitamin D dependant tubular calcium reabsorption (156-159).

1.6. AIMS OF THE PROJECT

The aims of this project were to further define the clinical characteristics of ERS and to determine the genetic cause of this disorder. At the start of this project we had access to, and the full cooperation of, a large, consanguineous kindred in which 2 of 6 sibs had been diagnosed with ERS.

1. Complete a clinical evaluation of family X including assessment of renal function, metabolic profiling and review of dental records.
2. Perform candidate gene linkage analysis on family X. The size and consanguinity of the family would be a powerful resource to *exclude* candidate genes by this method. We planned to study candidate genes within the "secretory calcium-binding phosphoprotein gene family". These genes are on the 4q21 locus to which the similar dental phenotype – Amelogenesis Imperfecta 2 (AIH2) – had been localised. We also planned to study the candidate genes bone gamma-carboxyglutamic acid protein (*BGLAP*, 1q12-q14), Matrix Gamma-Carboxyglutamic Acid (*MGP*, 12p13.1-p12.3), Vitamin D Receptor (*VDR*, 12q12-q14), Epithelial Calcium Channel 1 (Transient Receptor Potential Cation Channel Subfamily V, Member 5 *TRPV5, ECaC1*, 7q35) and Calbindin 1 (*CALB1*, 8q21.3-q22.1).
3. Invite the participation of the previously described ERS kindreds (as published in the medical literature) and their responsible clinicians, hopefully obtaining relevant clinical data and DNA samples. By advertising our interest in this disorder it was hoped we might also be able to recruit further, unreported kindreds with this disease into the project.
4. Given the potentially subclinical nature of nephrocalcinosis, we planned to screen a very large family (treated at the Eastman Dental Hospital) with ADAI for nephrocalcinosis with renal ultrasound. If there was evidence of nephrocalcinosis we would include them in our genetic study of ERS. If they were found to have AI in isolation we hoped to confirm linkage to Ch4 (as previously described Backman et al) with a view to possible further genetic study of this dental disorder.
5. If our candidate gene approach was unsuccessful we planned to perform a genome-wide search, using linkage analysis, through an appropriate collaboration with an appropriately resourced collaborator.

SECTION I – CHAPTER 2

MATERIALS AND METHODS

2. 1 RECRUITMENT OF PARTICIPANTS

Ethical approval was obtained from UCL Research Ethics Committee. The principal family in this study was under our care in the renal unit of The Middlesex Hospital, University College Hospitals, London. They had also received treatment at The Eastman Dental Hospital, University. They agreed to participate in this study and consented to access to their dental records and DNA extraction from whole blood samples acquired from venepuncture.

A further family, with autosomal dominant hypoplastic amelogenesis imperfecta, had undergone dental treatment by Dr Kathy Harley at The Eastman Dental Hospital. I was able to perform renal screening for nephrocalcinosis. I obtained whole blood samples from adult family members and mouth swab samples from the children.

We then approached the authors of previously case reports of ERS treated in other centres. DNA from these patients was provided by their respective physicians in collaboration with local genetics departments, with the exception of the Bordeaux patient who's DNA was sampled and extracted myself.

2.2 CLINICAL PHENOTYPING

Routine biochemistry and haematology was performed through the clinical pathology services at The Middlesex Hospital using standard methods. The 2 ERS patients underwent a full 'metabolic stone screen'. This involves a 7-day diet diary from which dietary intake of key factors (calcium, oxalate etc) may be calculated. During the last 2 days two 24-hour urine collections are performed (one acid, one without preservative). From this the urinary profile is obtained, including calcium, oxalate and amino acid excretion. The clinical radiology department of the Middlesex Hospital performed X-rays and renal ultrasonography for the ERS family and ADAI family. Dr Kathy Harley (of the Eastman Dental Hospital) provided information on the dental phenotypes. Data on the other ERS families was obtained from the available publications and by direct communication.

2.3 DNA SAMPLING

2.3.1 DNA sampling from whole blood

For this method the Qiagen DNA extraction QIAamp kit was used as per the manufacturers recommendations. Venous blood was obtained by standard sterile

venepuncture and the blood aspirated into EDTA primed vacuum, glass bottles. These were then frozen at -20°C prior to DNA extraction. At the start of the DNA extraction the samples were thawed and equilibrated to room temperature. 20ml of QIAGEN Proteinase K was added to the bottom of a 1.5ml microcentrifuge tube. 200ml of whole blood was then added over the proteinase K and this was thoroughly mixed. 200ml of Buffer AL was then added to the sample. This mix was then pulse vortexed for 15 seconds, incubated at 56°C for 10 minutes and then briefly centrifuged.

200ml of 100% ethanol was then added to the sample and mixed by 15 seconds of pulse vortexing. This mix was then briefly centrifuged. This mix was then added to the QIAamp Spin Column and centrifuged at 6,000 x g (8,000 rpm). This was repeated until the QIAamp spin column was empty.

The QIAamp spin column was then opened and 500ml of Buffer AW1 was added. The cap was closed and the column centrifuged at 6,000 x g (8,000 rpm) for 1 minute. The QIAamp Spin Column was then placed in a clean 2 ml collection tube (provided) and the filtrate collection tube was discarded. The QIAamp Spin Column was hen opened and 500ml of Buffer AW2 was then added. His was then centrifuged at 20,000 x g (14,000 rpm) for 3 minutes. The QIAamp Spin Column was then placed in a clean, 1.5 ml microcentrifuge tube and the filtrate tube was discarded. 200ml of Buffer AE was then added. This was then incubated at room temperature for 5 minutes and then centrifuged at 6,000 x g (8,000 rpm) for 1 minute. The DNA was then stored at -20°C.

2.3.2 DNA extraction from mouth swabs

Cotton bud swabs were rubbed on the inside of the cheek (x10) and then submerged in 2.5mls Slagboom buffer. These samples were stored in a dark room prior to extraction. At the start of the extraction the swab tubes were warmed in a water bath at 65 °C for 2hours. The cap was removed and the tubes were inverted and placed in conical flasks and spun at 647g for 10 minutes. The swabs were removed and the sample liquid was transferred into a clean tube. 0.3mls of Yeast Reagent 3 (diluted 1:1 WITH 100% ethanol) was added and mixed thoroughly. The mixture was then spun at 7,000rpm for 25 minutes. The supernatant was transferred to a clean tube. Step 5, 6, 7 were then repeated.

Precipitation was performed by adding 1.8mls of isopropanol and inverting the tube several times. This mix was then centrifuged at 7,000rpm for 25 minutes to form a

pellet of the precipitated DNA. The supernatant was discarded and the pellet was washed with 70% ethanol. The tube was spun for a further 10 minutes at 7,000rpm. The residual ethanol was poured off and the pellet was dried for 15 minutes. 0.4mls of DNA Hydration buffer (TE) was added and the sample was left overnight in a rocker to resuspend.

2.4 MARKER SELECTION

Possible candidate genes were selected according to our limited understanding of the pathophysiology of the disease and the association between certain genes and syndromes sharing aspects of the ERS phenotype (e.g. autosomal dominant, hypoplastic amelogenesis imperfecta and Keutel syndrome). The loci of these genes were then obtained from the **GDB Human Genome Database** (hosted by RTI International, North Carolina USA, http://www.gdb.org/gdb/) and the **UCSC Human Genome Browser** (hosted by The Genome Bioinformatics Group, the University of California Santa Cruz, http://genome.ucsc.edu/). Markers (CA repeats) were then selected which were suitably polymorphic to be informative and, initially flanked the candidate genes. In some instances the haplotypes were clarified further by selecting further polymorphic markers in the region were selected to provide more detailed haplotyping.

2.5 PRIMER SELECTION

Primers are oligonucleotides hybridising to opposite strands and flanking the target DNA. Primers, for the PCR of polymorphic markers flanking, or close to, candidate genes were selected using The Genome Database (see above) using the Amplimer online primer search on this website.

The following were considered for primer selection.

1. Primers were 12 to 30 bases in length.
2. There was no intra-primer homology.
3. The primers did not anneal with other non-target sites in the genome.
4. G/C content was 45-55%.
5. Secondary structure was avoided.

6. The forward and reverse primers had melting temperatures within 3°C of each other.

2.6 PCR OF MICROSATELLITE MARKERS FROM GENOMIC DNA

Prior to radiolabelled PCR for genotyping the amplimers and DNA were checked with a standard PCR reaction. A PCR mix was made up which comprised 1ml 500ng/ml genomic DNA, 2.5ml 10x PCR buffer (ICN), 0.75ml 50Mm $MgCl_2$, 2.5ml 2mM 10x dNTPs, 0.1ml 5U/ml Taq DNA Polymerase ("Amplitaq", Applied Biosystems), 12.5pmol forward primer and 12.5pmol reverse primer. This then was made up to 25ml with H_2O. Following mixing the PCR reaction was performed using the Phoenix Thermocycler PCR machine. The standard PCR programme is shown below. Annealing temperature was varied for some primers.

PCR STEP	TEMP (°C)	DURATION (secs)	CYCLES
Initial Denaturing	94	300	1
Denaturing	94	30	30
Primer annealing	50	30	30
Strand elongation	72	30	30
Final elongation	72	600	1

Table 2. PCR programme for genotyping ERS family

2.7 GEL ECLECTROPHORESIS OF MICROSATELLITE MARKERS FOLLOWING PCR FROM GENOMIC DNA

An agarose gel mix was made up which comprised 5mls of 10xTBE (0.9M Trios, 0.45 M Boric Acid, 0.02M EDTA), 95mls of H_2O and 2.5ml of Ethidium Bromide (5mg/ml). 0.8g of agarose was added to 40mls of the above mix in a heat-resistant flask. This was boiled under a Bunsen burner, cooled and poured in to the gel apparatus. The gel comb was then inserted and the gel set for 30 minutes.

60 mls of the original TBE and Ethidium Bromide mix was then poured into the gel apparatus as running buffer. 10ml of PCR product was mixed with 2ml of gel loading buffer (0.25% Bromphenol Blue, 0.25% Xylene Cyanol FF, 15% Ficoll type 400, Pharmacia). These 12ml aliquots were then loaded into the gel well. 2ml of a 100bp

ladder was mixed with 8ml of water and 2ml of gel loading buffer and added also loaded.

The apparatus cover and electrodes were applied and connected to the power supply. The gel was left to run for 45 mins at a current of 50 mA and a voltage of 60V. The running buffer was then drained off. The gel was then inspected under UV light, transillumination and photographed.

2.8 OPTIMISATION OF PCR REACTIONS

When PCR amplification was inadequate modifications were made to annealing temp and PCR program. Occasionally alternative PCR primers were selected or designed. For some more difficult PCR reactions "hot start" PCR was deployed using "Amplitaq Gold" (Applied Biosystems) with the recommended GeneAmp 10xPCR Buffer II (500mM potassium chloride, 100mM Tris-HCL (Ph 8.3), 15mM $MgCl_2$ and 0.01% (w/v) gelatin. The latter method is designed to prevent mispriming during pre-PCR set up. The Taq Polymerase is activated only when temperatures are high enough to suppress primer annealing to non-target sequences.

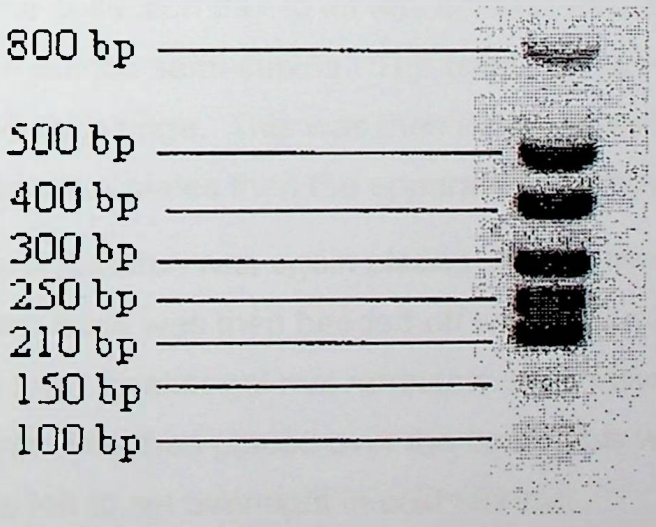

Figure 15. Kilobase ladder for agarose gel electrophoresis of PCR products of microsatellite markers.

2.9 GENOTYPING OF GENOMIC DNA USING P_{32}RADIOLABELLING

2.9.1 PCR of microsatellite markers from genomic DNA using P_{32} labeling

A radiolabelled PCR mix was made up. This comprised 1ml 60mM dCTPs, 1ml 10x PCR buffer (ICN), 0.3ml 50mM $MgCl_2$, 0.1ml dAdTdG, 12.5pmol forward primer, 12.5pmol reverse primer, 0.3ml 1/80 32p DCTP, 0.05ml 5U/ml taq polymerase and 2ml 500ng/ml genomic DNA. This was made up to 10ml with H_2O. The PCR reactions were optimised according to the non-radiolabelled PCR optimisations. All waste was disposed of as radioactive with regular Geiger counter monitoring of radioactivity in the work area.

2.9.2 Electrophoresis of radiolabelled PCR products of microsatellite markers for genotyping

A polyacrylamide gel mix was made up. This comprised 30 mls of acrylamide + urea, 150ml of Temed and 150ml of 25% AMPS. A gel comb mix was then made up which comprised 50 mls of acrylamide + urea, 100ml of Temed and 100ml of 25% AMPS

The gel apparatus was constructed. The gel mix was stirred in a beaker then added quickly between the plates of the apparatus. The apparatus was then stood upright in the collection tray to let any bubbles escape. The apparatus with poured gel was then placed semi-supine. The comb gel mix was stirred in a beaker then loaded into a 50 ml syringe. This was then added above the running gel mix; between the gel apparatus plates then the apparatus was placed upright to let bubbles escape.

The apparatus was again placed semi-supine and the gel comb was added. The comb edge was then beaded off with a 25 ml syringe and the remainder of the comb gel mix. Beaker gel mix remnants were observed for adequate gel setting. Wet tissue was then placed over the comb, this was covered with cling film and the gel was left to set overnight in cold storage.

The comb and base tray were removed and gel remnants trimmed off. The gel apparatus was then placed in power pack base and support screwed in. 400mls of 1xTBE was then poured into the power pack base tray. The rest was added to the glass plates of the apparatus up to 1 cm from the top. The electrodes were then added. The gel was warmed add at 90V until the front panel temperature gauge reached 50C. The voltage was then reduced to 60V.

10ml of gel loading buffer was added through paraffin cover to each PCR sample. The PCR samples (with loading buffer) were then spun at 1,500 RPM. The paraffin was then removed with a 200ml Gilson pipette. The PCRs were then warmed at 80C for 2 minutes. The electrodes were removed from the warmed gel apparatus and bubbles dispersed. The gel wells were then flushed and 2ml of PCR was added to each well. The electrodes were then added and the gel was run for at 60V. The duration of the gel run was around 2 hours. For smaller PCR products shorter runs (90 minutes) were used and run durations were often varied, the aim being to optimise separation of allele sizes and facilitate genotyping. The buffer was then drained off.

The apparatus was dismantled and blotting paper was applied across the gel, smeared and the gel and paper removed. This was then covered with cling film and placed in x-ray cartridge. Then, in the dark room, a BIORAD-MR radiology film was then added to the cartridge in proximity with the gel, separated by cling film. The x-ray cartridge was then placed in the -20C freezer overnight and developed. Where exposures were low, due to low radioactivity levels in the PCR products, films were placed for sequentially longer periods (up to 4 days) to aid accurate genotyping.

2.10 SCORING OF GENOTYPES

The genotypes were scored according to size by trans-illuminating the x-ray film and assessing migration of alleles on the gel. Mari-Wyn Burley, a senior laboratory geneticist, checked my genotyping scores. The genotyping data was entered into Cyrillic haplotype database software and haplotypes were constructed.

At times optimisation was required to provide clear resolution of alleles with this method. This included optimising the PCR, prolonging the gel migration stage and prolonging the exposure of the radiographic film to the radiolabelled gel.

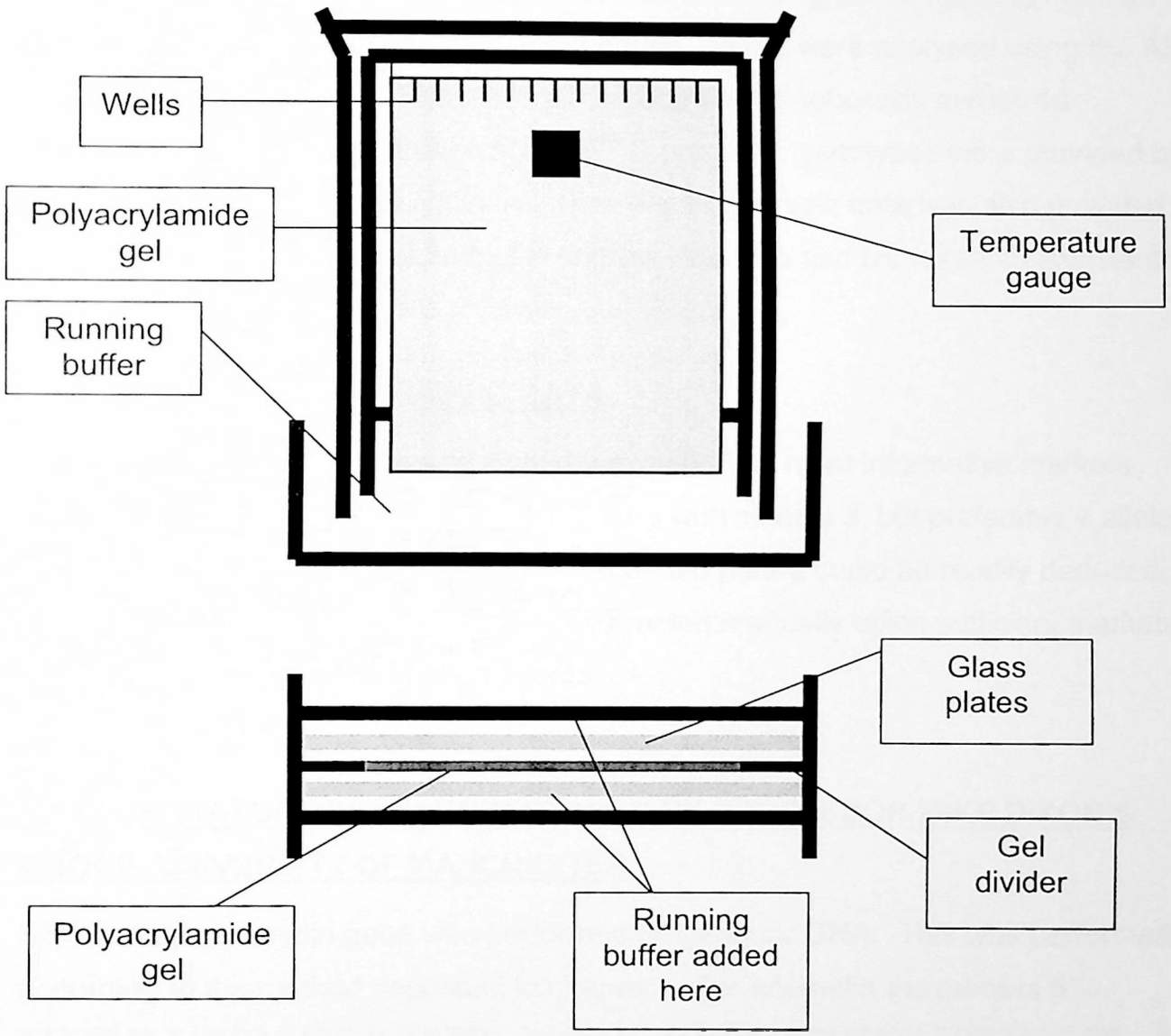

Figure 16. Schematic diagram of radiolabelled PCR gel electrophoresis apparatus.

2.11 LABORATORY WORK UNDERTAKEN BY HUMAN GENOME PROJECT RESOURCE CENTRE (HGMPRC), GENOME CAMPUS, CAMBRIDGE

Genotyping was performed on a large scale using integrated methods and technology supplied by Applied Biosystems. They performed standard PCR optimisations with amplitaq gold and hot start PCR. The manufacturer provided the fluorescent-labelled primers. This was a linkage mapping set comprising markers spanning the human genome at 10cM intervals. PCRs were analysed using the ABI PRISM genetic analyser. This performs capillary electrophoresis across 48 capillaries. Following laser detection of PCR products, genotypes were provided by the bundled data collection software. Raw electrophoresis data was also provided. This was work was undertaken by Dr Andrew Dearlove and his research assistants.

2.12 GENOTYPING OF HGMPRC DATA

The genotype data analysis was done by myself. The most informative markers were selected for the loci of interest. Markers with at least 3, but preferably 4 alleles, and those in which the genotype of the deceased parent could be readily deduced, were selected. Haploypes were then constructed manually using sufficient markers to clearly establish recombination events.

2.13 LABORATORY WORK UNDERTAKEN BY PROFESSOR MIKE DIXON'S GROUP, UNIVERSITY OF MANCHESTER

SSCP of the enamelin gene was performed on genomic DNA. This was performed according to the method described in chapter I. For enamelin the primers 5'-TTTTCAATACCACATCACTCTG – 3' and 5'- ACTGATTGGTATATGGTATTCC - 3' FOR PCR. Digestion with *Hph*I was used for screening the mutation of interest in our autosomal dominant amelogenesis imperfecta family. The method used was the same as that described in the methods section of chapter I. Sequencing of the enamelin gene was performed via di-deoxy chain termination method using dye primer chemistry.

SECTION I – CHAPTER 3

RESULTS

3.1 CLINICAL PHENOTYPING OF ERS KINDRED

3.1.1 Affected male sibling

On oral examination the brother had extremely thin, smooth enamel on the primary and erupted permanent teeth. The primary teeth appeared normal in colour but the erupted permanent incisors were a yellow colour. The teeth were widely spaced; the molar and pre-molar cusps were sharp and the incisal enamel razor edged. Pre-eruptive coronal resorption was evident in erupted permanent teeth. Dental radiographs showed minimal enamel. There was pre-eruptive coronal resorption of posterior teeth. There appeared to be intrapulpal calcification in the primary teeth and mandibular permanent incisors.

Extensive bridgework and crowns were applied to the erupted permanent teeth. Later he required further reconstruction and removal of an upper right premolar that had eroded through the mucous membrane, beneath the bridgework. Root canal treatment was required in 8 of the 13 teeth used to support the bridgework.

This sibling gave no history of urinary tract infections, nocturnal enuresis or haematuria. He was found to have proteinuria on a routine medical screen undertaken at the age of 32. This was investigated with renal ultrasonography, which demonstrated nephrocalcinosis. He was referred to The Middlesex Hospital Renal Unit aged 36 with polyuria and polydipsia. He reported having passed a renal calculus immediately prior to the assessment.

Physical examination was unremarkable other than the described dental abnormalities. Biochemical results are shown in table 3

	Affected male	Affected female	Normal
Plasma creatinine	161 µmol/l	89 µmol/l	50-125
Creatinine clearance	76mls/min	90mls/min	90-120mls/min
Plasma calcium	2.46mmol/l	2.44mmol/l	2.2-2.6
Plasma inorganic phosphate	0.92mmol/l	0.46mmol/l (max 0.71mmol/l)	0.7-1.5
Plasma alkaline phosphatase	234 IU/l	210	190
PTH	na	13.3 pmol/l	1.0-16.5
25(OH) vitamin D3	na	13 µg/l	3-30
Urinary protein	1g/24 hours	0.18g/24hrs	<0.06
Urinary calcium	0.9mmol/24hrs	0.5 mmol/24hrs	2.0-9.0
Urinary phosphate	24mmol/24hrs		15-50
Urinary amino acids	Strong presence of taurine and unidentified ninhydrin-positive species.	Not present	Not present
Random urine pH (glass electrode)	5.76	na	

Table 3. Clinical data on 2 affected siblings, ERS family X.

A water deprivation test was performed. Maximum urine concentration was 493 mmol/l, which is substantially reduced (normal >800mmol/l).

Renal ultrasonography revealed asymmetric kidneys (12.4cm left, 6.7cm right). The small right kidney had a bright parenchyma with multiple cysts, suggesting renal scarring. A Mag 3 isotope renogram with frusemide showed rapid clearance of isotope from this kidney, suggesting no obstruction was present. The right kidney was, however, only contributing 9% of overall renal function.

3.1.2 Affected female sibling

The enamel of the primary and permanent teeth was extremely thin and smooth. The incisor and canine teeth discoloured light yellow while the premolars and molars were yellow brown. The teeth were widely spaced with sharp molar and premolar cusps. There coronal reabsorption clinically. Radiographs showed extremely thin enamel with coronal reabsorption of the unerupted molar and premolar teeth, particularly marked in the maxillary first molars. There appeared to be intrapulpal

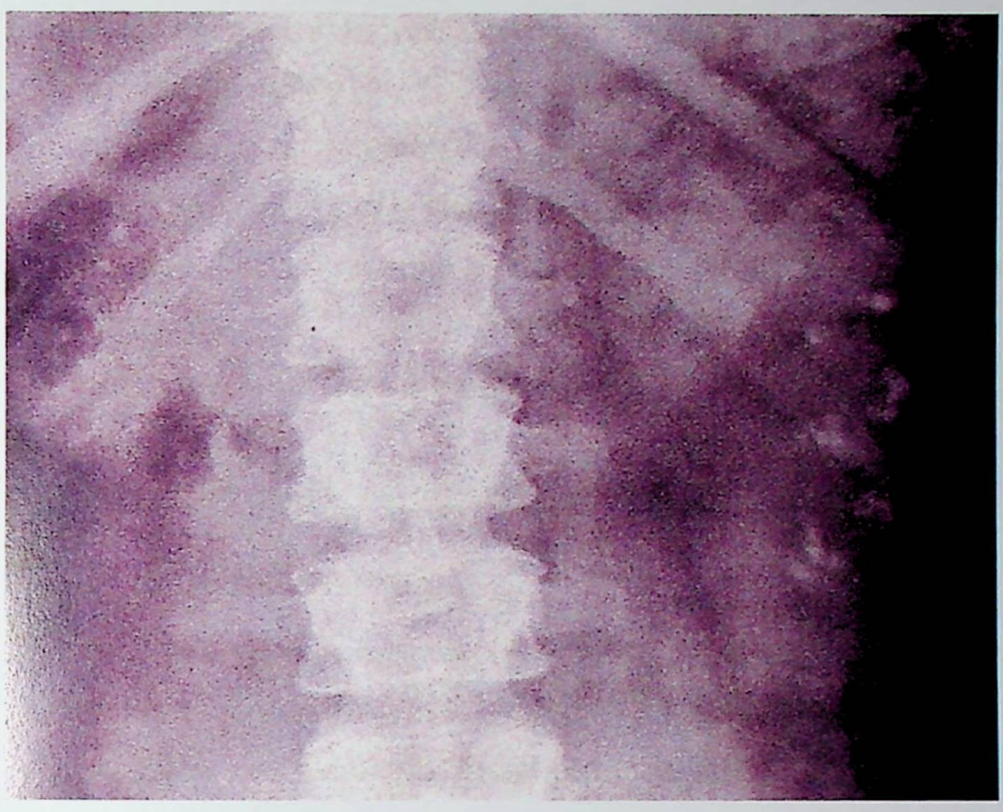

Figure 17. Medullary nephrocalcinosis in affected ERS family member.

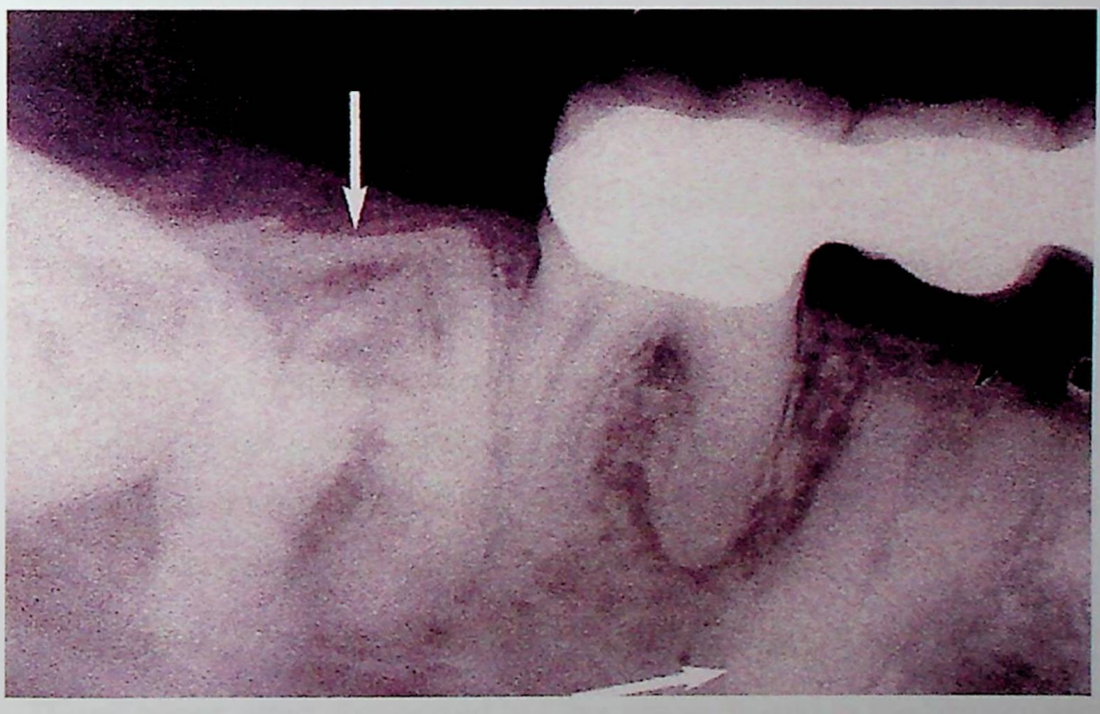

Figure 18. Hypoplastic enamel in affected ERS family member

calcification in all erupted and unerupted teeth. She had extensive fitting of crowns and bridgework to the permanent teeth.

Her diagnosis of nephrocalcinosis had been made following an episode of pyelonephritis during her first pregnancy aged 26 years. She suffered subsequent, infrequent urinary tract infections and was found to be hypertensive. Renal ultrasound showed symmetrical kidneys of normal size, with multiple medullary hyperechoic foci suggesting medullary nephrocalcinosis. Plain renal x-ray also confirmed multiple, 2-3mm flecks of calcification in both kidneys. These appearances have remained unchanged on follow up.

3.2 RECRUITMENT, AND DNA SAMPLING

3.2.1 London ERS kindred.

I was able to successfully recruit our own UK family. Whole blood samples were taken from the surviving mother and all 6 siblings, including the affected brother and sister. DNA was extracted and checked with PCR for the marker DS392 and found to be of good quality.

3.2.2 Queensland, Australia ERS kindred (MacGibbon)

Sadly at the time of initiating this project both of MacGibbon's ERS patients had died.

3.2.3 Nebraska, USA ERS kindred (Lubinsky et al)

I approached this group regarding recruitment of their ERS cases but unfortunately the patients did not wish to participate.

3.2.4 Melbourne, Australia ERS kindred (Hall et al)

The cases described by Hall et al agreed to participate. Blood samples were taken from the 2 parents, 2 affected children and 1 unaffected child by David McCreadie (a paediatric nephrologist in Melbourne). DNA was prepared in the Department of Genetics, University of Melbourne and mailed to me in London. Repeat sampling had to be performed due to the poor quality of the initial DNA samples. A second batch of samples was tested and found to be of better quality.

3.2.5 Upstate New York, USA ERS kindred (Scheinman et al)

These cases were unreported but this group, based in the Department of Nephrology, SUNY Upstate Medical University, approached us after an abstract and poster presentation of our family. They were treating two ERS patients who agreed to participate. DNA from the parents and two affected children was extracted from

whole blood samples locally, and then sent to me in London. The quality of the DNA was checked with PCR and found to be good.

3.2.6 Bordeaux, France ERS kindred (De La Tranchade et al)

This group approached Dr Kathy Harley (our dental collaborator at UCL) regarding a single, sporadic case of ERS. I contacted them, visited the patient in Bordeaux, acquired clinical data and performed mouth swab sampling for DNA. This was found to be of good quality with PCR. Her parents were not recruited into the study as, given that she was an only child from a non-consanguineous relationship, their participation was unlikely be informative genetically.

3.2.7 Brasilia, Brazil ERS kindred (Paula et al)

We made direct contact with the authors and their patient agreed to participate in our study. The parents and affected child gave whole blood samples and DNA was extracted locally at the Faculty of Health Science, Brasilia, Brasil and then sent to London.

3.2.8 Kobe, Japan ERS kindred (Jun Fu et al)

This case was reported some time after my period of research. I have attempted to recruit this case for our ongoing studies but regrettably the patient has been lost to follow up. Though they had obtained DNA for their own work they do not have ethical clearance for participation in further genetic studies.

3.2.9 Cardiff, Wales ERS kindred (Hunter et al)

This case was reported only two years ago. I have approached the group regarding our ongoing work on this syndrome and they are discussing participation with their patient.

3.3 CLINICAL PHENOTYPING OF ERS FAMILIES

Characterisation of the ERS phenotype was undertaken by a review of all the literature on this syndrome and direct communication with the clinicians involved. It is provided in the background chapter of this section.

3.4 PCR OPTIMISATION

I was able to perform satisfactory PCR of the majority of markers from the genomic DNA of ERS family X. Some markers required PCR optimisation as described in the methods section. I did not proceed to radiolabelled PCR until satisfactory standard PCR had been performed with a visible PCR product of the appropriate size seen on agarose gel electrophoresis.

Figure 19. Marker D4S1557 PCR with genomic DNA from ERS family X. This PCR was performed under standard conditions as described. The PCR is suboptimal

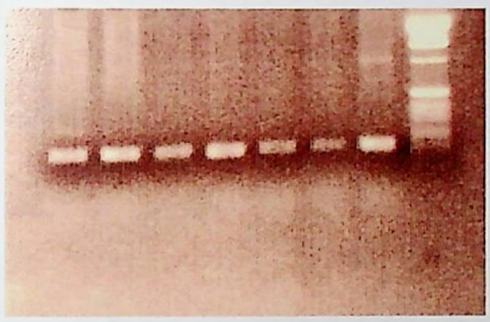

Figure 20. Marker D4S1557 PCR with genomic DNA from ERS family x. This PCR was performed following optimisation with "hot start" PCR using Amplitaq Gold.

3.5 RADIOLABELLED PCR OF GENOMIC DNA, ERS FAMILY X

Following optimisation of PCRs, P32-labelled PCR was performed and, following acrylamide gel electrophoresis, alleles for available family members were scored. Figures 21 and 22 are examples of P32-labelled PCR results with scoring.

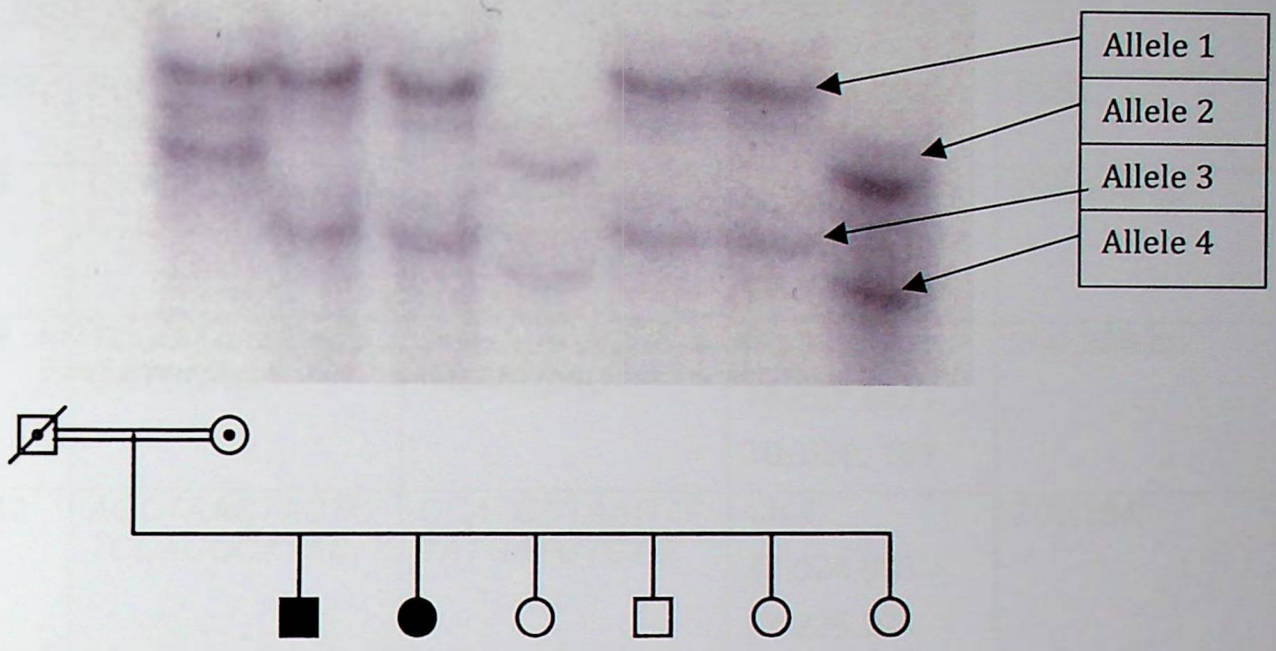

Figure 21. P32-labelled PCR of marker D4S392 with genomic DNA from ERS family X.

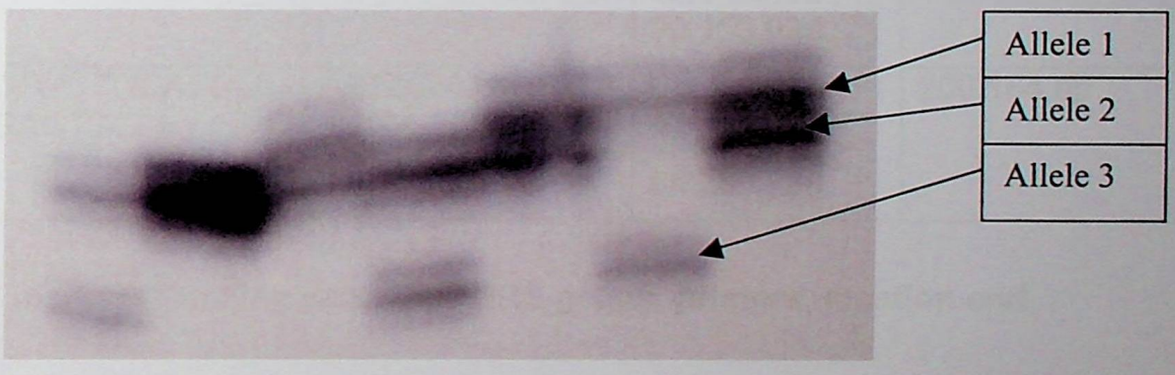

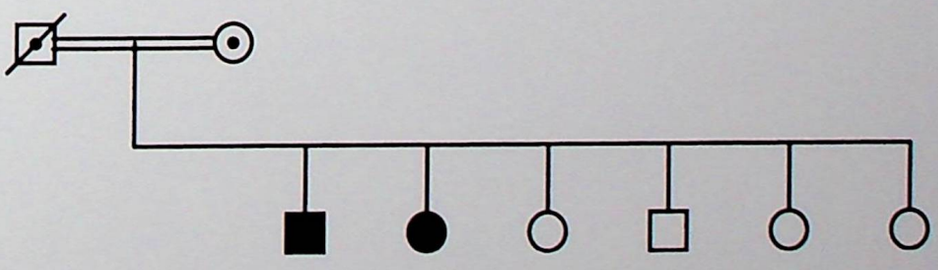

Figure 22. P32-labelled PCR of marker D12S1669 with genomic DNA from ERS family X.

3.6 GENOTYPING OF ERS – CHROMSOME 4 AND CANDIDATE GENES *AMBN, BMP 3, IBSP* AND *SPP1.*

MARKER	FORWARD PRIMER	REVERSE PRIMER	LOCATION	SIZE
D4S409	*CTTGCCGTCAGA CTCAAACT*	*CAACCTTTCAAT GTTAGGGC*	Ch4 67,906,464 - 68,106,761	200,298 bp
D4S392	*TCGGTAAACATT CATCCAGA*	*TGTCAAAATGGA CCAATCAG*	Ch 4 70,457,882 – 70, 658, 167	200,286 bp
D4S3042	*AGCTAACTACTC TCCACCCATAC*	*CCATGCTAAGTT TATGATGTCTG*	Ch 4 77,024,888 – 77,225,271	200,384
D4S395	*TACTCCAGCCTG GATGACAG*	*TGTTCCATAACA AGCACGTT*	Ch4 84,365,226 – 84,565,471	200,246 bp
D4S2460	*CCAAAATCATGT GAGCCA*	*GAGCAGCAGCC AACTGTAT*	Ch 4 89,952,672 – 90,153,035	200,364 bp
D4S1557	*CTGCTGCATGG GAGTT*	*ATTGGAAAGGCT GTGAATA*	Ch 4 95,083,073 – 95,283,236	200,164 bp

Table 4. Ch4 markers flanking candidate ERS genes, primers, location and size.

Gene	Chromosome 4 location	Size
Ameloblastin enamel matrix protein (AMBN)	71,492,590-71,507,593	15,004 bp
Bone morphogenetic protein 3 (BMP 3)	82,171,143-82,193,749	22,607 bp
Integrin binding sialoprotein (IBSP)	88,939,726 – 88,952,89	12,373 bp
Secreted phosphoprotein 1 (SPP1)	89,117,058-89,123,587	6,530 bp

Table 5. ERS candidate genes, Ch 4 locations and size.

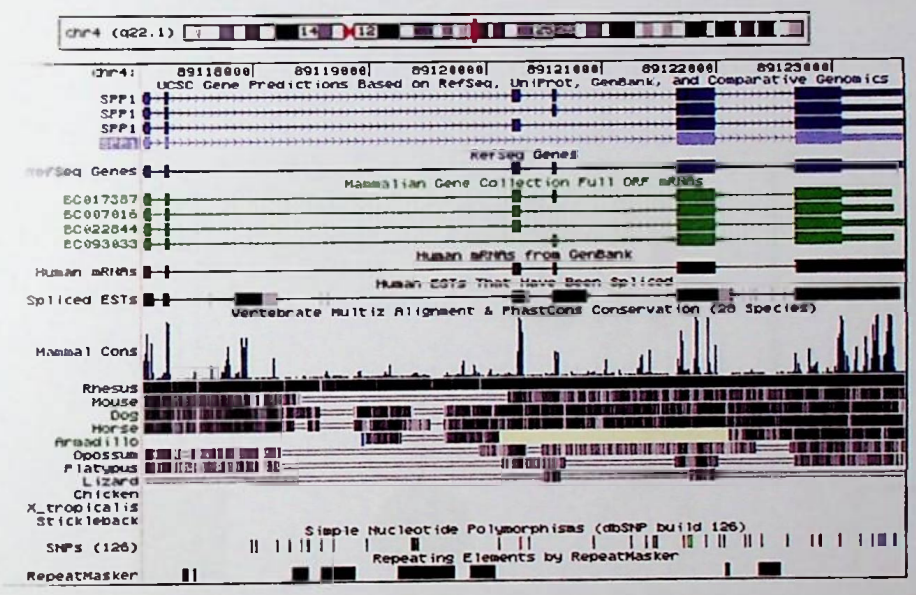

Figure 23. Sample of UCSC genome browser map showing the locus of secreted phosphoprotein 1 (SPP1).

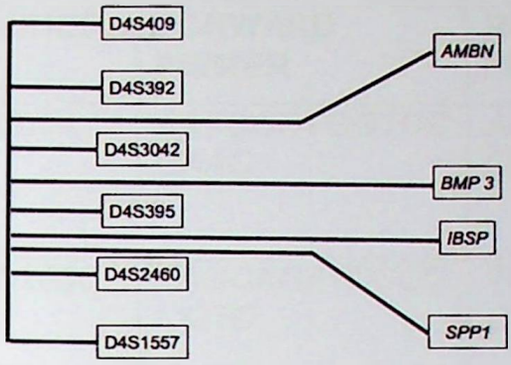

Figure 24. Physical map of Ch 4 demonstrating position of candidate ERS genes relative to the genetic markers used for this linkage study.

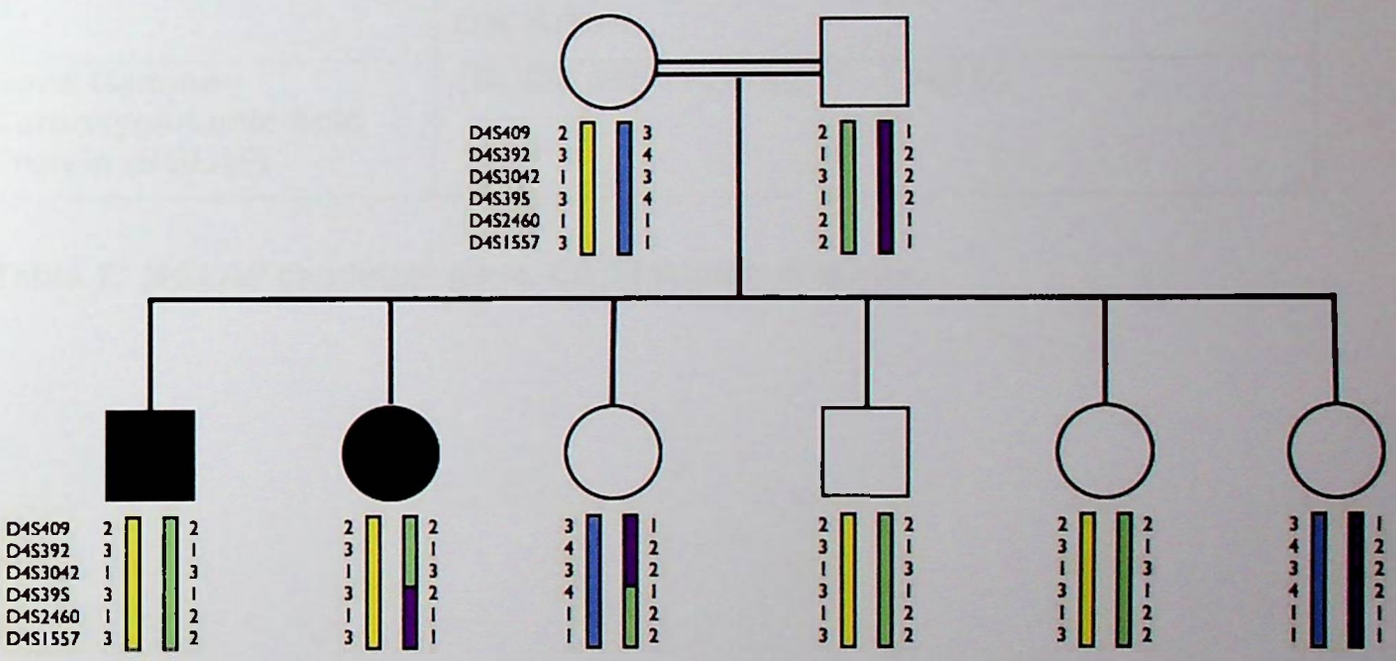

Figure 25. Haplotype of ERS family X with chromosome 4 markers flanking (and spanning) the loci of the *AMBN*, *BMP 3*, *IBSP* and *SPP1* genes. The Ch4 haplotypes are shown. There is no evidence of co-segregation of these loci with the disease. The affected siblings are not homozygous at these loci, and two unaffected siblings share their genotypes. Note that the genes of interest in this region are flanked by 2 markers on *each* side of the outer genes (*AMBN* and *SPP1*). On the basis of this data, there is no genetic linkage of ERS to the *AMBN*, *BMP 3*, *IBSP* and *SPP1* loci in this kindred. This complex of genes at 4q, which appears to regulate calcification processes in a number of tissues, is not implicated in ERS.

3.7 GENOTYPING OF ERS – CHROMOSOME 1 AND CANDIDATE GENE *BGLAP*

MARKER	FORWARD PRIMER	REVERSE PRIMER	LOCATION	SIZE
D1S514	*AATGCGTGGTCC CAAC*	*AATGCGTGGTCC CAAC*	Ch 1 119,970 – 120,170,620	200,344 bp
D1S2635	*TAGCAGATCCCC CGTC*	*TGAATCCTACCC CTAAGTAGAAT*	Ch 1 157,336,858 – 157,537,100	200,243 bp

Table 6. Ch1 markers flanking candidate ERS gene *BGLAP*, primers, location and size.

GENE	CHROMOSOME 1 LOCATION	SIZE
Bone Gamma-Carboxyglutamic Acid Protein (*BGLAP*)	154,478,636-154,479,577	942 bp

Table 7. *BGLAP* candidate gene, Ch 1 location and size.

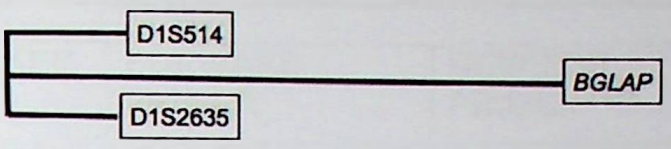

Figure 26. Physical map of Ch 1 demonstrating position of candidate ERS gene *BGLAP* relative to the genetic markers used for this linkage study.

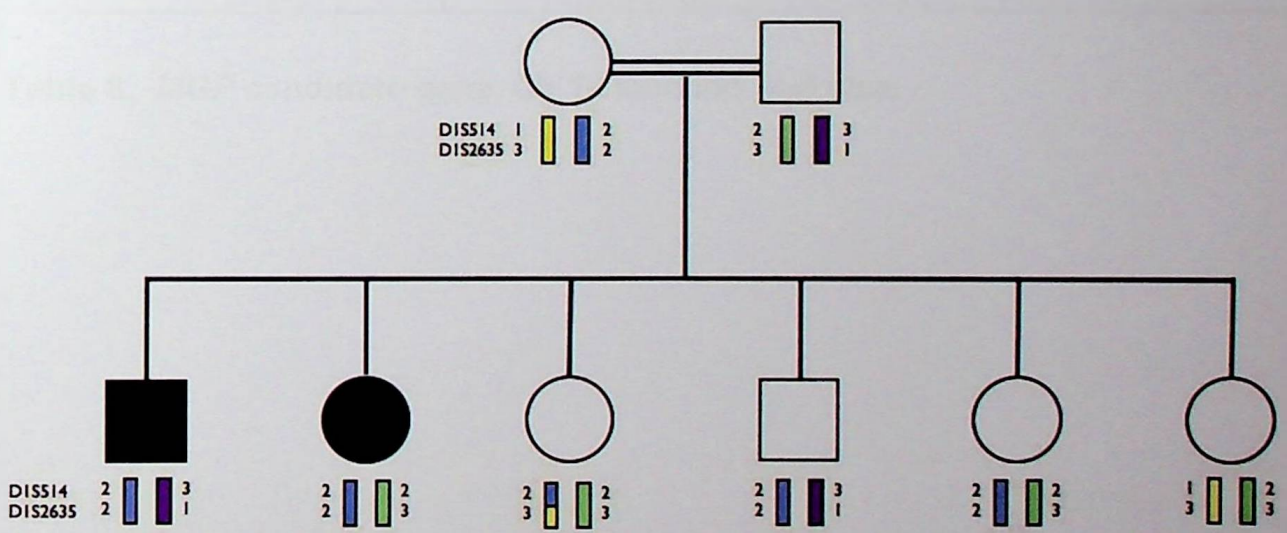

Figure 27. Haplotype of ERS family X with chromosome 1 markers flanking the *BGLAP* gene. The haplotype above shows that there is no co-segregation of this locus with the disease. The affected siblings are not homozygous at this locus, they have different genotypes and their genotypes are shared with unaffected family members. This effectively excludes a mutation in *BGLAP* as the cause of ERS in this family

3.8 GENOTYPING OF ERS – CHROMOSOME 12 AND CANDIDATE GENE *MGP*

MARKER	FORWARD PRIMER	REVERSE PRIMER	LOCATION	SIZE
D12S320	*GGCAGCCAAATA ACACATCT*	*AAAAAGGTGCCT CCCATTTA*	Ch12 13,413,310 – 13,613,571	200,262 bp
D12S1669	*GTTGCGCTTCAG CCTG*	*GCTTCCAAATCA GCGGTAGT*	Ch 1 19,29,661 – 19,529,982	200,322 bp

Table 7. Ch12 markers flanking candidate *MGP* gene, primers, location and size.

GENE	CHROMOSOME 12 LOCATION	SIZE
Matrix Gamma-Carboxyglutamic Acid (MGP)	14,926,094-14,930,095	4,002 bp

Table 8. *MGP* candidate gene, Ch 12 location and size.

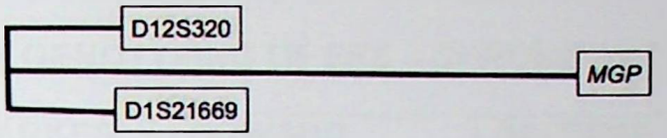

Figure 28. Physical map of Ch 12 demonstrating position of candidate ERS gene *MGP* relative to the genetic markers used for this linkage study.

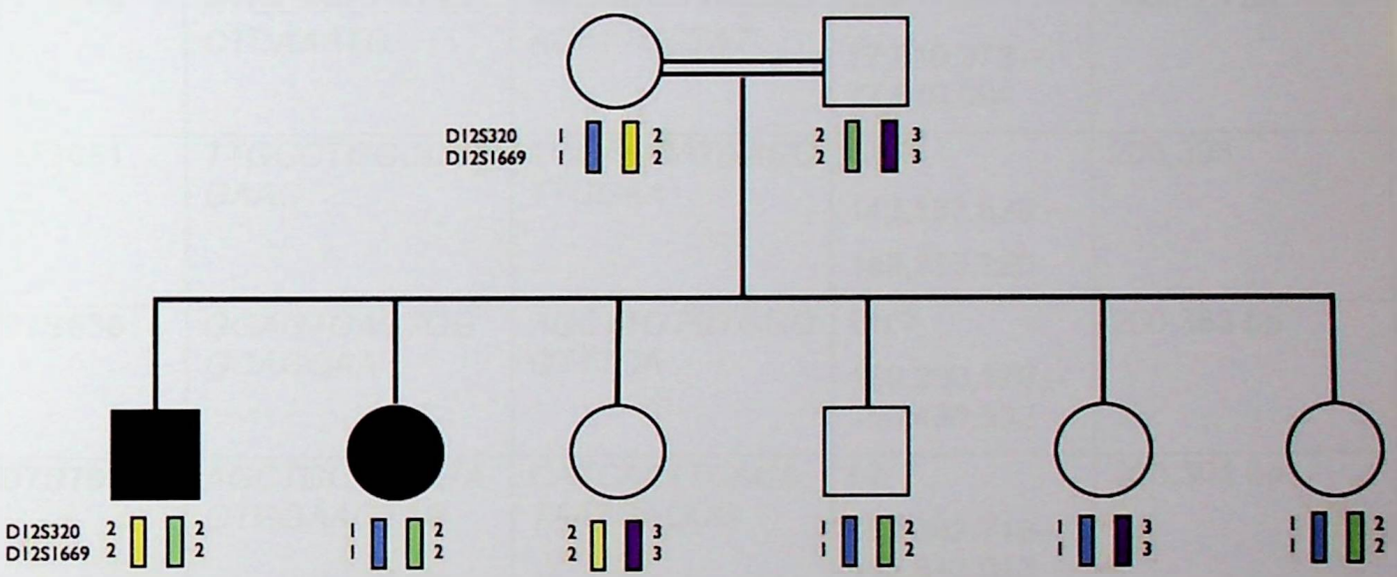

Figure 29. Haplotype of ERS family X with chromosome 12 markers flanking the *MGP* gene. The haplotype above shows that there is no co-segregation of this locus with the disease. The affected siblings are not homozygous at this locus, they have different genotypes and 1 of their genotypes is shared with unaffected family members. This effectively excludes a mutation in *MGP* as the cause of ERS in this family.

3.9 GENOTYPING OF ERS – CHROMSOME 7 AND CANDIDATE GENE *ECAC1*

MARKER	FORWARD PRIMER	REVERSE PRIMER	LOCATION	SIZE
D7S510	*CAGTGTGGAGG TTCCCAA*	*ACCCAGCCGCA AGATT*	Ch 7 39,056,237-39,256,573	200,377 bp
D7S502	*GGAAGGTATGTT GCGG*	*TAAGCCACCAAG AACACC*	Ch 7 66,594,972 – 66,795,314	200,343 bp
D7S669	*ATGCAACCTACC CTCAAATG*	*TACGGNTTACCC ACATTGCTAT*	Ch7 77,610,372 – 77,810,694	200,323 bp
D7S661	*TTGGCTGGCCCA GAAC*	*TGGAGCATGACC TTGGAA*	Ch 7 143,132,828 – 143,333,220	200,393
D7S636	*GGAGTGACTGG GCAGGAA*	*AGCTTGTGTGGG GTTTCA*	Ch 7 150,230,170 – 150,430,532	200,363 bp
D7S798	*AGCTGCAAAATA GTGGAAGTAG*	*CATCAATTCACA TAATGACCG*	Ch 7 152,342,713– 152,543,013	200,301 bp

Table 9. Ch7 markers flanking candidate genes ECAC1, primers, location and size.

Gene	Chromosome 7 location	Size
Epithelial Calcium Channel 1 (ECAC1, Transient Receptor Potential Cation Channel Subfamily V Member 5, TRPV5)	142,315,770 – 142,340,942	25,173 bp

Table 10. *ECAC1* candidate gene, Ch 7 location and size.

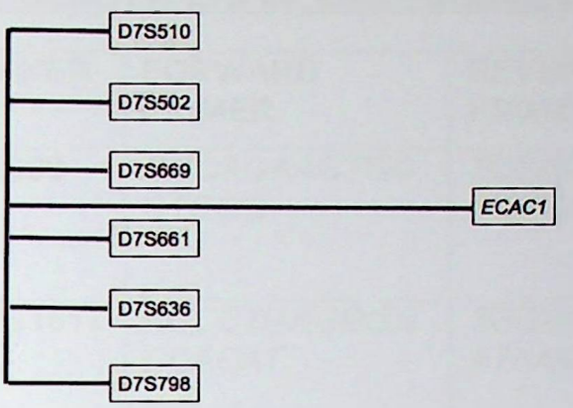

Figure 30. Physical map of Ch 7 demonstrating position of candidate ERS genes relative to the genetic markers used for this linkage study.

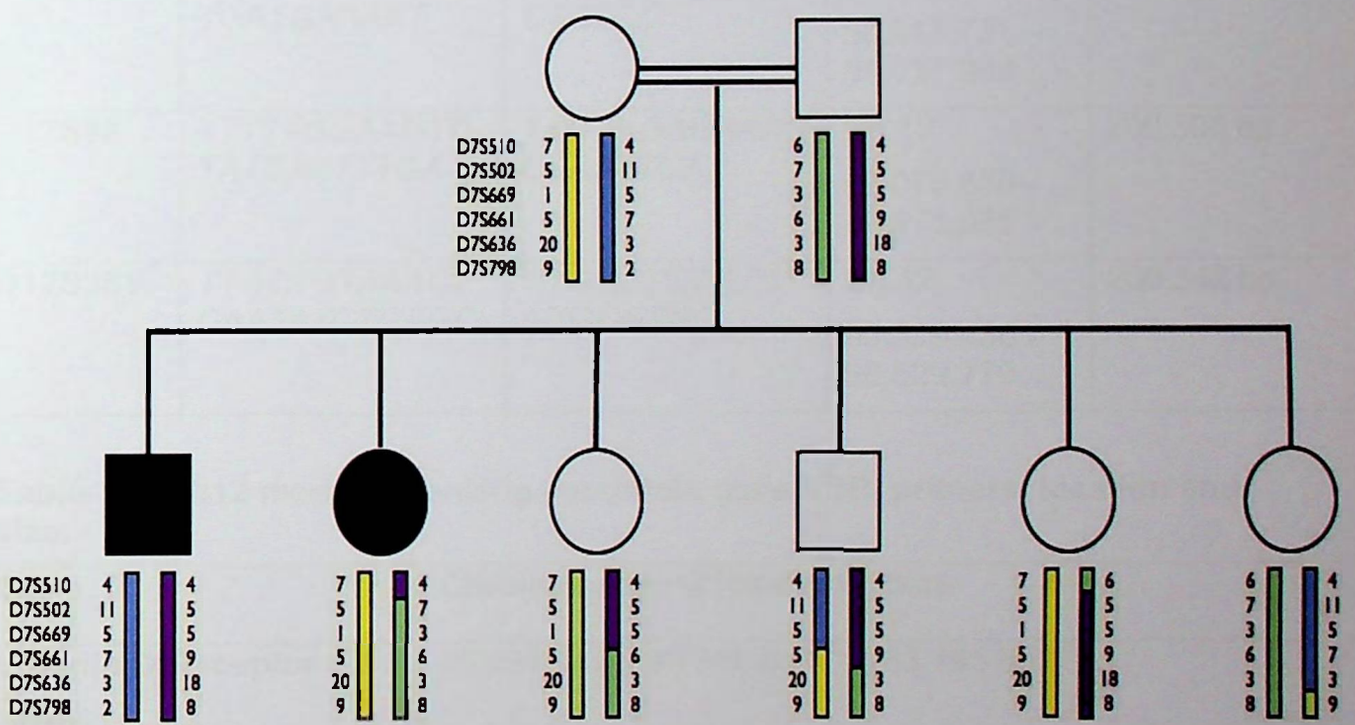

Figure 31. Haplotype of ERS family X with chromosome 7 markers flanking the *ECAC1* gene. The haplotype above shows that there is no co-segregation of this locus with the disease. While the affected brother is homozygous for the allele 5 at D7S669, the affected sister is not homozygous and has inherited different alleles at this locus. This effectively excludes a mutation in *ECAC1* as the cause of ERS in this family.

3.10 GENOTYPING OF ERS – CHROMSOME 12 AND CANDIDATE GENE *VDR*

MARKER	FORWARD PRIMER	REVERSE PRIMER	LOCATION	SIZE
D12S99	*GGCAGAAGTGC CTGGG*	*TCGAGGGTGCA GGTGG*	Ch 12 5,334,815 – 5,535,185	200,371 bp
D12S1617	*AGCCTGAGGGG CCACAT*	*TGGGCAACTTGG ATAAGAAACA*	Ch 12 24,891,279 – 25,091,586	200,308 bp
D12S345	*CAGCCTGGGTAA CAAA*	*AGCAATGTGTGC ATTC*	Ch 12 32,116,080 – 32,316,439	200,360
D12S368	*GCAACACCTTTG TGATGAAAAT*	*AGTCTGCACAGC CTGTCC*	Ch 12 50,817,731 – 51,017,990	200,260 bp
D12S83	*TTTTTGGAAGTC TATCAATTTGA*	*TAGCAGAGAAAG CCAATTCA*	Ch 12 59,075,650– 59,275,955	200,306 bp
D12S351	*TTGCTCTAAACT CAATATCTCAGC*	*GTGCATCTGTAT GTGCGTG*	Ch 12 90,329,438 – 90,529,779	200,342 bp

Table 11. Ch12 markers flanking candidate gene VDR, primers, location and size.

Gene	Chromosome 12 location	Size
Vitamin D Receptor (*VDR*)	46,521,587 – 46,585,081	63,495 bp

Table 12. *VDR* candidate gene, Ch 12 location and size.

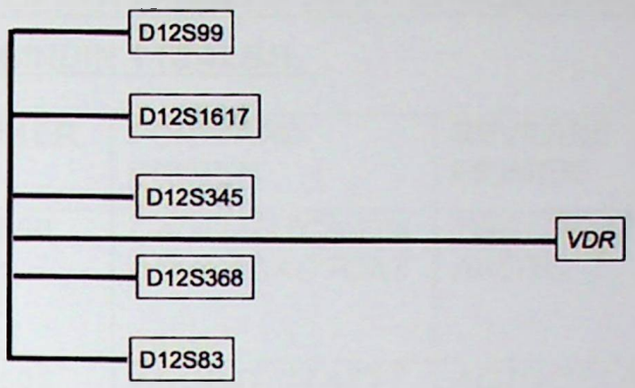

Figure 32. Physical map of Ch 12 demonstrating position of candidate ERS gene *VDR* relative to the genetic markers used for this linkage study.

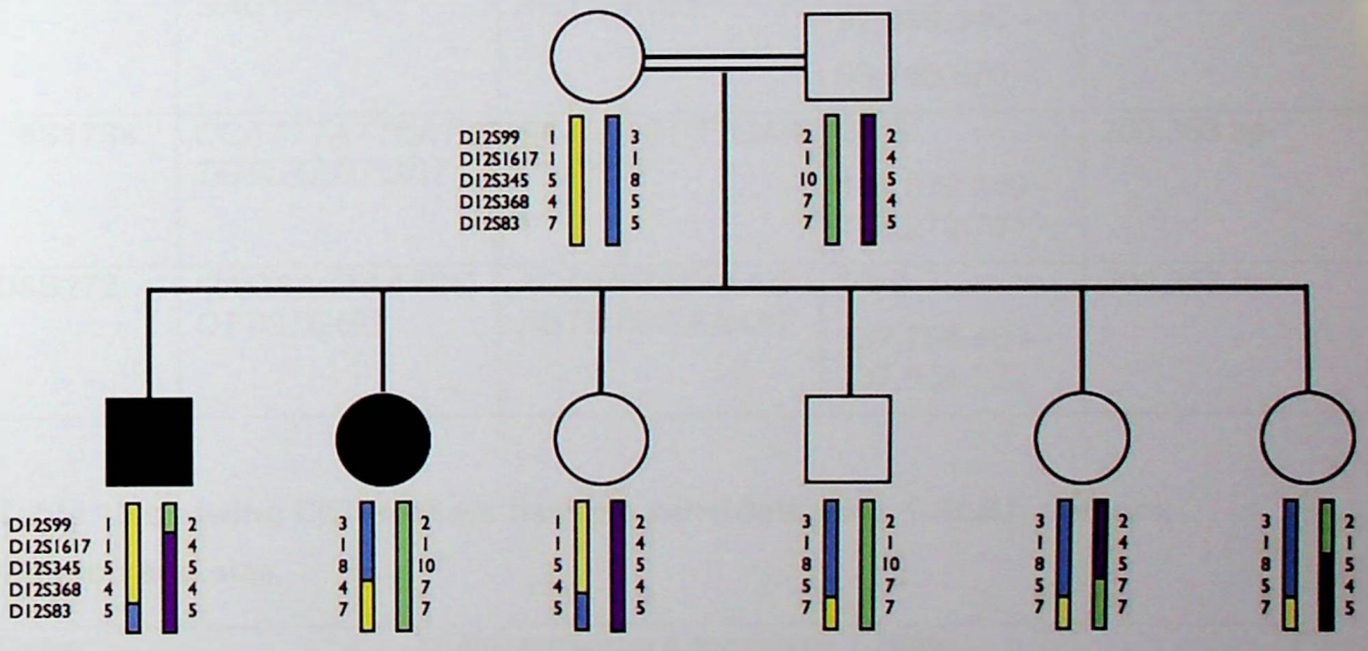

Figure 33. Haplotype of ERS family X with chromosome 12 markers flanking the *VDR* gene. The haplotype above shows that there is no co-segregation of this locus with the disease. While the affected brother is homozygous for the allele 5 at D12S345, the affected sister is not homozygous and has inherited different alleles at this locus. The converse applies for marker D12S1617 where the affected sister is homozygous but has a different genotype to the affected brother. Both the affected sibs genotypes are shared with other unaffected family members. This effectively excludes a mutation in *ECAC1* as the cause of ERS in this family.

3.11 GENOTYPING OF ERS – CHROMSOME 8 AND CANDIDATE GENE CALBINDIN 1 (*CALB1*).

MARKER	FORWARD PRIMER	REVERSE PRIMER	LOCATION	SIZE
D8S550	*CAGGAGTCAATA ACCCAAAGTCAT*	*TGGCACATCCCG AAGTC*	Ch 8 10,818,926-11,019,323	200,398 bp
D8S505	*AGCCTGCTATTT GTAGATAATGTT T*	*AGTGCTAAGTCC CAGACCA*	Ch 8 34,470,316 – 34,670,723	200,408 bp
D8S260	*AGGCTTGCCAGA TAAGGTTG*	*GCTGAAGGCTGT TCTATGGA*	Ch8 61,884,335 – 62,084,648	200,3l4 bp
D8S270	*ATTCAGAACGAT GAGGAAGC*	*AGAATGGCACAT AGTCNCGT*	Ch 8 92,989,546 – 93,189,870	200,325 bp
D8S1784	*CCATTTATTCATT TGTGTAGTGCT*	*GGCTGGCTTCAA CTTTCA*	Ch 8 106,072,349 – 106,272,701	200,353 bp
D8S272	*GAGAACTAATCC CTTCTGGC*	*AGCTTCATAAAG AGTCTGGAAAAT*	Ch 8 137,704,460– 137,904,722	200,263 bp

Table 13 showing Ch7 markers flanking candidate gene *CALB1*, primers, location and size.

Gene	Chromosome 8 location	Size
Calbindin 1 (*CALB1*)	91,159,777-91,176,863	17,087 bp

Table 14. *CALB1* candidate gene, Ch 8 location and size.

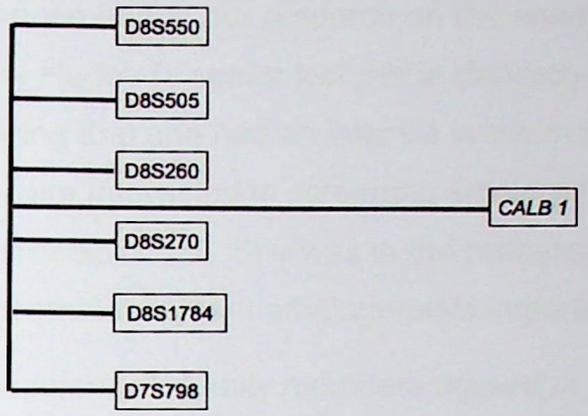

Figure 34. Physical map of Ch 8 demonstrating position of candidate ERS gene CALB1 relative to the genetic markers used for this linkage study.

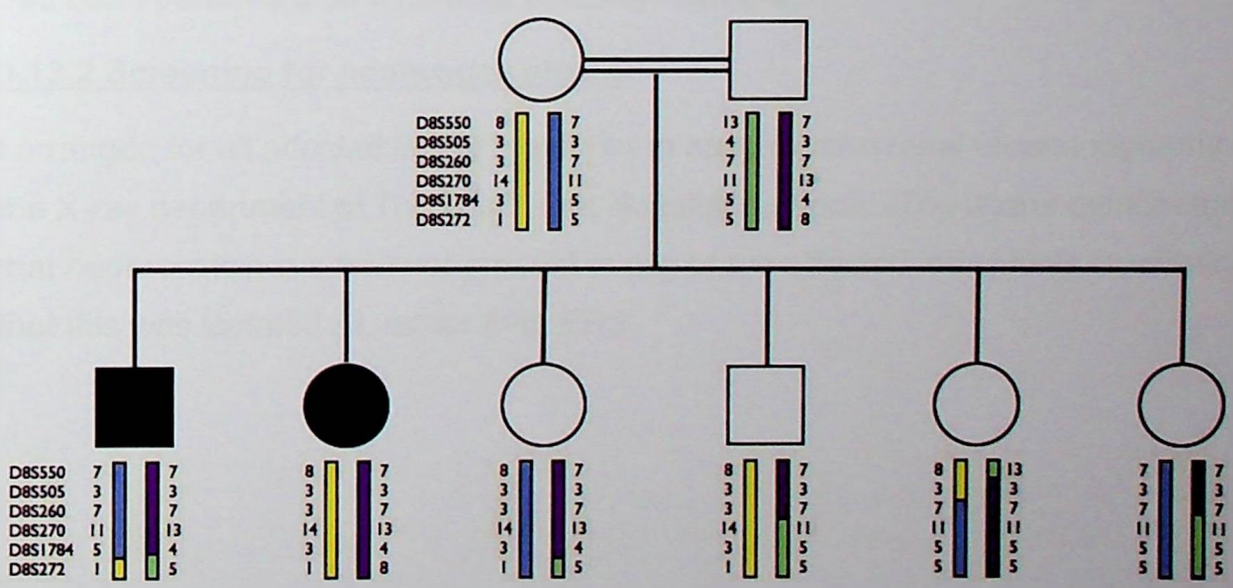

Figure 35. Haplotype of ERS family X with chromosome 8 markers flanking the *CALB1* gene. The haplotype above shows that there is no co-segregation of this locus with the disease. The affected siblings are not homozygous at this locus, they have different genotypes and their genotypes are shared with unaffected family members. This effectively excludes a mutation in *CALB1* as the cause of ERS in this family.

3.12 AUTOSOMAL DOMINANT AMELOGENESIS IMPERFECTA (ADAI) – RECRUITMENT AND SAMPLING

When we began our research on the enamel renal syndrome we approached Dr Kathy Harley (a senior lecturer in dentistry at The Eastman Dental Hospital, London) knowing that she had an interest in the management of inherited enamel defects. We were interested in screening amelogenesis imperfecta patients for undiagnosed nephrocalcinosis. She was in the process of treating a very large family with autosomal dominant amelogenesis imperfecta (family Y).

The majority of family members agreed to participate. I obtained DNA from whole blood samples in adults and from mouth swabs in children. DNA extraction was performed according to the previously described methods. All DNA was found to be of sufficient quality for PCR.

3.13 ADAI FAMILY – PHENOTYPING

3.13.1 Dental phenotype

This was a thin, smooth hypoplastic phenotype. Extensive reconstructive surgery had been performed on a number of family members.

3.13.2 Screening for nephrocalcinosis

I arranged for all affected family members to have routine renal ultrasonography at the X-ray department of The Middlesex Hospital, London. The scans demonstrated that nephrocalcinosis was not present in any of the affected individuals confirming that this was isolated AI, rather than ERS.

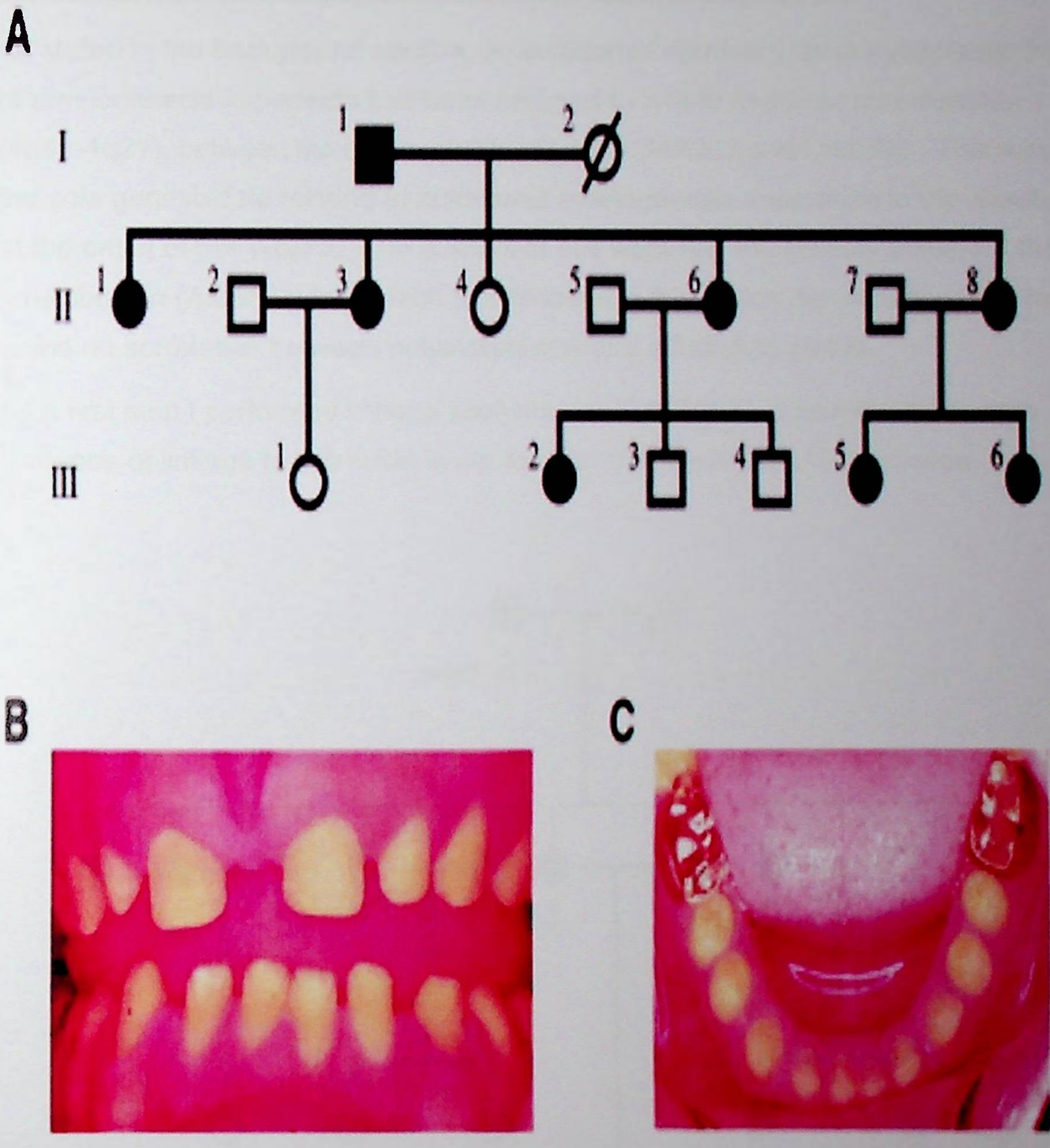

Figure 36. A is the pedigree of AI family Y. B and C are dental photographs of individual II:8. The teeth are small, discoloured and have undergone extensive wear. This is a thin, smooth, hypoplastic phenotype of autosomal dominant amelogenesis imperfecta.

3.14 RADIOLABELLED PCR OF GENOMIC DNA, ADAI FAMILY

As stated in the background section, an autosomal dominant, local hypoplastic form of amelogenesis imperfecta had been mapped to a 4Mb region of chromosome 4 (4q11-4q21), between the microsatellite markers D4S392 and D4S395. This was the sole genetic data relating to autosomal amelogenesis imperfecta in the literature at the onset of this project. The authors of this work had extensively screened the ameloblastin (*AMBN*) gene, which has its locus in this region, for mutations but had found no correlation between polymorphisms and affectation status.

As a first step I performed linkage analysis with D4S395 to establish if there was evidence of linkage to this locus in our family. The results are shown below.

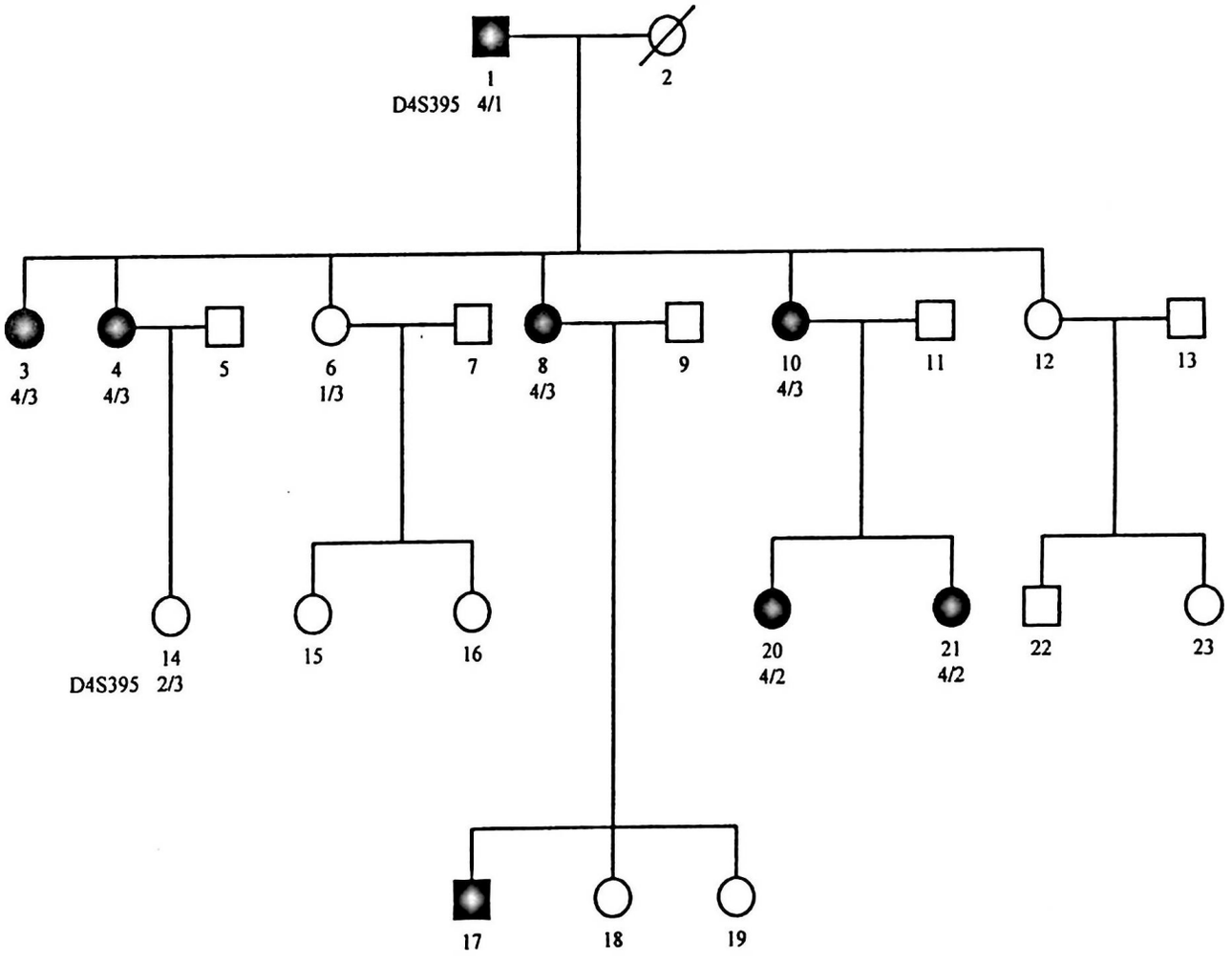

Figure 37. Haplotype of ADAI (autosomal dominant, hypoplastic amelogenesis imperfecta) family for the microsatellite marker D4S395. There is evidence of co-segregation of the allele 4 and the disease, supporting the hypothesis that this is the disease locus in this family.

There was strong evidence of linkage with this marker and the disease

3.15 MUTATION SCREENING 4q CANDIDATE GENES, ADAI FAMILY

At this point the best candidate gene in the region of 4q was still *AMBN*. At this stage I decided that it would be worth collaborating with a UK group who were already resourced to screen for dental genes at this locus. Professor Mike Dixon (Department of Dental Medicine and Surgery at the University of Manchester) was at that time involved in screening for mutations in *AMBN* in amelogenesis imperfecta cases. I visited his laboratory in Manchester, we decided to collaborate on this project and I provided him with my linkage data and the DNA from family Y, with their consent.

Helen M Rajpar performed the bulk of the Manchester laboratory work. Initially she performed mutation screening of *AMBN* and did not demonstrate any mutations that segregated with the disease.

In 2000 the gene for enamelin, *ENAM*, was mapped to the 4q21 locus, within 15kb of *AMBN*. I made further contact with Mike Dixon and discussed screening *ENAM* for mutations in enamelin in family Y. They performed *in silico* screening of the genomic sequence of human chromosome 4 with human cDNA sequence using the BLAST algorithm and identified 9 exons in the *ENAM* gene. SSCP was then performed on each exon and this demonstrated an abnormal conformer only in unaffected individuals.

In porcine enamel enamelin is synthesized and secreted by ameloblasts as a 186-kDa precursor, the unprocessed form concentrating along the secretory face of the ameloblast Tomes process. Proteolytic processing towards the C-terminus produces 142 kDa enamelin via a 155 kDa intermediate. Subsequent cleavages generate an 89-kDa polypeptide encompassing the first 627 amino acids of the secreted protein and a 34-kDa-polypeptide beginning at residue 632. Processing of 89 kDa enamelin results in polypeptides of 32 kDa (amino acids 136–238) and 25 kDa, commencing at residue 477. Intact enamelin and cleavage products containing the C-terminus are limited to the most superficial layer of the developing enamel matrix, while other cleavage products accumulate in the deeper layers of this tissue in the maturing rod and inter-rod enamel.

Direct sequencing revealed a heterozygous mutation in the splice donor site of intron 7, nt841+1 (G>A). As this mutation deletes an *HphI* site, *HphI* digestion was used to confirm the presence or absence of the mutation in family members. The mutation co-segregated with the disease entirely. HpHI digestion was used to screen 200

individuals of a similar ethnic origin for nt841+1 (G>A), but this mutation was not detected in any members of this control group.

Ameloblasts are transient during development and enamelin is only secreted by ameloblasts. It was therefore not possible to prepare cDNA from affected individuals to confirm the effect of the mutation on the enamelin transcript. It is likely however that this mutation has led to aberrant splicing.

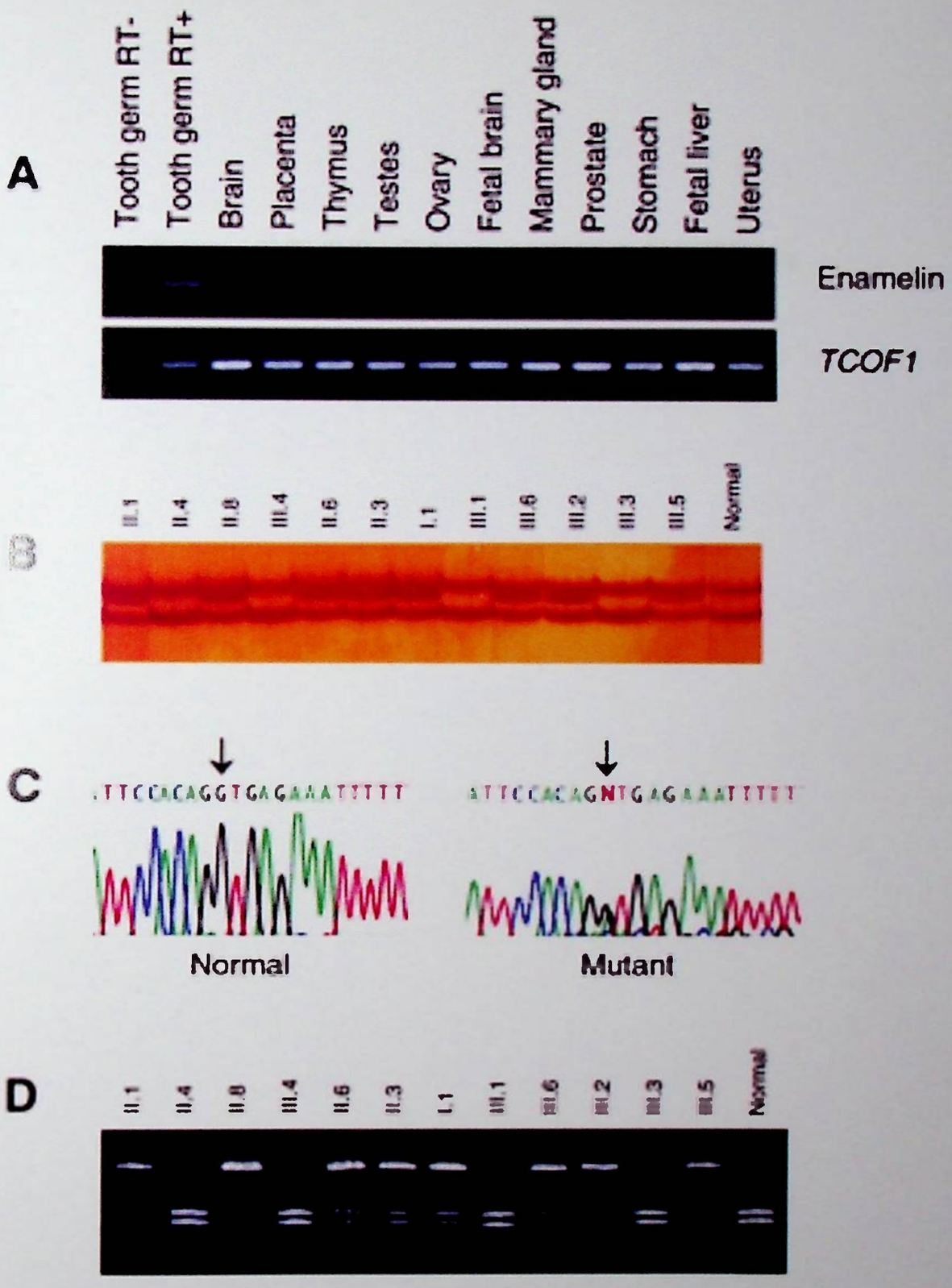

Figure 38. (A) RT-PCR of the enamelin gene demonstrates that it appears to be expressed exclusively in enamel. (B) SSCP analysis of genomic DNA from family Y reveals the presence of the abnormal conformer in individuals I.1, II.1, II.3, II.6, II.8, III.2, III.5 and III.6. This conformer is not present in unaffected family members. (C) Sequencing of DNA from individual II.1 reveals the presence of mutation nt841+1 (G>A) (arrowed) not present in control. (D) The mutation removes an *HphI* digestion site. Digestion of DNA from affected individuals produces bands of 214, 116 and 98 bp. The 214 band is not present in unaffected individuals. The mutation is therefore present in all affected and no unaffected family members.

SECTION I - CHAPTER 4

DISCUSSION

4.1 ENAMEL RENAL SYNDROME – THE CLINICAL PHENOTYPE

The nephrocalcinosis is medullary. It is evident radiologically and histologically and may be progressive. Nephrocalcinosis in ERS has been shown, from these reports, to be associated with tubular concentrating defects, recurrent pyelonephritis, loin pain and secondary renal tubular acidosis.

There is no evidence of generalised proximal tubular dysfunction, or Fanconi syndrome; sodium, potassium and phosphate wasting are not features, nor is generalised aminoaciduria. As regards renal function this is, on the whole, preserved and as such it follows a clinical course similar to other non-Fanconi causes of nephrocalcinosis. The exception appears to be Macgibbon's report in which the affected male sib developed progressive renal failure. It appears that this was as a result of accelerated phase hypertension that caused multiple organ dysfunction and an early death. Hypertension is associated with nephrocalcinosis, though malignant phase hypertension is rare, and this case must be regarded as unusual.

As regards metabolic profiling the only consistent abnormality has been hypocalciuria and this was a striking feature in our own affected sib pair. Lubinski demonstrated low levels of urinary osteocalcin (BGLAP) in the urine and this was not tested in other families (n.b. a mutation in the BGLAP gene was excluded in my linkage work). All other metabolic screening has been unremarkable. 1 patient was shown to have ectopic calcification in the pelvis, but there does not appear to be a generalised disorder of tissue calcification.

4.2 ENAMEL RENAL SYNDROME – RESULTS OF CANDIDATE GENE LINKAGE ANALYSIS

I have performed a positional candidate approach to investigate a number of candidate genes for ERS. While this approach is inevitably more speculative, particularly when the pathophysiological basis of a disease is not well understood, the participating family – consanguineous with 6 participating sibs and a surviving parent – clearly would be a powerful pedigree for *excluding* candidates. As such we felt this approach was worthwhile.

Initially I investigated the region of chromosome 4q, which has since become known as the *secretory calcium-binding phosphoprotein gene cluster.* Support for these

genes, on pathological terms, was described earlier. Further support for this region was provided by linkage of families with a similar inherited dental phenotype (without known nephrocalcinosis) to this region. Ameloblastin Enamel Matrix Protein (*AMBN*), Bone Morphogenetic Protein 3 (*BMP 3*), Integrin Binding Sialoprotein (*IBSP*), Secreted Phosphoprotein 1 (*SPP1*) were examined through genetic linkage analysis with microsatellite markers in Family X. There was no evidence of linkage of disease and these loci. I subsequently examined Bone Gamma-carboxyglutamic Acid Protein (*BGLAP*, 1q12-q14), Matrix Gamma-Carboxyglutamic acid (*MGP*, 12p13.1-p12.3) and these genes did not show evidence of linkage either.

These genotypes were generated by radiolabelled PCR and polyacrylamide gel separation and typed individually by myself and checked by Mari-Wyn Burley. Where genotypes had not been resolved clearly PCRs were further optimised, the duration of gel migration adjusted and the duration of radiographic exposure changed as appropriate. Additional markers for further genotyping were added as necessary to clarify the haplotype. Though this process was more laborious than some of the more automated genotyping technologies that have been developed (and more time consuming) I was satisfied with the accuracy of the results.

Having excluded this initial round of candidates I was able to broaden our study by enlisting the help of the HGMP-RC in Cambridge who, under the supervision of Dr Andrew Dearlove provided further genotyping data on a further tranche of candidates. I specifically examined genotypes at the loci of the Vitamin D Receptor (*VDR*, 12q12-q14), the Epithelial Calcium Channel 1(transient receptor potential cation channel subfamily V, member 5 *TRPV5, ECaC1*, 7q35) and Calbindin 1 (*CALB1*, 8q).

HGMP-RC used well-validated, semi-automated genotyping technology using fluorescent-labelled primers and laser genotype reading (as described in the methods section). We did get informative genotypes for the loci of these genes. I used the raw data to manually construct the haplotypes shown and found the data to be genetically consistent. I was able with this linkage data to exclude mutations of these genes as causative of this disease.

We were considering using genome-wide linkage analysis at this stage but were unable to get satisfactory data in some regions with the panel of markers used at HGMP-RC. It is also unlikely that this would be sufficiently powered as a study, and

the latter point has motivated my subsequent attempts to acquire DNA from further reported families.

It is disappointing to not have found evidence of linkage to this disease and a candidate gene. I have however been able to successfully exclude the candidate genes selected at the conception of this study as well as several others. As such the project was successful in its intended aims, even if the results were not those we desired. This project demonstrated the power of linkage analysis, deployed with a suitably sized family, to be able to exclude putative candidate genes. Inevitably, however, a candidate gene approach is speculative, and this is particularly true of a disorder of this complexity in which the underlying physiological mechanism is not well established.

4.3 COULD ENAMEL RENAL SYNDROME HAVE AN ENVIRONMENTAL AETIOLOGY?

One must always entertain the possibility that one may not be looking at a genetic disorder, but an environmental exposure that (in, for example Family X) has been shared by some siblings, but not others.

An alternative hypothesis that I considered was that ERS is caused by Hypervitaminosis D. It is well established that excessive vitamin D supplementation can result in hypercalciuria, hypercalcaemia and nephrocalcinosis. This may be due to a single episode of massive intoxication. In a case of a family reported (Down et al) in 1979 a family ingested a vitamin D-rich nut oil and all became ill with symptomatic hypercalcaemia. Eleven years later one was proven to have biopsy confirmed nephrocalcinosis. It is also the case that in less severe, but more chronic toxicity, there may be nephrocalcinosis without symptomatic hypercalcaemia. One of the commonest causes of this is vitamin D supplementation for the treatment of X-linked hypophosphataemic rickets (see Background, Chapter 1).

Though the nephrocalcinosis seen in vitamin D toxicity may be related to hypercalciuria, it is also possible that vitamin D affects renal, or other organ calcification more directly. It is also worth noting that in one of the reported ERS cases there was unusual punctate calcification of the internal iliac vessels (Hall et al).

While it is well recognised that vitamin D deficiency may affect dentition adversely, so may toxicity. Giunta et al described, in 1998, a case of nephrocalcinosis and amelogenesis imperfecta (of the permanent dentition) in a girl who had consumed milk incorrectly fortified with vitamin D (prior to eruption of permanent teeth) (160). Interestingly enamel hypoplasia and *focal pulp calcification* was noted. The latter is a rare finding that I have only been able to find reported in ERS or this case. Clearly it is possible to induce a very close approximation of this syndrome by vitamin D intoxication while the permanent teeth are still in development. We were, however, unable to find any history of vitamin D exposure in the patients we recruited, though the possibility of inadvertent exposure should be considered. What is not clear is why this should result in sustained hypocalciuria as a persisting feature.

Though I am not convinced of this as a hypothesis, the striking similarities between the single, isolated case of AI with pulpal calcification and nephrocalcinosis does make the vitamin D pathway attractive as regards selection of further candidate genes.

4.4 THE ENAMEL RENAL SYNDROME – FURTHER WORK

During my research fellowship, and since, I have been able to recruit and obtain DNA from 3 families and 2 sporadic cases with ERS. I am hopefully in the process of recruiting a third sporadic case (Hunter et al 2007). This will hopefully provide a platform for future research in this condition. Genotyping technology has advanced rapidly and it now possible to provide far more detailed mapping at greatly reduced expenditure in terms of time and cost. The bioinformatics analysis of this high throughput data is, however, critical. Certainly detailed homozygosis mapping would clarify potential areas of interest in this family. The relatively small size, and lack of consanguinity in the other families and sporadics may mean they are less informative.

With a view to taking this forward I have provided professor Robert Kleta (Centre for Nephrology, UCL) with the DNA samples from these participants. He is in the process of having genome-wide typing performed in collaboration with his previous institution, NIH Washington, and has an interest in genetic bioinformatics.

There are aspects of the dental phenotype (such as intrapulpal calcification) that appear to be specific to this syndrome and may alert dentists to the possibility of the

presence of ERS. There remains, however, the possibility that there are a number of patients who are thought to have standard AI in isolation, and have undiagnosed nephrocalcinosis. As with much renal disease it is conceivable that patients may only develop symptoms very late in their illness. As a consequence there would be a case for routine renal screening of patients with recessive AI and this would make an interesting project. As we have no underlying mechanism for the nephrocalcinosis there would not be a specific renal therapy. There are, however, a number of therapies for complications of nephrocalcinosis such as hypertension (which may in itself cause further renal damage), urinary tract infection and stones and establishing the presence of this syndrome would benefit patients.

4.5 AUTOSOMAL DOMINANT AMELOGENESIS IMPERFECTA

We were, as described in this section, the first group to determine a genetic basis for autosomal amelogenesis imperfecta, which is the commonest form of AI. We found that, in one large family with autosomal dominant AI, that a mutation in the enamel matrix protein enamelin *(ENAM)* was responsible. Prior to this project the only form of AI for which the gene was known was the X-linked form. This was known to be caused by mutations in X-chromosome amelogenin *(AMELX)*.

Enamelin is the largest enamel matrix protein, constituting around 5% of human dental enamel. Porcine enamelin was cloned and characterised in 1997. It was found to be a 186-kDa phosphorylated glycoprotein that underwent cleavage into smaller products. It was found, in the pig, to be present in the crystallites of the rod and inter-rod enamel.

In 2000 Hu et al reported on in situ hybridisation in a day 1 mouse-developing incisor. They found enamelin to be expressed by ameloblasts, but not other cells (such as odontoblasts). They subsequently cloned human enamelin cDNA and used radiation hybrid mapping and fluorescent in situ hybridisation to localise the gene to 4q. Dong et al mapped human enamelin to the same location. The gene maps for a protein 1142 amino acids in length. It was the localisation of the enamelin gene *(ENAM)* to 4q21 that informed my proposal to Professor Mike Dixon's group that we look for enamelin mutations in our AI family, given that I had confirmed linkage to this location. As described in the previous section, we identified a splicing mutation in the splice donor site of intron 7 of *ENAM* (161).

March et al went on to report a an *ENAM* mutation causing local hypoplastic autosomal dominant AI. This phenotype is very common in Sweden, where it accounts for 27% of autosomal AI. This was a nonsense mutation that results in a severely truncated form of the protein 52 amino acids, rather than 1142 amino acids, in length. This was a milder form of AI than that present in our family (162).

Kida et al described an enamelin mutation in a Japanese family with autosomal dominant AI. This was a similar phenotype to that seen in our family. The mutation was a single G deletion within a series of 7G residues at the boundary of exon and intron 9 (163).

Hart et al identified previously unreported autosomal dominant AI kindred in which the disease segregated with a g.344del G mutation (164). They subsequently published data on light and electron microscopy analyses of unerupted teeth. The enamel was markedly reduced in thickness and lacked prismatic structure. This group subsequently performed homozygosity mapping for 5 candidate genes, including *ENAM,* in 20 consanguineous Turkish families with autosomal recessive AI. There was homozygosity at the *ENAM* locus for probands in 3 families. These individuals had a generalised hypoplastic AI. Mutational analysis demonstrated homozygosity for a 2 bp insertion mutation in these probands. This caused a premature stop codon in exon 10. Of note heterozygous carriers had localised hypoplastic enamel pitting, but not 'full-blown' AI. This implied a dose-dependent effect of this mutation (164-166).

Kim et al identified 2 different *ENAM* mutations in families with autosomal dominant, hypoplastic AI. They found the previously reported g.344delG mutation in one family, which had a fairly mild phenotype with generalised hypoplastic enamel and horizontal ridges in the middle 1/3 of the anterior teeth. They also found a novel mutation, g.4806A>C, IVS6-SA>C) which resulted in a more severe phenotype, with much deeper grooving of teeth due to ridges of marked enamel hypoplasia (167).

Ozdemir et al reported on 2 further Turkish families with hypoplastic AI. In one family a novel missense mutation (g.12263C>A; p.S246X) was found to cause autosomal dominant disease. In another family probands were compound heterozygotes for a novel insertion mutation (g.12946_12947insAGTCAGTACCAGTACTGTGTC), and a further previously described insertion mutation (g.13185_13186insAG). Heterozygotes with either mutation in isolation had mild enamel pitting only (168).

More recently Kang et al reported on a further autosomal dominant mutation (g.14917delT) and autosomal recessive mutation (g.13185-13186insAG) in a further two Turkish families with hypoplastic AI.

Since our original report *ENAM* mutations have been shown to cause both autosomal dominant and recessive hypoplastic AI in several families of varied nationality and ethnicity (cases have been reported in the UK, Sweden, Japan and Turkey) (169-172).

AMELX and ENAM encode enamel proteins and mutations result (in both human cases and transgenic mouse models) in enamel thinning (or hypoplasia). More recently mutations in *MMP20* and *KLK4*, which encode the enamel *proteinases* enamelysin and Kallikrein 4 respectively, have also been shown to cause AI. These appear to be hypoplastic/hypopigmented AI forms. Enamelysin appears to act in concert with ameloblastin, amelogenin and enamelin to promote enamel crystal elongation, and therefore enamel thickness (173-181). Kallikrein 4 appears to act later, in the final stages of enamel maturation. *FAM83H* mutations have, recently, been shown to cause hypocalcified AI in two families. The function of the protein this gene encodes is as yet unknown (182-186).

While it appears that several mutation sin several genes have now been shown to cause AI there are a great number of AI cases (around 75%) in which the genetic cause has not been determined. As such this complex disease appears to have not only great clinical, but also genetic heterogeneity.

SECTION II

AUTOSOMAL DOMINANT DIABETES INSIPIDUS

SECTION II-CHAPTER 1

BACKGROUND

1.1 INTRODUCTION

Diabetes insipidus was first differentiated from diabetes mellitus in the 17th century. It has two types – the central, or neurohypophyseal form, in which AVP secretion is reduced, and the nephrogenic form, where there is renal resistance to AVP. Patients with either form may have a dramatic phenotype, passing large volumes of urine per day, sometimes up to 30 litres. These conditions demonstrate the remarkable concentrating reserve of the renal tubule and how it is modulated by AVP.

We were providing renal care for a patient with presumed nephrogenic diabetes insipidus during the period of my research. He had a typically striking phenotype, with very high urine volumes and water requirements. In addition he had developed significant impairment of renal function, probably related to chronically high intravesical pressures and 'functional obstruction'. The diagnosis of nephrogenic diabetes insipidus had been made in his infancy. There was a strong family history, with his father, brother, sister and her three children all affected.

In this chapter I will present the results of a clinical and genetic investigation of the disease affecting this family performed by myself, and collaborators at the Galton Laboratory, UCL.

1.2 FREE WATER HOMEOSTASIS

Human free water excretion is determined by arginine vasopressin (AVP), also known as antidiuretic hormone (ADH). It is a polypetide hormone synthesized in the supraoptic and paraventricular nuclei of the hypothalamus. ADH is contained within secretory granules that travel through the supraopticohypophyseal tract to the posterior lobe of the pituitary. Here they are stored, then released into the circulation. ADH has a very short half-life of around15mins as it is rapidly metabolised by the kidneys and liver.

AVP regulates renal excretion of free water. It acts independently of mechanisms that determine salt and water excretion, such as the renin-angiotensin system, though both may be provoked by a hypovolaemic challenge. AVP acts on the principal cells of the renal cortical and medullary

collecting tubules to increase water permeability. The interstitium is hypertonic at this site, so increasing permeability, rather than active transport, is all that is required for water to move from urine to interstitium. This action is mediated by V2 receptors. When these are activated protein kinase is released. This, in turn, stimulates cytoplasmic vesicles containing water channels (principally aquaporin 2, AQP2) to migrate to the luminal membrane and fuse with it. This results in increased luminal permeability. Water then moves to the basolateral membrane and is exported to the basolateral circulation via aquaporin 3 and 4 (AQP3 and AQP4), (Figure 1). Basolateral transfer of water is not ADH dependent, and the luminal, AQP2 mediated stage is the rate limiting factor. When AVP levels fall AQP2 proteins fold into clarithrin coated vesicles and is returned to the cytosol.

AVP also acts on systemic V1 receptors, promoting phosphatidyl turnover, which causes vasoconstriction. AVP action on V1 receptors also stimulates renal prostaglandin release. These prostaglandins inhibit the vascular and permeability actions of AVP, and may represent a negative feedback loop. The V3 receptor is located on the anterior pituitary, and here AVP seems to have a role in modulating ACTH release from this site. AVP also regulates the release of factor VIII and von Willebrand factor from vascular endothelium.

AVP release is governed by osmoreceptors and baroreceptors. Verney, in his classic studies, infused hypertonic saline into large vessels and noted an increase in local, but not systemic osmolarity when the infusion was directed at the carotid artery. This implied that osmoreceptors were located in the brain. We now know that these osmoreceptors are mainly hypothalamic. It is likely that these osmoreceptor cells are sensitive to osmotic shifts. Water moves in and out of the osmoreceptor cells via water channels as the osmotic gradient with the plasma rises. Consequent cellular shrinkage affects the activity of stretch inactivated cation channels. Membrane depolarisation then stimulates AVP production.

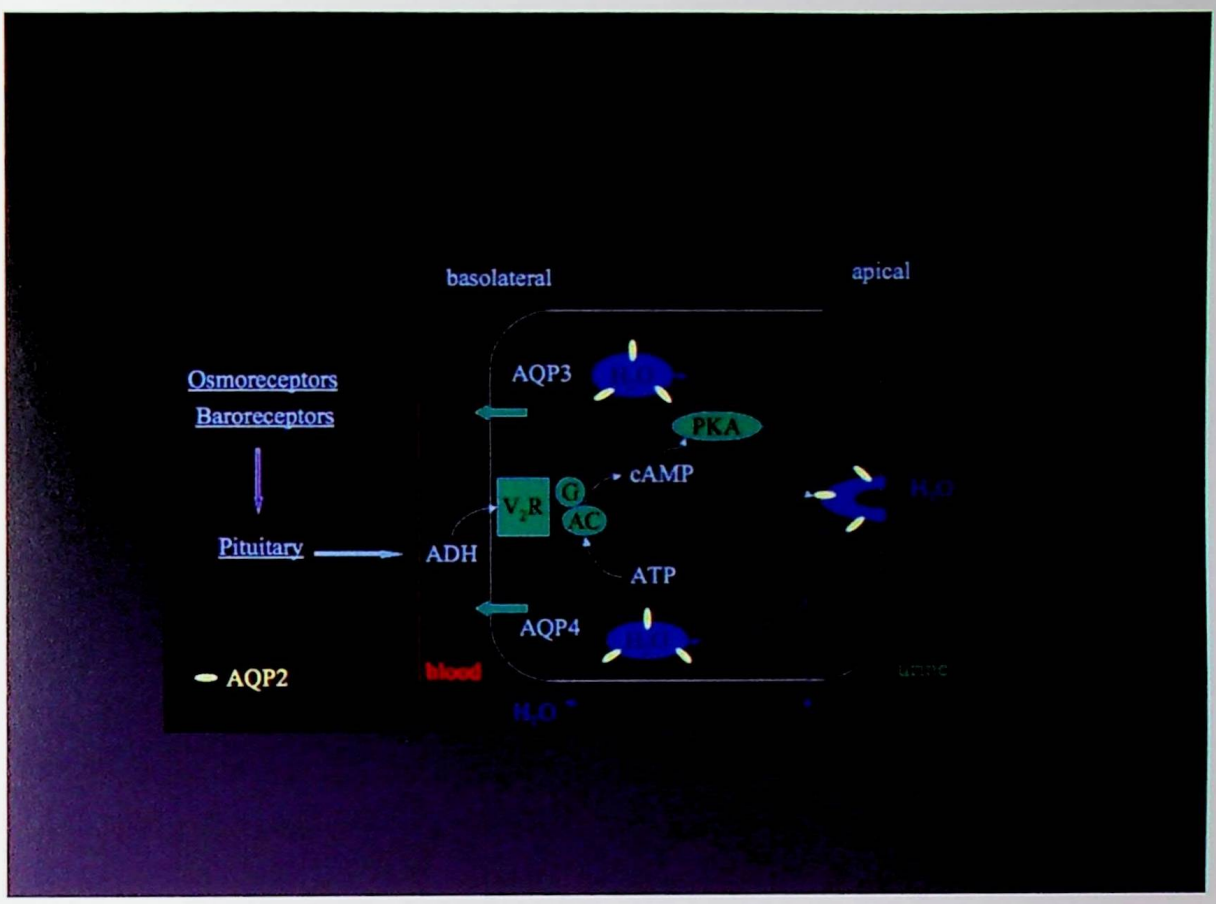

Figure 1. Cellular mechanism of ADH action. V_2R = vasopressin receptor 2 or V2. PKA = protein kinase A. Free water flows from apical to basolateral membrane and thence to blood via AQP2, 3 and 4 water channels. AQP2 activity is mediated by ADH action on V2 via protein kinase A.

Sodium is the most abundant osmole in the ECF. Unlike urea it does not diffuse into the osmoreceptor cells and so exerts greater osmotic effect on them. Glucose is a major extracellular solute, but rises in insulin cause a movement of glucose into osmoreceptor cells, diminishing their osmotic impact. In insulin deficiency, such as type I diabetes, this effect does not happen, and ECF glucose will stimulate ADH production.

In humans, when plasma osmolarity is less than 280mosmol/l, AVP release is almost completely suppressed and urine will be maximally dilute. Above this osmotic threshold, rises in ADH secretion are linear. Plasma osmolality does not normally vary by more than 1%. Thus the very large filtration of water at the glomerulus provides a mechanism for large amounts of water excretion if necessary. Should osmolality be high, however, this free water diuresis can be almost completely, and instantaneously switched off. This potential for

tight control of plasma osmolality in the face of very different water intakes has likely developed, in evolutionary terms, due to the variability of human water supplies.

A rise in plasma osmolality results in an increase in thirst, again centrally controlled. The "thirst threshold" is a change in plasma osmolarity of 2 to 5 mmol/l. The danger of this mechanism is that the lag time between water intake and change in plasma osmolarity, due to gut absorption, might mean excess water is consumed, resulting in potentially dangerous rebound hyponatraemia. To protect against this, the sensation of thirst is sated by stimulation of oropharyngeal mechanoreceptors that are stimulated by consuming large volumes of water.

AVP secretion is also under the influence of baroreceptors. These are likely to be parasympathetic fibres in the carotid sinus. These feedback to the vasomotor centre in the medulla, which in turn influences hypothalamic secretion of AVP. It is likely that this happens to facilitate the pressor effects of AVP, as free water reabsorption (as opposed to salt and water reabsorption) is an ineffective way of expanding ECF volume. It seems, however, that large changes in ECF volume are required to influence AVP secretion, unlike small shifts in osmolality. Chronic hypo or hypervolaemia may result in chronic changes to ADH secretion and tolerance of an abnormal plasma osmolality. An example is in heart failure, where there is perceived hypovolaemia by the offloading of baroreceptors, and AVP activation may result in chronic hyponatraemia. If this persists the new "normal osmolality" may be tolerated even if the volume insult abates. This phenomenon is called "osmostat resetting"

Numerous other factors stimulate ADH release, including stress, pain and nausea. Postoperative surgical patients, particularly the young, are vulnerable to hyponatraemia due to excess ADH activation. If such patients are maintained on hypotonic solutions, such as 5% dextrose, this can result in catastrophic hyponatraemia.

1.3 DIABETES INSIPIDUS

Polyuria is defined as a urine volume of >3l/24 hours in adults and 2l/24 hours in children. In the assessment of the polyuric patient common and reversible causes such as hyperglycaemia and post-obstructive polyuria should be excluded. If these have been excluded three important diagnoses remain: primary polydipsia, neurohypohyseal diabetes insipidus (or central diabetes insipidus, CDI) and nephrogenic diabetes insipidus (NDI).

Primary polydipsia is when there is an inappropriate consumption of water. The polyuria is appropriate and represents a homeostatic effort to excrete excess water and maintain plasma osmolality. AVP levels will be undetectable. Primary polydipsia may be seen in psychiatric patients and hypothalamic disease (infiltrative or vascular).

CDI is due to defective ADH secretion. This may be inherited, or acquired due to autoimmune disease (idiopathic CDI), anoxic brain injury, trauma, pituitary surgery or infiltration. Familial CDI, or familial neurohypohyseal diabetes insipidus (FNDI), is an autosomal dominant disease caused by mutations in the arginine-vasopressin gene *(AVP)*.

The *AVP-NPII* gene is located at the distal end of the short arm of chromosome 20 (20p13). This encodes the AVP protein, the carrier protein neurophysin II (NPII) and the signal peptide domain. FNDI has been associated with 56 different *AVP-NPII* mutations in 87 kindreds. Most reported mutants have been single base pair substitutions, however, dinucleotide substitutions and deletions have been reported. These correlate with a heterogeneous collection of mutants of the AVP protein product, including amino acid substitutions, deletions and truncations in the AVP moiety, neurophysin II, and signal peptide domains. The great majority of mutations occur in the coding region for neurophysin II.

In spite of genetic heterogeneity, the phenotype is surprisingly consistent. In an effort to explain this, the delayed onset of the phenotype, and the dominant-negative affect of mutant alleles a uniform mechanism for genotype-phenotype correlation has been hypothesised. This "misfolding neuro-toxicity hypothesis" proposes that all such mutant hormone precursors, after failing to

fold or dimerise properly, are retained in the endoplasmic reticulum, resulting in cytotoxic accumulation and degeneration of magnocellular, AVP-producing neurons (13).

Nephrogenic diabetes insipidus is due to renal AVP resistance. It has a number of acquired and inherited causes. Hypercalcaemia is an important cause of acquired nephrogenic diabetes insipidus. The calcium sensing receptor (CaSR) is expressed on the basolateral membrane in the thick ascending limb of the loop of Henle. Calcium binds to this receptor, reducing calcium reabsorption in the thick ascending limb. CaSR activation also results in reduced NaCl reabsorption. This, in turn, causes inhibition of the medullary osmotic gradient and, as a consequence, urine cannot be adequately concentrated. In hypercalcaemia more calcium is delivered to the collecting duct where it binds with CaSR. This reduces AVP mediated increases in luminal water permeability. Some animal studies have suggested that hypercalcaemia also results in reduced expression of aquaporin 2.

Lithium toxicity is an important cause of nephrogenic diabetes insipidus. Twenty percent of patients on chronic therapy will have symptomatic polyuria, while thirty percent will have a subclinical concentrating defect. Lithium accumulates in the renal tubular cells, where it probably reduces the expression of AVP.

Chronic hypokalaemia reduces collecting duct AVP responsiveness, probably through reduced AQP2 expression. As in hypercalcaemia, there is probably reduced thick ascending limb reabsorption of NaCl, which disrupts the countercurrent concentrating mechanism.

NDI may be seen in other forms of drug toxicity (cidofivir, demeclocycline and orthostat). It may be seen transiently in pregnancy and has been associated with autoimmune disease such as Sjogren's syndrome. It has also been reported in sickle cell disease and amyloidosis. Bartter's syndrome causes polyuria but this is not strictly a disorder of free water excretion and is therefore not usually categorized as NDI.

Inherited NDI is a rare but important cause of polyuria and polydipsia. Ninety percent of hereditary NDI is due to mutations of the vasopressin 2-receptor

gene *AVPR2*. This disease was first reported in 1955 in a Mormon family traced to 1813 in which Cannon reported on apparent male-to-male transmission of diabetes insipidus. In 1974 Bell et al demonstrated that some NDI patients did not have increased cAMP levels in urine in response to ADH administration. This suggested a "back-stream" defect, before the cAMP step. Bichet et al showed that in a proportion of patients, extrarenal effects of ADH (factor VIII and VWF) were absent, suggesting a vasopressin receptor problem not confined to the kidney.

Knoers et al were the first to successfully localise the gene for this disease to Xq28. Van den Ouweland et al were first to demonstrate expression of a vasopressin receptor in hybrid cell lines containing this locus. Rosenthal et al were first to demonstrate AVPR2 mutations in an X-linked NDI kindred. Since then, several hundred AVPR2 mutations have been found to be associated with this disease. Mutant AVPR2 is usually folded and trapped in the endoplasmic reticulum and cannot be expressed on the basolateral principal cell membrane. This stops it interacting with AVP. As expected the non-renal effects of ADH not mediated by AVPR2 are intact (vasoconstrictor and prostaglandin) while those that are AVPR2 dependent (factor VIIIc and von Willebrand's factor) are impaired in this condition. Females have a lesser phenotype and are usually asymptomatic, though severe polyuria in females has been reported when there is skewed normal-X activation.

Autosomal NDI accounts for 10% of nephrogenic diabetes insipidus. This disease has been found to be associated with mutations in the gene encoding AQP2. In 1975 Zimmerman and Green reported a normal increase in urinary cAMP in response to ADH in a subset of NDI patients. This indicated a *post*-cAMP defect. Several kindreds with apparently autosomal inheritance were subsequently reported. Deen et al were first to report on mutations in AQP2 causing NDI in 1994, when they reported compound heterozygosity for 2 mutations in the AQP2 gene in NDI patients. AQP2 mutations have subsequently been shown to cause dominant-negative effects in xenopus oocyte models. In patients with AQP2 mutations, the extra renal effects mediated by AVPR2 receptors are intact.

I.4 THE WATER DEPRIVATION TEST

The water deprivation test is used to assess AVP production and response and will differentiate between primary polydipsia, CDI and NDI. When serum osmolality reaches 300 mosmol/Kg endogenous AVP secretion is maximal. Elevation of urine osmolarity above 600 mosmol/kg in response to this is considered normal and will be seen in psychogenic polydipsia. In CDI there will be a sub-maximal rise in urine osmolarity in response to water deprivation (usually >300mosmol/kg) and a 100% rise in response to dDAVP (15-50% in partial CDI states). In NDI urinary concentration is attenuated (<300mosmol/kg) with no response to dDAVP in complete NDI, with a small (<45%) rise in incomplete NDI (11). Where diagnostic uncertainty remains (as in incomplete forms) this can be resolved by formal AVP measurement (12). An alternative to water deprivation testing is the infusion of hypertonic saline (0.05ml/Kg for 2 hours). Patients undergoing these tests must be monitored assiduously.

	Inherited	Acquired
Neurohypophyseal diabetes insipidus (central or cranial diabetes insipidus)	**Familial neurohypophyseal diabetes insipidus** OMIM 125700. *AVP* (arginine vasopressin) mutations Locus 20p13 **Wolfram Syndrome** OMIM 222300 (DIDMOAD syndrome) Autosomal dominant and recessive Diabetes insipidus and mellitus, optic atrophy and deafness. *WFS1* (Wolframin) mutations Locus 4p	**Idiopathic (autoimmune) DI** **Neurosurgery or brain trauma** **Primary or secondary brain cancer affecting the hypothalamic pituitary axis** **Anoxic brain injury (Sheehan's syndrome)** **Sarcoidosis** **Wegener's Granulomatosis** **Histiocytosis X** **Autoimmune Lymphocytic hypophisitis** **Anorexia Nervosa** **Gestational DI** (placental vasopressinase)
Nephrogenic diabetes insipidus	**X-linked nephrogenic diabetes insipidus** OMIM 304800 *AVPR2* (vasopressin receptor) mutations Locus Xq28 **Autosomal dominant nephrogenic diabetes insipidus** OMIM 125800 *AQP2* (aquaporin-2) mutations Locus 12q13 **Autosomal recessive nephrogenic diabetes insipidus** OMIM 222000 *AQP2* mutations Locus 12q13 **Nephrogenic diabetes insipidus with mental retardation and intracerebral calcification** OMIM 22195	**Lithium** **Sjogren's syndrome** **Hypokalaemia** **Hypercalcaemia**

Table 1. Causes of diabetes insipidus

I.5 CANDIDATE GENES IN AUTOSOMAL DOMINANT DI IN THIS FAMILY

At the onset of this project the DI affecting this family had been classified as nephrogenic. As stated above the commonest genetic cause of NDI is mutation of AVPR2. This is in X-linked disease, which, for reasons described later, is possible (though unlikely) in this pedigree. As regards autosomal dominant NDI this is rare (recessive disease being more common). The only known genetic cause of this was mutations of AQP2.

At the time of the onset of this research the gene CLCK-1 was found, in a mouse transgenic model, to be critical for urinary concentration, as a knock out model had resulted in a severe NDI phenotype. CLCK-1 mediates transepithelial chloride transport in the thin ascending limb of the loop of Henle. Its human homolog is CLCK-A, which, in the light of this animal data, represented a further potential candidate in human NDI.

FNDI has been found to be solely due to mutations in AVP-NPII. The great majority of cases have been autosomal dominant, with a small number recessive. Cases of FNDI with no evidence of AVP-NII mutation have been reported, and their genetic cause is unknown.

1.6 AIMS OF THE PROJECT

These were as follows

1. To formally characterise the clinical phenotype of DI in this family, one of who was under our care at The Middlesex Hospital. This would include assessment of renal and bladder function, extent of polyuria, water deprivation testing, correction with exogenous AVP and assay of endogenous AVP.
2. To obtain DNA sampling of the family and perform a candidate gene linkage analysis for candidates for DI. If evidence of linkage were found we would perform mutational analysis in an effort to determine the genetic cause of DI in this family.

SECTION II - CHAPTER 2

MATERIALS AND METHODS

2.1 RECRUITMENT AND DNA SAMPLING

I obtained contact details of other family members from our index case. I travelled to their homes, which were in the South East and South West of England to discuss our research and invite them to participate. Several family members subsequently agreed to attend The Middlesex and Royal Free Hospitals for clinical evaluation and water deprivation testing.

DNA sampling and extraction was according to the methods described in Section I.

2.2 MARKER IDENTIFICTION, PRIMER DESIGN, PCR AND P_{32} LABELLED GENOTYPING AND LINKAGE ANALYSIS

This was according to the method described in Section I.

2.3 GENOTYPING USING THE ALFEXPRESS DNA SEQUENCER

In addition to the radiolabelled PCR analysis we performed non-radiolabelled PCR analysis using the ALFexpress. This provides automated detection of fluorescently labelled DNA molecules separated by gel electrophoresis. A fixed laser beam is directed into the gel perpendicular to the direction of band migration. This excites the fluorescently labelled DNA fragments and the light emitted is detected by photo-detectors located behind the gel. The photo-detector signals are digitised and sent to the computer for storage and processing.

The oligonucleotide primers were labelled at their 5' prime end. These were ordered from Sigma Genosys.

2.3.1 PCR reactions for ALFexpress

The PCR mix shown below was used. Of the 10ml product 5ml were used for a check agarose gel electrophoresis, the remainder for loading on the ALFexpress.

PCR reagent	Volume (ml)	Concentration	Mix concentration
Blood DNA sample	1	500ng/ml	50ng/ml
Buccal cell DNA sample	1	100ng/ml	10ng/ml
10x Abgene PCR Buffer IV	1	10x	1x
10x dNTPs	1	2mM	0.2mM
Abgene taq polymerase	0.05	5U/ml	0.5U/ml
Forward primer	1	5mM	0.5mM
Reverse primer	1	5mM	0.5mM
H_2O	4.95	-	-

Table 2. PCR mix for DI family genotyping

The optimisation of PCR running conditions and agarose gel electrophoresis was performed as per the method described in Section I.

2.3.2 ALFexpress protocol

1. ALF short plates, combs and spacers were washed and cleaned with isopropanol
2. Bind silane was applied to the two plates in the area where the comb would sit in order to maintain the integrity of the wells when removing the well comb.
3. The plates were set up for gel pouring.
4. Gel mix
    a. 5ml sequagel complete buffer reagent
    b. 20ml sequagel-6
    c. 200ml of 10% AMPS (ammonium persulphate)
5. The gel, following mixing of gel mix and pouring, was left to set for three hours
6. The comb was removed and the plate placed at an off-vertical angle on the ALFexpress machine to allow ease and safety of gel loading.

7. The buffer chambers were filled with 2 litres of 1xTBE, which acts as the buffer for the electrophoresis.
8. The buffer chambers were filled with 1 x TBE, in order to clear excess gel and urea.
9. Water was circulated from the integral water circulator through one of the plates of the cassette to control temperature.
10. 1ml of labelled PCR product were added to a 5ml mix of formamide buffer and two size markers
11. After the 6ml samples were loaded, the two electrodes were connected and the gel set to run.
12. The gel was run for 180 minutes at a set current of 40 Amps with a voltage of 1500 volts.

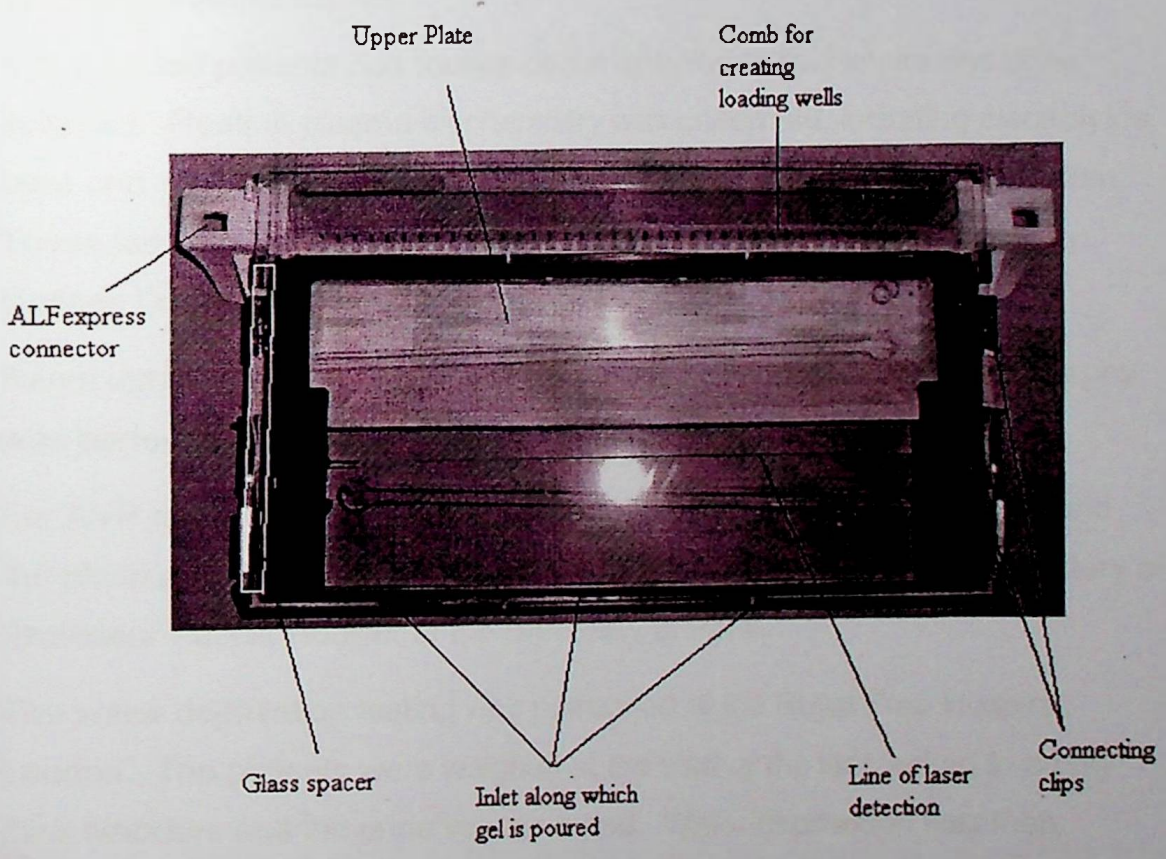

Figure 2. ALFexpress gel apparatus (photo William James White)

2.3.3 ALFexpress data analysis

The raw data from ALFexpress is presented as a sequence of peaks against the time they crossed the laser. The "Fragment Manager" software provided with the apparatus was used. This realigns peaks so that they can be compared in terms of size. Haplotypes were then constructed manually and with *Cyrillic* software.

2.3.4 Sequencing of genomic DNA

Sequencing of genomic DNA was done commercially. Standard automated sequencing was performed using automated methods with fluorescent labelling, gel migration and laser scanning. Sequencing of the AQP2 gene was performed by Professor Nine Knoers group using similar methods.

2.4 CLINICAL STUDIES

The affected patients had routine documentation of fluid intake and urine volumes. Routine plasma biochemistry was performed, including electrolytes, urea and creatinine, liver function tests, bone biochemistry and magnesium. These tests were performed in the biochemistry department of University College London Hospitals with routine assays.

Renal ultrasonography, magnetic resonance imaging and mag 3 renography was performed in the radiology department of The Middlesex Hospital.

For AVP assays whole blood samples were taken, spun at 4,000 RPM and the plasma frozen at -20C. These samples were then sent to the laboratory of Professor Pascal Houllier at the University of Paris.

The water deprivation testing was performed at the Royal Free Hospital, London. The patients were weighed at the start of the test, asked to empty their bladders and the urine volume noted. Water deprivation was then performed. O.2mg of exogenous AVP (DDAVP) was administered and weights, bladder voids, urine and plasma sodium and urine and plasma osmolality were checked at 0, 2 and 4 hours.

SECTION II-CHAPTER 3

RESULTS

3.1 CLINICAL EVALUATION

Our index case presented as a male infant with failure to thrive, vomiting of feeds, hypernatraemia and polyuria. He was diagnosed with autosomal nephrogenic diabetes insipidus (DI) due to the early onset and strong family history of this condition. He was appropriately hydrated and his parents were given advice regarding long-term fluid requirements. He enjoyed normal development, but continued to have marked polyuria and polydipsia, passing 10-15 litres of urine per day, which he was able to replace orally.

Routine renal ultrasonography was performed at the age of six. This demonstrated bilateral hydronephrosis, more marked on the left, with a grossly distended bladder. It was assumed that anatomical obstruction was present and this defined much of his subsequent investigation and management. Temporary bilateral nephrostomies were inserted followed by open myotomoy of the bladder neck. When the ultrasound appearances persisted a further transurethral bladder neck incision was performed. These procedures rendered him partially incontinent.

Over the years the hydronephrosis continued to worsen and this led to further urological investigation. Cystourethoscopy demonstrated a trabeculated bladder but no outflow obstruction. Pressure, video and ambulatory cystometrograms demonstrated a bladder of normal contractility with increased capacity. There was, however, evidence of-right sided vesicoureteric reflux. A left-sided anterograde pyelogram, serial intravenous pyelograms and Mag 3 renograms (with frusemide) did not demonstrate obstruction. The latter studies did demonstrate progressive cortical thinning and decline in renal function, particularly on the right (Figure 3).

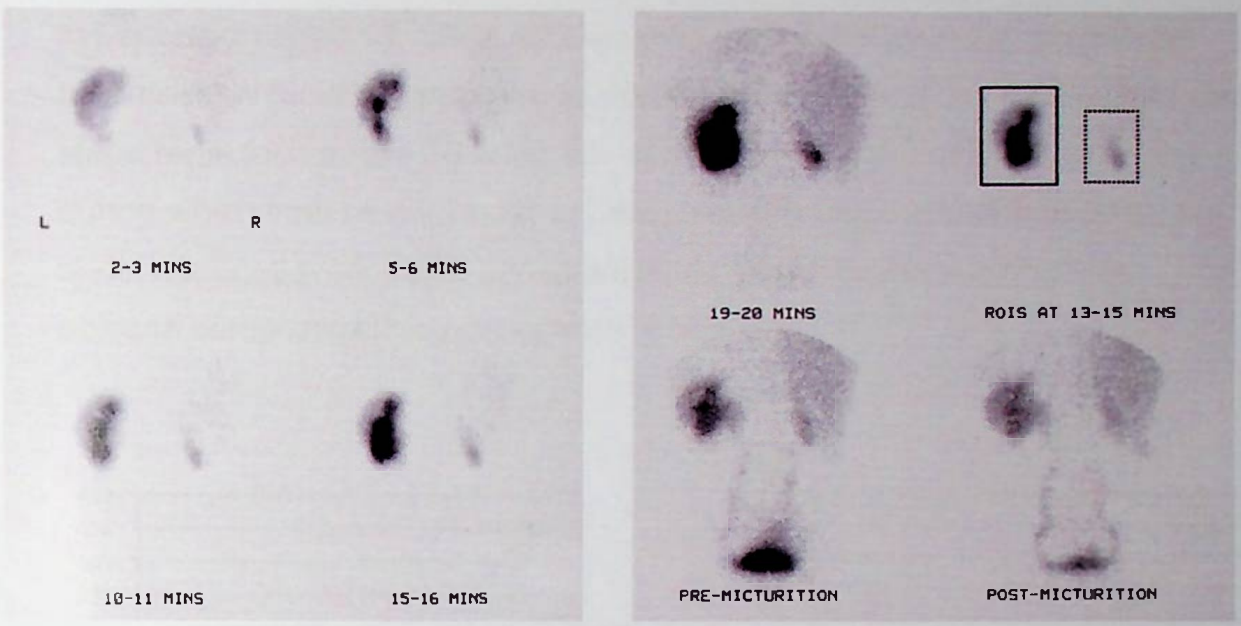

Figure 3. MAG3 renogram of proband II:3. Function in the left kidney is reduced; the right kidney is virtually non-functional. The frusemide excretogram does not demonstrate obstruction.

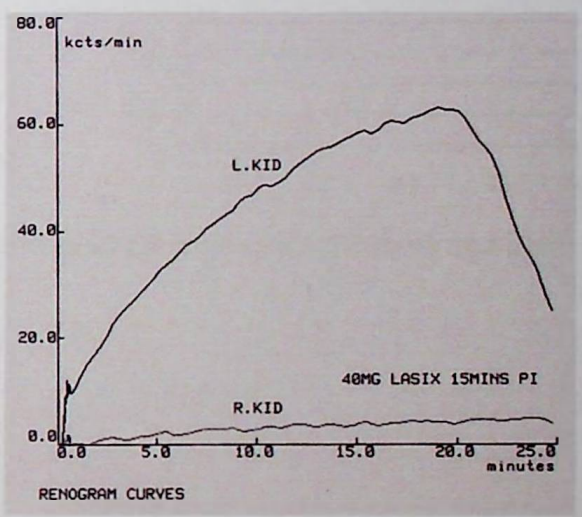

At the age of 14 he developed proteinuria and started treatment for hypertension aged 19. Over subsequent years the proteinuria progressed and his renal function continued to decline (figures 2 and 3). He reached end-stage renal failure (ESRF) aged 40. After a short period of haemodialysis, during which time he continued to pass relatively large volumes of urine, he underwent cadaveric renal transplantation. Dramatic worsening of his polyuria complicated his post-operative recovery.

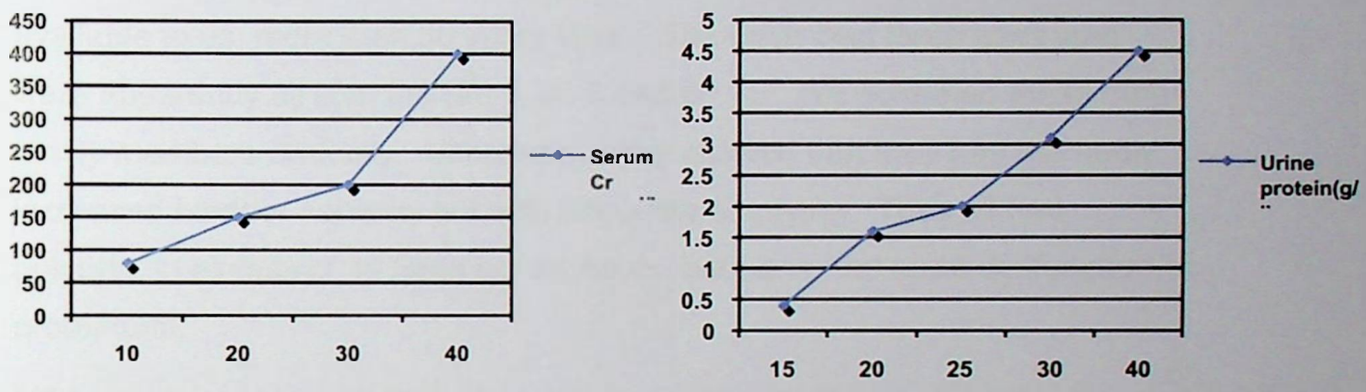

Figure 4. Graphs of serum creatinine and proteinuria plotted against age (in years) for proband II:3.

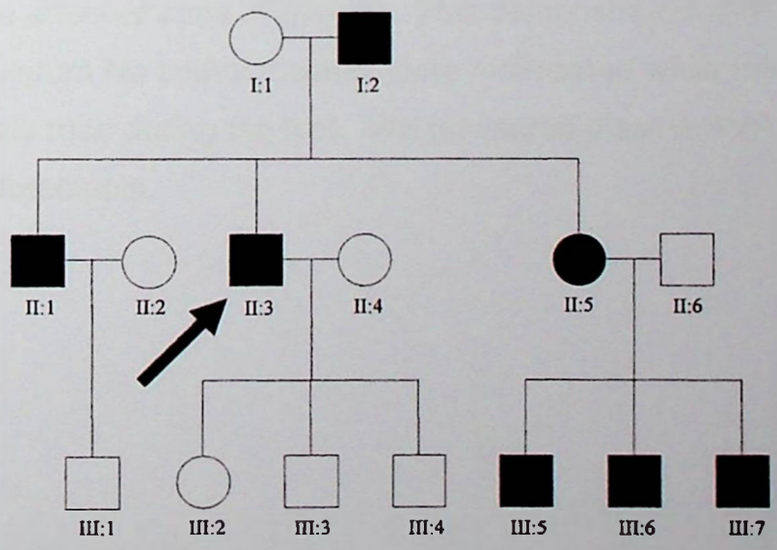

Figure 5. DI family tree. The index case is indicated with the arrow.

We revisited the original diagnosis of autosomal nephrogenic DI. There was clearly a family history of a polyuric illness (Figure 5). His father (I: 2) suffered lifelong polyuria and polydipsia and could recollect severe thirst as a child, often resorting to drinking puddles of rainwater. His elder brother and sister (II: 1 and II: 5) had presented with vomiting and failure to thrive in infancy. Initially their mother supplemented their nutrition by feeding them ground vitamins in bottled water. This judicious fluid therapy probably prevented hypernatraemic neurological damage. They were subsequently diagnosed with nephrogenic DI, though investigations undertaken at that time were not available to us, more than 30 years later. The sister had three sons who were apparently all affected (III: 5, III: 6 and III: 7). We screened these other family members clinically. Ultrasonography showed that they had markedly increased bladder capacity but with adequate emptying. They all had polyuria, in excess of 10 litres per 24 hours, but none had renal dysfunction or proteinuria.

MRI scanning of the pituitary showed abnormalities consistent with neurohypophyseal DI in II: 3 and II: 5 (Figure 7). We performed water deprivation testing with desmopressin (dDAVP) in our proband, his sister and her three affected sons (Figure 8). This demonstrated AVP responsiveness; weight, serum Na and osmolarity were maintained while urinary sodium and osmolarity rose during the test. We measured plasma AVP in III: 5 and this was undetectable.

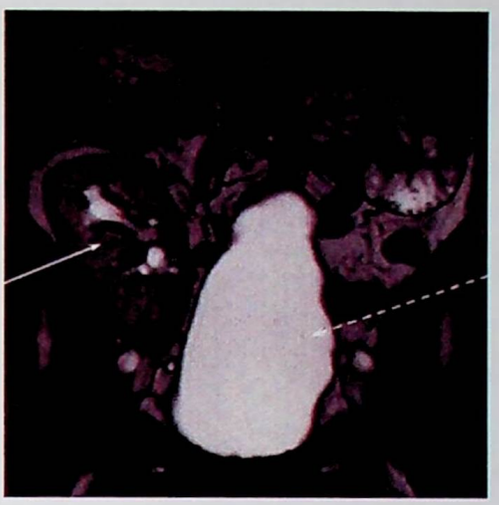

Figure 6. MR of proband II: 3 showing cadaveric renal transplant (arrow) and bladder distension (dashed arrow)

Figure 7. T1 weighted sagittal pituitary MR images of proband II: 3. The T1 hyperintensity associated with the posterior lobe of the pituitary is reduced (arrow) and the pituitary stalk appears thin in its inferior half (dashed arrow). This is more consistent with a diagnosis of neurohypophyseal diabetes insipidus (118,119).

3.2 WATER DEPRIVATION TESTING

II: 3 (patient RS) DDAVP dose 0.2mg

	Bladder volume/void	Weight Kg	Urine Na mmol/l	Urine Osmo. mosmol/kg	Plasma Na mmol/l	Plasma Osmo. mosmol/kg
0 min	**500 ml**	**90.9**	**35**	**150**	**138**	**284**
2 hours	**520 ml**	**93.0**	**62**	**263**	**136**	**281**
4 hours	**220 ml**	**92.7**	**79**	**407**	**135**	**280**

II: 4 (patient EH) DDAVP dose 0.2 mg

	Bladder volume/void	Weight Kg	Urine Na mmol/l	Urine Osmo. mosmol/kg	Plasma Na mmol/l	Plasma Osmo. mosmol/kg
DDAV0 min	**500 ml**	**60.4**	**17**	**88**	**140**	**288**
2 hours	**500 ml**	**61.8**	**53**	**233**	**132**	**268**
4 hours	**100 ml**	**62.3**	**48**	**379**	**132**	**273**

III: 5 (patient SH) DDAVP dose 0.2 mg

	Bladder volume/void	Weight Kg	Urine Na mmol/l	Urine Osmo. mosmol/kg	Plasma Na mmol/l	Plasma Osmo. mosmol/kg
0 min	**125 ml**	**77.9**	**18**	**165**	**143**	**292**
2 hours	**520 ml**	**78.5**	**31**	**253**	**144**	**293**
4 hours	**320 ml**	**78.8**	**66**	**408**	**141**	**293**

III: 6 (patient PH) DDAVP dose 0.2 mg

	Bladder volume/void	Weight Kg	Urine Na mmol/l	Urine Osmo mosmol/kg	Plasma Na mmol/l	Plasma Osmo mosmol/kg
0 mins	**Approx. 750**	**49.2**	**22**	**108**	**142**	**287**
2 hours	**150**	**48.9**	**40**	**246**	**142**	**286**
4 hours	**50**	**49.4**	**46**	**443**	**140**	**294**

III: 7 (patient TH) DDAVP dose 0.2 mg

	Bladder volume/void	Weight Kg	Urine Na mmol/l	Urine Osmo mosmol/kg	Plasma Na mmol/l	Plasma Osmo mosmol/kg
0 min	**500**	**50.4**	**19**	**119**	**138**	**287**
2 hours	**100**	**48**	**17**	**325**	**142**	**288**
4 hours	**20**	**49.1**	**11**	**400**	**143**	**293**

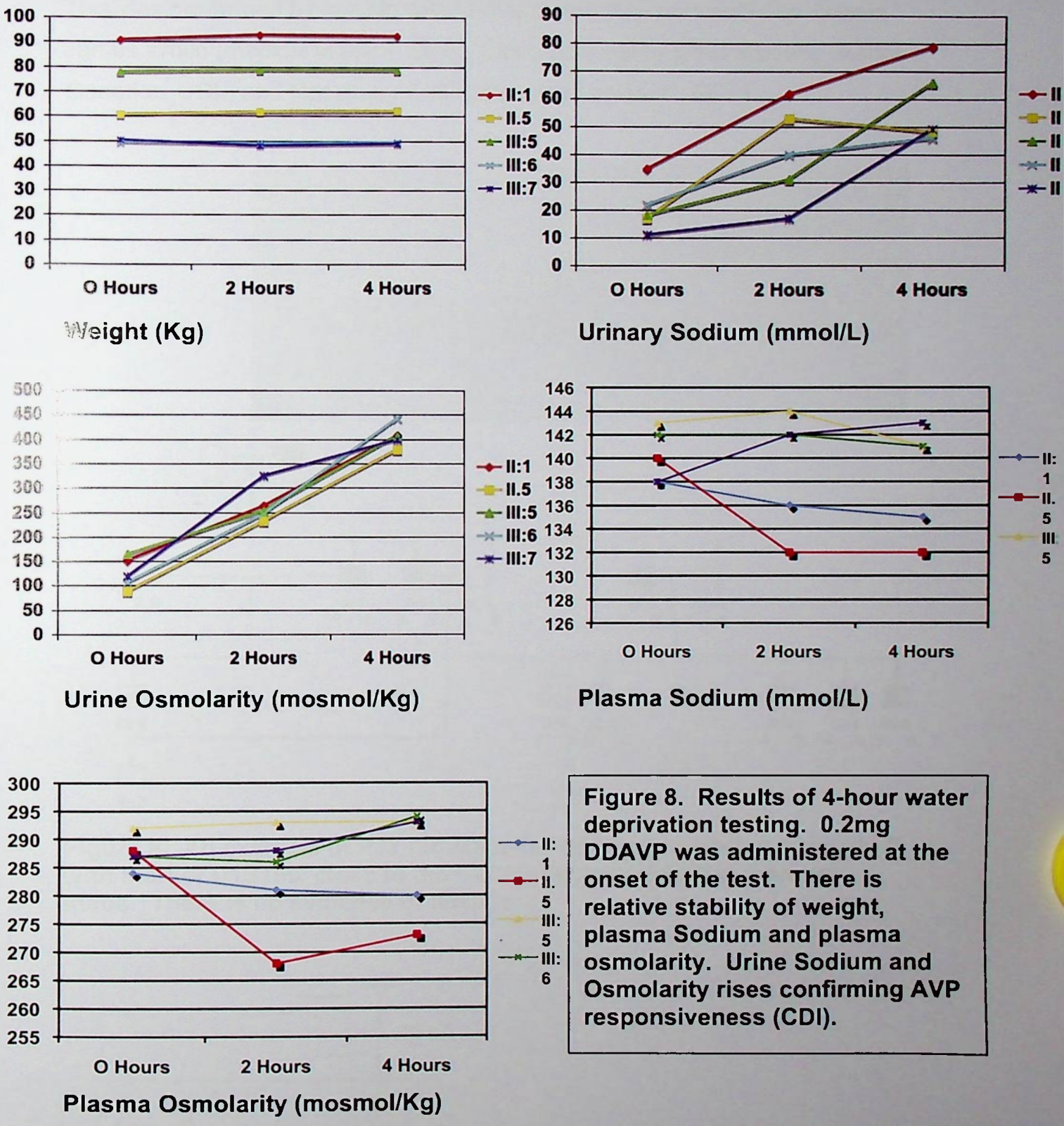

Figure 8. Results of 4-hour water deprivation testing. 0.2mg DDAVP was administered at the onset of the test. There is relative stability of weight, plasma Sodium and plasma osmolarity. Urine Sodium and Osmolarity rises confirming AVP responsiveness (CDI).

3.3 MUTATION SCREENING FOR AQP2 MUTATIONS IN DI FAMILY

Professor Nine Knoers group in Holland performed this. No mutations were found in 1 affected family member

3.4 GENOTYPING DI FAMILY

This was performed by myself, with further genotyping performed by William James White (medical student, UCL), Claire Willoughby (PhD student, Human Genetics, UCL) and Rosemary Ekong (research scientist, UCL)

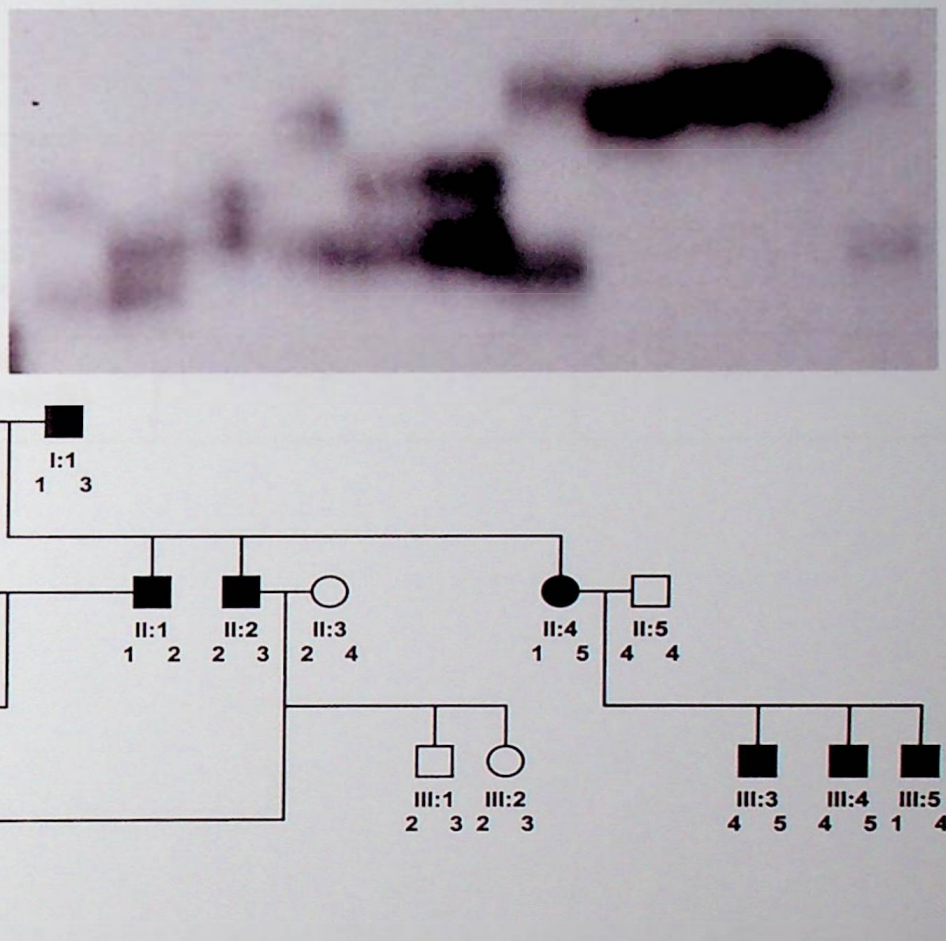

Figure 9. An example of P32 radiolabelled PCR gel migration of family D with marker D1S199, close to the CLCKA (kidney chloride channel) locus. There is no evidence of linkage.

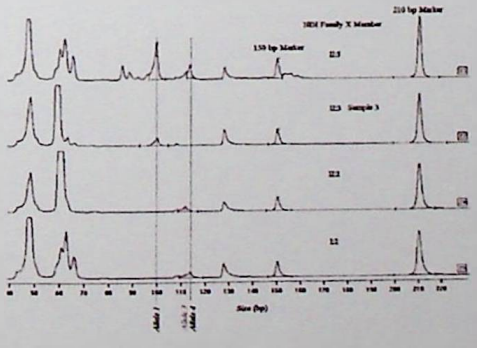

Figure 10. Sample genotypes from ALFexpress using fluorescent labelled primers, gel migration and laser genotyping.

3.5 GENOTYPING OF DI – CHROMOSOME 1 AND CANDIDATE GENES KIDNEY CHLORIDE CHANNELS A AND B (*CLCNKA, CLCNKB*)

MARKER	FORWARD PRIMER	REVERSE PRIMER	LOCATION	SIZE
D1S199	*GGTGACAGAGT GAGACCCTG*	*CAAAGACCATGT GCTCCGTA*	Ch 16 19,729,580-19,929,739	200,160 bp

GENE	CHROMOSOME 1 LOCATION	SIZE
CLCNKA (kidney chloride channels A)	16,221,073-16,233,132	12,060 bp
CLCNKb (kidney chloride channel B)	16,242,939-16,256,063	13,125 bp

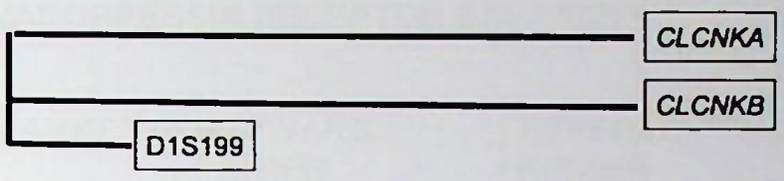

Figure 11. Figure 35. Physical map of Ch1 demonstrating position of DI candidate genes *CLCNKA* and *CLCNKB* relative to genetic marker D1S199.

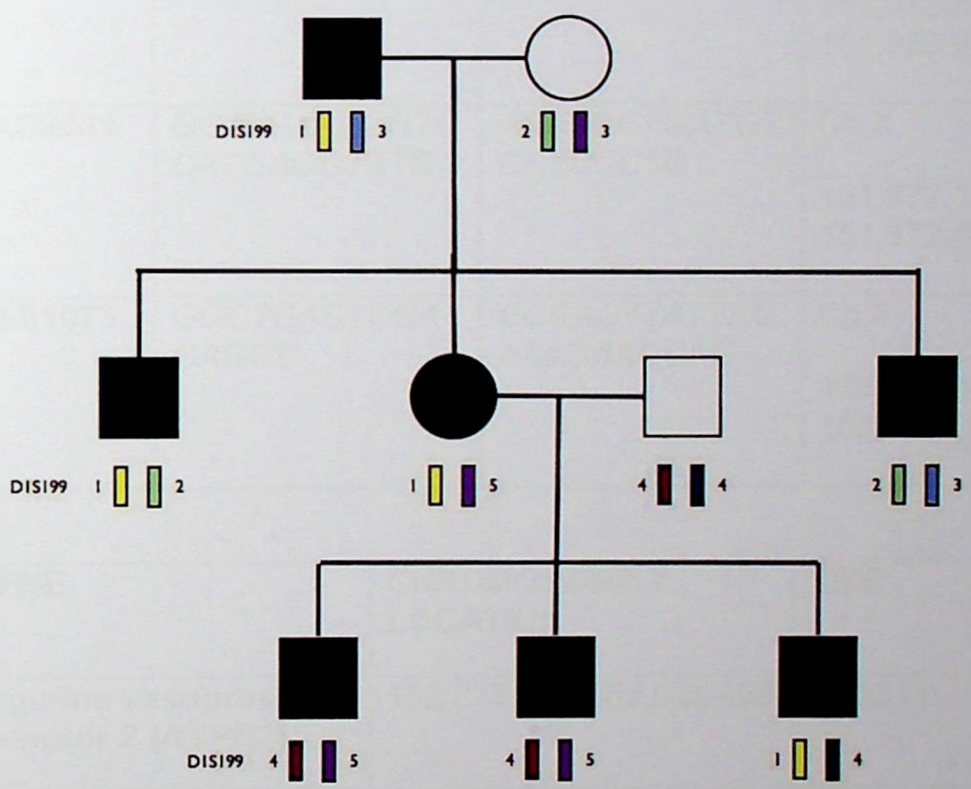

Figure 12. Haplotype of DI family with chromosome 1 marker D1S199, that is adjacent to the loci of the *CLCNKA* and *CLCNKB* genes. There is no evidence of co-segregation of the loci with the disease. The affected individuals do not share a common allele. Though I did not have flanking markers at this locus it is highly unlikely that 3 affected individuals would have recombination events between D1S199 and the genes of interest. This made it highly unlikely that the disease gene was at this locus.

3.6 GENOTYPING OF DI – CHROMOSOME X AND CANDIDATE GENE VASOPRESSIN RECEPTOR 2 (*AVPR2*)

MARKER	FORWARD PRIMER	REVERSE PRIMER	LOCATION	SIZE
DXS8091	*CACATTCAGGTT CCACAGG*	*CAAGATCCAGGC AAAAGTC*	Ch X 147,310,492-147,510,825	200,344 bp
DXS8069	*AACAGTCATTGT AGGCATCG*	*GAATTGCCAGTC ATCCC*	Ch X 151,073,054-151,383,976	310,923 bp
DXS8061	*GCTTGAAGTGTC CATGAGGTATC*	*AGAAGCTGATGT GCTCCCTG*	Ch X 151,672,164 - 151,872,488	200,325 bp
DXS1073	*GGCTGACTCCA GAGGC*	*CCGAGTTATTAC AAAGAAGCAC*	Ch X 153,382,042 - 153,582,362	200,321 bp

GENE	CHROMOSOME X LOCATION	SIZE
Arginine vasopressin receptor 2 (AVPR2)	152,823,622-152,825,429	1,808 bp

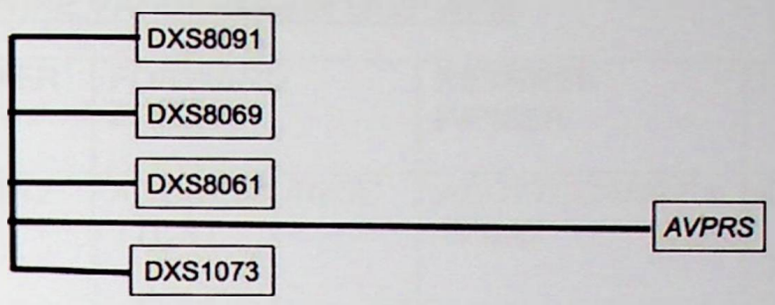

Figure 15. Physical map of Ch18 demonstrating position of DI candidate gene *AQP4* relative to genetic markers D18S819 and D18S1151.

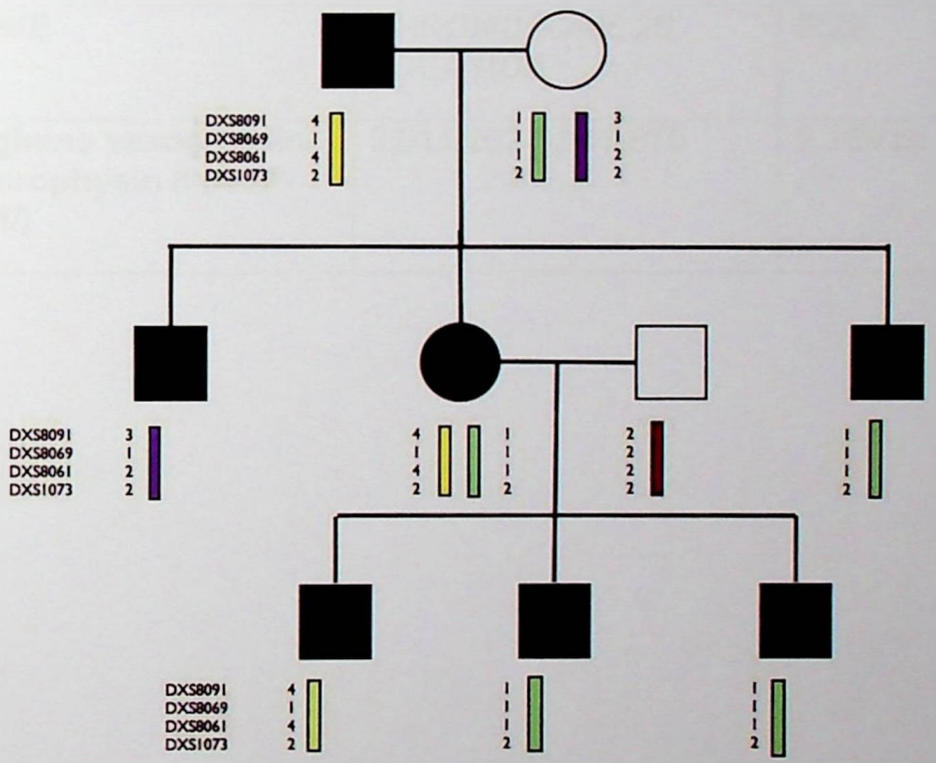

Figure 16. Haplotype of DI family with chromosome X markers. These flank the *AVPR2* gene. This locus was examined, as X-linkage is feasible under the following circumstances. If the grandfather had an AVPR2 mutation (passing this mutation to the affected female sibling) and the grandmother was also an AVPR2 carrier (passing this to the affected male sibling). Though this scenario may seem unlikely AVPR2 mutations are by far the most common cause of what is a rare disease. This hypothesis was therefore worth examining. Though the datasets were not complete it is clear that affected male family members do not share the maternal allele. X-linkage is therefore excluded.

3.7 GENOTYPING OF DI – CHROMOSOME 20 AND CANDIDATE GENE ARGININE VASOPRESSIN (*AVP-NPII*)

MARKER	FORWARD PRIMER	REVERSE PRIMER	LOCATION	SIZE
D20S842	*AGCGCACAGCC TTCAT*	*AGCTTCCANCCA TTCAT*	Ch 20 2,534,204-2,734,509	200,306 bp
D20S181	*ATCCCTCTAAGC ATGGGC*	*GGGTCTCTGTCA ATGGGT*	Ch 1 3,020,512-3,220,894	200,383 bp

GENE	CHROMOSOME 20 LOCATION	SIZE
Arginine vasopressin-neurophysin II (*AVP-NPII*)	3,011,202-3,013,370	2,169 bp

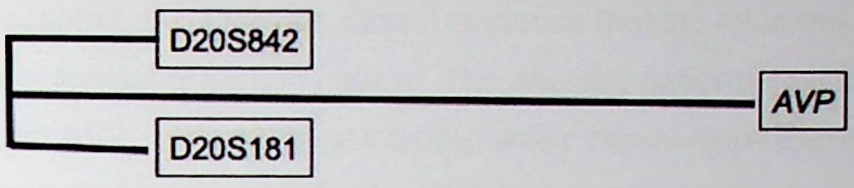

Figure 17. Physical map of Ch20 demonstrating position of DI candidate gene *AVP* relative to genetic markers D20S842 and D20S181

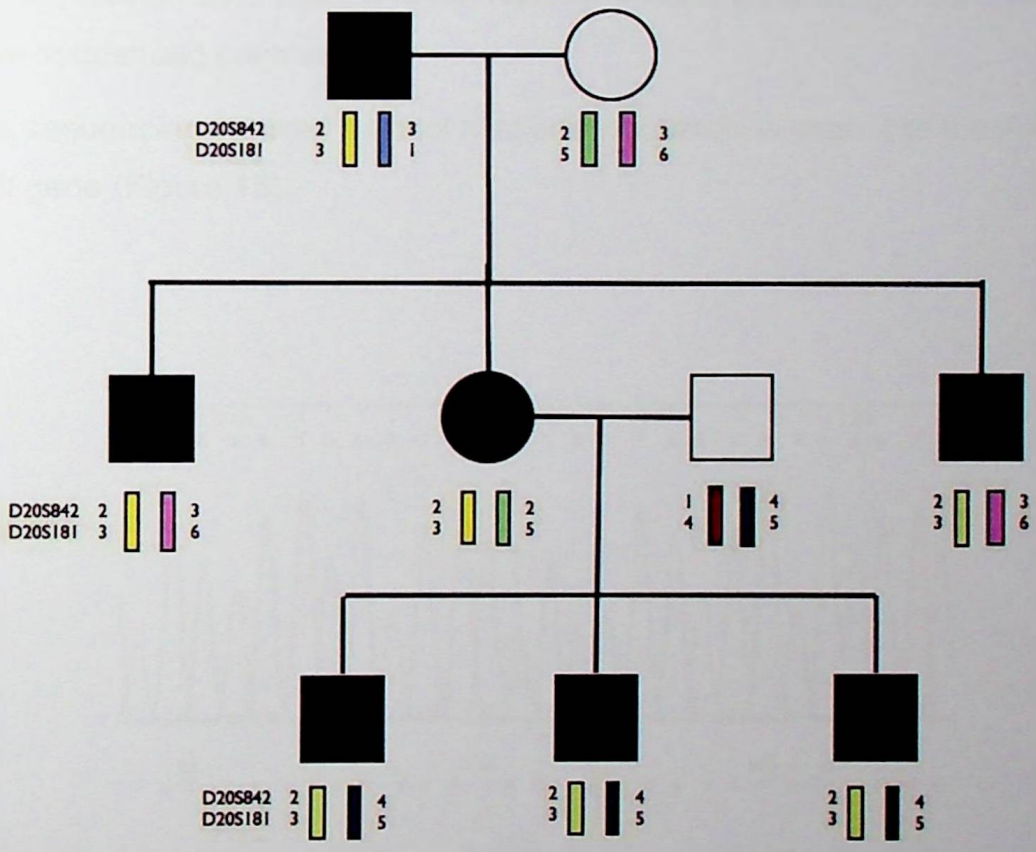

Figure 18. Haplotype analysis with the microsatellite markers *D20S842* and *D2OS181*, which flank the *AVP-NPII* gene. This shows co-segregation of the disease and *AVP-NPII*.

3.8 SEQUENCING OF THE AVP-NPII GENE IN DI FAMILY

We had collated considerable clinical evidence that the DI in this family was neurohypophyseal (FNDI) in nature. The affected patients had undetectable AVP levels, AVP responsiveness during water deprivation testing and typical pituitary appearances on MRI. Genetically we excluded the nephrogenic form (NDI) due to *AQP2* mutation by direct sequencing (N Knoers) and X-linked NDI due to *AVPR2* mutation by genetic linkage. We also excluded potential NDI candidates *CLCKA*, *CLCKB* and *AQP4* through linkage analysis. There was however evidence of genetic linkage to the *AVP-NPII* locus. This and the strong clinical evidence led us to revise the historic diagnosis of NDI to that of FNDI. Having found linkage to the *AVP-NPII* locus we arranged for this gene to be sequenced commercially.

This sequencing showed a novel missense mutation in exon 2 of the *AVP-NPII* gene (Figure 18).

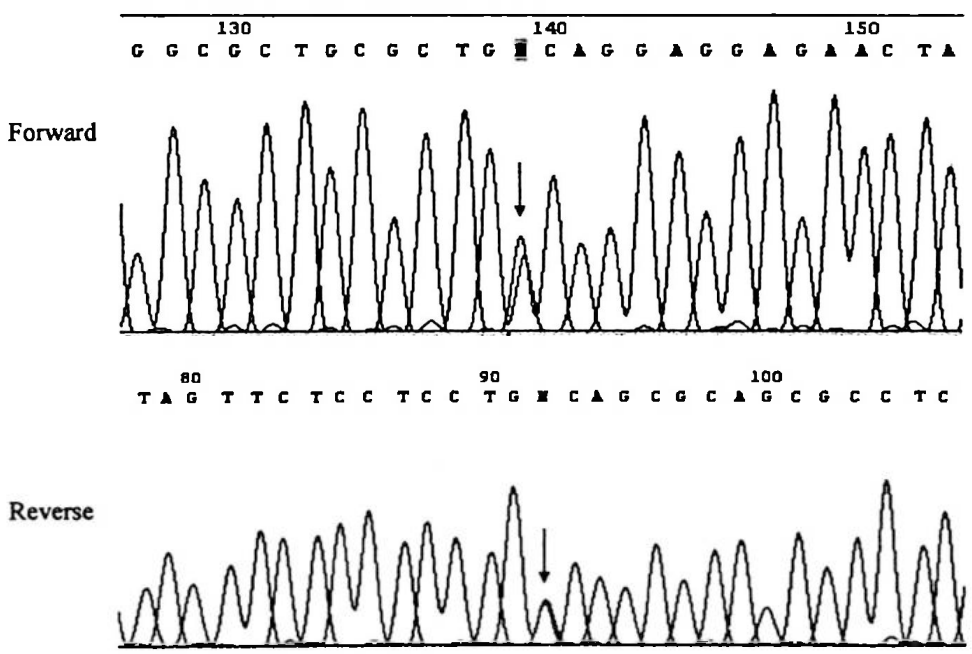

Figure 19. Bidirectional sequencing of AVP-NPII in family X demonstrating a novel missense mutation in exon 2 c.225C>G. All affected family members are heterozygous for this mutation.

SECTION III - CHAPTER 4
DISCUSSION

4.1 FAMILY A, DI PHENOTYPE

Our patient has suffered lifelong, severe polyuria as a consequence of what has been established clinically as familial neurohypophyseal diabetes insipidus (FNDI). We have demonstrated undetectable AVP levels, AVP responsiveness on water deprivation testing and pituitary abnormalities consistent with this diagnosis. The inheritance in this family suggests autosomal dominance, which is the classic mode of inheritance in FNDI. One of the younger family members I felt had mildly dysmorphic facies, and such dysmorphia is recognised in autosomal dominant FNDI.

Our patient (and his affected sister) had both been diagnosed as having the nephrogenic form of DI in the 1960s. As they had been investigated at major teaching paediatric renal units we had initially assumed this classification to be sound, though have subsequently revised this diagnosis. Unfortunately the medical notes from the period of diagnosis are no longer available and it is not clear whether AVP responsiveness was assessed. It is likely that exogenous AVP administration would have substantially improved symptoms in affected family members and may have mitigated against the serious complications seen in our index case.

Severe hypernatraemia has been prevented by early recognition and adequate fluid replacement in infancy. The family provide an anecdote of the grandmother, faced with neonatal vomiting of feeds, grinding vitamins into water for bottle-feeding. Subsequently compensatory thirst and polydipsia will have protected against hypernatraemia.

In our index case significant urinary tract dilatation (with bladder distension and bilateral hydronephrosis) was detected at six years and progressed thereafter. Neither anatomical obstruction or bladder dysfunction was found in spite of exhaustive investigation. Nonetheless he has developed progressive renal dysfunction associated with hypertension, proteinuria and radiologically apparent thinning of the renal cortices.

We believe that "functional obstruction" – chronically high urinary tract pressures due to severe polyuria and incomplete bladder emptying – emerges as the likeliest cause of his chronic kidney disease. The bladder trabeculation

seen on cystoscopy suggests chronically high intravesical pressure. The parenchymal renal damage is likely to represent progressive, irreversible glomerular and tubulointerstitial scarring and will correlate with the kidney damage seen in chronic anatomical obstruction. The incidental right-sided vesicoureteric reflux is the likely explanation of the more rapid decline in function and size of the right kidney demonstrated on the Mag 3 renograms. The increase in polyuria following transplantation was dramatic, as one might expect following grafting of a healthy kidney with a urine volume unmodulated by AVP.

The other affected family members all have severe polyuria and large capacity bladders but have no proteinuria and renal function has been preserved. It is not clear why our patient has, comparatively, done so badly, however, he appears to have had the most severe polyuria. He was able to achieve full bladder emptying when formally tested, thus the problem appears to have been progressive "tolerance" of high intravesical pressures resulting in inadequate micturition, or voluntary retention. There is clearly a complex relationship between bladder distension, intravesical pressure and desire (or willingness given social constraints) to void.

Functional obstruction is a recognised complication of both neurohypophyseal and nephrogenic DI. Urinary tract dilatation has been widely described, including one report of traumatic bladder rupture due to overdistension. Progressive renal dysfunction is uncommon and we believe this is the first report of such a case reaching end-stage renal failure. It is likely that, analogous to anatomical obstruction, there is a period of reversible renal dysfunction, followed by progressive renal damage (120-123).

Early diagnosis of DI is critical to prevent neurological damage from hypernatraemia. If there is a family history of DI, genetic screening of the newborn may be faster and more practicable than clinical testing. In the treatment of central DI, free water replacement is critical. Usually thirst stimulation promotes polydipsia and plasma sodium is high normal. The volumes of enteral water consumed may result in gastro-oesophageal reflux, in which case H2-antagonists, metoclopramide and domperidone may be used to reduce symptoms. Obviously infants, the cognitively impaired and

those with impaired thirst or limited access to water, are particularly vulnerable. Weight, temperature, growth and development should be monitored. If oral intake becomes inadequate, water may be administered through a nasogastric tube. Intravenous infusion of 5% dextrose is an effective way of replacing free water when enteral intake cannot be maintained, but the large volumes required in DI may exceed metabolic capacity and result in clinically significant hyperglycaemia, requiring insulin therapy.

As central DI is a defect of AVP production, it is treated with AVP analogues. Desmopressin (dDAVP) differs from AVP by two amino acid substitutions. It may be administered intranasally, subcutaneously, sublingually or by ingestion. dDAVP is usually introduced as a nocturnal dose prior to establishing a maintenance regime. This will normally require 10-40mg intranasally or 0.2 to 0.8 mg orally, usually as 2 or 3 divided doses. There is a risk of hyponatraemia if a precipitous fall in polyuria is induced, particularly as some patients will be habitually polydipsic. Treated patients may wish to consume more fluids than required for social reasons and will be unable to mount a diuresis as required.

Other pharmacotherapies have been utilised. Chlorporpamide is thought to enhance AVP secretion while carbamazepine may increase renal responsiveness to AVP, though neither of these is used widely in DI. Thiazide diuretics are used in the treatment of nephrogenic DI, often in tandem with salt restriction. They reduce distal tubular sodium reabsorption, increasing natriuresis and causing hypovolaemia. This in turn increases proximal tubular reabsorption of sodium and water, thereby decreasing distal tubular water delivery and polyuria. NSAIDS reduce the renal synthesis of prostaglandins, which in turn inhibit the renal action of vasopressin. They also reduce glomerular filtration and these combined effects mean that they have been used, with thiazides and salt restriction, to reduce polyuria in nephrogenic DI (124-126).

Functional obstruction in DI should be diagnosed as early as possible, indeed we would recommend screening renal tract ultrasonography in patients with severe polyuria, regardless of the cause. Inappropriate surgical intervention,

in the absence of anatomical obstruction, should be avoided. Polyuria should be managed with appropriate medical therapy as described previously. Patients should be advised to monitor their urinary frequency and voiding volumes. Regular emptying (avoiding where possible voluntary retention) is essential. These patients should undergo renal surveillance with serial ultrasonography, GFR measurement and urinary protein-creatinine ratio measurement. If renal tract dilatation, renal dysfunction or proteinuria progresses in spite of conservative measures, other means of bladder emptying, such as intermittent self-catheterisation or long-term suprapubic catheterisation, may be necessary to prevent progressive renal failure (120-123).

4.2 FAMILY A, DI GENOTYPE-PHENOTYPE CORRELATION

4.2.1 Family A Genotype

Initially, as our case had been diagnosed as having the nephrogenic form of diabetes insipidus, we examined candidate genes for NDI. The only known cause of autosomal NDI is mutation of AQP2. Professor Nine Knoers investigated this, with mutation screening of the gene in genomic DNA from this family (supplied by us). No mutations were found. Genetic linkage for the candidate genes *AVPR2*, *CLCKA* and *CLCKB* was negative.

We subsequently demonstrated clear co-segregation of the disease and the locus for the *AVP* gene. Sequencing revealed a novel mutation in *AVP-NPII.* This is a missense mutation in exon 2 (c.225C>G), for which all affected family members were heterozygous. This is consistent with the autosomal dominant inheritance usually evident in kindred's with familial neurohypophyseal diabetes insipidus (FNDI).

4.2.2 The AVP-NPII gene and translation of AVP-neurophysin II

Land et al determined the sequence of AVP and neurophysin II from bovine hypothalamic cDNA in 1982 (127). The *AVP-NPII* gene encodes a precursor protein arginine vasopressin (AVP) as well as neurophysin II and a glycopeptide copeptin. This gene is 2.5kb and resides on chromosome 20 (20p13). Exon I encodes the signal peptide, vasopressin and the NH_2

terminal domain of neurophysin II. Exon 2 encodes the central region of neurophysin II. Exon III encodes the COOH terminal of neurophysin II and the copeptide (Figure 21) (128). Recent transgenic studies have suggested that DNA sequences in the intergenic region downstream of *AVP-NII* may be regulators of cell-expression.

The preprovasopressin protein (prepro-AVP-NPII) is synthesised in the magnocellular neurons of the supraoptic and paraventricular nuclei of the hypothalamus. The protein is translocated into the endoplasmic reticulum of these cells due to the presence of the signal domain. The signal peptide is then cleaved as this AVP prohormone folds, disulphide bridges are formed and glycosylation and dimerisation occurs. AVP is then processed in the Golgi apparatus, packaged into neurosecretory granules in the trans-Golgi network and transported axonally in the stalk of the posterior pituitary. The pre-hormonal precursor undergoes further post-translational modification during axonal transport prior to storage in the posterior pituitary. Neurophysin II acts as a carrier protein, and facilitates transport of AVP along axonal neurons to the posterior pituitary. Here it is stored in herring bodies prior to release in response to a hypovolaemic or hyperosmotic stimulus (Figure 21). Some passes directly the brain and circulation, bypassing pituitary storage.

AVP is a nonapeptide comprising the nine amino acids Cys-Tyr-Phe-Gln-Asn-Cys-Pro-Arg-Gly. There is an internal disulphide bridge between C1 and C6 that results (in the fully processed hormone) in a cyclic N-terminal domain and a 3-amino acid residue C-terminal tail (Figure 20). It has a similar structure to oxytocin, the gene for which resides 8Kb away from the *AVP* gene. This results in some cross-reaction between the two hormones.

The NP-II domain is the largest part of the AVP-NPII prohormone, comprising 93 amino acid residues. Its central region, which is encoded by exon 2, is highly conserved among species. The protein has 2 internal segments that are closely homologous (amino acid residues 12-31 and 60-79). An a-helix and an inter-domain disulphide bridge link these.

The C-terminal domain of the prohormone, copeptin comprises 39 amino acid residues. Its function is not known, thought it has been proposed that it may

help refold misfolded prohormone through its interaction with the endoplasmic reticulum.

Cellular processing and folding of the prohormone is complex. Chaperones and folding enzymes regulate the orderly folding of the prohomone, prevent trafficking of misfolded prohormone and promote degradation of abnormal prohormone by cytosolic proteasome. These chaperones include Grp78, Grp94, calnexin and calreticulin. Sorting within the Golgi apparatus appears to be partly regulated by a sorting signal within amino acid residues 10-27 of neurophysin II. Proteolytic cleavage of the prohormone is necessary to form biologically active AVP. The enzyme Furin appears to provide some cleavage in the ER and Golgi complex. Most cleavage occurs, however, in the secretory vesicles. Enzymes include lysine-arginine calcium-dependent endopeptidase, carboxypeptidase B-like enzyme, peptidyl-hydroxyglycine lyase and an amidating peptidyl-hydroxyglycine lyase. While NPII and AVP reside within the pituitary they retain some reversible, noncovalent interaction then dissociate upon release into the circulation (129-135).

As discussed, AVP is a potent antidiuretic and vasconstricter and its release is mediated by osmoreceptors and baroreceptors in response to osmotic and hypovolaemic stress. The baroreceptors are located in the heart and carotids. Osmoreceptors are located in the nuclei, which manufacture AVP in the hypothalamus, as well as in the anterior wall of the third ventricle. As well as its principal actions of the kidney and circulation (expanded upon in the background chapter of this section) it is a brain hormone, and affects cognitive and behavioural function (such as memory, sexual behaviour, bonding and maternal instinct). It also promotes release of factor VIII and Von Willebrand factor

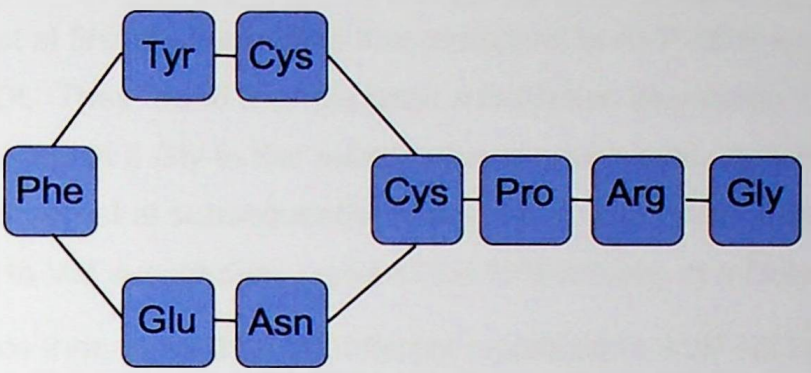

Figure 20. Vasopressin. The cyclical structure is due to the disulphide bond between the cysteine residues.

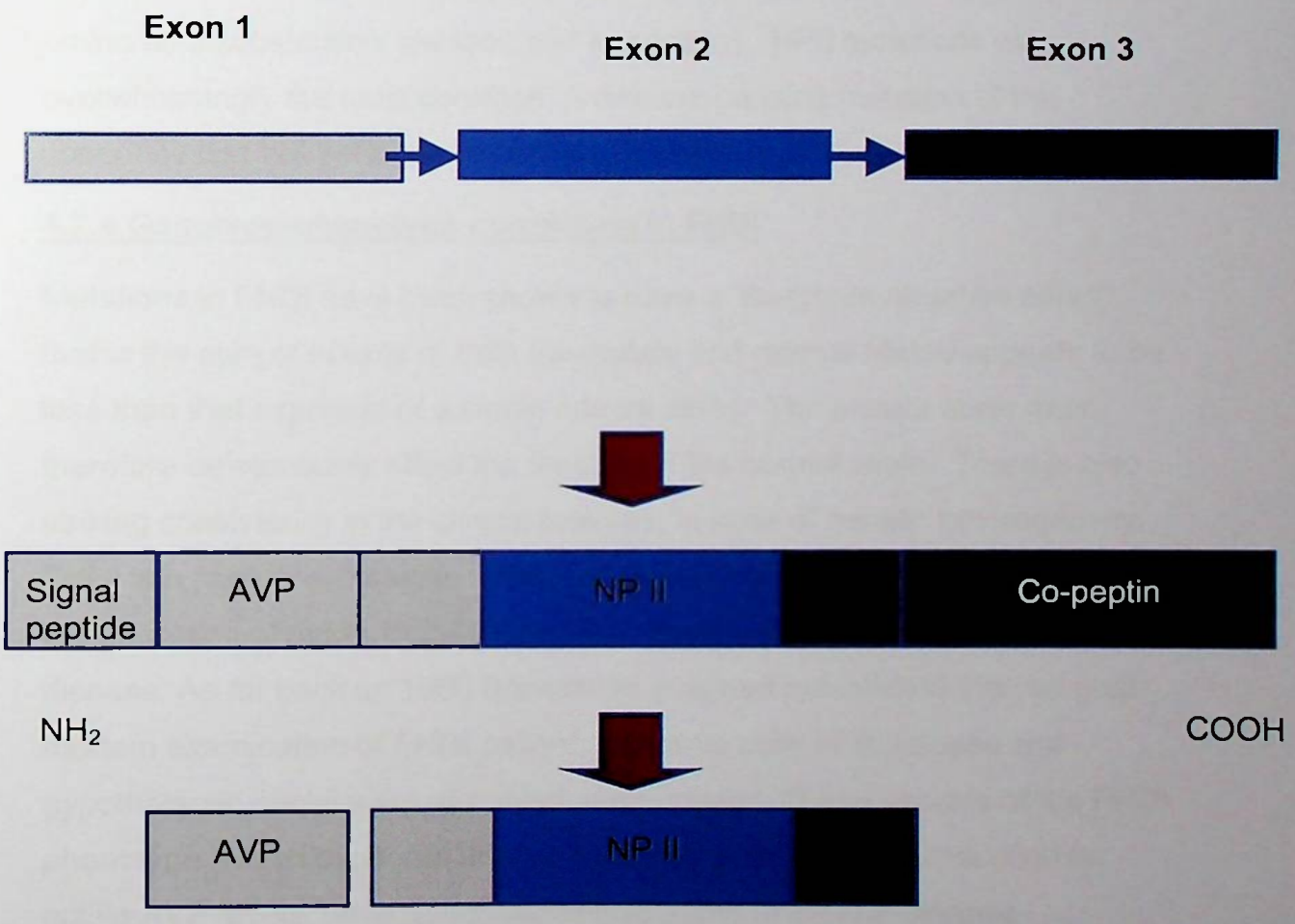

Figure 21. 3 exons on chromosome 20 encode the *AVP* gene. They encode a polypeptide precursor, which comprises a carboxy-terminal peptide co-peptin, the AVP peptide and a mid-molecule peptide called neurophysin II. (Neurophysin I is the equivalent mid –molecule peptide in the oxytocin molecule).

4.2.3 Previously found *AVP – neurophysin II* mutations and FNDI

Ito et al first demonstrated that mutations in AVP-NPII were associated with FNDI. They found a single base substitution at position 1859 in exon 2, resulting in a Gly to Ser substitution at amino acid position 57 in NPII. Bahnsen et al subsequently detected a similar point mutation (resulting in a Gly to Val substitution, again in the NPII moiety, in a Dutch family.

Since then more than 50 different mutations in AVP-NII have been found to be associated with FNDI. These are nearly all single-base substitutions, though dinucleotide substitutions and deletions have been reported.

The mutations are heterogeneous in terms of location (occurring in the signal peptide, AVP and NPII moiety) and effect on amino acid translation (causing amino acid substitution, deletion and truncation). NPII mutations are overwhelmingly the most common. A disease-causing mutation of the copeptide has not yet been identified (136-141).

4.2.4 Genotype-phenotype correlation in FNDI

Mutations in FNDI have been shown to have a "dominant-negative effect", that is the sum of activity of both the mutant and normal alleles appears to be less than that expected of a single normal allele. The mutant allele must therefore deleteriously affect the function of the normal allele. There is also striking consistency in the clinical features, in spite of genetic heterogeneity. FNDI is a postnatal disease, which develops *progressively* in tandem with degeneration of magnocellular neurons. Finally, FNDI is a *degenerative* disease. As far back as 1965 Braverman et al had established that, on post-mortem examination of FNDI patient, the nerve cells of supraoptic and hypothalamic nuclei were atrophied and depleted. These aspects of the FNDI phenotype, which might not be expected from a simple 50% reduction in active AVP levels, have generated considerable interest in disease mechanisms.

It has been hypothesized that abnormal folding and/or dimerisation of the NP-II domain are responsible. This will cause abnormal AVP to NPII binding (which occurs at a single site on NPII) and cause the accumulation of abnormal AVP-NPII complexes in the endoplasmic reticulum. This would also

explain why most FNDI causing mutations are in the NPII part of the prohormone.

In vitro studies, nuclear magnetic resonance imaging and crystallization studies have provided considerable data on NPII folding and binding. Initially 8 disulphide bridges form, which cause NPII to fold. The N-terminal domain of AVP is then inserted into the NPII binding site. For this last stage the α-amino group and phenyl ring of tyrosine are important, rather than the Pro-Arg-Gly tail of AVP. Dimerisation then occurs.

FNDI mutations can be seen to affect this process in several ways. Some mutations interfere with disulphide bridge formation by altering the sequence of cysteine residues while some alter the molecules ability to maintain its structure by eliminating glycine of introducing proline residue. Other mutations introduce stop codons into NP-II, truncating it. Finally mutations may affect AVP to NPII binding due to mutation of the signal peptide domain (which causes cleavage), the N-terminal domain of AVP critical to binding or through mutation of the NPII binding pocket. In vitro and transgenic studies (with bovine or human AVP prohormone) have confirmed that all described FNDI mutations affect folding or dimerisation on NPII.

It has long been hypothesised that this mis-folding/dimerisation leads to retention of mutant prohormone in the endoplasmic reticulum. Dimerisation of mutant and wild-type prohormone will cause retention of both, and a dominant-negative effect. This has now been demonstrated in cell culture. Nijenhuis et al expressed mutant AVP prohomones in neuroendocrine cell lines. These mutants were found to accumulate in the endoplasmic reticulum. These authors, and others, have hypothesised that the progressive nature of the disease, and the pathological degeneration of neurohypophyseal neurons, may be explained by cytotoxic accumulation of mutant prohormone complexes in the endoplasmic reticulum. This has become known as the "misfolding neurotoxicity hypothesis". Russell et al developed a murine model of FNDI. This was a "knock-in" of the previously reported Cys67Ter substitution. The authors demonstrated a progressive FNDI phenotype in the Cys67Ter mice as well as progressive loss of neurons in the periventricular nucleus. The authors concluded that the accumulation of abnormal AVP-NPII

complexes within the ER produces cell toxicity and long-term loss of neurons. More recent cell-line studies have suggested that mutant prohormone may provoke autophagy which, coupled with excitatory stress, leads to neuronal cell apotosis (142-150).

The variability of phenotype, which may be seen between affected members of the same family, can be attributed to the efficiency of the individuals sorting mechanisms in the endoplasmic reticulum, the timing of initiation of therapy (delayed exogenous AVP administration will lead to continued mutant AVP overproduction, accelerating the neuronal degeneration) and the individual's neuronal susceptibility to stress.

Precise clinical evaluation of these patients over time (with repeated water deprivation testing and AVP measurement) is laborious and expensive. The lack of precise clinical data makes it difficult, therefore, to assess differences in phenotypes caused by the various *AVP-NII* mutations. It appears, however, that mutations affecting the NPII domain lead to an earlier onset than those affecting the common signal peptide domain mutation.

The mutation affecting this family is in the highly conserved region of the NPII domain encoded by exon 2 of *AVP-NPII.* As such it is likely that this mutation affects folding of the prohormone, and the relatively early onset of disease in this family is expected. In vitro cell, or indeed transgenic, expression would potentially characterise the functional behaviour of this novel FNDI mutation. This would therefore be worthwhile future work.

SECTION III

AUTOSOMAL DOMINANT RENAL FANCONI SYNDROME

SECTION III - CHAPTER 1

BACKGROUND

1.1 INTRODUCTION

Renal Fanconi Syndrome (RFS) bears the name of Guido Fanconi, a Swiss Paediatrician whose considerable achievements include the definition of several inherited syndromes (including Fanconi anaemia) and his pioneering work on the use of intravenous fluids in children. In 1936 he described the syndrome of "nephrotic glycosuric dwarfism with hypophosphataemic rickets". He based his report on a patient he had reported in 1931, the 2 further cases he had treated and similar cases reported separately by Toni and Debre. Many know the syndrome as "Toni-Debre- Fanconi syndrome", however, the term "Renal Fanconi Syndrome" (RFS) is more commonly used. Fanconi et al described glycosuria with urinary wasting of phosphate, albumin and inorganic acids. He hypothesised correctly that the severe rickets, seen in this syndrome, was a consequence of hypophosphataemia from urinary phosphate wasting (1-6).

We now know that, as well as the glycosuria, aminoaciduria and albuminuria Fanconi described, renal Fanconi syndrome also results in wasting of bicarbonate, potassium, calcium and tubular proteins. This is due to disordered proximal renal tubular reabsorption.

While defects in isolated transporters may result in specific defects in transport function (as in inherited distal renal tubular acidosis), the reabsorptive failure seen in Renal Fanconi Syndrome is clearly more diffuse and may be profound. It has therefore been hypothesised that RFS is a consequence of defects in proximal tubular cellular energy metabolism or generalised changes in the permeability of the tubular epithelium (7-9).

Autosomal Dominant Renal Fanconi Syndrome (ADRFS) is a rare, inherited form of this disease. It causes significant morbidity in affected subjects, many of whom develop end-stage renal failure. In spite of the presumed common genetic defect, the phenotype varies between affected individuals and evolves over decades.

Affected members of the first two families with this condition to be reported (Dent and Harris 1951, Luder and Sheldon 1954) were being followed up in the renal

unit at the Middlesex Hospital when I began my research fellowship. Collating current and historical data on these families would provide an opportunity to characterise the evolution and long-term sequelae of this disease. Determining the underlying disease gene could provide useful information on proximal tubular transport biology, information that might have implications beyond the disorder itself.

In this section I present original research that I, and my collaborators, undertook on ADRFS with the participation of these families. As background I will outline proximal tubular transport physiology, give an overview of RFS in all its forms, and then give an in-depth account on the published reports of ADRFS. I will then present new clinical and genetic data on this condition.

1.2 PROXIMAL RENAL TUBULAR FUNCTION

To achieve adequate waste excretion, the glomerulus produces a massive filtrate and filters many substances almost freely. It is left to the renal tubular structures to save the "baby from being thrown out with the bathwater", avoiding excess depletion of solutes, water and other substances. In this role the proximal tubule is certainly the "workhorse" of the kidney – reabsorbing the majority of organic nutrients, solutes and water. It is left to the more distal tubular segments to "fine-tune" excretion and reabsorption according to the influence of homeostatic control mechanisms.

1.2.1 Reabsorption of organic nutrients

The glomeruli filter large amounts of organic nutrients. The most notable include amino acids and glucose. Others include acetate, acetoacetate, lactate, Krebs cycle intermediates and water-soluble vitamins. These are absorbed actively, usually via co-transport with sodium, against their electrochemical gradients. For some substances reabsorption is 100%, the transport maximum (Tm) for each substance exceeding the filtered load, resulting in reserve reabsorptive capacity.

This may be overwhelmed in disease states such as diabetes mellitus when glycosuria develops.

An enormous range of proximal tubular transporters of organic nutrients has now been identified. It is not possible to describe these in any depth. Amino acids, for example, undergo transport via 16 separate transport systems (e.g. System ASC, System A, System B, System T) and these systems represent families of discrete transporters. Some substrates share transporters, but the system is quite specific and, as a consequence, isolated reabsorptive defects (such as isolated aminoacidurias) may exist (10-14).

1.2.2 Protein and peptide reabsorption

The protein content of glomerular filtrate is low (10mg/L) but it is significant due to the large quantities of filtered fluid (180L/day). Proximal tubular reabsorption is therefore necessary to reduce protein excretion to normal levels (usually less than 100mg/day). This reabsorption may be saturated by excess protein filtration due to glomerular disease.

Filtered proteins bind to specific receptors on the luminal membrane and activate endocytosis. Intracellular vesicles are formed that merge with lysosomes. Proteins are then degraded to amino acid constituents that exit the basolateral membrane into the interstitium and, in turn, the peritubular capillaries.

While the filtration of albumin (the major plasma protein) is limited, smaller proteins such as polypetide hormones are more freely filtered and reabsorption is greater. Several "low molecular weight proteins", such as retinol binding protein, may be measured in clinical practice (10-14).

1.2.3 Bicarbonate reabsorption and ammonium secretion

The kidney facilitates acid-base homeostasis via the reabsorption of filtered bicarbonate and the excretion of titrateable acid. Eighty to eighty five percent of bicarbonate reabsorption occurs in the proximal tubule, ten percent occurs in the thick ascending limb of the loop of Henle and the remainder in the distal convoluted tubule and cortical collecting duct.

Renal bicarbonate reclamation is linked to tubular secretion of hydrogen ions. Filtered bicarbonate combines with these excreted protons and, via luminal carbonic anhydrase, forms carbonic acid that dissociates into water and carbon dioxide. This diffuses into the cell and, again via carbonic acid, dissociates into bicarbonate and hydrogen ions. The latter again exits luminally (providing a continuing source for further bicarbonate reclamation) while the bicarbonate is transported basolaterally. Chloride/bicarbonate exchangers and sodium/bicarbonate co-transporters provide Basolateral bicarbonate transport. H-ATPases, Na/H-co-transporters and H, K-ATPases provide luminal hydrogen ion transport.

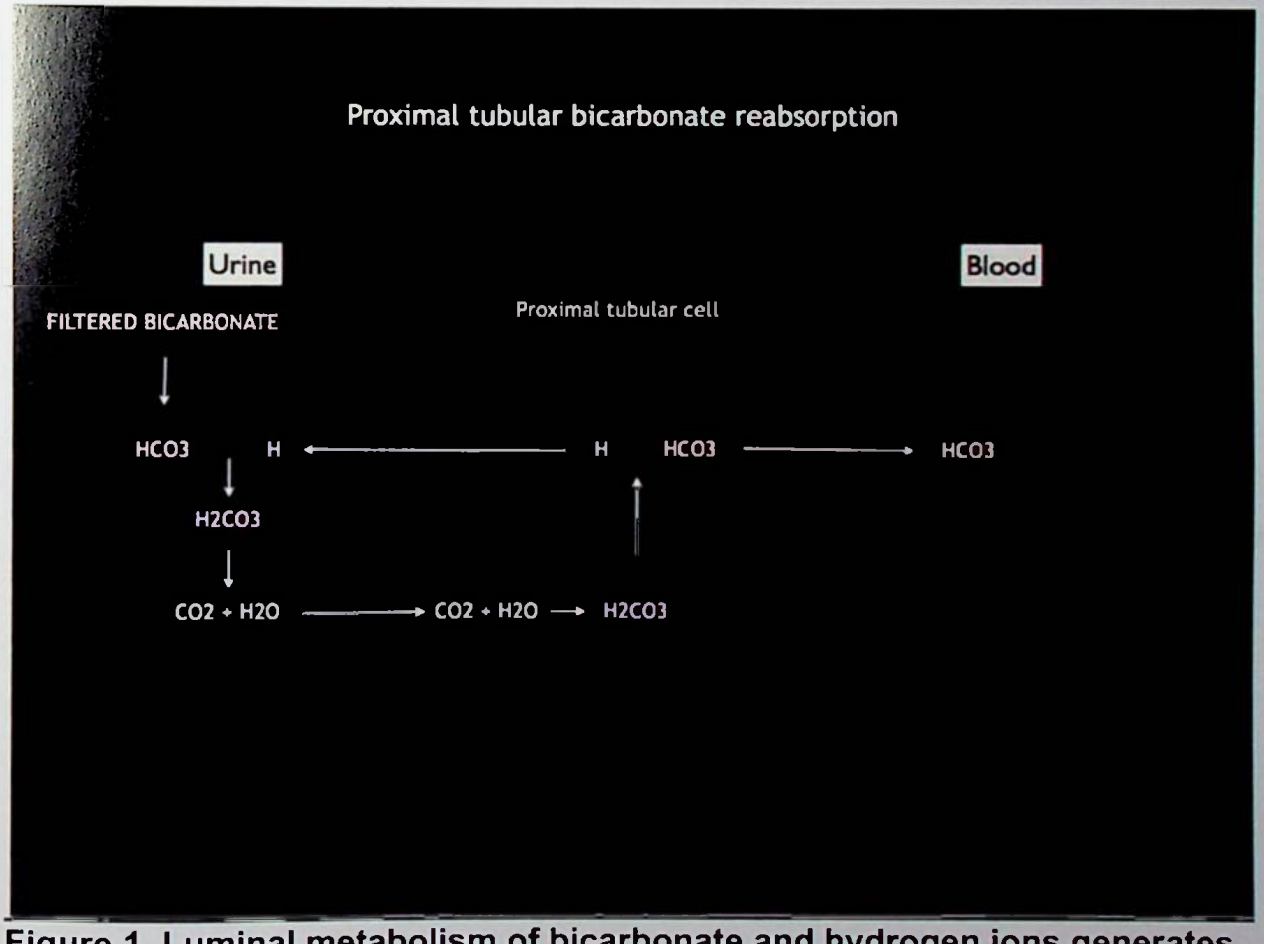

Figure 1. Luminal metabolism of bicarbonate and hydrogen ions generates carbonic acid that dissociates and diffuses into the cell. This is the source of bicarbonate for basolateral transport.

The other main role of the proximal tubule in acid-base homeostasis is in glutamine catabolism. Glutamine is extracted from the glomerular filtrate and peritubular capillary blood. It is hydrolysed to glutamate and ammonia.

Glutamate is metabolised to α-ketoglutarate that is, in turn, metabolised, generating free bicarbonate that is reabsorbed. Ammonia metabolism and excretion is complex, but results ultimately in net proton excretion.

Though proximal tubular bicarbonate reclamation is the aspect of renal acid-base homeostasis that is of relevance to ADRFS several other processes occur distal to this. The majority of the remainder of filtered bicarbonate is reabsorbed in the thick ascending limb of the loop of Henle. In the distal convoluted tubule and collecting-duct the remainder of bicarbonate is reabsorbed. It is also here that the a-intercalated cells secrete titrateable acid and (in response to alkalosis) the b-intercalated cells excrete bicarbonate (15-20).

1.2.4 Sodium, chloride and water transport

Around 65% of filtered sodium is reabsorbed in the proximal tubule. This, combined with sodium reclamation in the loop of Henle and distal convoluted tubule, results in less than 1% of filtered sodium being excreted in the urine. This is regulated by neural and hormonal inputs (such as the renin-angiotensin system). In the proximal tubule, as elsewhere, the majority of basolateral sodium transport occurs actively via the NaK-ATPase. The exit of potassium from the tubular epithelium results in negative polarity in the cell interior that, in turn, facilitates passive entry of sodium from the lumen into the cell. This sodium entry occurs via active transport with organic nutrients (e.g. glucose) or phosphate. There is also counter-transport with hydrogen ions which (as described previously) facilitates bicarbonate reabsorption

Chloride transport may be trans-cellular or paracellular. Paracellular transport of chloride is diffusive. Proximal tubular reabsorption of salt, water and other solutes increases chloride concentration, creating a downhill gradient into the peritubular capillaries into which chloride passes via the intercellular junctions. Paracellular chloride transport is initiated by luminal transport. This is an active process that, in the proximal tubule, is dependent principally on Na, H and Cl/base counter-transporters. Basolateral transport is passive (due to increased

intracellular chloride concentration) and dependent on K, Cl co-transporters and chloride channels.

65% of water reabsorption occurs in the proximal tubule, which is highly permeable to water. Thus solute reabsorption, by the methods described, creates an osmotic gradient that drives water reabsorption. As all proximal tubular solute reabsorption is linked to sodium transport, water and sodium reabsorption are very closely matched (21-29).

1.2.5 Potassium and phosphate reabsorption

The proximal tubule reabsorbs around 55% of filtered potassium. It does this regardless of total body potassium. Conversely the distal convoluted tubule or cortical collecting duct may provide net secretion or reabsorption depending on potassium intake. Proximal tubular potassium reabsorption occurs through paracellular diffusion, facilitated by a 'solvent drag'. This is established by water reabsorption that is, in turn, dependent on sodium reabsorption.

Phosphate is the sixth most abundant element of the body and essential for cell function and bone health. Phosphate balance is controlled by the gut and kidney. Eighty percent of proximal tubular phosphate reabsorption is via the proximal tubule. This is mediated by sodium-phosphate co-transporters (NaPi IIa and NaPi IIc) located at the apical border of the proximal tubular cells. This reabsorption is tightly controlled (according to phosphate balance) by parathyroid hormone, vitamin D, insulin, growth hormone, insulin-like growth factor, cathecholamines, dopamine and serotonin (30-35).

1.3 THE RENAL FANCONI SYNDROME

1.3.1 Clinical features of renal Fanconi syndrome

RFS is a generalised disorder of proximal tubular transport function. Typically, there are variable degrees of phosphate, glucose, bicarbonate, potassium, sodium, calcium and amino acid wasting. This results in a range of metabolic disorders and clinical problems.

The delivery of large amounts of sodium to the distal nephron, and activation of the renin-angiotensin-aldosterone system (due to hypovolaemia) leads to increased potassium secretion. Hypokalaemia often ensues. In acute forms of this disease the hypokalaemia may be precipitous, causing increased myocardial excitability and life threatening cardiac arrhythmias. Profound hypokalaemia may also lead to generalised muscle weakness, paralysis and respiratory failure.

Bicarbonate wasting in RFS causes a hyperchloraemic, normal anion gap metabolic acidosis. This proximal RTA (pRTA) is also known as 'type 2' RTA. Unlike distal RTA, the urine can acidify to a pH of less than 5.4, when bicarbonate depletion is severe (Figure 2)

Tubular reabsorption of phosphate is systematically reduced resulting in reduced serum phosphate. This, alongside reduced proximal tubular 25-hydroxylation of vitamin D_3, renal insufficiency and the aforementioned acidosis (which may in turn cause hypercalciuria) results in abnormal bone metabolism. Various bone disorders may be manifest including rickets, osteoporosis, osteomalacia, and osteitis fibrosa. Chronic forms, presenting in adulthood, may have bony pain and muscle weakness as a consequence of this hypophosphataemia and metabolic bone disease.

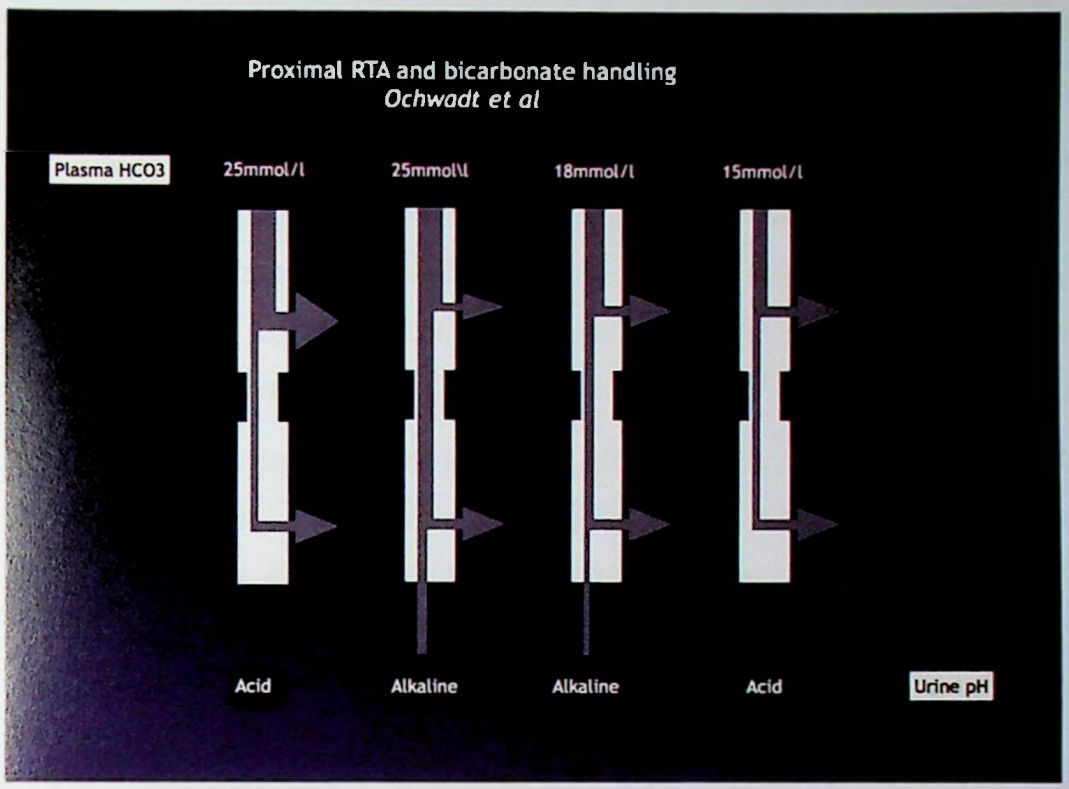

Figure 2. Schematic representation of proximal renal tubular acidosis (pRTA) development. The diagram on the left represents the norm, with around 85% of bicarbonate reabsorption occurring in the proximal tubule and 15% in the distal tubule. A net acid urine is produced. The second left image represents early Fanconi – proximal tubular bicarbonate reabsorption has been reduced, overwhelming distal tubular reabsorption and resulting in urine alkalinity. As serum bicarbonate depletion occurs filtered bicarbonate is reduced and eventually distal tubular bicarbonate delivery is lowered to the point that bicarbonate reabsorption is again complete. Urine acidity then returns at the expense of a low serum bicarbonate. (Adapted from Seldin and Geibisch, The Kidney, in turn adapted from Ochwadt et al, Am J Physiol 1956)

Glycosuria may be present and ranges from 0.5 to 10g/24 hours. This is not sufficient to result in any systemic consequences, and plasma glucose is maintained.

Usually, 98% of amino acids are reabsorbed. In RFS there is *generalised* aminoaciduria, that is, abnormally high excretion of all amino acids that undergo renal excretion. These are quantified by chromatography. Aminoaciduria is most profound in those amino acids that have highest 'normal' excretion such as

glycine, lysine, cystine, serine and histidine. RFS does not lead to amino acid deficiencies and, like glycosuria, is generally tested for diagnostic purposes.

Albuminuria may be present, but usually in much smaller quantities than in glomerular disease. More recently it has become possible to measure excretion of 'tubular proteins'. Excretions of these are diagnostic of proximal tubular injury or dysfunction. B_2-microglobulin and human retinol binding proteins are commonly assayed tubular proteins.

Polyuria is common, particularly in acute RFS. This may relate to a failure to reabsorb sodium. As sodium reabsorption is the osmotic engine for proximal tubular water reabsorption water wasting follows sodium wasting. Normally distal tubular water reabsorption (mediated by AVP) may overcome this, however the hypokalaemia seen in RFS also causes distal tubular dysfunction (36-45).

1.3.2 Causes of renal Fanconi syndrome

RFS may be due to inherited defects or environmental insults.

Inherited RFS occurs most commonly in Dent's disease (X- linked autosomal recessive nephrolithiasis). A typical presentation is with early onset nephrocalcinosis and renal failure. This disease has now been associated with mutations in the ClC5 gene (46,47). Autosomal dominant renal Fanconi syndrome (ADRFS) is a much less common form, and is the subject of the research in this section.

Renal Fanconi syndrome may also complicate a number of inherited systemic metabolic diseases: Fanconi-Bickel syndrome, Wilson's disease, Lowe's syndrome, glycogen storage disease (type I), cystinosis, tyrosinaemia and galactose deficiency (48-56). Fanconi syndrome has also been found to be a feature of inherited mitochondrial cytopathy (57-60). A case of RFS in paroxysmal nocturnal haemoglobinuria has also been described, in which the authors found evidence iron deposition in proximal tubules (61).

Acquired RFS is usually due to a toxic or immunological nephrotoxic insult. Severe tubular toxicity causes acute tubular necrosis (ATN). The causes of this

are legion and include sepsis, rhabdomyolysis, hypotension and nephrotoxic agents including radiological contrast and drugs. Often in cases of ATN the proximal tubule dysfunction is not a dominant feature and renal impairment or distal tubular concentrating defects may predominate.

RFS is more usually a feature of certain *specific* nephrotoxic agents. These include heavy metal poisoning and specific drugs including the chemotherapeutic agents Cisplatin and Ifosfamide and the antiretrovirals Adefovir and Tenofovir (62-75). Acquired RFS may be due to acute or chronic interstitial nephritis (IN), although more commonly IN presents with a decline in renal excretory function. Eosinophilia or eosinophiluria may be present and renal biopsy will show a tubulointerstitial inflammatory cell infiltrate. IN may be drug-induced and has been particularly associated with administration of methicillin, COX-2 inhibitors, cimetidine, sulphonamides and 5-aminosalicylates. IN may also be a feature of certain infections, including leptospirosis, corynebacterium, diphtheria and viral infections, including polyomavirus and cytomegalovirus. Tubulointerstitial nephritis and uveitis (TINU) syndrome is a specific, presumed autoimmune syndrome (76,77).

RFS may also present in light chain nephropathy due to multiple myeloma. Often the urinary excretion of light chains leads to their precipitation in the distal tubule with consequent renal failure (known as cast nephropathy). Less commonly, filtered light chains may be reabsorbed in the proximal tubule, accumulating in the tubular epithelium and causing toxicity, in which case RFS predominates over renal failure. This variation in proximal tubular reabsorption may be a function of specific biochemical characteristics of the excreted light chains. Similarly, RFS has been described from proximal tubular toxicity due to peritubular deposition of amyloid in systemic amyloidosis and in monoclonal gammopathy of undetermined significance (78-86).

Autosomal dominant RFS has also been reported, which causes renal failure as well as Fanconi syndrome. Though this has been genetically localised to Ch15, the underlying gene defect has not been established. This form of RFS is the

subject of the research undertaken in this chapter, and will be described in more detail.

1.3.3 Treatment of renal Fanconi syndrome

Treatment of this condition is directed at the underlying cause (e.g., withdrawal of causative drugs, treatment of underlying Wilson's disease, etc). The remainder of therapy is aimed at replacing pathological losses of phosphate, potassium and bicarbonate, and alleviating metabolic bone disease.

In acute RFS (from for example Cisplatin chemotherapy), intravenous therapy with sodium bicarbonate, potassium chloride and sodium phosphate may be necessary. Formulae exist to calculate total body deficits, however, in the context of ongoing losses therapy must be titrated against response.

More chronic forms are treated with oral therapy. Sodium bicarbonate is commonly used for treatment of pRTA. Potassium may be supplemented as oral potassium chloride. The use of potassium citrate or acetate provides both bicarbonate and potassium supplementation. Sodium chloride supplementation may be necessary if salt wasting is a predominant feature. Phosphate may be replaced as magnesium glycerophosphate or sodium phosphate. Oral vitamin D will not only improve serum calcium, but will improve bone health in osteomalacia. Carnitine supplementation may improve muscle function. Amino acid losses do not require replacement (36-44).

1.4 AUTOSOMAL DOMINANT RENAL FANCONI SYNDROME (ADRFS)

1.4.1 Definitions

In this thesis I have referred to this condition as "Autosomal Dominant Renal Fanconi Syndrome", or ADRFS. In the genetic diseases database Online Mendelian Inheritance in Man (OMIM); it has been given the number **134600**.

OMIM also acknowledges several other names used in the literature for this condition. "Idiopathic Renal Fanconi Syndrome" has been widely used, but it is less satisfactory as this disease is not genuinely idiopathic, but genetic. "Adult

Fanconi Syndrome" has also been used; however, as we shall see, the disease clearly presents in early childhood. "Fanconi Syndrome without Cystinosis" and "Fanconi Renotubular Syndrome" are less commonly used. "Luder-Sheldon Syndrome" has been used, but the syndrome described they later acknowledged as being a classical "Fanconi Syndrome" (which is in itself eponymously titled) and of an inherited variety that appears identical to that described by Dent and Harris in 1954, 3 years prior to the Luder-Sheldon.

1.4.2 Dent and Harris (1951) and Brenton et al (1981)

In their 1951 paper Dent and Harris provide the first report of ADRFS in the literature. This is the main ADRFS family I investigated in this project. Thirty years later Brenton et al revisited this family and described their findings. This is the main ADRFS family we investigated in this project. By the time of Brenton's paper it was clear that the inheritance in the family was dominant rather than recessive. Both papers provide case histories of the affected family members, which I have collated as follows.

DP, the index case for the family, presented to University College London Hospital in 1949. She gave a 6-year history of progressively worsening, generalised bone pains. Clinical examination revealed diffuse bony tenderness. Her illness had been labelled for some time as psychological. Investigations demonstrated renal glycosuria, aminoaciduria, low plasma phosphate and high alkaline phosphatase. There were multiple Looser's zones on a chest radiograph. These linear, fracture-like, radiolucencies are due to poorly mineralised osteoid matrix and are pathognomic of osteomalacia. She was commenced on a high calcium diet, high dose vitamin D and bicarbonate supplementation. Her creatinine clearance at diagnosis was 30mls/min/1.73mls/min/m^2. She developed progressive renal failure and carcinoma of the vulva.

BL, the index case's sister was investigated in 1950, following the diagnosis of ADRFS in her sister. From the Dent paper it appears she had glycosuria during pregnancy on 3 occasions. When assessed by Dent she not only had glycosuria,

but also gross aminoaciduria. She was essentially asymptomatic with no evidence of osteomalacia or renal dysfunction. She died of metastatic cancer of the cervix aged 47. The cervical cancer had originally been treated 12 years previously.

HN index case's brother was also screened after her diagnosis. He had renal glycosuria, aminoaciduria, chronic acidosis and hypophosphataemia. He subsequently developed back and foot pain with bony tenderness on examination. His creatinine clearance at this stage was 48mls/min/1.73m^2. He was commenced on high dose bicarbonate and vitamin D. He died at the age of 66 from recurrent carcinoma of the small bowel.

Another brother PN was also found to have aminoaciduria and glycosuria on screening in 1950. There was a history of peptic ulcer disease and recurrent haematemesis, resulting in a partial gastrectomy aged 38. For 5 years after his renal screening he was asymptomatic, but then developed clinical evidence of osteomalacia (with Looser's zones in both femoral necks), hypophosphataemia and acidosis. He was commenced on sodium bicarbonate and vitamin D. His renal function remained normal; however he died of a myocardial infarction at the age of 51.

DN, the son of PN, was screened for the disease at the age of six and a half. He was found to have only a trace of proteinuria and was not followed up. Subsequently, at the age of 30, glycosuria and proteinuria were diagnosed at an insurance medical. At the age of 32 he presented to Southend Hospital with bony pains and was found to have a femoral Looser's zone. He was referred back to UCH and found to have hypertension and renal impairment, with a creatinine clearance of 55mls/min/m^2. He was hypophosphataemic and hypouricaemic with aminoaciduria and glycosuria. He was treated with vitamin D and antihypertensives.

SN, the son of DN, was screened at age 6 and found to have lactic aciduria, aminoaciduria and elevated urinary b_2-microglobulin.

Patient KP was first seen at the Royal National Orthopaedic Hospital with low backache and pain in his right shoulder. There were no radiological abnormalities, but bone biopsy showed evidence of osteomalacia. He had glycosuria and generalised aminoaciduria. An adenocarcinoma of the colon was resected in 1977.

Patient CP, the son of KP, was found to have (at the time of this publication) glycosuria, mild polycythaemia, hypophosphataemia, aminoaciduria, lactic aciduria and raised urinary b_2-microglobulin. MP, the brother of CP, though asymptomatic, was found to have glycosuria, aminoaciduria and elevated urinary b_2-microglobulin.

The authors pointed out that excess lactic acid and b_2-microgloblin excretion appeared to predate glycosuria and aminoaciduria and that GFR tended to be 30-50% of normal in middle life, with end stage renal failure developing subsequently. They also pointed out a high incidence of cancers in this family (87,88).

1.4.3 Luder and Sheldon (1954), Sheldon et al (1961) and Patrick et al (1981)

The authors present female twins that they treated as children at Great Ormond Street Hospital, London. The first was brought for assessment at the age of 5 due to thirst, anorexia and failure to thrive. It was noted that the paternal grandfather had been found to have "sugar in the urine" but the parents were well. She appeared well, but had moderate growth retardation (the authors, in the vernacular of the time, refer to her as "considerably stunted"), without overt rickets. Chromatography of urine demonstrated marked, generalised aminoaciduria. Proline, lysine, tyrosine, threonine, alanine, glutamine, b-alanine, α-aminobutyric acid and methionine were all present. There were also abnormal quantities of protein, glucose and fructose. A glucose tolerance test was normal.

The twin was also admitted. She appeared in better health and was described by the authors as "...a sturdy, cheerful child. Her weight was slightly low for age, but height was normal." Again, generalised aminoaciduria was present, as well as excess urinary glucose and fructose. These were in smaller amounts than the

twin. Neither twin had evidence of cystine crystals on bone marrow smears (used diagnostically at the time) and renal function was normal.

Their father was also found to have the same urinary abnormalities, but to a much lesser degree than either twin. The authors reviewed the notes on the paternal grandfather had been described as "...a short spare man", weighing only 7 stones. He had been found, at the age of 30, to have glycosuria due to an impaired renal threshold. He also suffered from chronic back pain and intercostal neuralgia. A diagnosis of osteoporosis and then Paget's disease was made. At the age of 56 he complained of severe muscle weakness and, when glycosuria was detected, he was treated with "a diet that rendered his urine sugar free". He developed ketosis and died. The authors felt, justifiably, that he had been misdiagnosed, that he in fact had a unifying diagnosis of Fanconi syndrome and that the carbohydrate restriction initiated when he became ill induced an iatrogenic (and fatal) ketotic coma. The authors do not comment on his renal function at the time of his death.

The disease in this family appears to have been inherited in an autosomal dominant fashion, and has probably spanned 3 generations. At the time of the original publication there appeared to be marked aminoaciduria, glycosuria, fructosuria and mild proteinuria early in life. Phosphaturia was not a major feature in this family. Though there was no evidence of overt rickets, alkaline phosphatase levels were raised in both twins (suggesting osteomalacia), while the grandfather appeared to have bone disease. Renal excretory function was preserved at the time of publication. Given the young age of the twins, this would not imply that this was necessarily a different syndrome to that described by Dent and Harris, and the renal function of the father and deceased grandfather (which we would expect to be abnormal) is not stated. The authors state that the disease gene has "...acted with different force in the three generations", a concept, which we would now describe as "variable penetrance".

Sheldon et al revisited these twins in a subsequent publication in 1961, although it appears this manuscript was presented for publication in 1959. The smaller

twin had developed genu valgum while bony X-rays showed rachitic changes at the end of the long bones, with retardation of bone age to 5-6 years (she was aged 8). She was acidotic and hypophosphataemic, with evidence of a urinary phosphate leak. GFR was calculated at 65% of normal, with a normal intravenous pyelogram (excluding structural abnormalities). The other twin also had a reduced serum phosphate with abnormally high phosphate excretion, though no clinical evidence of rickets. She was also acidotic with a reduced GFR. Both twins were treated with a mixture of injected vitamin D and oral phosphate and this caused a clinical improvement in the rickets seen in the first twin. The authors acknowledged that this syndrome appeared to be the more complete "renal Fanconi syndrome" than they had acknowledged in their first paper. Of note they screened a further sib who had been born since the original paper and appeared to be unaffected. Slit lamp examination as repeated and did not show evidence of Kayser-Fleischer rings, excluding Wilson's disease.

Patrick et al revisited the family in 1981. By this time (27 years on from the original publication) the twin's father had reached end-stage renal failure, had undergone renal transplantation and had died of complications of this. The twins now had significant renal failure that progressive decline in renal function is part of the ADRFS phenotype (89,90).

1.4.4 Smith et al (1976) and Harrison et al (1991)

In this paper Smith et al reported on a large ADRFS family in which the disease spanned 4 generations. The index case, a female, was found to have glycosuria in 1967 at age 17. At the age of 20, she appears to have developed symptomatic osteomalacia (with bony pain and a waddling gait) but this was not diagnosed until 3 years later when she was found to have pathological rib fractures, a proximal myopathy, osteomalacia (confirmed biochemically, radiographically and on bone biopsy), a hyperchloraemic acidosis, tubular proteinuria, glycosuria and aminoaciduria were found (along with proteinuria and glycinuria). She was treated with oral phosphate.

She stated that her father had died of 'nephritis', so the authors re-examined their case. He was found to have renal glycosuria in 1940 at the age of 24. By the time he was 40 he had clinical symptoms suggestive of osteomalacia. At age 46 he had clinical evidence of osteomalacia, hyperchloraemic acidosis and renal failure. Pyelography demonstrated small kidneys, suggesting irreversible renal scarring. His osteomalacia grew progressively worse in spite of supplementation treatment begun in 1964, at the age of 48. Though the authors do not state this it can be presumed he was deemed 'too old' for dialysis – a very restricted therapy in this era. He died of gastrointestinal haemorrhage in 1972 at the age of 58. Certainly uraemia can cause gastritis and ulceration, though no post mortem was done to exclude other gastric pathology.

This patient's brother (the uncle of the propositus) was found (in 1917) to have rickets and then developed knee pain at the age of 18, for which he was treated with vitamin D (for presumed osteomalacia). He was noted to have glycosuria at that assessment. He had further quite serious problems with pathological bony fractures and died, at the age of 32. The cause of death is not clear from the report.

The paternal grandfather of the index case was born in 1884. From the age of 42 years he had problems with traumatic leg fractures (that failed to heal) and muscle weakness. Both of these problems suggest osteomalacia. He was also

reported to have polydipsia. He died at the age of 52. His two sisters became 'deformed' and 'weak' and died at the ages of 45 and 47. The paternal great grandfather appears to also have had 'bony deformities' and died some time before 1920 (under the age of 60). His brother had 'advanced bone disease' and died at the age of 19.

The sister of the index case was investigated by the authors and found, at the age of 31, to have glycosuria, proteinuria, hypophosphataemia, renal glycosuria and generalised aminoaciduria. The 2 children of the propositus were found to have proteinuria, but no other abnormality.

Though the clinical data are not complete there appears to be strong evidence that this family suffered ADRFS. There is clearly a strong family history of bone disease, muscle weakness and premature death. Where this has been thoroughly investigated, osteomalacia has been found. Renal failure and other features of RFS syndrome (glycosuria, proteinuria, aminoaciduria, hyperchloraemic acidosis) were evident. The trait appears to be autosomal dominant.

There is some ambiguity as to whether 4 of the affected individuals in this family had diabetes. They were variously polydipsic and had glycosuria on dipstick testing, though either of these could be attributed to RFS. One patient certainly was diabetic, but overall the evidence does not support a clear association between ADRFS and a diabetic trait, and indeed the authors acknowledge this.

In 1992 Harrison et al published a follow up clinical report on this family. The index case from the Smith et al paper had initially improved with treatment of her osteomalacia with phosphate supplements. At the age of 36 she was found to have significant renal failure with a plasma creatinine of 218mmol/l and a creatinine clearance of 20mls/min^{-1}. She was also hypokalaemic and had evidence of a tubular acidification defect with systemic acidosis, which was treated with oral bicarbonate. She was hypocalcaemic, and vitamin D therapy resulted in secondary toxicity and hypercalcaemia. She was stabilised and her

renal failure (though significant) did not appear to be progressing rapidly. Her children (aged 2 and 6) had not developed aminoaciduria.

The index case's sister, who had been diagnosed in the previous publication, had also developed renal failure with a creatinine of 195μmol/l. Her children had dipstick proteinuria and low plasma bicarbonate levels, but no other features. This report verified that in this syndrome renal failure appears to develop in early adulthood and progresses slowly thereafter (91,92).

1.4.5 Sung-Feng et al (1981) and Lichter-Konecki et al (2001)

Sung-Feng et al reported on an ADRFS family that was subsequently the subject of a genetic positional cloning study by Lichter-konecki et al. The index case had suffered long-bone fractures after relatively minor injuries due to osteomalacia, and had been known to have 'renal glycosuria' for 20 years. She was assessed for renal dysfunction aged 39 and was found to have a reduced GFR at 31ml/min, proteinuria at 1.2 g/24 hours, hyperchloraemic acidosis and a raised fractional excretion of phosphate, uric acid and potassium. Tubular proteinuria was confirmed with urinary electrophoresis and osteomalacia was evident on x-ray imaging. Screening for other causes of RFS (e.g. heavy metal poisoning, Wilson's disease) was negative. Of note her father had died of renal disease in his 40s.

Her son had suffered a traumatic fracture of the left wrist at the age of 11. At the age of 14 he was screened for ADRFS after the diagnosis was made in his mother. He was found to have renal glycosuria and a reduced creatinine clearance at 52 mls/min. Urine electrophoresis showed tubular proteinuria, while plain X-rays demonstrated nephrocalcinosis. A renal biopsy was performed which showed tubular atrophy, interstitial atrophy and calcium oxalate deposition.

Urine chromatography showed generalised aminoaciduria in both patients. A bicarbonate-loading test demonstrated proximal RTA (reduced proximal bicarbonate reabsorption) in the mother but not the son. This may represent, as in other families, phenotypic heterogeneity; though it is possible pRTA may have been a late-onset feature in this family.

Lichter-Konecki et al reported on this same family 20 years later. They had recruited 10 affected and 11 unaffected members across 2 generations. Detailed clinical information on previously unreported affected members was not provided but it can be assumed the phenotype was similar

They performed a genome-wide linkage analysis with a 300-marker set. This yielded a maximal LOD score of 3.01 at marker D15S659. They then performed fine mapping with 24 further markers in this region and defined the disease locus as residing at 15q15.3- between markers D15S182 and D15S143. Maximal LOD scores of 4.4 and 4.68 were obtained. They estimated a physical distance of 3Mb for this region (93).

1.4.6 Long et al (1989)

In this publication the authors present a further case of renal Fanconi syndrome. The patient had been found to have asymptomatic glycosuria and mild proteinuria at a medical for the Navy in 1968, aged 21. Further evaluation showed him to have significantly impaired renal function and heavy, generalised aminoaciduria. He was referred to Leon Rosenberg at Yale and underwent further evaluation. There was little in his history to suggest a harmful environmental exposure, and urinary mercury, arsenic and lead were normal. Blood count, caeruloplasmin, calcium, phosphate and serum electrophoresis were normal. An intravenous pyelogram showed two stones. Bony x-rays showed osteomalacia. The bone marrow itself was sampled and showed no abnormality and neither bone marrow, nor slit-lamp examination, revealed deposition of cystine crystals.

Renal biopsy showed swollen, distorted tubular cells with granulated, vacuolar cytoplasm. Some tubular epithelia were simply flattened. There was medullary interstitial fibrosis.

He was maintained on bicarbonate, phosphate and potassium chloride supplement, and in time required vitamin D supplementations. He also commenced a thiazide, and then a beta-blocker for hypertension. Aminoaciduria,

proteinuria and renal failure progressed. Much of the proteinuria was of the low molecular weight variety.

In 1987 a bone biopsy was performed which showed a mixture of renal osteodystrophy, hyperparathyroidism and osteomalacia. There was reduction in renal size on IVP, consistent with progressive scarring. At this stage he was being worked up for renal transplantation.

His son was found to have cerebral palsy and, in 1986, at the age of 5 years, he was seen by the paediatric nephrology service and found to have generalised aminoaciduria, glycosuria and hypophosphataemia. Again, there was no evidence of cystinosis and it was assumed the child had inherited renal Fanconi syndrome from his father, confirming dominant inheritance (94).

1.4.7 Wen et al (1989)

The authors presented the case of a 39 year-old, white female with osteomalacia (causing recurrent fractures), hypophosphataemia, hypouricaemia, hypokalaemia, metabolic acidosis and renal glycosuria. Acid, bicarbonate and phosphate loading tests confirmed phosphate wasting and type 2 RTA. GFR was reduced. Her 15 year-old son was found to have glycosuria with nephrocalcinosis on X-ray. A percutaneous renal biopsy was performed and this confirmed the deposition of calcium oxalate crystals, interstitial fibrosis and tubular atrophy. Cystinosis was excluded by measurement of leucocyte cystine level, and slit-lamp examination excluded Wilson's disease (95).

1.4.8 Tolaymat et al (1992)

This was a clinical report on a large Afro-American family based in Florida. Their index case presented at two years and six months with vomiting and dehydration. She was found to have rickets, a hyperchloraemic acidosis (consistent with pRTA), glycosuria, aminoaciduria, low molecular weight proteinuria and hyperphosphaturia. Replacement therapy with potassium phosphate, sodium-potassium citrate and vitamin D, as well as a thiazide diuretic (to reduce hypercalciuria), resulted in clinical improvement.

There was a family history of short stature and 'bowed legs' so they proceeded to screen 21 family members for RFS. They performed a clinical examination and bony radiology, as well as 24-hour urine collections and measuring excretion of urate, creatinine, glucose, phosphate and protein (the latter as a surrogate for tubular proteinuria), and serum biochemistry.

Eight family members had rickets while five had short stature while PTH was normal when measured (in five of the rickets patients). Eight patients had hypophosphataemia and seven of these had an elevated fractional excretion of phosphate. One patient had a high fractional excretion of phosphate with a normal serum phosphate. Five patients had hypercalciuria. Thirteen patients had aminoaciduria. Four out of ten tested patients had low-molecular-weight proteinuria. Glycosuria was found in seven patients. Four patients had significant hyperchloraemic metabolic acidosis. One patient had a high excretion of urate.

Renal failure is clearly an important feature of this syndrome in other families and is generally evident by the onset of adulthood. Thirteen of the patients Tolaymat studied were aged thirteen or under, while three patients were under five. Tolaymat presents the serum creatinine levels and 24-hour creatinine clearance measurements. I have calculated eGFR (estimated GFR) values from their age and creatinine data using the abbreviated MDRD calculation correcting for sex and assuming black ethnicity using the following formula

$186 \times (\text{creatinine}/88.4)^{-1.154} \times (\text{age})^{-0.203} \times (0.742 \text{ if female}) \times (1.210 \text{ if black})$

eGFR is only validated for patients eighteen and over, so I have not included eGFR calculations in the paediatric patients. Below are renal function results for all the Tolaymat patients who had any other abnormality that suggested Fanconi syndrome, even if not the full syndrome (96).

Age	Sex	Serum creatinine	Creatinine clearance mls/min (Male 97-137/female 88-126)	eGFR
58	F	97.2	67	66
35	F	88.4	90	82
31	F	79	100	95
24	F	114	69	65
34	F	97	84	73
31	F	128	71	54
29	M	NA	NA	NA
7	F	70	80	x
9	F	53	113	X
2	M	53	73	X
2	F	35	NA	X
5	M	53	103	X
9	M	61	114	X
13	M	88	90	x

Table 1. Renal function data on affected individuals, Tolaymat et al ADRFS family, with calculated MDRD eGFR in adult patients

Serum creatinine is an unreliable marker for renal function (GFR) though it may 'track' *changes* in renal function accurately, particularly in mild renal dysfunction. This is primarily because creatinine production is dependent on muscle mass that, while stable for individual patients, varies between patients. Creatinine also undergoes tubular secretion. Thus, in patients with intact tubular function, it tends to overestimate GFR. The latter also applies to the creatinine clearance measurement, although this is preferable to the simple serum creatinine. eGFR

has been validated, but loses its reliability with GFR>60 mls/min and is not validated in children.

If one examines the eGFR and creatinine clearance values shown in the Table above it appears that renal function is better preserved in this family than in other ADRFS kindred's. Of those with modest renal impairment, it is not clear however whether there were reversible factors, such as intravascular volume depletion, at the time of the investigations. Patient 2 had serum bicarbonate of 10 at the time of the study, so it seems likely that the patient was in the throes of de-compensation and hypovolaemia at the time of renal function measurement. Thus the renal dysfunction in this patient, aged 2, may not represent irreversible, progressive renal damage, as seen in other ADRFS patients.

Regrettably, there are no data on urinary tubular proteins in this patient, indeed the tubular proteinuria and 24-hour urinary protein (which may be a surrogate) data are very incomplete.

Overall, it appears there is a wide variation in phenotype in this family, with some family members apparently expressing less than the full set of traits and some only expressing isolated defects. It also appears that there is mild renal impairment in adulthood. The study is, however, somewhat limited by the variable completeness of the clinical data.

Interestingly Tolaymat et al named their paper 'Idiopathic Fanconi Syndrome in a Family. Part 1. Clinical study". This implied a subsequent genetic study on this family, but this has not yet appeared in the literature.

1.4.9 Other reported cases

Hunt et al presented a large family with this disease. The index case had rickets, short stature, hypophosphataemia, hypokalaemia, acidosis, aminoaciduria, proteinuria, and glycosuria. 6 relatives were screened and found to have isolated aminoaciduria but no bone disturbance. Autopsy and biopsies showed no cystine deposits in tissues (97). Lee et al (1972) presented a further case of idiopathic (presumably sporadically inherited) non-cystinotic renal Fanconi syndrome

alongside two other cases with acquired disease (secondary to myeloma and laxative/enema abuse.) (98).

1.5 AIMS

The aims of this project were to further define the clinical characteristics of ADRFS and to determine the genetic cause of this disorder. This would be undertaken by studying the two kindreds with ADRFS described by Dent and Harris (FAN1) and Luder and Sheldon (FAN2). Members of these families were still being followed up at The Middlesex Hospital. I would, with collaborators, use the following approach

1. I would contact trace affected and family members who might wish to participate in the project.
2. I would clinically characterise affected members and confirm unaffected status in other family members.
3. We would perform linkage analysis, using genomic DNA, to determine genetic locus of ADRFS in these kindreds. Following the publication of the Lichter-Konecki paper, linking ADRFS to 15q, we decided to study this region in the first instance.
4. If linkage to Ch 15 was confirmed, we hoped that recombination events in our families might reduce the size of this large region and narrow the number of candidate genes for this disease.
5. Should we exclude linkage to Ch15, we would deploy a genome wide linkage-analysis approach to determine the disease locus in these families.

SECTION III – CHAPTER 2

MATERIALS AND METHODS

2.1 RECRUITMENT OF PARTICIPANTS AND DNA SAMPLING

I was in contact with 2 affected members of FAN1 family, who we were treating at University College London Hospital. I was also in contact with two patients from the FAN2 family who we were also treating. From these contacts I was able to contact a large number of affected and unaffected family members, who provided blood samples for genomic DNA preparation. The samples were collected from the homes of family members around the South East of England. One FAN1 family member was screened by her GP in Canada and provided us with an "isocode stix" blotted blood sample for DNA preparation.

Two patients from the FAN1 family died during the course of this study. One of these cases was cared for by us, and the family consented to post-mortem examination and sampling of renal tissue. The other patient, who we had not recruited, died in her local hospital in Brighton. She had heard of our research, had bequeathed her remains to us for further research and her family contacted us at the time of her death. The local pathologist performed the autopsy and provided us with both kidneys and blood for DNA extraction that I transported from Brighton to UCL.

The methods used for DNA extraction are described in Chapter I. The majority of samples were collected as whole blood samples. Others were collected as buccal cell swabs and blotting of pinprick blood samples with "isocode stix".

2.2 CLINICAL PHENOTYPING

Clinical data were collated from our own records on the patients we were treating. By far the largest resource of data regarding phenotype and affectation status from our principal family was available from the study performed by Brenton et al published in 1981. For understandable reasons, the family were reluctant to have these tests repeated. These data are presented in detail in the background section above. Other records were acquired from other physicians treating the relevant patients (all affecteds were under the care of nephrology

specialists). We obtained fresh urine samples from several affecteds to perform new urinary proteomics (as part of a separate project). Most unaffecteds had already been screened, however some were screened directly by us or, in 1 case, by the participants general practitioner (in Canada) under my supervision. Two male participants from FAN1, whose affectation status was unknown, were found to have the disease following screening by us.

For screening we performed urinary retinol binding protein assay (performed by Martha Lapsley, St Helier NHS Trust), which we viewed as a gold standard for diagnosis. We also checked for dipstick glycosuria and proteinuria, as well as laboratory measurement of total protein and phosphate excretion. Bloods were sent, where possible, for routine assessment of renal, liver and bone biochemistry. Renal ultrasonography had been performed on all affected participants, and was undertaken in the two newly diagnosed cases. The post-mortem kidney and blood samples from patient PV were taken in accordance with the Human Tissue Act, at the advance directive of the patient and with the signed consent of her son. The post-mortem kidney tissue from patient KP was also taken in accordance with this legislation and with the consent of his son.

2.3 MARKER SELECTION

We selected the markers spanning the 15q region that yielded the maximum lod score for ADRFS in the study by Lichter-Konecki *et al.* Ten markers in all were selected, with an average spacing of 0.5285Mb. We referred to the UCSC genome browser (http://genome.ucsc.edu) and the EnsEMBL database (http://www.ensembl.org) to confirm marker location. In their study Lichter-Konecki *et al* had stated that D15S643 was telomeric to D15S527, when in fact the reverse is the case. Of the markers chosen D15S641, D15S537, D15S222, D15S172, D15S659, D15S161, D15S643 and D15S527 were dinucleotide repeats. D15S182, D15S172 and D15S143 are tetra-nucleotide repeats.

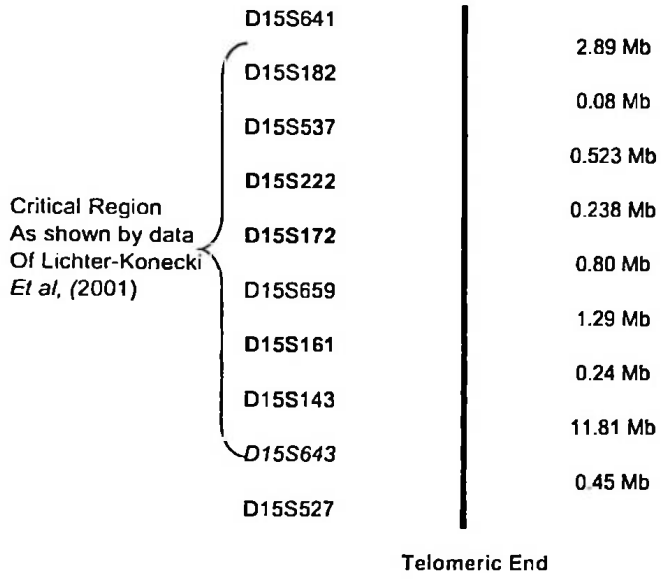

Figure 3. Diagram of selected markers in the 15q15.3 with physical distances (Nicole T Eady).

The markers presented in normal print were included on the "first run" linkage study. The markers in bold were subsequently also included.

2.4 PRIMER DETAILS

All genotyping was performed using the ALFexpress DNA sequencer, the use of which is described in Chapter III. For this system the antisense primers are fluorescently tagged with Cy5, allowing PCR products to be sized by a scanning fluorescent detector as they migrate through an acrylamide gel. The primers were ordered from SigmaGenosys. They were suspended in 1 ml of sterile water at 100nmol concentrations and stored in darkness.

Primer name	Primer sequence	Annealing temperature ^{0}C
D15S641 Forward	AACAAAGGGAGACCCTCATC	61.9
D15S641 Reverse	GACACCCCAGTAGCAATGAG	62.1
D15S182 Forward	GGTGACAGAGTAAGGTCCC	58.5
D15S182 Reverse	TCACCTTGTTGCTCAGACTG	61.7
D15S537 Forward	CCCAGCAGTAATCCCACCATT	66.8
D15S537 Reverse	CTGGTCACTGTCTGTCCTGT	69.9
D15S222 Forward	CCTCAGCGTCCTCTCTTG	61.3
D15S222 Reverse	CTGGTCACTGTCTGTCCTGT	60.4
D15S172 Forward	AGCAAGACGCTATCTCAAAA	59.2
D15S172 Reverse	AGGCTCATCCACTCACATAT	58.5
D15S659 Forward	GTGGATAGACACATGACAGATAGG	61.2
D15S659 Reverse	TATTTTGGCAAGGATAGATACAGG	60.7
D15S161 Forward	TCTGTGATTTTGCCATTATGAG	61.4
D15S161 Reverse	TAAACTGGAATTTTTGACTATGAGC	61.2
D15S143 Forward	CTAAGGAGGCAACAGCAAAG	61.5
D15S143 Reverse	TAAACTGGAATTTTTGACTATGAGC	59.2
D15S527 Forward	TTCCTCCAATGCAATGCAGT	65.5
D15S527 Reverse	CCAGAGCGACAGATACCTA	579

Table 2. Details of primers used in ALFexpress genotyping in FAN 1 and 2 families. The reverse primers were tagged with the Cy-5 fluorophere.

2.5 POLYMERASE CHAIN REACTION

The Galton laboratory has a collection of human genomic DNA from a CEPH (Centre d'Etudes du polymorphism humain) reference family (number 884). These were known to be good quality DNA preparations and were used to test the performance of the ADRFS primers in PCR reactions.

The *Taq* polymerase was purchased from ABgene™ and supplied at 5U/ml. The companies own buffer IV was used, containing 15 mmol $MgCl_2$. Amersham Biosciences supplied dNTPs at a concentration of 2 mM. Sterile water was used as a DNA control for the PCR reactions.

PCR reagent	**Volume (X1)/ml**	**Concentration (X10)/ml**
Buffer IV	1	10
DNTPs	1	10
Primer-forward	0.1	1
Primer-reverse	0.1	1
Abgene Taq polymerase	0.05	0.5
H_2O	6.75	67.5

Table 3. PCR mix for ADRFS genotyping

The Phoenix™ thermal cycler was used for PCR reactions. Annealing temperatures were as described in table 1, or as an average of the forward and reverse primer annealing temperatures when these differed.

The thermal cycler settings are shown below.

Pre-denaturing	95 C for 5 minutes
Denaturing	95 C for 30 secs (x30)
Annealing	58.9-62 C for 30 secs (x30)
Extension of primers	72 C for 30 seconds (x30)
Final extension	72 C for 30 secs (x30)

Table 4. Thermal cycler settings for genotyping PCR

When PCR was not optimal temperature graded PCR was performed to ascertain optimum annealing temperatures. For this the DNA Engine Tetrad, PTC-225 Thermal Gradient Cycler was used for a range of annealing temperatures from 48 to 62°C.

To check PCR product quantity and size, agarose gel electrophoresis was performed as per the method described in Chapter II.

2.6 GENOTYPING USING THE ALFEXPRESS

The ALFexpress was used for the genotyping in this project. This method, including gel preparation, sample loading, gel migration and analysis of results using the supplied Fragment Manager software, version 3.02, has been described in Chapter III.

2.7 HAPLOTYPE CONSTRUCTION

Haplotypes were constructed manually, by selecting haplotypes with minimal recombination events, using the PC software Cyrillic version 2.23.

SECTION III – CHAPTER 3

RESULTS

3.1 CLINICAL PHENOTYPING

3.1.1 Clinical features of ADRFS Family 1 (FAN1)

Patient PV, year of birth 1941

This patient was unknown to us at The Middlesex Hospital. She had been followed up for AD RFS with the renal unit at the Royal Sussex Hospital in Brighton. This had been diagnosed in childhood due to family screening. She had reached ESRF in her late 40s and had been commenced on haemodialysis. She died in 2001, at the age of 60, of non-Hodgkin's Lymphoma and bequeathed her remains to research into Fanconi syndrome. After being contacted by her sons I was able to obtain post-mortem kidney samples, as well as venous blood for DNA

Patient DS, year of birth 1968

I offered this patient, one of the sons of PV, screening for ADRFS in the course of this research. He was found to have retinol binding protein in his urine on 2 occasions with urine retinol binding protein: creatinine ratios of 564 and 799. Renal function was normal and he had no evidence of nephrocalcinosis on ultrasound. He, therefore, had a mild form of the disease and indeed his renal function has remained essentially normal (estimated GFR 79mls/min 2009). He is now followed up at the Royal Free Hospital.

Patient RS, year of birth 1965

This patient, the other son of PV, was traced during the course of my research. He had bilateral ureteric re-implantations at the age of 10 for management of reflux nephropathy. Through most of his childhood and adult life he had glycosuria (without diabetes) and low-grade dipstick proteinuria. Urinary retinol binding protein: creatinine ratio was 8537. He had intermittent loin discomfort, though it is not known to me whether he has radiological evidence of nephrocalcinosis. Electrolytes have remained normal, though he was found to have significant renal impairment with an estimated GFR of 40mls/min and a serum creatinine of 170 μmol/l. This is likely to be due to a combination of renal

parenchymal scarring from reflux nephropathy and progression of ADRFS. Currently, he has long-term follow up at Nottingham City Hospital.

Patient KP, year of birth 1933

This patient was described in the aforementioned papers of Brenton et al and Dent and Harris. He had colonic adenocarcinoma successfully resected in 1997. He presented again with backache in 1978 and was found to have glycosuria, aminoaciduria, and a bone biopsy confirmed osteomalacia. He reached end-stage renal failure in his early-50s and underwent renal transplantation at the age of 58. He developed type II diabetes and progressive graft dysfunction. Renal transplant biopsy showed evidence of diabetic and chronic allograft nephropathy. He had to restart dialysis in 2000 and, after a prolonged period of weight loss and hospitalisation died. Though imaging for malignancy had been negative he was found to have pancreatic cancer at post-mortem. His family consented to my sampling of kidney tissue at post-mortem.

Patient CP, year of birth 1957

This patient, also described early in his illness by Brenton, is the son of KP. He was having follow up at The Middlesex Hospital. He had been found to have renal glycosuria at insurance medical and, at the time of Brenton's report, low normal serum phosphate and elevated urinary amino acids and B_2-microglobulin. Creatinine clearance at this stage (aged 24) was reduced at 51 $mlmin^{-1}/1.73m^2$. Since then he had gone on to develop end-stage renal failure at the age of 45. He underwent cadaveric renal transplantation 4 years later. He has been found to have multiple skin tags and a diagnosis of Lynch syndrome (an inherited predisposition to cancer) has now been made.

Patient MP, year of birth 1960

This patient, the second son of KP, was found (by Brenton) to have asymptomatic elevation of urinary B_2-microglobulin at the age of twenty-one. Though the clinicians who have been looking after him have not been forthcoming with more clinical data, it seems his clinical course has been similar

to that of his brother, and he is reaching end-stage renal failure. He also has diabetes and has been worked up for combined kidney-pancreas transplantation. He has been offered screening for Lynch syndrome.

Patient DN, year of birth 1946

This patient was initially diagnosed at the age of six when his family were screened for the disease. He was lost to follow up initially, but was then found to have glycosuria and proteinuria at the age of thirty. Two years letter he was diagnosed as having osteomalacia, with Looser's zones on bony x-rays of the ribs and femur, hypophosphataemia, generalised aminoaciduria and glycosuria. Since then he has had regular follow up at the Middlesex Hospital, Southend and (following the transfer of renal services from the Middlesex Hospital) The Royal Free Hospital. He has developed progressive nephrocalcinosis, proteinuria and renal failure. He has had persistent glycosuria and low molecular weight proteinuria, and he has been dependent on phosphate, vitamin D, potassium and bicarbonate supplementation.

He has also developed mild coronary artery disease as well as renal stones, and in 2000 had a left ureteroscopy and stone extraction for ureteric obstruction. Currently his estimated GFR is 15mls/min and it is likely he will require renal replacement therapy.

Patient SN, year of birth 1973

This patient, the son of DN, was screened by Brenton et al at the age of 8 and found to have B_2-microglobulinuria and lactic aciduria. It is not clear if he had follow up after this publication, but in 1994 was found to have proteinuria and glycosuria with a serum creatinine of 130mmol/l. After a period of follow up at The Middlesex Hospital his care was transferred to Southend Hospital. He too has developed progressive renal dysfunction and his estimated GFR has now fallen to 38ml/min. He has also become hypertensive and has around 1.5g/24hr of proteinuria.

Screening of other family members

MS (sister of PV) resides in Canada. We asked her GP to measure serum creatinine and 24-hour excretion of phosphate, potassium and protein. These results were normal. She sent us urine for retinol binding protein assay. Retinol binding: creatinine ratio was <5. As she was already middle-aged we were able to conclude that she was unaffected. Her two sons (KS and PS) approached us for screening. KS had a retinol binding protein: creatinine ration of <5, KS had a ratio of 4. Both results exclude ADRFS as expected from the diseases inheritance and unaffected status of their mother. GR (the sister of SN), DP and JP (brother and sister of MP and CP) were also found to be unaffected, as per Brenton's earlier study. A number of affected family members described in Dent and Harris's original paper (SN, BN, JN, and DN) were now deceased and unavailable for further characterisation, or DNA sampling.

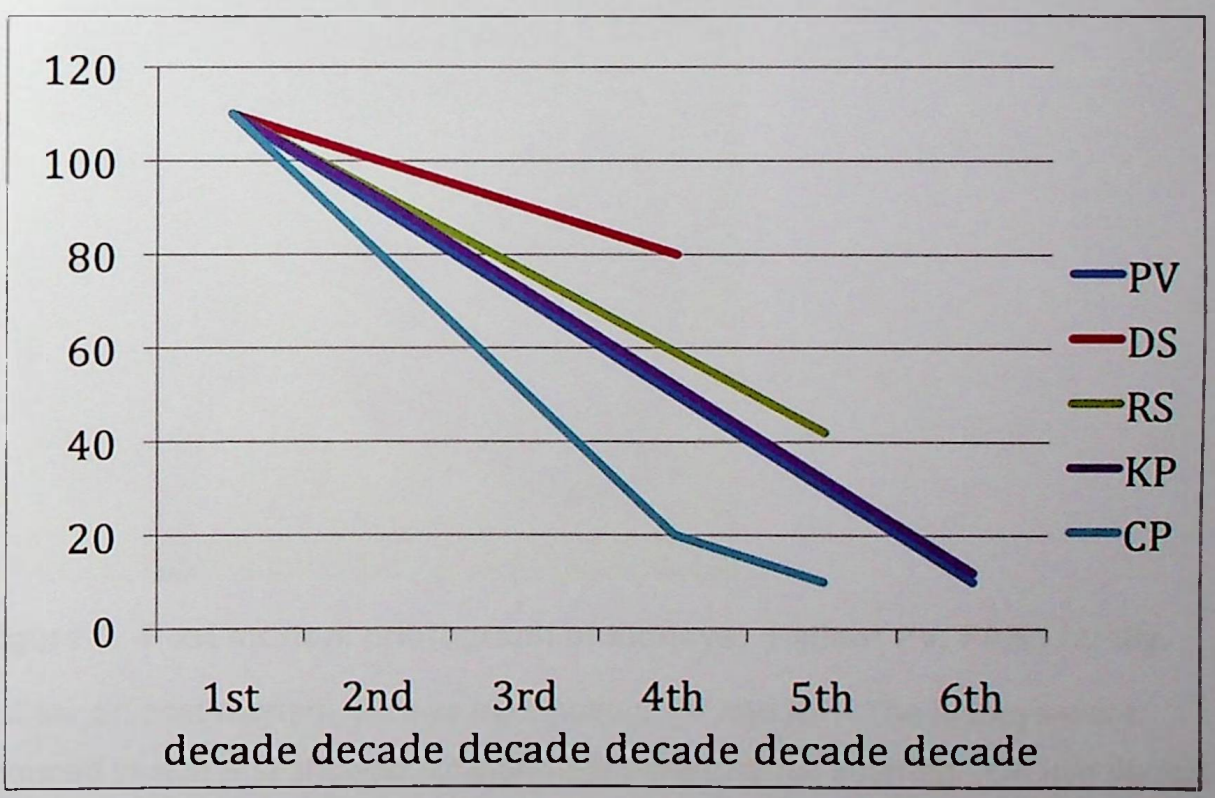

Figure 4. Decline in renal function with ADRFS FAN1 family – data on 5 patients (estimated GFR Vs decade of life)

3.1.2 The FAN1 family and cancer

Of the affected FAN1 members, one patient has had cancer of the cervix, one patient had carcinoma of the bowel, and 1 patient had carcinoma of the vulva. One patient (KP) sadly suffered carcinoma of the skin, bowel and pancreas, the latter proved to be fatal. There does appear, from the data, to be an unusual predisposition to cancer in this family. In view of this history several family members were having surveillance colonoscopy for colonic carcinoma and had undergone formal cancer genetic counselling. There also appears to be a somewhat higher than expected incidence of diabetes in this family.

3.1.3 Renal pathology in ADRFS, FAN1 family

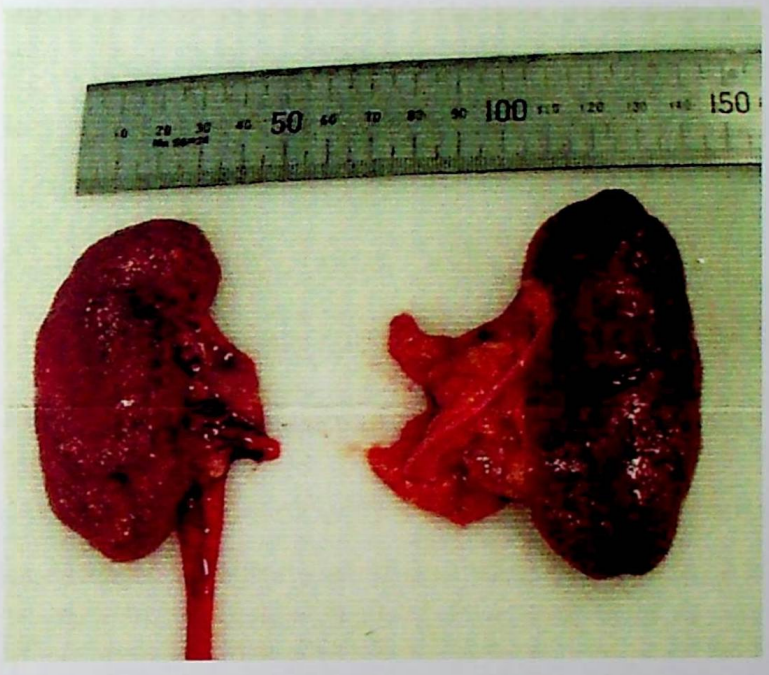

Figure 5. Post mortem photograph of kidneys. Patient PV, FAN1 family.

I obtained post-mortem kidneys from patient PV and KP. The kidneys were reduced in size and showed considerable parenchymal scarring. On histological examination there was nephrocalcinosis, glomerulosclerosis and severe tubulointerstitial fibrosis. As these kidneys were end-stage the findings were fairly non-specific, and the severe distortion of the renal architecture made

detailed ultrastructural analysis (e.g. mitochondrial morphology) of the tubular epithelium impossible.

3.1.4 Clinical features of ADRFS Family 2 (FAN2)

Patient GM, year of birth 1948

This patient, who had rickets in early childhood, had developed progressive renal impairment and reached end-stage renal failure in her 40s. Renal impairment had been first noted at the age of 8 years. She had commenced haemodialysis privately and had continued on this treatment ever since. Urinary retinol binding protein: creatinine ratio, measured in 2000, was 30849. This is a very high level, but advanced renal failure makes interpretation difficult. Her first son, **BM**, was found to have aminoaciduria, increased excretion of retinol binding protein and significant renal impairment (serum creatinine >200) by his early 20s. His half brother **CS**, 3 years his junior, had a similar level of renal impairment at age 20. Retinol binding protein: creatinine ratio was 30849. Both therefore, are affected and are having follow up outside London.

Patient LB, year of birth 1948

This patient had also reached end-stage renal failure in her 40s and underwent cadaveric renal transplantation in 1996. After periods of follow up at the Middlesex and Royal Free renal units her care was transferred to Brighton. She continues to be well with a functioning renal transplant, though she has an increased creatinine at 180 μmol/l, likely related to cyclosporine toxicity.

3.2 GENOTYPING 15q REGION IN ADRFS FAMILIES

3.2.1 Genotyping results FAN1/FAN2

Marker	Ch 15 locus	Size
D15S641	39,531,200-39,731,493	200,294
D15S182	42,423,500-42,623,937	200,438
D15S537	42,502,705-42,703,014	200,310
D15S222	43,132,922—43,333,128	200,207
D15S172	43,263,511-43,463,571	200,061
D15S659	44,061,167-44,261,529	200,363
D15S143	45,590,446-45,790,769	200,324
D15S643	57,401,059-57,601,337	200,279
D15S527	57,854,546-58,054,763	200,218

Table 5. Markers used for genotyping FAN1 and FAN2

Claire Willoughby, Timo Heikkla and Nicole Eady performed the genotyping according to the method outlined previously. After initial work the markers D15S222, D15S172 and D15S161 were added

It proved possible to optimise PCR reactions adequately by the described method, with the exception of the marker D15S161. The latter difficulty persisted in spite of using a range of annealing temperatures and $MgCl_2$ concentrations. Results from D15S641 and D15S527 were incomplete.

As regards scanning fluorescent analysis of genotypes, most of the raw data were adequate for scoring. Some background interference of other bands made

scoring more difficult. Dinucleotide, rather than tetra-nucleotide repeats, were more difficult to score because the allele peaks wee closer together and were harder to differentiate from "stutter bands" (due to polymerase slippage). Several gels had to be repeated to resolve these technical issues.

FAN1 members RS and DS were initially thought to be unaffected due to provisional results from urinary screening. When they appeared to have the disease genotype they were retested and found to have significant excretion of urinary retinol binding protein, and were, therefore, affected.

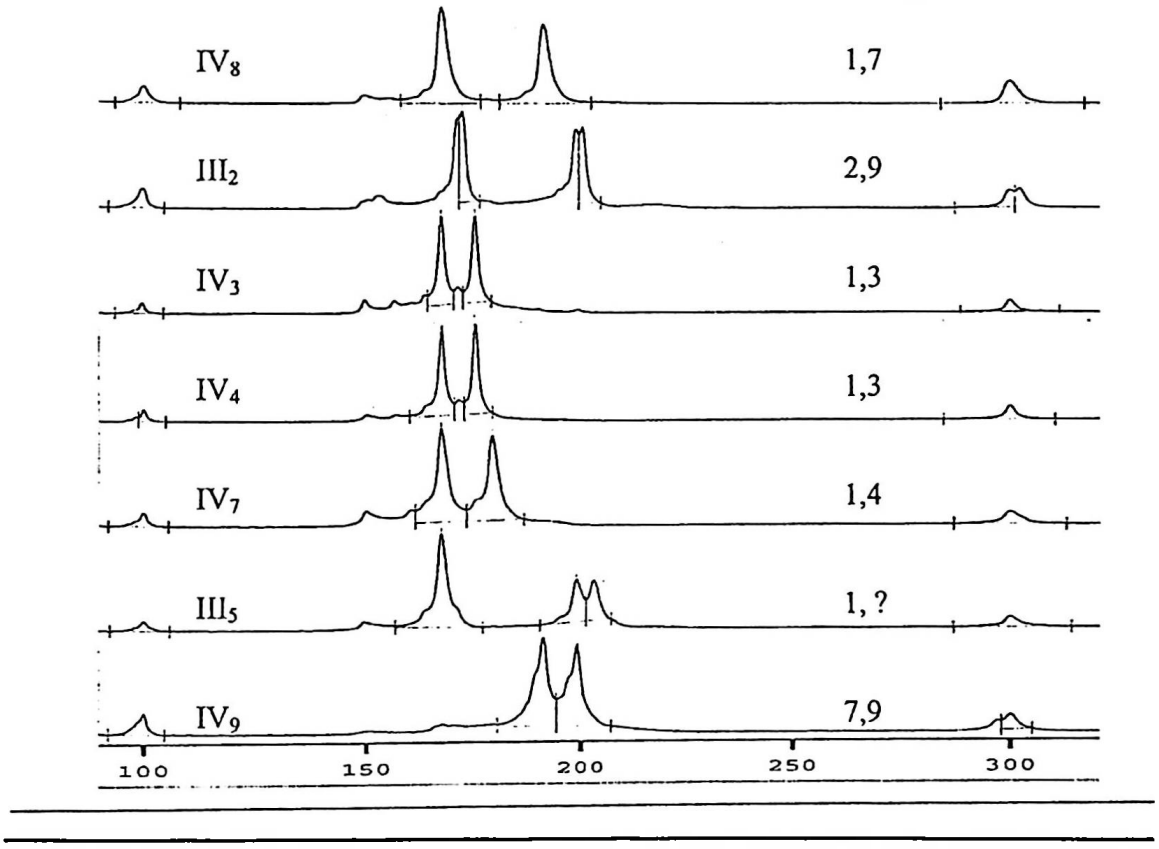

Figure 6. Output from Sigma Genosys Fragment Manager software for the FAN1 pedigree with the marker D15S659. The small peaks to the right and left indicate the 100bp and 300bp markers. The genotype allocations are shown on the right. Individual III_5 has 3 allele peaks, likely due to a somatic mutation.

Individual III_5, who was affected by the disease, displayed three alleles for D15S659. The best explanation for this is that she possessed a mosaic somatic mutation in D15S659 microsatellite region, representing alleles 9 and 10. This would result in her having both the 3,9 and 3,10 haplotypes.

3.2.2 Haplotypes FAN1/FAN2 for Ch15 markers

Following genotyping, haplotypes were constructed by arranging alleles in a manner that resulted in the lowest apparent number of recombination events. Haplotypes are shown below. These results are a collation of genotyping work performed by Claire Willoughby, Timo Heikkla and Nicole Eady.

There is clear evidence of linkage of the ADRFS locus to 15q15.3 in these kindred's. We can say confidently that the disease locus resides between the markers D15S641 and D15S643, a region defined by key recombinations in patients from both families.

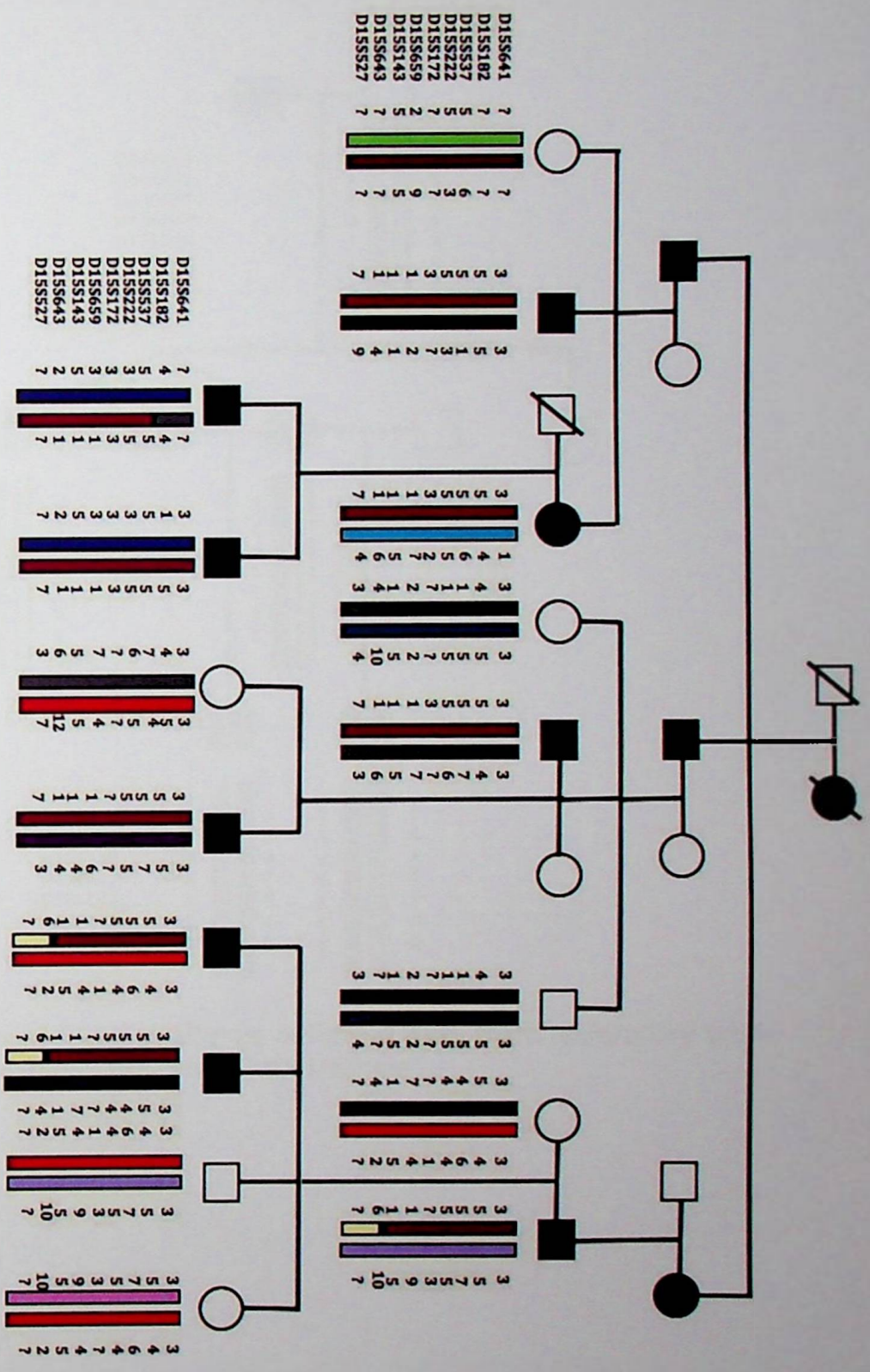

Figure 7. Haplotypes of FAN1 pedigree collating genotyping data from laboratory work performed by Claire Willoughby, Timo Heikkla and Nicole Eady. Genotypes for additional markers D15S222, D15S172 and D15S161 are shown.

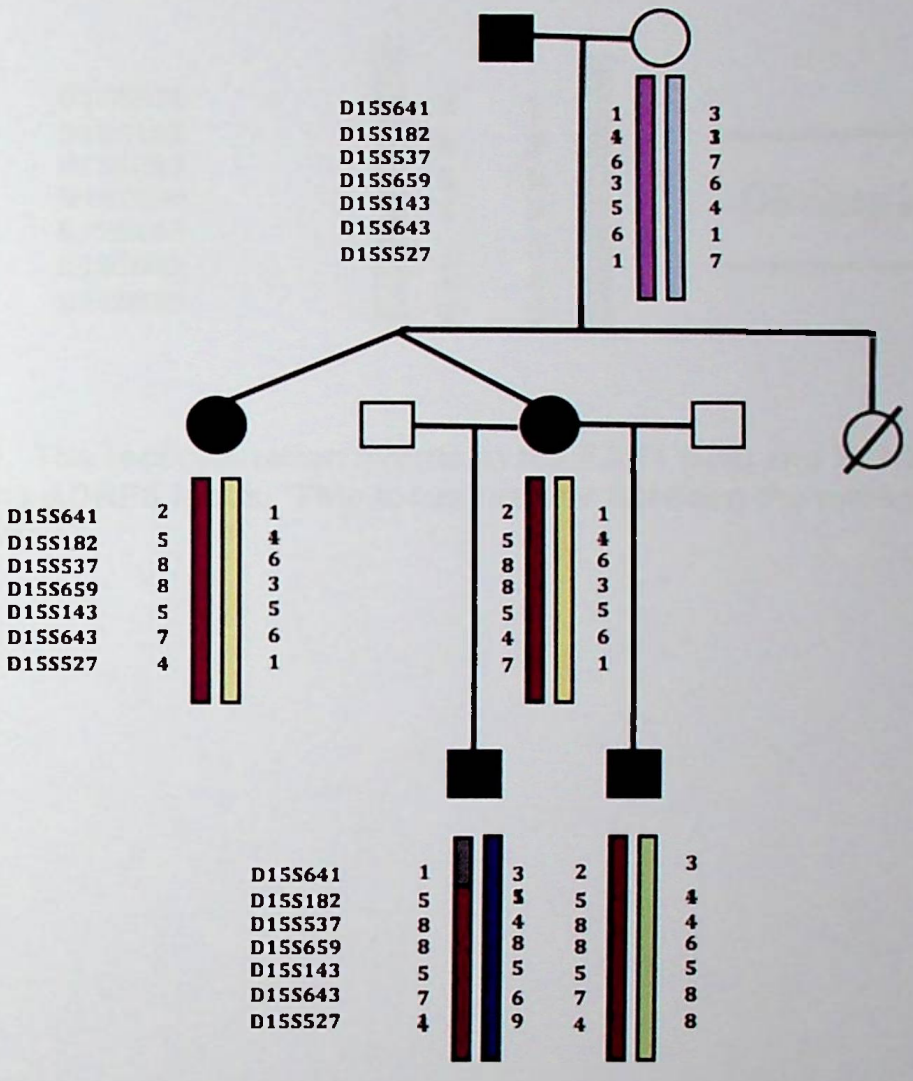

Figure 8. Haplotypes of FAN2 pedigree collating data from laboratory work performed by Claire Willoughby and Timo Heikkla.

Figure 9. The recombination events in the FAN1 (left) and FAN2 (right) that define the ADRFS locus. This locus resides between the markers D15S641 and D15S527.

SECTION III – CHAPTER 4

DISCUSSION

4.1 THE ADRFS CLINICAL PHENOTYPE

In collating clinical data on these families, we have provided further information on the clinical characteristics of this disorder that appears to be one of the more severe inherited nephropathies. From a review of the previously published reports on this disorder (summarised in the background section), and review of the clinical course of the families described in the Dent and Harris 1954 paper (FAN1), and the Luder and Sheldon 1957 paper (FAN2), whom we have studied genetically, several characteristics emerge.

It appears that ADRFS is evident on clinical screening from an early age and has been diagnosed as young as 5 years. Glycosuria appears to be evident in early childhood, as does low molecular weight proteinuria and lactic aciduria. We have used a retinol binding protein assay, but other investigators have used, for example, b2-microglobulin. Aminoaciduria, which is also present at this age, is generalised, severe and proportionate to the normal amounts of various amino acids excreted. This does appear to cause a proportionate fall in serum amino acids, though this is not clinically significant. Dent and Harris suggest that, based on their own report, b2-microglobulin and lactic aciduria precedes glycosuria and aminoaciduria, though other authors have not verified this. It is likely that that estimation of low molecular weight proteinuria (as retinol binding protein or b2-microglobulin) represents the best available 'screening test' for early disease.

Phosphaturia appears to develop later. This is apparent from measurement of urinary excretion, a reduction in serum phosphate or from the development of osteomalacia. Osteomalacia is clearly common in this condition, and is often a presenting feature (with bony pains, rickets or pathological fractures). It has been shown to be arrested/reversed with phosphate and vitamin D therapy. This osteomalacia has had classical radiological appearances, with Looser's zones, reduced bone maturity, reduced trabeculation and reduced bone density all evident. Bone biopsy has shown osteomalacia overlapping with

hyperparathyroid changes and renal osteodystrophy (the latter a consequence of renal failure and reduced vitamin D hydroxylation).

Acidosis is a later, but common feature, and has been shown to be (via bicarbonate loading and calculation of fractional excretion of bicarbonate) type 2 proximal RTA. This necessitates bicarbonate supplementation. Hypokalaemia is also common, the mechanism perhaps being increased NaCl delivery to the distal tubule. This results in 'fast' sodium reabsorption by ENaC. The negatively charged Cl^- in the luminal fluid stimulates K^+ excretion. Potassium supplementation is often also required.

Some patients have been found to be hypercalciuric. Nephrocalcinosis is a common, though not universal, finding on X-ray and has been confirmed on renal biopsy in 2 patients. The latter demonstrated calcium oxalate deposition. Stones are also a common, though not universal finding, are radio-opaque and are likely calcium based.

Renal failure, that is reduction of excretory capacity or GFR, is a striking feature. This is not explained by recurrent pyelonephritis, obstructive nephropathy from stones, or nephrocalcinosis. Stones are uncommon and nephrocalcinosis does not, *per se*, cause renal failure in other diseases, unless it is associated with severe, recurrent infection. Renal failure in ADRFS is often apparent in childhood and results in significant elevations in serum creatinine in adult life. End-stage renal failure by the 5^{th} or 6^{th} decade is common.

Several patients have undertaken dialysis or renal transplantation as a consequence of this disorder. The relationship between GFR and serum creatinine is well known to be exponential, and indeed creatinine rises do not appear to be linear in this condition. When one plots calculated or estimated GFR against time, there does, however, appear to be a steady, linear decline in renal function. I have demonstrated this in FAN1 and FAN2 while Luder and Sheldon demonstrated this in their follow up report of the father of the twins in FAN2.

Renal biopsies and post mortem examination of ADRFS kidneys have shown tubular flattening, tubulointerstitial fibrosis and glomerulosclerosis. These tubular findings are fairly non-specific and present in all tubulointerstitial diseases causing renal failure. The relationship between tubulointerstitial and glomerular scarring (and their relative impact on renal function) is less clear. Glomerulosclerosis is common in chronic tubulointerstitial damage, though the mechanisms of this are not clear.

There is some variation in 'penetrance' in ADRFS, even within kindreds, suggesting that environmental factors (such as diet or other genes working in concert with the ADRFS gene) are contributing to phenotype expression. Luder and Sheldon commented on this in 1957, noting that the father of their affected twins was much less affected than they were, in spite of his advanced years. Another example is patient RS in FAN1. At the time we diagnosed him he had only low molecular weight proteinuria, in spite of being in his fourth decade. Similarly there is considerable variation in the expression of various *components* of ADRFS (such as phosphaturia, acidosis, etc) both between and within families. This is perhaps not unexpected given the complexity of the disease phenotype.

In the Tolaymat kindred renal failure appears to be much less of a feature, often with only stage 3 chronic kidney disease in the 3rd decade (96). This is the only Afro-American family with ADRFS to be reported. Professor Robert Kleta (UCL) and his group have now performed genetic linkage on this family. This confirmed that the disease locus does not in fact reside on 15q in this family. This group do have some data on disease gene localisation for this putative 'Fanconin' gene though I am not able to present this at this stage.

4.2 ADRFS, CANCER AND FAN1 KINDRED

More recently, FAN1 family member CP (the son of KP) was investigated for unusual cutaneous skin lesions. These had been detected during his attendance at transplant clinic. Biopsy, microsatellite instability testing,

immunohistochemistry and mutation screening confirmed a diagnosis of Lynch syndrome due to a mutation in the MSH2 gene. This work was undertaken at St Mark's Hospital in London, which has a special interest in this disorder. The surviving family members have been offered screening for Lynch syndrome

Lynch syndrome, also known as hereditary non-polyposis cancer (HNPCC), is one of several inherited disorders that increase the risk of cancer, in particular, colorectal cancer. Other cancers associated with this syndrome are those of the endometrium, ovary, skin, pancreas, urinary tract and brain. The disorder is autosomal dominant. The great majority of cases are due to mutations in the MLH1 (mutL homolog 1, colon cancer, non-polyposis type 2) and MSH2 (mut S homolog 2, colon cancer, nonpolyposis type 1). MLH1 is at the locus 3p21.3, MSH2 at chromosome 2p21-22. Mutations of these genes result in DNA mismatch repair and microsatellite instability, which is carcinogenic. MLH1 and MSH2 mutations account for 50% and 40% of HNPCC cases, respectively (99-106).

This MSH2 mutation is likely to explain, finally, the predisposition to cancer in FANI. I did consider that carcinogenesis may be an extension of the ADRFS phenotype (due, for example, to mitochondrial dysfunction), but there has been no evidence of cancer disposition in other ADRFS pedigrees. There is no evidence of Ch2 linkage to ADRFS in FAN1, and one must conclude that two distinct autosomal dominant disorders have been inherited in the same family.

4.3 THE ADRFS DISEASE LOCUS AND FURTHER WORK

By demonstrating genetic linkage to 15.q15.3 in 2 affected families we have provided further evidence that the ADRFS locus is at this region. The study reported by Lichter-Konecki at al is the only other report of genetic localisation of this disease. As the latter study was concerned with only 1 family, our study hopefully represents a useful advance in our understanding of the genetics of this condition.

Some markers, such as D15S222 and D15S172, were insufficiently polymorphic to be informative, but the evidence of linkage, from haplotype analysis, is conclusive.

Unfortunately, we were unable to significantly narrow the region of interest from the original Lichter-Konecki study, as we could not demonstrate new recombinations in this region in our families. The disease locus (as shown above) appears to reside between the markers D15S641 and D15S643. Taking the central, flanking end of these markers it appears (from the UCSC browser) that this region extends to 17,669,566 base pairs and around 200 genes. The size of this region, unfortunately, has limited further progress with this project. One might select candidate genes that appear promising of physiological grounds, however the sheer number of possible candidates makes this approach speculative.

The degree of localisation of the gene in this project is limited entirely by the number of recombination events in the family members. There is considerable variation in recombination frequency throughout the human genome with an average recombination rate of 1 cM/Mb. Within this average there is a range of recombination frequencies from "hot" to "cold" spots and, although these have not been well characterised, it is possible that the ADRFS locus resides within a "recombination cold spot".

It is worth noting that there is colonic cancer susceptibility locus within this 15q region. Tomlinson et al reported on a large Ashkenazi Jewish family with a dominantly inherited predisposition to colonic adenoma and adenocarcinoma. No linkage was found to previously identified loci for hereditary nonpolyposis colorectal cancer. They subsequently demonstrated linkage to 15q, with a maximal lod score of 3.06 at marker D15S118. Jaegar et al published similar data linking 15q and colonic adenocarcinoma (107). Park et al performed a high-density loss of heterozygosity study for 13 microsatellite markers spanning 15q15.3-q22.1 in 70 cases of colonic adenoma and adenocarcinoma and confirmed a disease susceptibility locus at this site (108). Daley et al reported on

their colon neoplasia sibling study. Through sib-par analysis they identified strong evidence of linkage between the subgroup of patients with oligopolyposis or young onset and the locus 15q14-q22. Of note these were all European, rather than Ashkenazi, families (109).

Our large Fanconi kindred also have Lynch syndrome, however I have not yet found a family member to suffer cancer without *also* having Fanconi syndrome. One family member, KP, had skin, colonic and pancreatic cancer. If one hypothesised that the Fanconi disease gene also contributed to the cancer susceptibility, which has been mapped to this same region it is conceivable that this gene mutation, with the Lynch mutation on chromosome 2, acted as a 'double-hit' for cancer susceptibility. This is, however, speculative.

There is a recognised association between Fanconi syndrome and mitochondrial disorders. It is seen in inherited disorders such as mitochondrial cytopathy, while Fanconi syndrome is a recognised complication of mitochondrial toxicity seen in highly active antiretroviral therapy. The proximal tubule clearly has high metabolic demands, given its transport functions (57,58,71,75). The tubulointerstitium, particularly in the medulla, has a very low oxygen tension, existing in what is often described as a 'hypoxic precipice'. As such tubular epithelium is susceptible to bioenergetic failure, either due to excessive demand or disordered mitochondrial function. The tubular dysfunction seen in this context is often profound and generalised, resulting in Fanconi, rather than a more specific defect (such as NDI).

Genes involved in normal mitochondrial dysfunction in renal tubular cells would therefore represent good candidates for ADRFS. Within the Fanconi 15q locus resides the *CKMT1B* gene. Creatine kinase isoenzymes encoded by nuclear DNA are cytoplasmic muscle (CKM), cytoplasmic brain (CKB), ubiquitous mitochondrial (CKMT1B) and sarcomeric mitochondrial (CKMTS). CKMT1B has high levels of expression. The mitochondrial creatine kinases appear to be critical to the functional coupling of phosphocreatinine production to oxidative phosphorylation. As such they are essential to bioenergetic health of cells, and

may be particularly important to those cells with high-energy requirements, such as the renal tubular cells (110-117). As the CKMT1B gene resides within our locus it may be worth pursuing as a candidate for ADRFS.

Though I have continued participation in this project I have now largely handed it over to Professor Robert Kleta, a colleague in the Centre for Nephrology UCL. We have considered candidate gene mutational analysis and identification of further families. Due to the improvements in sequencing technology the costs of direct sequencing have been greatly reduced. As such we are considering 'deep sequencing' of the entire ADRFS region. Establishing the genetic basis of this disease will not only enhance our understanding of this condition, which has high morbidity for affected patients, but may also provide further understanding of proximal tubular cell biology.

SECTION IV
AUTOSOMAL DOMINANT RENAL TUBULAR ACIDOSIS

SECTION IV - CHAPTER 1

BACKGROUND

1.1 THE PHYSIOLOGY OF RENAL TUBULAR ACIDIFICATION

1.1.1 Introduction

To understand clinical renal tubular acidosis (RTA) and the role of the kidney in acid-base balance, normal renal acid-base handling must be reviewed briefly. The current model of renal acid excretion depends on the capacity of the renal tubule to reclaim filtered bicarbonate (HCO_3^-) and to excrete net protons (H^+) as titrateable acid and ammonium (NH_4^+). Reabsorption of filtered HCO_3^- takes place mainly in the proximal tubule, while net acid excretion (~1mmol/kg body wt/day to balance what is generated from food and metabolism) occurs in the distal nephron (mainly the collecting duct.

1.1.2 Proximal tubule bicarbonate reabsorption

Filtered bicarbonate (HCO_3^-) is almost completely reabsorbed along the proximal tubule. The mechanism of reabsorption is indirect: H^+ and HCO_3^- ions are generated in tubular cells (facilitated by carbonic anhydrase type II, CA (II)); the H^+ ions are then secreted into the lumen via a Na^+/H^+ exchanger in the apical membrane and the HCO_3^- ions transferred via a basolateral Na^+-HCO_3^- co-transporter (Unwin et al., 2002). There is also some primary active H^+ secretion by an H^+-ATPase. The secreted H^+ ions react with filtered HCO_3^- to form H_2CO_3, which is rapidly converted to CO_2 and H_2O by another form of CA (CA (IV) present in the luminal membrane of the proximal tubule; the CO_2 and H_2O then diffuse into the cell: the net result is removal of a filtered HCO_3^- and its replacement by another in plasma. However, this process is neutral in terms of net urinary H^+ excretion, because the secreted H^+ are used to reclaim only filtered bicarbonate.

1.1.3 Distal tubule and collecting duct acid excretion

Net urinary elimination of H^+ depends on its buffering and excretion as titrateable acid (mainly phosphate - $HPO_4^{2-}+H^+ \leftrightarrows H_2PO_4^-$), and excretion as NH_4^+. Importantly, the production of NH_4^+ from glutamine by the proximal tubule, and its subsequent excretion in the urine, also generates 'new' bicarbonate, which is added to plasma. Availability of phosphate as a buffer depends on its filtration, whereas NH_4^+ depends on normal function of the proximal tubule, as well as a complex process of secretion, reabsorption, and

secretion again along the nephron. The final secretory step for NH_4^+ excretion is 'diffusion trapping' in the collecting duct. Anything that interferes with H^+ secretion in the collecting duct will reduce diffusion trapping and cause a decrease in excretion of both H^+ and NH_4^+[1]. Chronic metabolic acidosis stimulates renal NH_4^+ synthesis and excretion.

The alpha-intercalated cell (a-IC) of the distal nephron secretes H^+ and is responsible for net acid excretion. These cells secrete H^+ into the lumen of the distal tubule and collecting duct via an H^+-ATPase and (possibly) an exchanger, H^+/K^+-ATPase; they also transport HCO_3^- via a Cl^-/HCO_3^- exchanger into the blood (see Figure 1). The Cl^-/HCO_3^- exchanger is homologous with the red cell anion exchanger known as 'band 3' (eAE1)[2]; after the red cell, the kidney is the next richest source of this protein (kAE1). Proton secretion varies with systemic pH and it is also aldosterone-dependent and voltage-dependent (1,2,3).

1.2 CLINICAL FEATURES OF INHERITED RTA

1.2.1 Introduction

The current model of how the nephron reabsorbs HCO_3^- and secretes H^+ has led to a clinical and functional classification of *proximal* (tubule) versus *distal* (tubule and collecting duct) forms of RTA. This represents a move away from previous classifications of types 1 – IV RTA.

1.2.2 Distal (or Type 1) RTA (dRTA)

In dRTA, distal nephron net acid secretion is impaired. This leads to a high urine pH, even in the presence of systemic acidosis. However, there is often no metabolic acidosis and the blood bicarbonate concentration normal - so-called 'incomplete' dRTA - and a defect in renal acid excretion must be demonstrated by a failure to lower urine pH below 5.5 following an NH_4Cl load or a modified frusemide test. Acquired dRTA is often secondary to

---

In uraemic acidosis, urinary excretion of NH_4^+ and titrateable acid are also decreased, but unlike in the distal form of RTA, urine pH is low, and when the amounts of titrateable acid and NH_4^+ excretion are corrected for the low GFR, both are normal or increased.

[2] It is known as 'band 3', because of its relative position on gel migration analysis of red cell membrane proteins.

autoimmune diseases, such as Sjogren's syndrome. Inherited dRTA is rare and there are essentially 3 types: autosomal dominant dRTA (the commonest form) and autosomal recessive dRTA with and without sensorineural deafness. There is another inherited condition, pseudohypoaldosteronism type II or Gordon's syndrome, which while it can be associated with a form of dRTA (and hyper- rather than hypo-kalaemia), it is not usually regarded as a true genetic type, i.e., directly linked to mutation of an acid or base transporter (see later)[3].

In the complete forms of both dominant and recessive dRTA bone disease is common (rickets or osteomalacia), as well as nephrocalcinosis (often) complicated by renal stone disease. The occurrence of renal stones is attributed to the combination of hypercalciuria, low urinary citrate excretion (due to systemic and intracellular acidosis) and high urine pH, all favouring calcium phosphate stone formation. Hypokalaemia, another characteristic feature, is less troublesome than in the acquired autoimmune form of dRTA, but it can become symptomatic (though its cause is still unclear), especially if a thiazide diuretic is prescribed to reduce hypercalciuria. In recessive dRTA, some patients suffer from sensorineural deafness, which can be late in onset (2,3,4).

1.2.3 Proximal (or Type 2) RTA (pRTA)

In pRTA, reabsorption of bicarbonate is impaired, leading to 'bicarbonate wasting' and, at least initially, a high urine pH. As plasma HCO_3^- levels fall and the amount of filtered HCO_3^- decreases, urine pH eventually becomes more acid (unlike in dRTA). The extent of the HCO_3^- leak can be judged by intravenous loading with $NaHCO_3$ and recording a high fractional excretion of HCO_3^- (>15%). Hypokalaemia often occurs due to the osmotic diuretic effect of the 'wasted' HCO_3^-, but nephrocalcinosis and renal stones are less common than in dRTA, perhaps due relatively normal citrate excretion.

Proximal RTA typically manifests as part of a generalised defect of proximal tubule function, namely the renal Fanconi syndrome (with glycosuria, low

[3] An autosomal dominant form of this syndrome has been characterised with a gene defect encoding a protein whose exact function is still incompletely understood (Wilson et al., 2001).

molecular weight proteinuria, urinary phosphate wasting, hypophosphataemia and hypouricaemia). Isolated pRTA occurs rarely and usually presents as growth retardation in childhood. Like dRTA, it can be divided into 3 types: autosomal recessive pRTA with ocular abnormalities, autosomal recessive pRTA with osteopetrosis and cerebral calcification, and autosomal dominant pRTA.

Autosomal recessive pRTA with ocular abnormalities is the commonest form of isolated and inherited pRTA, but even this is rare. Ocular abnormalities include band keratopathy, glaucoma and cataracts. Short stature is usual; dental enamel defects, mental retardation, hypothyroidism, abnormal pancreatic function and basal ganglia calcification are also features. In inherited CA (II) deficiency, isolated pRTA presents with osteopetrosis (due to impaired osteoclast function), cerebral calcification and variable mental retardation (Sly et al., 1983). Although this form of inherited RTA is clinically more proximal in type, it can also present with a mixed proximal and distal phenotype, which reflects the presence of CA (II) in cells all along the renal tubule (2,3,4).

1.3 THE MOLECULAR BASIS OF INHERITED DISTAL RENAL TUBULAR ACIDOSIS

1.3.1 The electroneutral anion exchanger, AE1

The Cl^-/HCO_3^- anion exchanger AE1 is one of a family of anion exchangers (Alper, 1991). It is abundant in the red cell membrane (eAE1). Here, it's NH_2-terminal 40kDa cytoplasmic domain provides a membrane anchorage site for the red cell cytoskeleton, playing a key role in maintaining its structural integrity. Here, it also has a key role in normal gas exchange (CO_2 transfer). The C-terminal 55kDa membrane domain (Tyr_{359} to C-terminal) provides anion transport function. It is also expressed in the basolateral membrane of the collecting duct acid secreting a-IC cell, though as a truncated form (kAE1). Here the 65 NH_2 terminal residues are absent, with a renal promoter in intron 3. kAE1 transports intracellular HCO_3^- out of the cell in exchange for Cl^-. The membrane domain has 12 spans, a high proportion of which are α–helical.

The *AE1* gene has been completely sequenced and is designated *SLC4A1* on chromosome 17; it is a member of the *SLC4* gene family, comprising 10 genes of which 8 encode bicarbonate (or carbonate) ion transporters, including the electrogenic Na^+-HCO_3^- co-transporter, NBC1, present in the proximal tubule (see later) (Romero et al., 2004). The related anion exchanger pendrin (*SLC26A4*), also known as AE4, is sited apically on the HCO_3^- secreting b-IC; although pendrin mutations can cause deafness in humans, dRTA has not been reported (4,5,6).

Several inherited mutations of the *AE1* gene have been found to cause red cell disorders such as hereditary spherocytosis (HS) and Southeast Asian Ovalocytosis (SAO) (7). SAO in heterozygous form appears to be a benign abnormality of red cell morphology that is endemic to Southeast Asia, possibly because it may provide some protection against cerebral malaria (7,8).

Early case reports had suggested an association between SAO and dRTA, which in light of AE1's physiological role in the a-IC prompted Bruce *et al* to investigate it as a candidate gene for autosomal dominant dRTA in Caucasian patients. Though red cell morphology was unremarkable, initial studies of red cell band 3 protein found slower migration than normal on gel electrophoresis. Genetic linkage analysis was significant for a marker close to the *SLC4A1* locus and gene sequence analysis of *AE1* showed distinct and family specific point mutations in exons 14 or 15, producing R589H, R589C or S613F amino acid substitutions. An inhibitor of anion exchange, the stilbene derivative DIDS, was used to titrate SO_4^{2-} (a more easily measured substitute for Cl^-) influx across the red cell membrane to measure band 3 transport activity. While SO_4^{2-} influx was reduced by ~20% (compared with controls) in those subjects with the R589H mutation, it was significantly *increased* in subjects with the S613F mutation who were phenotypically similar. Furthermore, when the band 3 mutants were heterologously expressed in *Xenopus* oocytes they showed no consistent reduction in measured Cl^- transport.

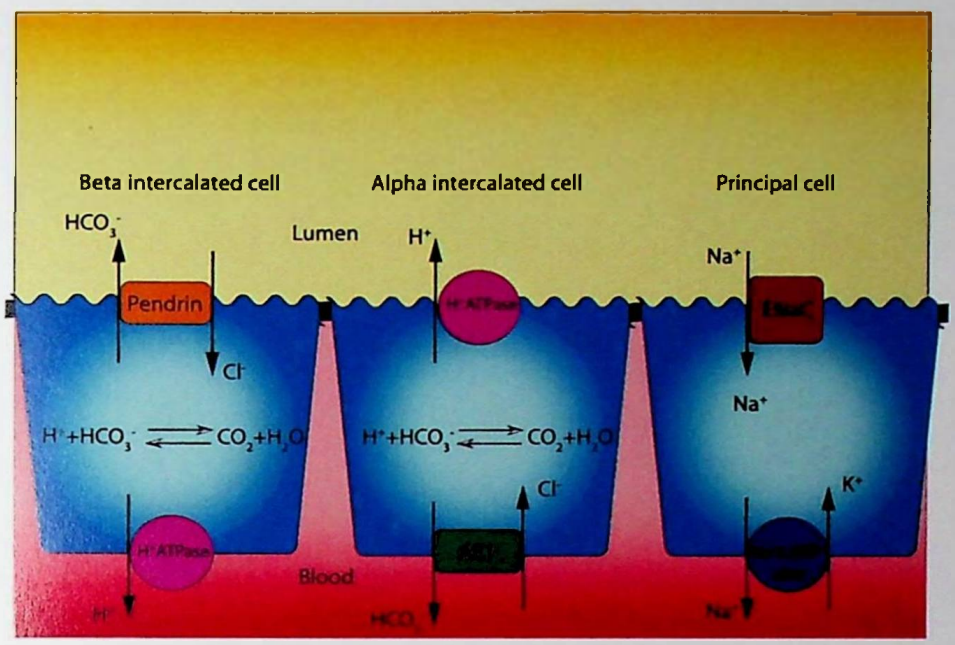

Figure 1. Distal tubular epithelial cells and their contribution to acid-base homeostasis.

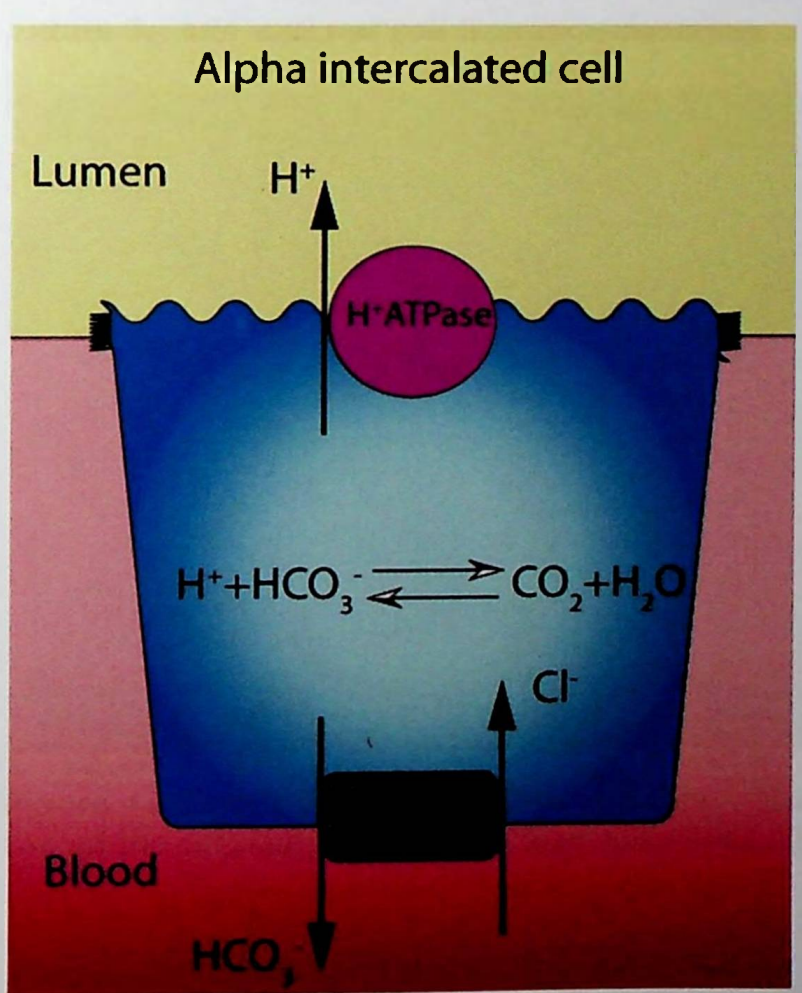

Figure 2. Transport function of the alpha intercalated cell.

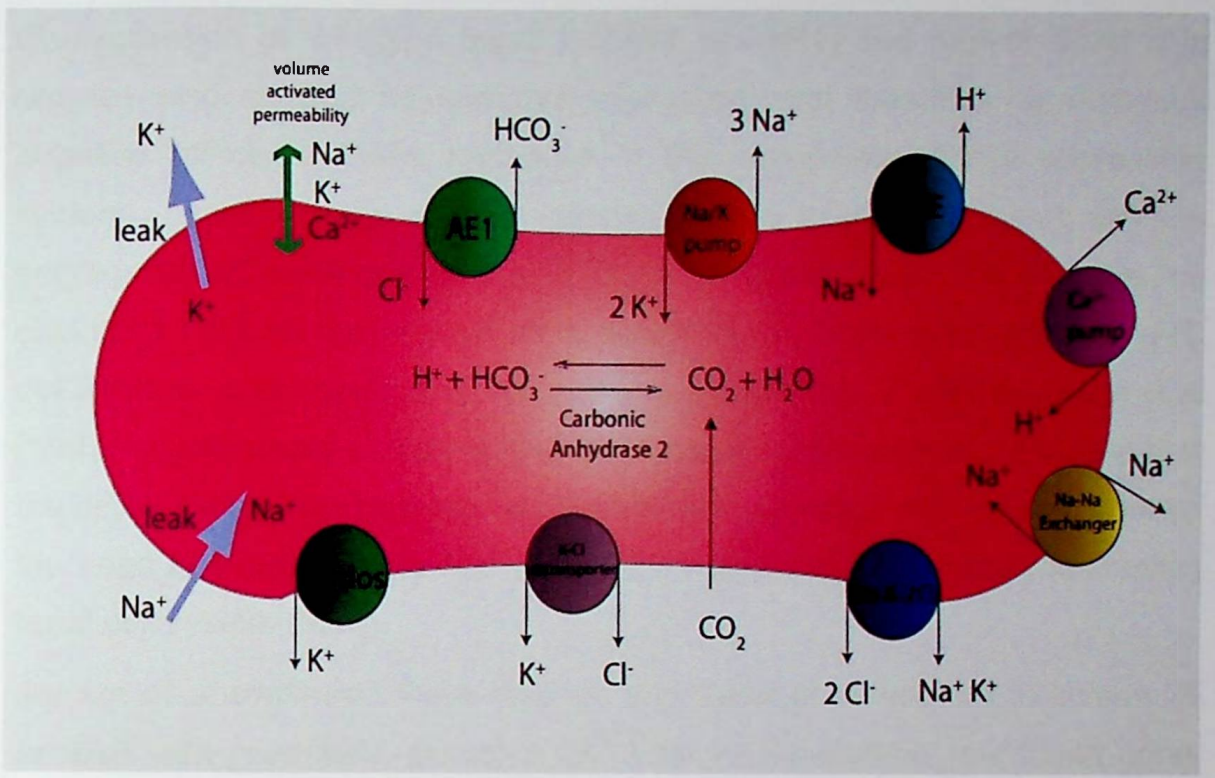

Figure 3. AE1 and red cell transport function.

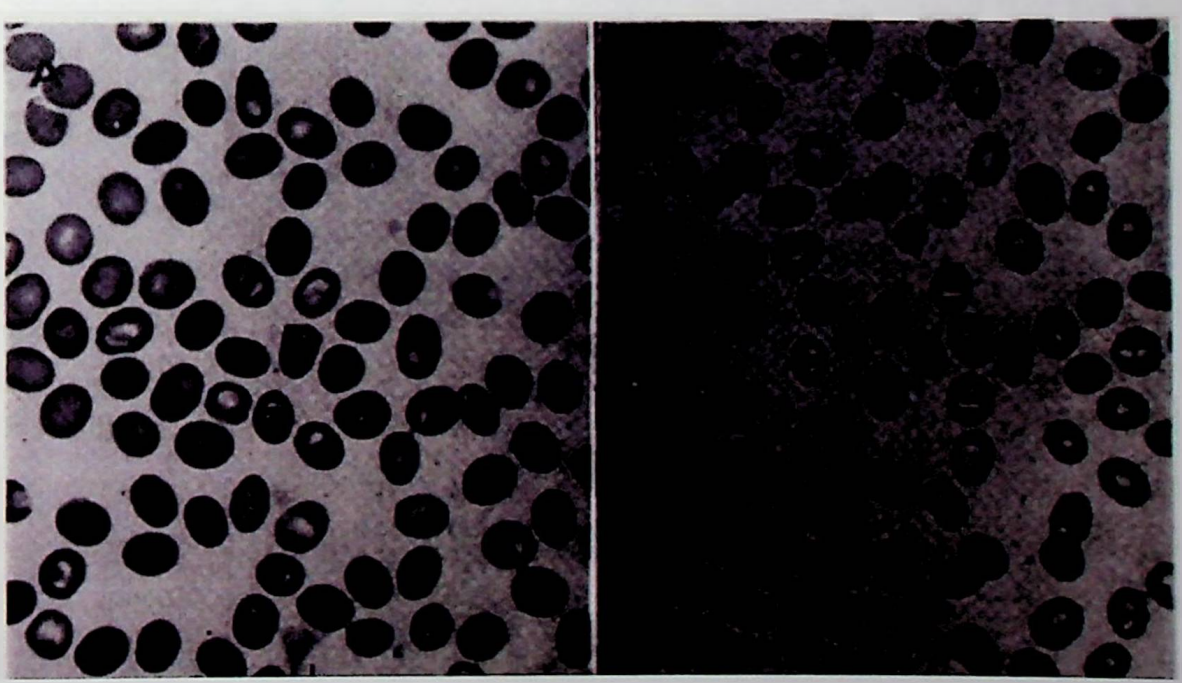

Figure 4. South East Asian Ovalocytosis. These are blood films from two of the original family described with SAO. (Honig et al, 1971).

Co-expression of wild-type band 3 (eAE1 or kAE1) and mutant band 3 in oocytes also showed no apparent interaction, and therefore no *dominant negative* effect, of these mutations in this non-polarised cell expression system. Thus, in spite of clear genetic linkage to the *AE1* locus and co-segregation of mutations in the Cl^-/HCO_3^- exchanger with the disease, no obvious functional mechanism for a defect in this transporter affecting a-IC cell function, and therefore H^+ secretion, was apparent. Therefore, Bruce *et al* (1997) hypothesised a mistargeting mechanism (expression of AE1 protein at the apical rather than basolateral membrane of polarised a-IC cells and hence the need to express these and other AE1 mutants in a polarised mammalian renal cell system (9,10).

Jarolim *et al* confirmed these findings and Karet *et al* went on to screen 26 families with presumed recessive dRTA for *AE1* mutations, but found none, except for a sporadic case with a *de novo* A589S mutation (11,12). Strippayawan *et al* also reported a R589C mutation, indicating that this AE1 protein site is a mutation 'hotspot'. In contrast, 2 affected brothers, initially thought to have recessive dRTA, were found to have a mutation in exon 20 causing a C-terminal truncation (R901X) and later called band 3 Walton (13,14).

These initial observations appeared to establish AE1 as a cause of dominant, but not recessive, dRTA until Tanphaichitr and colleagues reported 2 novel homozygous AE1 mutations, G701D and M31T (as well as K56E, a common polymorphism), in an affected sib pair (with unaffected parents) from North-eastern Thailand who also had haemolytic anaemia. Their red cells had normal AE1 content and SO_4^{2-} transport. However, oocyte expression of G701D showed significantly decreased transport function; but when this mutation was co-expressed with the eAE1 chaperone protein glycophorin A, which is not present in a-IC, normal function was restored (15). In the presence of glycophorin A, G701D can traffic to the red cell membrane and transport normally, but may not provide enough structural integrity for the red cell membrane and so cause haemolytic anaemia. In contrast, in the a-IC, trafficking to the plasma membrane is presumably reduced, as in the oocyte, resulting in decreased AE1 function and dRTA. Further expression studies

confirmed that no dominant negative effect was present on co-expression with wild type kAE1 and that M31T behaviour was no different from wild type. Yenchitsomanus and co-workers have also confirmed the association of AE1 mutations and recessive dRTA, and the importance of the previously reported G701D mutations in Southeast Asian cases of dRTA (16).

Vasuvattakul *et al* addressed directly the reported association between red cell SAO and dRTA by performing AE1 mutation screening in 2 individuals with dRTA and SAO from different families. Both turned out to have G701D mutations in compound heterozygosity with the SAO allele. As well as producing clinical dRTA, this mutation caused a 40% reduction in red cell SO_4^{2-} flux. Twenty patients with SAO alone were also screened for dRTA, but none had it, confirming that SAO itself does not cause dRTA and that it needs to be inherited with another AE1 mutation as a compound heterozygote (17). Bruce *et al* (2000) also investigated this association and identified 3 mutations: G701D in 2 families causing dRTA when inherited with the SAO allele (as already described); a D850 deletion in 6 families causing (recessive) dRTA in homozygous individuals, and when present as a compound heterozygote with the SAO allele; an A858D mutation present in 2 families causing incomplete (dominant) dRTA alone, and complete dRTA when inherited with SAO or the D850 deletion as compound heterozygotes. Again, those with SAO alone did not have dRTA (18,19).

Ribeiro *et al* (2000) have described a case of homozygosity for a V488M mutation called band 3 Coimbra, known to cause the red cell defect HS. Homozygosity had previously been diagnosed *in uteri* in an earlier failed pregnancy requiring termination and both parents were known to be V488M heterozygotes. Antenatal testing was declined in the second pregnancy and at birth the baby had severe and transfusion-dependent haemolytic anaemia, and absent red cell band 3; there was also evidence of dRTA with nephrocalcinosis detectable at 3 months of age (20).

Thus, it now seems clear that only AE1 mutations cause dominant dRTA, but that some AE1 mutations can (more rarely and perhaps confined to Southeast Asian populations) cause recessive dRTA (Tables 1 and 3). Clearly the next step in understanding the molecular basis of this form of dRTA would clearly

require investigation of the behaviour of individual AE1 mutations in mammalian renal cell expression systems.

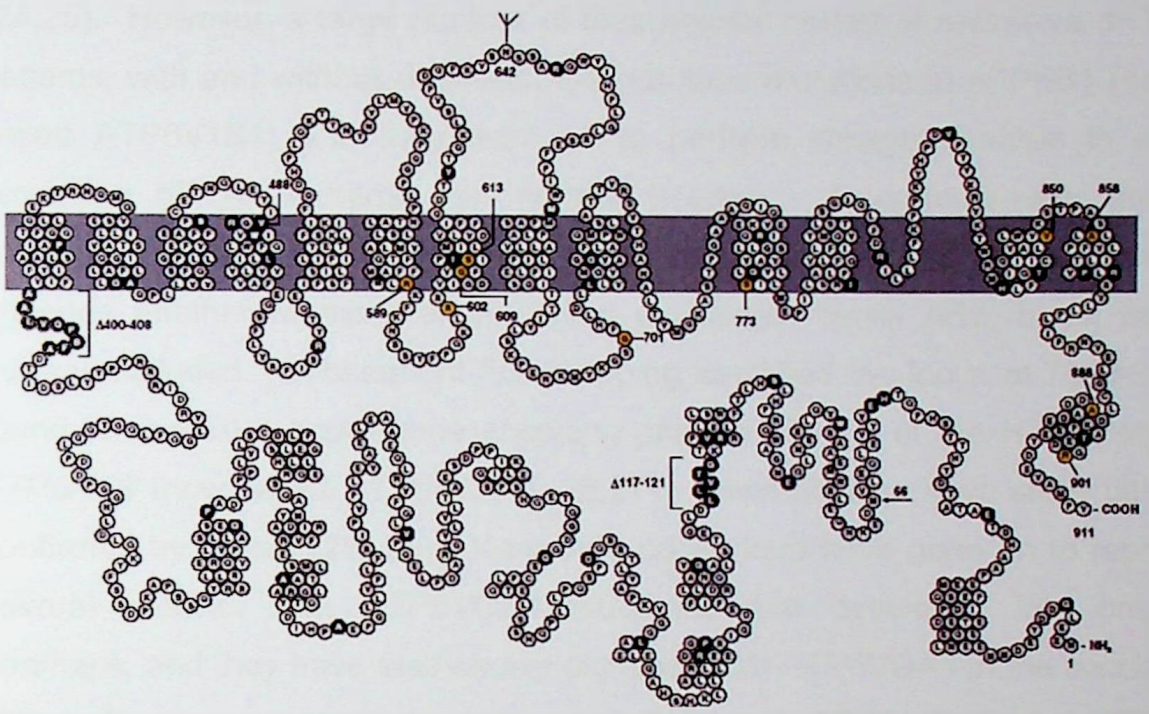

Figure 5. Schematic representation of the secondary structure of AE1. Yellow residues mark the sites of mutations causing hereditary dRTA. Black residues signify mutations causing red cell disease.

1.3.2 The electrogenic (positive) proton pump, H^+-ATPase

The renal H^+-ATPase is a member of the ubiquitous family of vacuolar H^+-ATPases that require ATP to drive protons across intracellular and (in specialised cells like the a-IC – Figure 1) plasma membrane (21). Karet and co-workers investigated this transporter as a candidate gene for recessive dRTA, since they had already excluded *AE1* mutations in a large cohort of recessive dRTA patients (12). Moreover, the H^+-ATPase had previously been shown to be absent, or abnormally expressed, in studies of autoimmune dRTA (as well as absent AE1 immunoreactivity) and also to be present in the inner ear, establishing a potential link with hearing (22,23). In many unrelated kindreds with recessive dRTA, a genome wide scan showed linkage to chromosome 2p13 in which the gene encoding the B1-subunit of H^+-ATPase (*ATP6B1)* is located. Mutation screening in affected cases identified several loss of function mutations. All mutations segregated with the disease and were not detected in unaffected or unrelated individuals. Bilateral hearing

loss was associated with these *ATP6B1* mutations, linking them to deafness and expression of the ATP6B1 subunit in the cochlea was also demonstrated (24,25). However, a large number of their original cohort of recessive dRTA patients, with and without deafness, did not have mutations in ATP6B1 (now called ATP6V1B1) and they went on to perform linkage analysis in the recessive dRTA kindreds with normal hearing. A genome-wide scan established linkage to chromosome 7q, which contains the *SLC4A2* gene that encodes another member of the anion exchanger family AE2, but it was quickly excluded. Subsequent fine mapping identified the locus at 7q33-34, found to contain a novel gene encoding another subunit of the H^+-ATPase, *ATP6N1B* (now called *ATP6VOA4*) (26,27) - these findings have since been confirmed by others (28, 29). Karet and co-workers have gone on to report several patients with *ATP6VOA4* mutations that developed late onset deafness, and they have also shown expression of ATP6VOA4 in the cochlea (31). Thus, in contrast to autosomal dominant dRTA, recessive dRTA appears to be genetically more heterogeneous, as the gene defect in several families with recessive dRTA is still unknown.

1.4 THE MOLECULAR BASIS OF INHERITED PROXIMAL RENAL TUBULAR ACIDOSIS

1.4.1 The electrogenic (negative) sodium-bicarbonate co-transporter, NBC1

As already mentioned, the renal Na^+-HCO_3^- co-transporter, NBC1, is expressed in the basolateral membrane of the proximal tubule and is responsible for most of the HCO_3^- transport across this membrane (32) and thus net bicarbonate reabsorption. It is expressed at a low level in the cornea and duodenum, while a modified form is highly expressed in pancreatic tissue; lower levels are also found in other epithelia and in endothelial cells.

Igarashi *et al* investigated this transporter as a candidate gene (*SLC4A4)* for inherited isolated pRTA in 2 patients with autosomal recessive pRTA. Both had systemic acidosis, mental retardation and short stature, and glaucoma, cataracts and band keratopathy. Sequencing of *SLC4A4* revealed 2 different homozygous mutations, R289S and R510H - both mutations were shown to

significantly reduce NBC1 activity. Another patient with pRTA and glaucoma was found to be homozygous for a nonsense mutation Q29X (34), while more recently Dinour *et al* found a S427L mutation in a patient with pRTA, short stature, glaucoma, cataracts and dental enamel defects (35).

The ocular phenotype seen in this disease has been investigated and several groups have demonstrated the presence of both kidney NBC1 and pancreatic NBC1 in ocular tissues, including corneal endothelium, trabecular meshwork and lens epithelium (36,37), and that pancreatitis can be associated NBC1 mutations (38). Autosomal dominant pRTA has also been reported in a single large Costa Rican family, but its molecular basis is still unknown (39).

1.4.2 Carbonic anhydrase II, CA (II)

Carbonic anhydrase II (CA (II)) is a cytoplasmic enzyme and a member of the large CA family that catalyse the hydration/dehydration of CO_2 and H_2CO_3. It is expressed in the renal proximal tubule, the loop of Henle and in IC of the collecting duct, as well as in brain glial cells and bone osteoclasts. Because of its importance in normal bicarbonate reabsorption, Sly *et al* investigated the possibility that CA (II) (the only CA present in kidney and brain) deficiency could be the cause of familial pRTA and published convincing biochemical and immunological evidence for the absence of CA (II) in erythrocytes of affected patients (40,41). Not long after the gene for CA (II) had been cloned and sequenced, Venta *et al* reported gene mutations in CA (II) deficient patients, later confirmed by Roth *et al* and shown to have reduced enzyme activity (42,43). Several other mutations have since been described (44,45,46) and it is now clear that CA (II) deficiency can be caused by a variety of mutations and that the clinical presentation is also variable, even with the same underlying mutation. Lai *et al* have attempted to correct RTA in CA (II) deficient knockout mice by gene therapy. The mice had a baseline blood pH of 7.0±0.03 and were unable to acidify their urine after acid loading. Using gene transfer methods, human CA (II) cDNA was injected into each renal pelvis via the ureter. Messenger RNA expression of CA (II) in mouse kidney was maximal at 3 days, but undetectable at 1 month. Urinary acidification did improve in the mice with a baseline urine pH of 6.7±0.06 the ability to lower urine pH to 6.2±0.09 after an acid load. Immunohistochemistry

showed localisation of CA (II) to the outer medulla and cortico-medullary junction. This does at least demonstrate the feasibility of *in vivo* and targeted gene therapy of the distal nephron (47).

Finally, another potential and novel mouse model of dRTA is related to a basolateral K^+-Cl^- co-transporter, KCC4, which when its gene (*SLC12A7*) is deleted causes deafness, but also an alkaline urine pH and reduced systemic base excess (on blood gas analysis) (48). As yet, there is no known human equivalent of this form of dRTA.

1.5 SUMMARY: ADVANCES IN UNDERSTANDING OF THE MOLECULAR BASIS OF RENAL TUBULAR ACIDOSIS

Our molecular understanding of inherited RTA has been transformed in the last two decades by a successful correlation of careful clinical phenotyping, positional cloning, mutational analysis and *in vitro* expression studies. In most instances this has confirmed existing cell models of renal acidification, but it has improved our understanding of how this complex machinery might be regulated at the cellular level. Such progress will also help refine our clinical classification of RTA and, hopefully, its earlier diagnosis. Furthermore, if gene therapy proves a viable option, the renal tubular defect itself might be targeted directly. It is also possible that less deleterious polymorphisms in these 'acid-base' genes might contribute to more complex polygenic diseases like osteoporosis (49-51).

At the time of the onset of my research, the 'next step' in investigating inherited renal tubular acidosis was the development of relevant transgenic cell and animal models to facilitate definition of the functional characteristics of disease causing mutants. This would help RTA genotype-phenotype correlation, and expand our understanding of this disease.

1.6 THE $RCCD_1$ CELL LINE

Clearly the ideal cell model for the study of AE1 mutants and dRTA would be a cortical collecting duct cell line. MDCK and LLC-PK cells had been in longstanding use as renal tubular cell lines. Both these lines do, however,

exhibit properties of both proximal and distal tubular epithelium. The amphibian TBM cell line had been in use as a more specific mode for mammalian CCD, but these cells have many different properties from their mammalian counterparts.

Marcel Blot-Chabaud *et al* sought to establish a mammalian cell line with tight transepithelial resistance to study ion transport properties and regulatory pathways in the distal nephron. A primary culture of rat kidney cortical collecting ducts was performed using a modified Percoll gradient technique. Cultured cells were then infected with wild type SV40 virus, resulting in transformation with persistent expression of the SV40 T antigen in successive passages of $RCCD_1$.

When grown on petri dishes $RCCD_1$ cells had epithelioid shape and formed domes. When grown on filters they formed monolayers of closely apposed cuboidal cells separated by junctional complexes. Electron microscopy showed at least two cell types, with features of principal (light) and intercalated (dark) cells. Immunostaining with DBA showed around 50% of cells to be principal cells. A very high transepithelial resistance (1800-4000 ohms/cm^2) was demonstrated and this was maintained over multiple passages.

Morphological examination, immunocytochemical study, ion concentration and short-circuit current measurements indicated that the cell line was polarised. $RRCD_1$ were able to establish concentration gradients with Na^+, K^+, HCO_3^-, and H^+. They also exhibited junctional complexes, basolaterally located Na-pumps and amiloride sensitive Na channels.

Ultrastructural studies, DBA binding and Isc experiments suggest this cell line expresses at least two different types of cell corresponding to principal and intercalated cells of the CCD. The principal cells appeared to express mRNA of the α-, β-, and γ- subunits of the epithelial sodium channel as well as the a- and b- subunits of the N^+, K^+, -ATPase.

$RCCD_1$ appeared to have AVP responsiveness, supporting the presence of functional principal cells. There was, however, no convincing responsiveness to aldosterone. The authors suggested that culture conditions might not be optimal for mineralocorticoid receptors or the response to aldosterone.

As regards intercalated cells (which are the desired model for RTA studies) half the cells were not stained with DBA. This and ultrastructural and Isc studies suggested around half of cultured $RCCD_1$ were intercalated cells, though the possibility of a single cell line with plasticity between both cell types could not be excluded (52).

1.7 TETRACYCLINE-INDUCIBLE GENE EXPRESSION IN $RCCD_1$

Around the time of the onset for this project a number of inducible gene expression systems had been developed. These had the advantage of producing translation of the gene in question in a timed fashion 'on demand'. This obviously facilitated study of a number of properties, such as targeting or transport properties, in a more controlled fashion, with the non-induced state acting as a negative control.

We established collaboration with Frederic Jaisser in INSERM U478 and his group and I performed the bulk of the work in this section in his lab, under his supervision. He had developed tetracycline-dependent gene expression in $RCCD_1$ cells and we felt this would be the ideal model in which to study dRTA mutants.

Their tetracycline-inducible (tet-ON) system was built on previous work performed by Bujard *et al.* The tet system was based on the use of a fusion protein between a strong transcription factor (VP16 from Herpes Simplex Virus) and the tet repressor isolated from E. Coli. This fusion transcriptor factor (denoted rtTA) can interact with Tet operon sequences (tetO) linked to a minimal cytomegalovirus promoter.

In this tet-ON system, transcription requires the presence of two transgenic constructs in target cells: the transactivator construct and the responder construct. Transgene transcription is, in this system, only activated in the presence of an exogenous ligand (in this case Tetracycline or its derivative Doxycycline) and will be turned off in its absence. This contrasts with more standard constitutive expression systems in that this allows temporal (and to some extent quantitative) control of gene expression.

This group first stably transfected $RCCD_1$ with the CMV-rtTA transactivator construct (provided by H Bujard). Transient transfection with the responder construct was then performed. The responder construct used initially was pminLacZ. The best transactivator cell-line, with the highest expression of LacZ, was then selected

Am IRES-Hygromycin resistance gene was excised from pCMV-IRES-Hygro (Clontech) and incorporated into the pminLACZ construct, resulting in the bi-directional pminHygroLacZ construct. This provides coordinate expression of both Hygromycin resistance and the LacZ reporter gene under a bi-directional reporter. The $RCCD_1$ clone with good rtTA expression was then stably transfected with the pminHygroLacZ responder construct. 24 hours after transfection Doxycycline stimulation was initiated by adding Dox to the culture medium (5μg/ml) with, in tandem, selection with Hygromycin (400μg/ml). The Dox was therefore switching-on transcription of both Lacz and Hygromycin resistance. The latter greatly improved efficiency. The selection process resulted in only clones with expression of the responder construct surviving, reducing the need for laborious screening of clones. They were able to demonstrate inducible LacZ expression in a number of clones. Western blotting showed dose-dependant expression of LacZ in one clone. Induction of expression was rapid, reaching a plateau in 48 hours and was fully reversible on withdrawal of Dox.

Their results showed that they had a functional tet-ON inducible system in $RCCD_1$. The use of a bi-directional construct that includes a selection marker (in this case a Hygromycin resistance gene) reduced the need for laborious screening of non-expressing clones. This model obviously had great potential applications for expressing genetic mutants that cause disease in the cortical collecting duct (53).

1.8 AE1 MUTANTS AND THE MISTARGETTING HYPOTHESIS

As previously described, initial studies on the behaviour of AE1 mutants in xenopus oocytes had not shown evidence of a dominant negative effect when co-expressed with wild type AE1, and these mutants had similar transport activity when expressed in isolation (Bruce *et al*). Furthermore, when the red

cells of patients with dRTA due to AE1 mutations were studied there appeared to be no consistent, significant abnormality in sulphate flux (a surrogate for anion exchange). In one family, with the DS613F mutation, anion transport appeared to be significantly increased. The conclusion could not be drawn that dRTA was caused by reduced transport function of AE1 in a-IC cells, and the mechanism of this disease remained unclear.

An alternative hypothesis, originally proposed by our collaborators (Bruce, Tanner *et al*), was that, in the a-IC cell, mutant AE1 may mistarget to the apical membrane, uncoupling the acidification mechanism (Figure 6). This would clearly not be problematic in the erythrocyte, which is not polarised.

Even if true mistargeting were not present, it might be that mutant AE1 is sequestered in more highly differentiated mammalian cell lines, due to the more complex protein sorting machinery present in the cells (but not in the xenopus oocyte). Either of these mechanisms could, conceivably, have a dominant-negative effect via wild type dimerisation and joint mistargeting/sequestration of mutant-wild type dimers.

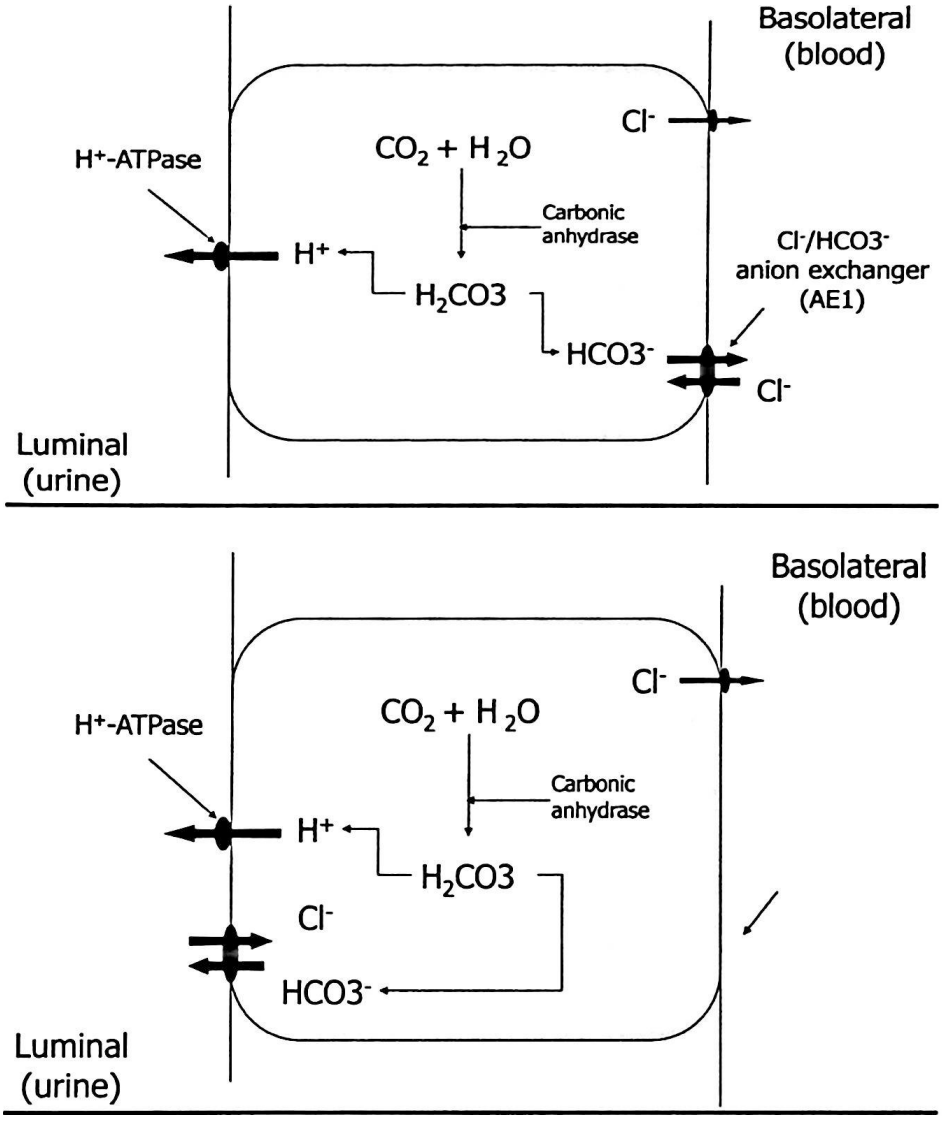

Figure 6. The AE1 mistargeting hypothesis. The top diagram represents the physiological norm. The lower diagram shows the hypothetical mechanism for dRTA secondary to AE1 mutation. Mutant AE1 is misdirected to the luminal membrane resulting in urinary bicarbonate wasting.

1.9 THE AE1 WALTON MUTATION

We were (at the Department of Nephrology, Middlesex Hospital) looking after 2 brothers who had both been diagnosed with dRTA. They both presented in adult life with kidney stones, and were found to have nephrocalcinosis, acidosis and hypokalaemia. Distal RTA was confirmed after a urine acidification test. One has remained well, however the other has suffered progressive nephrocalcinosis, renal failure and is now under the care of our low clearance nephrology team. His does, therefore, seem a severe phenotype of dRTA.

As there was no known family history, it was considered that they may have recessive dRTA, however mutation screening of AE1 showed that they were both heterozygous for the exon 20 mutation shown below.

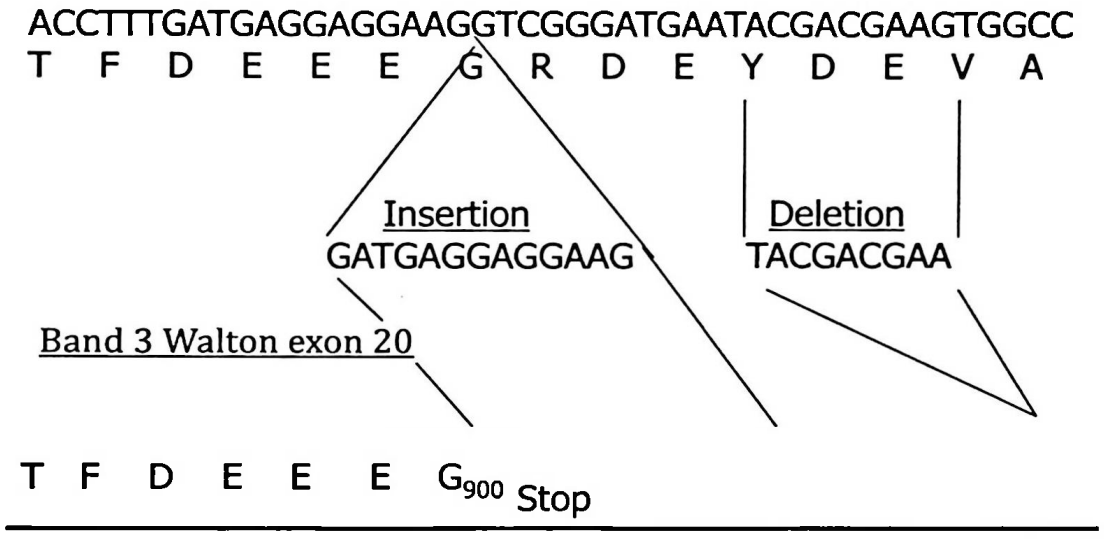

Figure 7. The AE1 'Walton' mutation. An insertion deletion mutation results a premature stop codon at exon 20. This truncates the protein, removing the last 11 amino acid residues at the carboxy-terminal end.

This apparently dominant mutation was named band 3 "Walton" after the town from which the brothers came. This unique insertion-deletion resulted in deletion of the 11 carboxy-terminal amino acids of the protein.

We felt, as we were caring for the brothers directly, their phenotype was apparently more severe in 1 brother and this was the only truncation mutation yet reported, that this would be a good mutation to study functionally (9,54).

1.10 AIMS OF THE PROJECT

1. The broad aim of the project was to examine the hypothesis that protein trafficking or mistargeting, rather than abnormal transport function, may be the mechanism of disease in dRTA due to AE1 mutations.

2. This hypothesis would be tested by expressing the AE1 'Walton' mutation (comprising an 11 amino acid truncation at the carboxy-terminal end critical for anion transport) in the mammalian cortical collecting duct cell line $RCCD_1$, (which had been developed by our collaborator Marcel Blot-Chabaud).

3. Walton would initially be transfected transiently in $RCCD_1$, with and without GFP-AE1 tagging, for basic trafficking information. Transient transfection would be performed by cloning AE1 (with and without GFP-tagging) into the PCDNA3 expression vector, which has a strong CMV promoter.

4. Walton would also be constitutively expressed in the rtTA $RRCD_1$ cell line. This would provide tet-dependent expression of wild type and Walton AE1 in $RCCD_1$. A bi-directional responder construct (incorporating the Hygromycin resistance gene) would be utilised as per Puttini et al original experiments.

5. Establishment of such a stably infected cell line would facilitate examination of mistargeting or otherwise disordered trafficking of AE1. Interaction of wild type and Walton AE1 would be examined by concurrent transient transfection of, for example, wild type AE1 in $RCCD_1$ in which mutant AE1 expression had been induced.

6. The functional behaviour of wild type and Walton AE1, in polarised $RCCD_1$, could then be studied by growing clones expressing both AE1 types in monolayers and, after inducing expression, measuring net luminal acidification and basolateral chloride transport.

7. This research would be conducted in INSERM U478 under the supervision of Frederic Jaisser with the collaboration of Marcel Blot Chabaud (also based in U478) and Mike Tanner's group in the University of Bristol.

8. Please note that a more detailed description of the specific strategies deployed in the molecular construction of the plasmids used in $RCCD_1$ transfection and the methods used for immunodetection of expressed AE1 is provided in the materials and methods and results chapters of this section.

9. As well as my cell-line expression studies I was also, during this period of research, to perform screening for AE1 mutations in patients with known RTA, in whom the underlying genetic cause had not been established.

SECTION IV - CHAPTER 2
MATERIALS AND METHODS

2.1 METHODS USED IN FORMATION OF MOLECULAR CONSTRUCTS

2.1.1 "Maxiprep" method for propagating DNA.

This method was used for large-scale propagation of plasmid DNA crucial to the project such as the source plasmids for Band 3 gene and the completed expression vectors.

2mls of E. coli (stored at –20C) were thawed slowly on ice. 1ml of DNA plasmid suspension was mixed gently in 2ml eppendorf with 100ml of E. coli and left on ice for 30 minutes. A water bath was set up to 42C with thermometer monitoring. "Heat shock" was then performed – an eppendorf with a mix of DNA and bacteria were added to the water bath for 1 minute, and then left on ice for 1 minute 30 seconds. 300 ml LB growth medium was then added to mix and incubated at 37 C for 1 hour. The mix was then applied to ampicillin-resistant bacterial growth plates and smeared until plates dry. These bacterial plates were then covered and incubated at 37 C in incubator.

Ampicillin stock at 100mg/ml was diluted to 100mg/ml. 20ml of this was then added to 20mls of LB growth medium and vortexed to mix. 5mls of ampicillin-LB mix was added to 20 ml tubes. Colonies of plasmids growing on ampicillin plates were then sampled with cocktail sticks and added to the 5ml ampicillin-LB mix and incubated at 37 C overnight.

800mls of LB growth medium was measured into large glass flasks and 200ml of 100mg/ml ampicillin added to each. 5mls of E.coli solution was then added to flasks and incubated at 37 C overnight on shaking incubator. Following overnight incubation the contents of the flasks were poured into large plastic centrifuge tubes and centrifuged at 5000rpm for 20 minutes.

10mls of *Qiagen* P1 buffer was added to each pellet, the pellets were re-suspended and then the suspension was added to 50ml plastic tubes. 10mls of *Qiagen* P2 lysation buffer was then added and mixed gently, then incubated at room temperature for 5 minutes. 10mls of *Qiagen* P3 buffer was then added to this lysate. *Qiagen* '"maxiprep" filter cartridges were then labelled and filter tips (*Qiagen* –tip 100) were added. The tips were then equilibrated with *Qiagen* QBT buffer by adding buffer to cartridges and

allowing the buffer to drain through the filter tips with gravity. Lysate was then added to *Qiagen* filter syringes and syringed into equilibrated filter cartridges. The elutant was then allowed to pass through the cartridge by gravity (DNA passes through filter in syringe but is retained in filter in cartridge). DNA, suspended on filters in cartridges, was then washed with *Qiagen* QC buffer by passing 30 mls through the cartridge twice. DNA was then eluted by adding 15 mls of *Qiagen* QF buffer to each cartridge and allowing it to drip through into a collection tube. 5 mls of isopropanol was then added to eluted DNA and the mix centrifuged at 10,000rpm for 1 hour. The supernatant was then drained; the DNA was re-suspended in sterile water and was then quantified by photometry

2.1.2 Enzymatic digestion of plasmids

This was performed frequently during the molecular stage of this project to facilitate ligation of DNA into plasmids for the formation of molecular constructs for expression. It was also used diagnostically to confirm that the various steps in the manufacture of the molecular constructs had been carried out successfully.

A digestion mix was prepared consisting of 10ml of *Qiagen*10x Tp buffer, 10mg of DNA plasmid, 50Us of restriction enzyme (typically 5ml at 10U/ml, various manufacturers). Sterile water was added to make up to a total volume of 100ml. This was mixed and incubated at 37 C for 1 hour and stored at 4C.

The DNA was then precipitated. 250ml of cold, 100% ethanol was added to 100ml of digestion mix following incubation. 10ml of Sodium Acetate, 3 molar (pH5.2) was then added. This was then mixed with a vortex, and then placed at –20C for 1 hour. This mix was then centrifuged at 13,000 rpm, at room temperature for 30 minutes. The supernatant was removed and 1ml of 70% ethanol was added. This was then centrifuged at 14,000 rpm for 5 minutes at room temperature, the supernatant removed and the pellet dried at room air. Finally, the pellet was re-suspended in 85 ml of sterile water.

2.1.3 Gel analysis of enzymatic digestions of plasmids

5g of powdered agarose was added to 50mls of KBL buffer solution. This agarose/buffer mix boiled briefly with a Bunsen burner. 50ml of fluorescent

dye was added to agarose solution. The agarose solution was poured into gel electrophoresis tray, the well insert added and cooled until agarose solidified. KBL buffer solution was then poured into electrophoresis tray over the solidified gel.

Digested plasmid DNA was diluted to 0.1mg per ml. A DNA running mix was prepared consisting of 1 ml of DNA at 1mg/ml, 3 ml of BB4 dye and 9ml of sterile water. The well insert was removed and the DNA running mix was added after mixing. 5 mls of Kilobase Ladder (*Eurogentec*) mixed with BB4 was added to the running well.

50V was applied across gel electrophoresis tray for 30 plus minutes depending on size of digestion fragments. Progress of electrophoresis was regularly reviewed under fluorescent light. Completed electrophoresis was reviewed and photographed under fluorescent light.

2.1.4 Kilobase ladder

The Eurogentec Kilobase ladder was used for simultaneous quantification and sizing of DNA fragments. 5 mls was used in each well

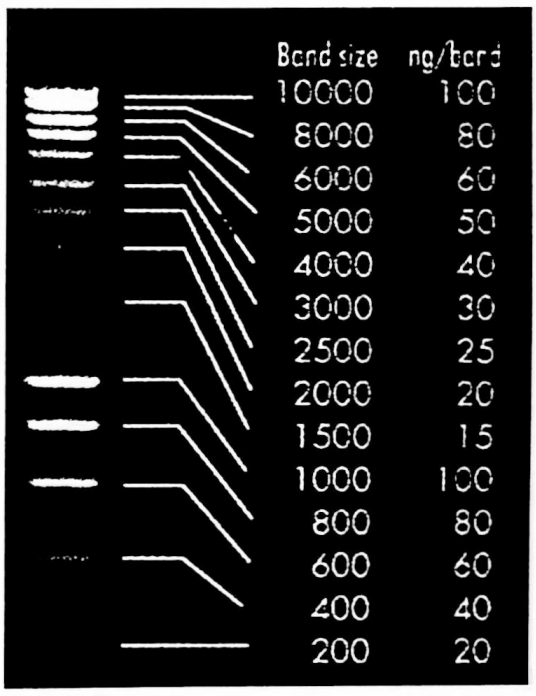

Figure 8. The Eurogentec Kilobase ladder.

2.1.5 Gel Purification of digested DNA

Running buffer was added to DNA mix (4ml per 100ml). Agarose gel preparation was performed as described previously using long well inserts. DNA/running buffer mix was added to long wells. Gels were run out with

periodic review under UV guidance to ascertain separation of fragments. When separation was adequate to allow excision, DNA fragments were excised under UV guidance with a scalpel.

The gel slices were weighed and 300 ml of *Qiagen* QG buffer was added to each 100ng of gel in *Qiagen* "QIAquick" columns. The buffer-gel mix was incubated at 50C for 10 minutes using a heated block. Isopropanol was added at 100ml for every 100ng of gel in original mix, then mixed. The "QIAquick column" was then placed onto a collection tube and spun. 800ml loaded and samples spun at 13,000 rpm for 1 minute, then the waste in the collection tube was discarded. The samples were reloaded, 800ml each time, until the entire sample had passed through "QIAquick" column.

DNA was then washed by adding 0.75 mls of *Qiagen* buffer PE to each column. This was left to stand for 5 minutes then centrifuged at 13,000 rpm for 1 minute. The flow-through was discarded and the samples were centrifuged again for 7 mins at 13,000 rpm. The "QIAquick" columns then placed into a clean 1.5 ml microfuge tube. 50 ml of *Qiagen* buffer EB was added to the centre of the membrane and centrifuged for 1 minute at 15,000 rpm. Eluted DNA passing through the filter at this stage and was collected in a clean tube below. This eluate was then diluted with 80ml of sterile water. The concentration of DNA was then checked on quantitative agarose gel electrophoresis. For this 2ml of DNA was added to each well with 8ml of sterile water and 3ml of running buffer.

2.1.6 Dephosphorylation of digested plasmids

This was performed on plasmid fragments after digestion and prior to subsequent ligation steps. 1.5 ml of 10 U/mg calf intestine phosphatase (CIP) was added to 100 ml of digestion mix and mixed with vortex. This was heated for 15 minutes on a heat block at 37 C, then for 15 minutes on a heat block at 56 C. 1.5 ml of 10 U/mg CIP added and mixed with vortex. This was again heated for 15 minutes on heat block at 37 C, then heated for 15 minutes on heat block at 56 C

2.1.7 "Blunting" of digested DNA fragments

This was performed when ligation of blunted DNA fragments was required for a cloning step in molecular construction. 50 ml of digested DNA was mixed with 2 ml of DNTPs at 2.5 mM, 2.5 ml of T_4 DNA polymerase, 5 ml of TpH buffer. This was made up to 100ml with sterile water. This was mixed and placed in 12 C cooling bath for 20 minutes. 2.5 ml of Klenow (2U/ml) was added and the mix was heated on a heat block at 37 C for 15 minutes. 4 ml of running buffer was then be added to each 100ml of blunted mix. This would then be gel purified using the gel purification of digested DNA technique described previously.

2.1.8 Ligation of plasmids

A ligation mix was initially prepared. This comprised quantities of insert and vector mixed at insert: vector ratio of 7:1 for blunt ligation, 3:1 for sticky ligation. To this was added 1 ml of ligase enzyme and 1 ml of ligase buffer. Sterile water was added to make the mix up to a volume of 10 mls. This was mixed, wrapped in saron and left at 16 C overnight. Ligation mixes were also prepared for insert-insert ligation to check there was no residual Ampicillin-resistance from plasmid from which the DNA fragment for insertion was derived. A vector-vector ligation control was also performed to check that there was no auto ligation of the vector due to inadequate dephosphorylation.

2.1.9 Transformation of ligated plasmids

Bacteria were stored at –80C. 5ml of ligated plasmid was added to 100ml of freshly thawed bacteria, mixed gently and kept on ice for 30 minutes. This was then warmed in a water bath at 42 C for 1 minute 30 seconds. 900ml of LB growth medium was added and the mixture as agitated for 1 hour in an incubator at 37 C. 1 ml of the incubated sample was then taken and centrifuged at 3500 rpm for 5 mins. 900ml of supernatant was removed, with 100ml of supernatant left covering the pellet. The pellet was resuspended by pipetting gently up and down with the residual supernatant. 100ml of resuspended bacteria was smeared across Ampicillin-coated growth plate and the plate was then incubated overnight at 37 C. Following overnight incubation plates were kept refrigerated at 4 C until use.

2.1.10"Miniprep" propagation and isolation of DNA from transformed plasmids

This method was used for smaller scale propagation of transformed DNA plasmids after, for example, a ligation step in an expression vector construction, prior to diagnostic digestion.

Colonies on Ampicillin-coated growth plates were sampled using a sterile cocktail stick and placed in 5 mls of LB growth medium. This was then left to incubate, agitating, overnight at 37 C. 2mls of this was added to *Qiagen* "miniprep" tubes and centrifuged at 13,000 rpm for 5 minutes. The bacterial pellet was then re-suspended in 250ml of *Qiagen* Buffer P1 (with *Qiagen* RNase A) and transferred to a micro-centrifugefuge tube. 250ml of Qiagen Buffer P2 was added and the sample was mixed by gentle inversion 4-6 times. This caused bacterial lysis at which point the sample became clear. 350ml of QIAGEN Buffer N3 was then added and the sample was quickly inverted 4-6 times. This caused precipitation at which point the solution became cloudy. Rapid mixing was performed to avoid localised precipitation. The sample was then centrifuged at 13,000 rpm for 10 minutes.

A *Qiagen* "QIAprep" spin column was placed in a 2ml collection tube and the supernatant from step 6 was pipetted into this column. The sample was then centrifuged at 13,000 rpm for 60 seconds, and the flow-through was discarded. The "QIAprep" spin column (with adherent DNA plasmids) was then washed by adding 0.5 mls of *Qiagen* Buffer PB and centrifuging for 30-60 seconds (to remove trace nuclease activity). The flow through was again discarded. The "QIAprep" spin column was washed by adding 0.75mls of QIAGEN Buffer PE and centrifuging at 13,000rpm for 60 seconds. The flow through was then discarded and centrifugation was performed for an additional 1 minute.

The QIAprep column was then placed in a clean, 1.5ml micro-centrifuge tube. 50ml of Buffer EB (10mM Tris-Cl, pH 8.5) was then added to the centre of the column, which eluted the DNA. This was left to stand for 1 minute then centrifuged at 13,000 rpm for 1 minute. The DNA was then quantified by photometry.

2.2 METHODS USED IN CULTURE, TRANSFECTION AND PROPAGATION OF $RCCD_1$ CELL LINE

2.2.1 $RCCD_1$ cells and culture

Marcel Blot-Chabaud, who worked in the same INSERM unit, provided the RCCD1 cells (52). Primary cultured rat cortical collecting duct cells by an adapted from Vinay et al, Bello-Reuss and Weber. These were then immortalised by infecting with wild-type simian virus 40 (SV-40). When grown on petri dishes they become organised as monolayers of cuboidal cells and, when confluent, form domes. High transepithelial resistance was noted when $RCCD_1$ was grown on permeable filters.

Sterile plastic culture dishes were first coated with sterile collagen. 1ml of collagen was added to dishes and the collagen spread evenly. This was repeated a further two times. Dishes were then left in a sterile area under a cell culture canopy to dry.

Cells were split by adding 5 mls of trypsin to each culture dish. Trypsin was then left on the cells for 1 hour at 37C. 5 mls of culture medium were then added to each tray and mixed by pipetting x 4. The cell/trypsin/medium mix was then placed in centrifuge tube and centrifuged at 1500 rpm for 6 minutes. The supernatant was then discarded. Cells were then rapidly resuspended in 5 mls of growth medium and mixed gently with a pipette. A cell count was performed under a calibrated glass slip with light microscopy. A cell count/ml figure was then obtained.

For ongoing cell culture 2.5×10^6 cells were added to a large (10ml) culture dish. This meant cells would be confluent and ready for further splitting at 4-5 days. For transfection work 2.5×10^6 would be added to each small (2ml) culture well in 6 well cluster 24 hours prior to transfection. This meant the cells would be 25% confluent on the day of transfection and confluent (and ready fro further splitting) 48 hours after this. Large culture dishes were topped up to 10mls of culture medium. Small wells in 6 well clusters were topped up to 2 mls. The growth medium was changed every 48 hours

Cells were split again when a dense, continuous monolayer had been formed (approximately 10 million cells for large culture dish, 2 million cells for small

wells transfection dishes). Cells were checked daily for health and growth under light microscopy.

2.2.2 $RCCD_1$ cell culture medium

The culture medium was as follows: HAM's F12, DMEM 1:1, 14mM Na HCO_3, 2 mM glutamine, 5mg/l transferring, 5mg/ml insulin, 10mg/ml EGF, 5 x 10^{-8} M T_3, 10 U/ml penicillin-streptomycin, 20mM HEPES, pH 7.4.

2.2.3 Transient transfection of $RCCD_1$ cells using $PCDNA_3$ vector with CMV promoter

Cells were split onto 6 well clusters 24 hours prior to transfection. Approximately 2.5 x 10^6 cells were added to each cluster such that 5x 10^6 cells were in culture (around 25% confluence) on the day of transfection. 1mg of DNA, 100ml of OPTIMEM (serum free medium) and 4ml of PLUS reagent were mixed and left to incubate for 15 minutes at room temperature. Simultaneously 3 ml of lipofectamine reagent and 100ml of OPTIMEM serum free medium were mixed and left to incubate for 15 minutes at room temperature.

DNA, lipofectamine reagent, PLUS reagent and OPTIMEM mixes were then combined by dropping the lipofectamine mix onto the DNA mix slowly with a 10ml pipette. This combined mix was then incubated for a further 15 minutes at room temperature. The culture medium was then aspirated from the cells, growing in 6 well clusters. 800ml of OPTIMEM was then added and mixed gently by pipette. This mix, including the lipofectamine and DNA complexes was then dropped slowly over the cells. After 4 hours incubation at 37 C the medium containing the DNA complexes was replaced with fresh medium.

At 48 hours cells transfected with $PCDNA_3$ wild type and mutant Band 3 GFP fusion protein constructs were inspected for fluorescence. As well as this cells transfected with $PCDNA_3$-wild-type and mutant Band 3 constructs were lysed for protein preparation (Western blotting), lysed for RNA for Northern Blotting and examined directly with immunofluorescence.

2.2.4 The $RCCD_1$-rtTA cells

The CM-rtTA construct was provided by H Bujard (INSERM Paris). It allows constitutive expression of the reverse transactivator (rtTA) under the control of the CMV-IE promoter. It also contains a Neomycine-resistance gene under the control of the SV40 constitutive promoter.

Several clones of RCCD1 expressing the rtTA construct had been established by S Puttini (INSERM Paris) prior to my arrival in the lab (53). These were achieved by performing a transfection as described above. At 48 hours post transfection the cells were split to 1 x 10^6 per large culture dish and adding geneticine at 400ml/ml. Surviving colonies were isolated and amplified. The clones were characterised by performing transiently transfecting a reporter construct – a LacZ cDNA (whose expression was placed under control of the tetO-Pmin promoter (PB1-3). B-Galactosidase activity was then determined 2 days after transient transfection in the presence of Doxycycline 5mg/ml in the culture medium.

Several clones demonstrated inducible b-Galactosidase activity. "Clone B5" was selected for further use as it had a 40-fold increase in inducible expression. Maximal activity was reached with 0.5-1mg/ml of Doxycycline. Clone B5 was used for my constitutive expression experiments.

2.2.5 Transfection of vectors for constitutive expression

PBI4IREShygroAE1 (wild type and mutant) constructions were transfected into rtTA-$RCCD_1$. in order to achieve tet-dependent, constitutive AE1 expression. This transfection was performed by linearising the constructions with Hpa1. A lipofectamine-based transfection was then performed according to the previously described method.

2.2.6 Selection of clones using inducible expression of Hygromycin resistance

Doxycycline was used as a tetracycline surrogate as previously described in the method of Stefania Puttini (53). The transfected cells were stimulated with Doxycycline 5mg/ml (in cell culture medium) for 3 days for 3 days prior to a high dose Hygromycin selection. The latter was performed by adding Hygromycin at a concentration of 400mg/ml to the culture medium (with the

ongoing addition of Doxycycline). Only cells with tet-dependent stimulation of the PBI4 bi-directional promoter would have Hygromycin resistance (through transcription of the IREShygro selection cassette. It was hoped that these cells would also express AE1 (the transcription of which was also been driven by the PBI4 bi-directional promoter as described).

Cells were then separated two days after high dose Hygromycin. The Hygromycin and Doxycycline containing medium was then removed by centrifuge and the cells were resuspended in petri dishes with fresh, antibiotic-free medium. Clones were then isolated with wax and plastic isolation wells, removed from the petri dishes by pipetting with trypsin and culture medium then resuspended in isolated petri dishes. The clones were then propagated. After recovery of the cells was confirmed selection was maintained by ongoing Doxycycline stimulation and Hygromycin selection apart from culture immediately after passage, when the clones were allowed to recover in antibiotic-free medium.

2.2.7 Defrosting of frozen $RCCD_1$ cell clones for analysis

At points in the project it was necessary to freeze cell lines, such as after selection and propagation of key clones. Cells were frozen at -80C. To defrost cell lines cryotubes containing cells (frozen in culture medium) were warmed in a 37C water bath. Culture medium was then added in droplets, at an exponential rate, from a 10ml pipette up to a total volume of 10mls. The cell/culture medium mix was then added to a 10ml culture dish coated with collagen.

2.3 WESTERN BLOTTING FOR AE1 EXPRESSION IN $RCCD_1$

2.3.1 Western blotting gel and buffer preparation

For western blotting the following several buffer and gel solutions were constituted. Tris buffered saline (10 x) was made up by adding 12.5g of TRIZMA and 40.0g of NaCl to 500mls of water. This was adjusted to a pH of 7.6 and stored at 2-8 C.

TBS-T (1x) was made up with 100mls of TBS, 1ml of TWEEN 20 and made up to 1 litre with water stored at 2-8 C.

For the protein transfer buffer 3.03g of TRIZMA, 14.4g of glycine and 200mls of methanol were added to 650mls of water to dissolve constituents. The solution was then made up to 1 litre and stored at 2-8 C.

Resolving gel buffer was made up by adding 90.8g of TRIZMA base and 2.0g of Sodium Dodecyl Sulphate was added to 900mls of water. This was pH adjusted to 8.8 and the final volume made up to 1 litre with water. This was then stored at 2-8 C.

Stacking gel buffer was constituted by adding 30.3g TRIZMA base and 2.0g of Sodium Dodecyl Sulphate to 900mls water added, then mixed. This was pH adjusted to 6.8 and made up to of 1 litre with water and stored at 2-8 C.

To make up resolving gel sufficient for 4 gels 10.6mls of 30% acrylamide, 10.0mls of 1.5M TRIS pH 8.8, 0.4mls of 10% SDS, 0.4mls of 10% APS and 24ml of TEMED were added to 18.6 mls of water and mixed in a measuring cylinder.

Stacking gel solution sufficient for 4 gels was made up by adding 2.0mls of 30% acrylamide, 1.5mls of 1.0M TRIS pH 6.8, 0.12 mls of 10% SDS, 0.12 mls of APS and 12ml of TEMED to 8.2mls of water.

Running buffer (5x) was made up by adding 15.7g TRIS, 72.0g of Glycine and 5g of SDS were made up to 1 litre with water and stored at 2-8 C. (pH not adjusted). Blocking buffer (5% milk) was made up with100mls TBS-T (1x) and 5g of powdered milk

2.3.2 Western blot gel electrophoresis

Gel plates set up. Resolving gel solution was added slowly between plates up to 1 cm below comb margin. Water was then added slowly and the apparatus covered with damp paper to prevent evaporation. The gels were then refrigerated to solidify overnight. The following morning the stacking gel solution was made up. The water and combs were then removed from the resolving gels, the gels were placed in electrophoresis tank and the 1 x running buffer was added. Protein samples were added to 15ml or 20ml of APS buffer and made up to 30ml or 40ml with water. This mix was then heated at 95C on a heating block for 5minutes to denature the proteins. Samples were then loaded (30ml or 40ml each well). The electrophoresis

tanks were then filled with running buffer. The electrophoresis was run at 40mA, maximum voltage for 3 hours.

2.3.4 Western blot transfer

The gels were removed from the plates and soaked for 20 minutes in transfer buffer. The blots were then labelled were labelled, soaked in methanol for 1 minute, rinsed in water then soaked in transfer buffer (on tilting tray) for 10 minutes. The transfer pads were then soaked in transfer buffer. The transfer was then set up (blot – gel – pad) and rolled to remove bubbles. The transfer was run at 15V, maximum amplitude for 1 hour.

2.3.5 Western blot blocking

The blots were removed and soaked in TBS-T (1x) on tilting tray for 5 minutes. TBS-T (1x) was then drained and the pads were soaked in TBS-T (1x) 5% milk blocking solution overnight on tilting tray at 4C°.

2.3.6 Western blot primary antibody fixation

The following day the blots were washed twice with TBS-T (1x) solution. The antibody was then applied, diluted in 50 mls TBS-T (1x) 0.5% milk (NB differing concentrations were tried as will be discussed in results). This was left to soak on tilting tray for 1 hour at 4C°. The blot was then washed 3 times with TBS-T (1x)

2.3.7 Western blot secondary antibody fixation

Secondary antibody was then applied, diluted in 50mls in 50mls TBS-T (1x) 0,5 % milk and this was left to soak on tilting tray for 1 hour at 4C°. The blot was then washed 3 times with TBS-T (1x).

2.3.8 Western blot exposure

The blotting paper was partially dried. ECL solution was then applied (2 mls to each blot) such that each blot was evenly coated. The blots were dried and wrapped in plastic film. They were then placed in radiation cassette and exposed to Biomax MR radiographic film.

2.4 ISOLATION OF GENOMIC DNA FROM RTA PATIENTS AND KINDREDS

For some patients the method described in Section I was used. In some other patients the 'Isocode Stix' (Krackeler Scientific) method was used. A small drop of blood was added (after finger tip pinprick) to the triangle area on the isocode stix. This was then dried in a container overnight (without touching). When dried the triangle was cut off and added to a small eppendorf. 500μl of sterilised water was then added to the eppendorf and this was vortexed. This was then centrifuged and then the water was removed by pipette. 50μl of clean water was then added to the eppendorf and this was spun again. The eppendorf was then added to a 100^{o}C heating block. At this point the DNA moves from the triangle into the sterile water. The water was then pipetted off and stored, with the stix triangle discarded as waste.

2.5 SCCP AE1 MUTATION SCREENING IN RTA PATIENTS

Primers for PCR amplification of all exons of the AE1 gene were provided be Lee Bruce, who was performing the bulk of mutation screening for dRTA patients. PCR for SCCP (single stranded conformation polymorphism) was then used as a method for mutation screening these exons in five patients with dRTA in whom the genetic basis of their disease had not been ascertained. The PCR method has been described in Section I.

The gel mix for SSCP (50ms for 2 gels) was constituted with 10mls acrylamide, 2.5mls 10 x TBE and 37.5mls water. 80μl of AMPS and TEMED were then added to this mix. The gels were poured and the comb inserted. When this was set the combs were removed and the wells were filled with running buffer (0.5 x TBE).

1μl of PCR product was mixed with 3μl of water and 4μl of formamide loading buffer. PCR samples were denatured by heating on a block at 98°C for 8 minutes. Following this the samples were immediately plunged into a bath of ice and salt water. 1μl of Kilobase ladder (diluted 1 in 4) was added to 3μl of water and 4μl of formamide loading buffer. This was used as a size marker.

All samples were then added to the gel and the electrodes were connected to the running apparatus. The gel was then run at 300V for 4 hours at room temperature. Each series of PCRs was also run at 400V for 5 hours at 4°C in the laboratory cold room.

The running buffer was then drained and the gels separated from the plates and placed in a staining tray. The gels were then fixed by soaking twice in 10% ethanol/0.5% acetic acid (200mls per gel) for 3 minutes each soak. The soak solution was drained between each fixation. The gels were then stained in 1g/L $AgNO_3$ (200mls per gel) for 10 minutes. The silver stain solution was then drained off and the gels were rinsed 3 times in distilled water. He gels were then transilluminated and scanned.

2.6 SEQUENCING OF AE1 IN GENOMIC DNA OF RTA PATIENTS

Primers for PCR amplification of the AE1 gene from genomic DNA were provided by Lee Bruce. Purified DNA was suspended in distilled water and mixed with 10pmol and 2μl reaction buffer (Sequenase version 2.0 sequencing kit, Amerhsam Life Science). This mix was then heated at 65 °C for 5 minutes and cooled to allow the primer to anneal. This was then used for labelling reactions using ^{35}S-dATP as the labelled nucleotide. The termination reactions of the chain-termination Sequencing kit were then used according to the manufacturers instructions.

The Bio-Rad sequencing apparatus was used for gel migration. This is a 21 x 40cm gel with wedge-shaped spacers. The gel mix comprised 6% acrylamide, 1 x GTB, 7.67M urea, 100μl 25% APS and 100μl TEMED. To create the wells the sharks toothcomb was inverted to create a straight edge on the top of the gel. The comb was then inverted before loading. The running buffer was 1 x GTB.

The gel was warmed to 50°C (there is a thermometer on the front of the gel glass plate). Completed sequencing reactions were denatured by heating to 75°C for 2 minutes then placing samples in an ice and salt-water bath. 2μl of each sample was loaded. The gel was then run at 45W, maintaining a

temperature of 50°C, for 3-4 hours. Sometimes this would be extended for longer sequencing reads.

The gel was then cooled by running the gel plates under cold tap water. The plates were separated and the gel was then transferred to Whatman 3MM paper. The gel was then dried.

The dried gel on paper, wrapped in cling film, was then exposed to Biomax film at room temperature overnight. Sometimes an extended exposure was required. The sequence was then read.

SECTION IV

CHAPTER 3 - RESULTS

3.1 PREPARATION OF PCDNA$_3$-AE1 CONSTRUCTS FOR TRANSIENT TRANSFECTION IN RCCD$_1$

3.1.1 AE1 constructions

Wild type and mutant band 3 genes were cloned from constructs provided by A. Toye (Department of Biochemistry, Bristol University). Wild-type AE1 was provided in a construct denoted BSXG1KB3.SEQ, the mutant from the BSX1KB3BD.SEQ construct.

The plasmid DNA of these constructs was propagated using the 'Maxiprep" method as described and this DNA was quantified using photometry.

3.1.2 The pCDNA3 expression vector (Invitrogen)

This vector was chosen as it had been used successfully to transfect into RCCD$_1$. It has a strong CMV promoter and multiple cloning sites for gene insertion. It may be used for constitutive expression, but in this case was used for transient transfection.

3.1.3. Preparation of WT and MUT AE1 inserts and pCDNA3 vector for ligation– blunt strategy

The ECORV site, within the pCDNA3 multiple cloning site was selected for cloning the wild type and mutant AE1 inserts.

Initially a restriction enzyme digestion was performed on the AE1 plasmids with Xho1 and the PCDNA3 vector was digested at ECORV. The digestions were then checked with agarose gel electrophoresis and run alongside undigested controls. The results are shown overleaf

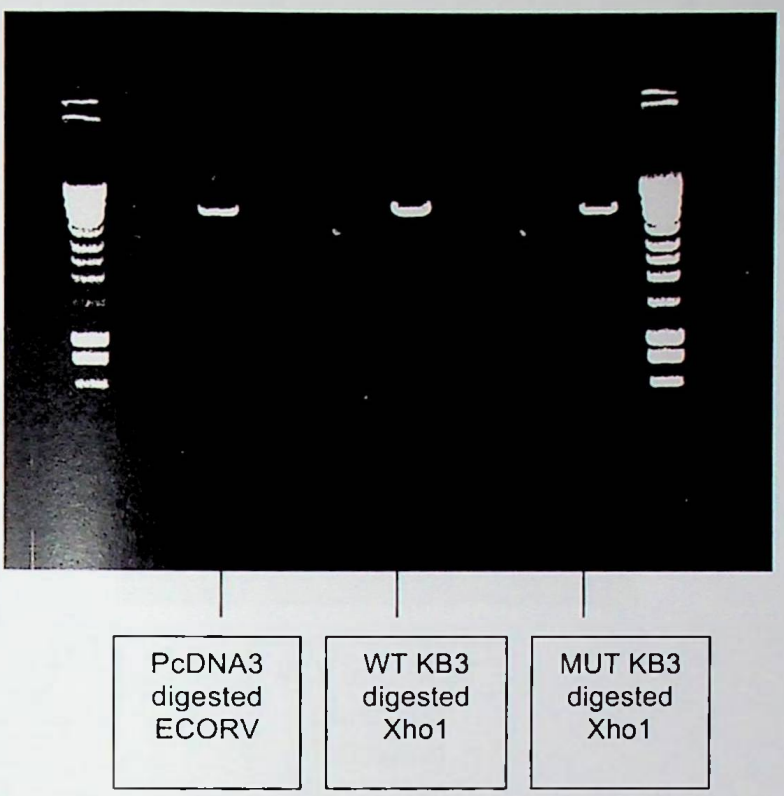

Figure 9. Agarose gel electrophoresis showing successful digestion of pCDNA3 with ECORV and WT and Mut AE1 plasmids with Xho1 digestions alongside undigested control

The Xho1 digested plasmids were then precipitated and digested with Sac1. This cut the plasmid into two similarly sized fragments, which were indistinguishable on gel electrophoresis (below).

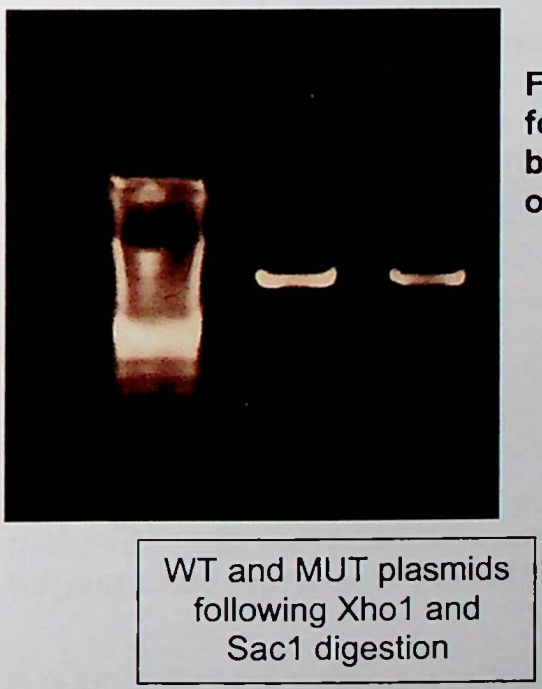

Figure 10. Agarose gel electrophoresis following Sac1 digestions. Only a single band is discernible due to the similarity of the fragment lengths.

As a consequence a further precipitation was performed and the plasmids were digested with Sca1. This resulted in 3 fragments of differing size, which were easy to distinguish on gel electrophoresis (overleaf).

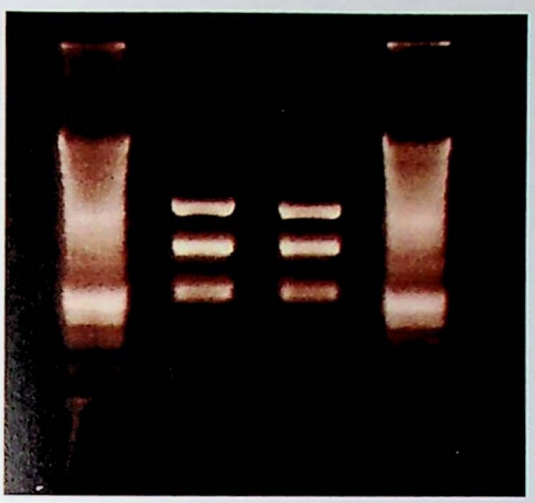

Figure 11. Agarose gel electrophoresis following digestion of WT and MUT plasmids with Xho1, Sac1 and Sca1

WT and MUT plasmids following Xho1, Sac1

These fragments were then blunted with DNTPs and T4 DNA polymerase. A precipitation of the ECORV digested PCDNA3 vector was then performed and this was then dephosphorylated. These fragments were then separated out and purified by gel electrophoresis (QIAGEN method as previously described. The gel separations are shown below

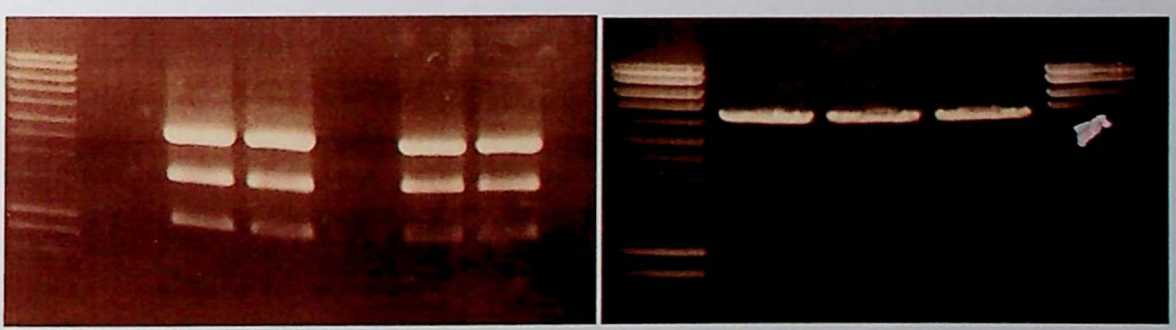

Figure 12. Gel separation and purification of digested WT and MUT AE1 plasmids (left) and pCDNA3 vector (right). In the left hand gel the largest band represents the KB3 inserts.

A quantitative gel analysis was then performed on vector and AE1 inserts. The results are shown overleaf.

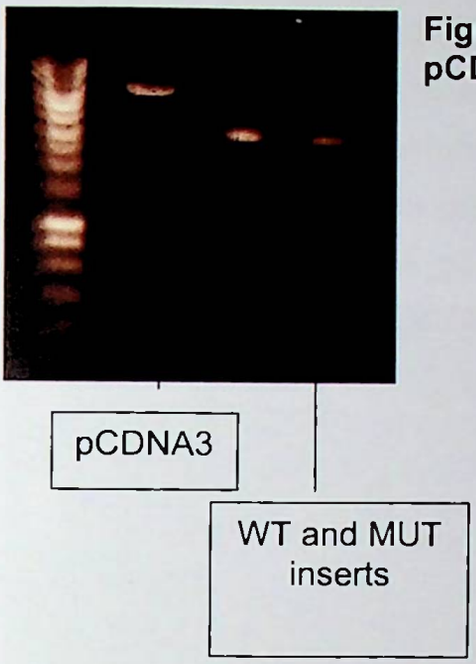

Figure 13. Quantitative gel electrophoresis of pCDNA3 vector and WT and MUT AE1 inserts.

3.1.4 Ligation of WT and MUT AE1 into pCDNA3 vector – "blunt ligation" strategy

6 ligations were performed. The ligation reaction was set up with a ratio of 7:1 and 14:1 for inserts: vector in view of this being a blunt ligation. Controls were set up with only insert in 1 ligation mix and with only vector in a further ligation mix.

a. Ligation 1: wild-type AE1: vector (7:1)
b. Ligation 2: wild-type AE1: vector (14:1)
c. Ligation 3: mutant AE1: vector (7:1)
d. Ligation 4:mutant AE1: vector (14:1)
e. Ligation 5: vector only
f. Ligation 6: insert only

The ligation mixes were incubated at 16C overnight. These were then transformed in e coli bacteria according to method to the previously described method and plated on ampicillin resistant culture plates and incubated overnight. Colonies were then selected and DNA extracted according to the QIAGEN miniprep protocol described previously.

Two diagnostic restriction enzyme digestions were then performed. Firstly, to determine whether the ligation was successful a BSTX1 digestion was performed. If the ligation had been successful 2 bands (5.4Kb and 2.5 Kb) would be present. If the ligation was unsuccessful only a 5.4 Kb band would

be present. Secondly a digestion was performed to determine whether the insert was in the correct orientation a combined digestion with Net1 and Nco1 was performed. If the orientation was correct 2 bands (5.4Kb and 2.5 Kb) would be discernible. If the orientation was incorrect 2 indiscernible 8Kb bands would be present on gel electrophoresis.

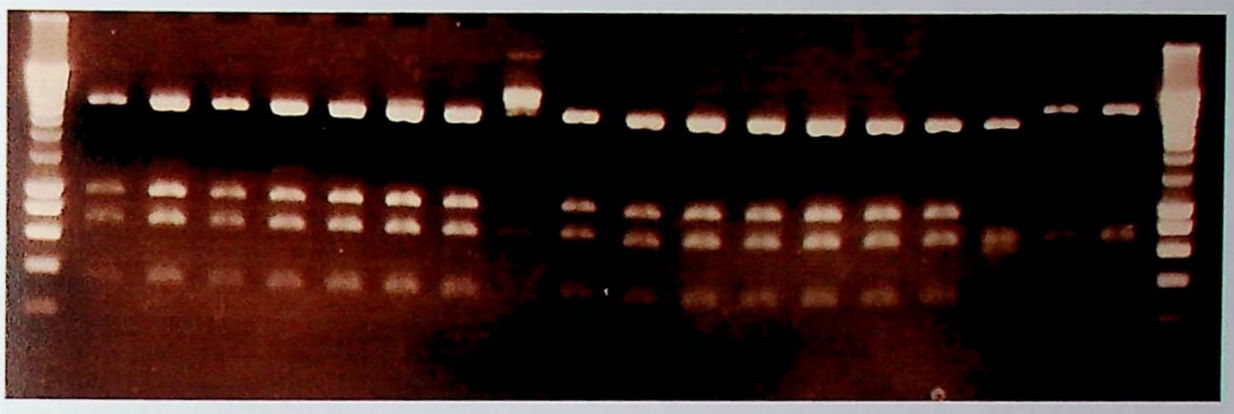

Figure 14. Agarose gel electrophoresis of ligated plasmids with NCO1/NOT1.

The digestions suggested only auto-ligated vector present, as the total fragment size was 5.4Kb.. This was confirmed by running with a vector control. Harvesting of a further 9 colonies confirmed this with further digestion yielded the same result.

3.1.5 Preparation of WT and MUT AE1 inserts and pCDNA3 vector for ligation – sticky ligation strategy

The strategy for the ligations was then changed. The restriction enzyme maps demonstrated a common Xho1 site in the PCDNA3 vector-cloning region as well as on the distal end of the band 3 on the BSXGKB3 and BSXGKB3BD plasmids. Using this restriction enzyme site would mean a "sticky" rather than blunt ligation at the distal end of the gene insert.
The new strategy for plasmid construction was as shown overleaf

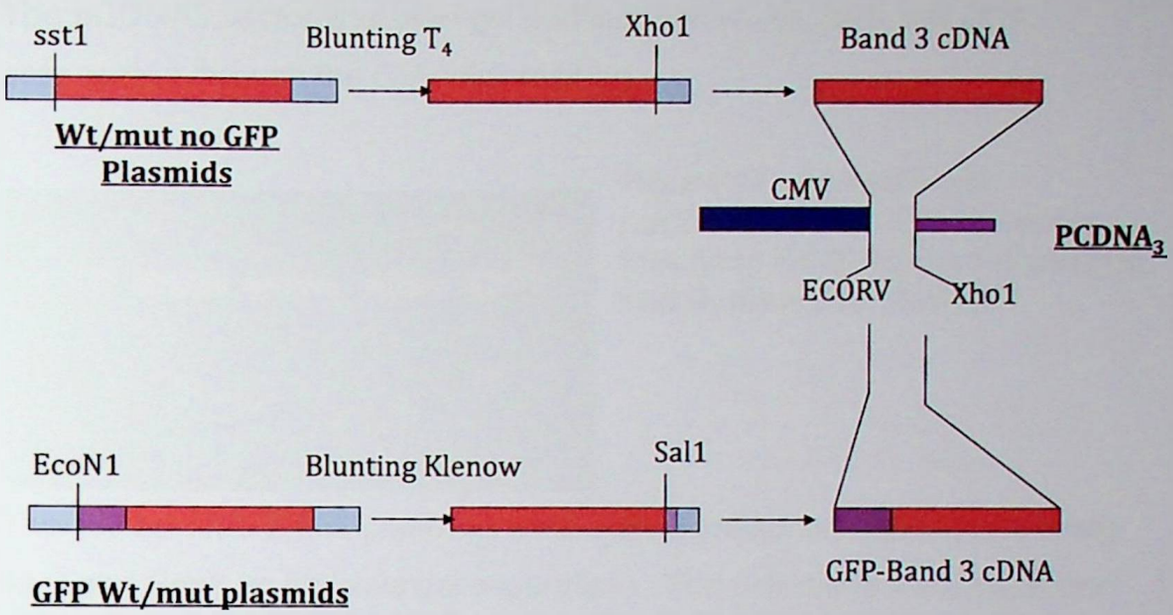

Figure 15. Strategy for construction of PCDNA$_3$band3 plasmid for transient transfection

A Sac1 digestion was then performed then blunted with DNTPs and T4 polymerase. The vector was then digested at the ECORV site then at the Xho1 site, and then dephosphorylated. These digestions were then checked on the gel below.

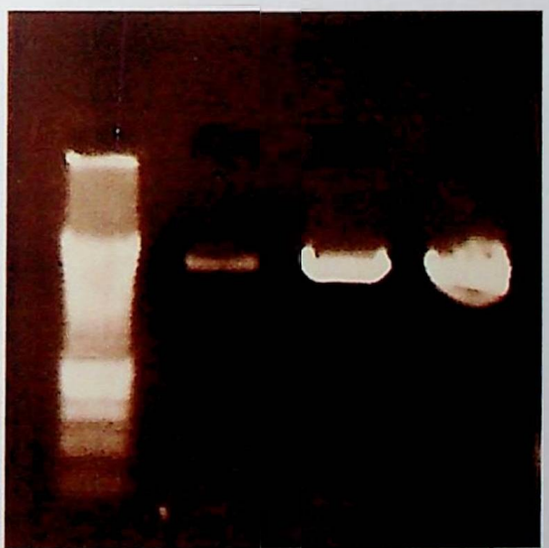

Figure 16. Agarose gel electrophoresis. New digestions of AE1 WT and MUT plasmids with Sac1 and digestion of pCDNA3 with ECORV and Xho1.

The pCDNA3 vector was then gel purified (below), excised and DNA propagated through the QIAquick method.

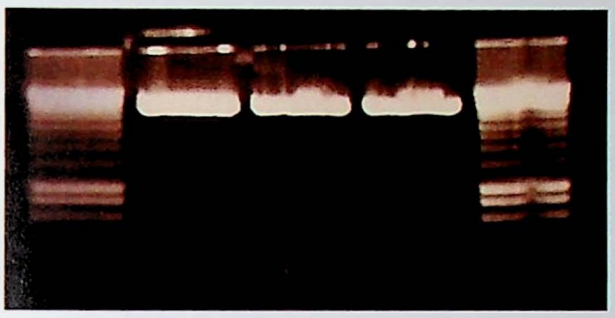

Figure 17. Agarose gel purification of pCDNA3 vector following ECORV/Xho1 digestion and dephosphorylation

The WT and MUT AE1 plasmids were then digested with Xho1 (for cloning site) and Sca1 (to improve gel separation). The fragments were separated and purified on gel electrophoresis (below)

Figure 18. Agarose gel purification of WT and MUT AE1 plasmids after further digestion Xho1/ Sca1.

A quantitative gel analysis was then performed for the vector and KB3 inserts (below).

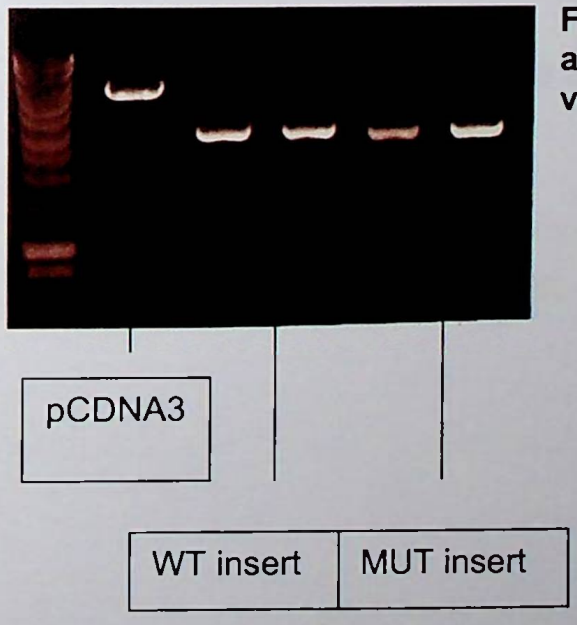

Figure 19. Agarose gel quantitative analysis of post digestion pCDNA3 vector and AE1 Wt and Mut inserts

3.1.6 Ligation of WT and MUT AE1 into pCDNA3 vector – "sticky ligation" strategy

The ligation reactions were then performed with a 7:1 ration of insert: vector with vector only and insert only controls. The ligation mixes were incubated at 16C overnight, transformed in e coli bacteria and plated on ampicillin resistant culture plates. These were then incubated overnight. Colonies were then selected and DNA extracted according to the QIAGEN miniprep method. Diagnostic digestions were then performed with the BSTX1 and Xba1 enzymes.

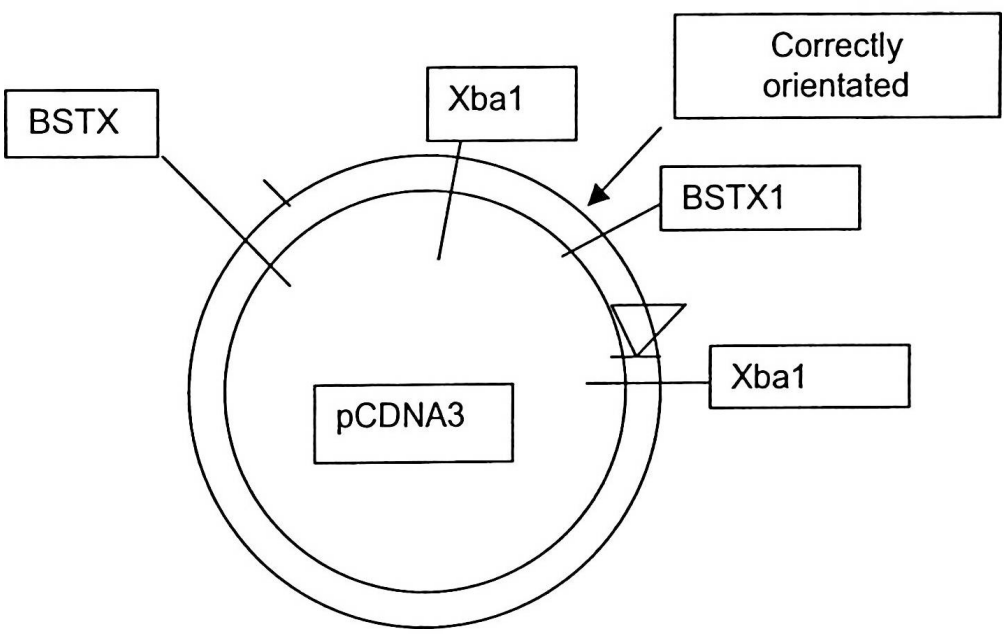

Figure 20. Diagram of pCDNA3 construction with Xba1 and BSTX1 digestion sites.

The Xba1 digestion yielded a vector and 1.5 Kb fragment. The BSTX1 digestion yielded a vector and 2Kb fragment.

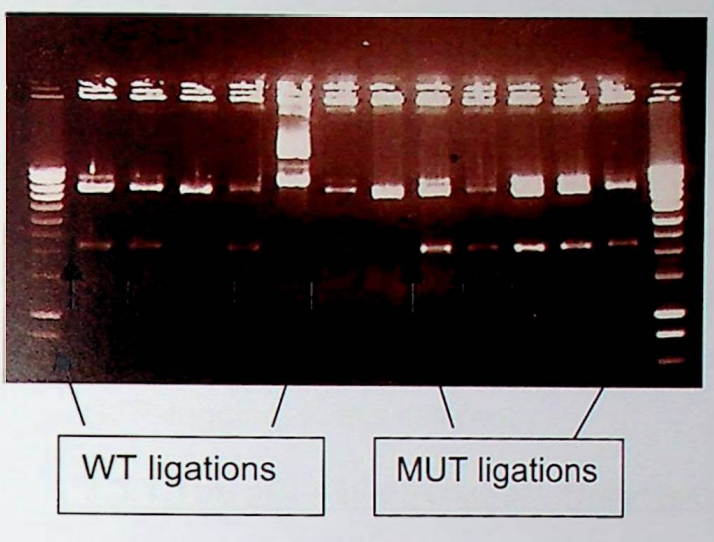

Figure 21. BSTX1 digestions of WT/MUT AE1 and pCDNA3 ligations. Arrows represent successful ligations.

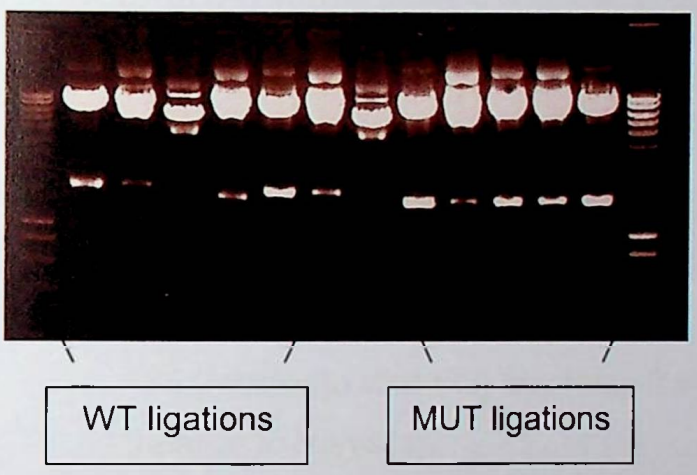

Figure 22. Xba1 digestions of WT/MUT AE1 and pCDNA3 ligations. The arrowed samples represent successful ligations.

3.1.7 Sequencing of pCDNA3AE1WT and pCDNA3AE1MUT constructs

I designed primers for direct sequencing across ligation sites. This sequencing was then performed commercially and the results checked by myself against the known sequences of the $PCDNA_3$ vector and the AE1 sequence.

3.2 GFP-TAGGED WT AND MUT AE1 PCDNA3 CONSTRUCTIONS

GFP-tagged band 3 CDNA was also available from plasmids provided by Ashley Toye. These were excised and cloned into the $PCDNA_3$ vector using a similar method. Again, the ligation sites were checked with commercial, direct sequencing.

3.3 PREPARATION OF CONDITIONAL EXPRESSION VECTOR FOR WILD-TYPE AND MUTANT AE1 EXPRESSION

In the last two sections I have outlined the preparation of the molecular constructs for transient transfection of $RCCD_1$ cells with WT, WT-GFP, MUT and MUT-GFP AE1. A main aim of this project was also to deliver constitutive, *conditional* expression of WT and MUT AE1, with and without GFP-tagging, in this cell line.

3.3.1 The pBI-4 bi-directional promoter construct

This is a vector constructed by A.G.H. Bujard and donated to Frederic Jaisser at INSERM U478. The plasmid consists of four main fragments.

1. The Pbr322 sequences including colE1-origin of replication and b-lactamase resistance gene with PBLA/P3 OF Tn2661.
2. The regulatory region with the bi-directional promoter Pbi-1: heptamerized *tet*-operator sequences flanked by two divergently orientated hCMV minimal promoters: Pmin-1 spanning position- -31 to +75 (relative to start site) and Pmin-2 spanning position -53 to +75 (relative to start site).
3. Multiple cloning site 1, followed by rabbit b-globin intron/poly (A) signal and transcribed from Pmin-2. Specific cleavage sites here are Pvu II, Mlu I, Nhe I and ECORV.
4. Multiple cloning site 2, followed by SV40 late poly (A) signal and transcribed from Pmin-1. Cleaving specificities of MCS 2 are Sal I, Not I, Pst I.

3.3.2 The pIRES1Hygro bicistronic expression vector

The pIRES1*hyg* Bicistronic Expression Vector (CLONTECH) contains the internal ribosome entry site (IRES) of the encephalomyocarditis virus (ECMV). This permits the translation of two open reading frames from one messenger RNA. It comprises the following.

1. The human CMV major immediate promoter/enhancer.
2. A multiple cloning site

3. A synthetic intron known to enhance the stability of the mRNA.
4. The ECMV IRES followed by the Hygromycin B phosphotransferase gene, and the polyadenylation signal of the bovine growth hormone.

Ribosomes can enter the bicistronic mRNA either at the 5' end to translate a gene cloned into the multiple cloning site or at the ECMV IRES end to translate the antibiotic resistance marker.

In this vector the antibiotic exerts selective pressure on the whole expression cassette. Thus, only cells expressing a high level of the gene of interest will survive when cultured in medium with added Hygromycin.

3.3.3 Strategy in constructing a vector combining pIRESHygro selection cassette and pBI-4 bidirectional promoter.

Our strategy here was to develop a construct in which the Hygromycin selection cassette *and* AE1 expression would be under influence of the *tet* operator. This would give me tet-dependant Hygromycin resistance and Band 3 expression. As a consequence I would, following tet-induction, be able to select cell clones with only strong expression of the Hygromycin resistance cassette and the AE1 gene inserts. This tet-dependant Hygromycin resistance would also, theoretically, give us the means to maintain stable AE1 expression during culture by performing intermittent Hygromycin selection.

To do this our plan was to clone the pIRES1*hyg* selection cassette into the pBI-4 vector on one side of the bi-directional, *tet*-dependant promoter. We would then clone our AE1 genes into the other end multiple cloning site at the other side of said promoter.

RCCD1 transfected cells would potentially have constitutive expression of AE1 genes which was entirely *tet*-dependant. That our antibiotic resistance was also *tet*-dependant would hopefully mean that only clones with strong expression of AE1 under *tet* influence would be selected.

The strategy for plasmid construction is shown in the figures on the next two pages.

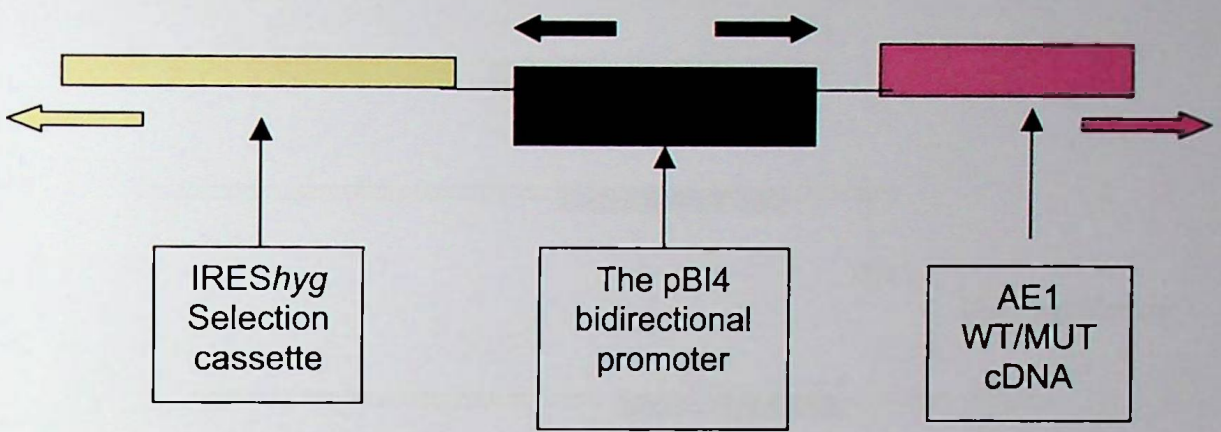

Figure 23. The intended pBI4IREShygroAE1-GFP responder construct

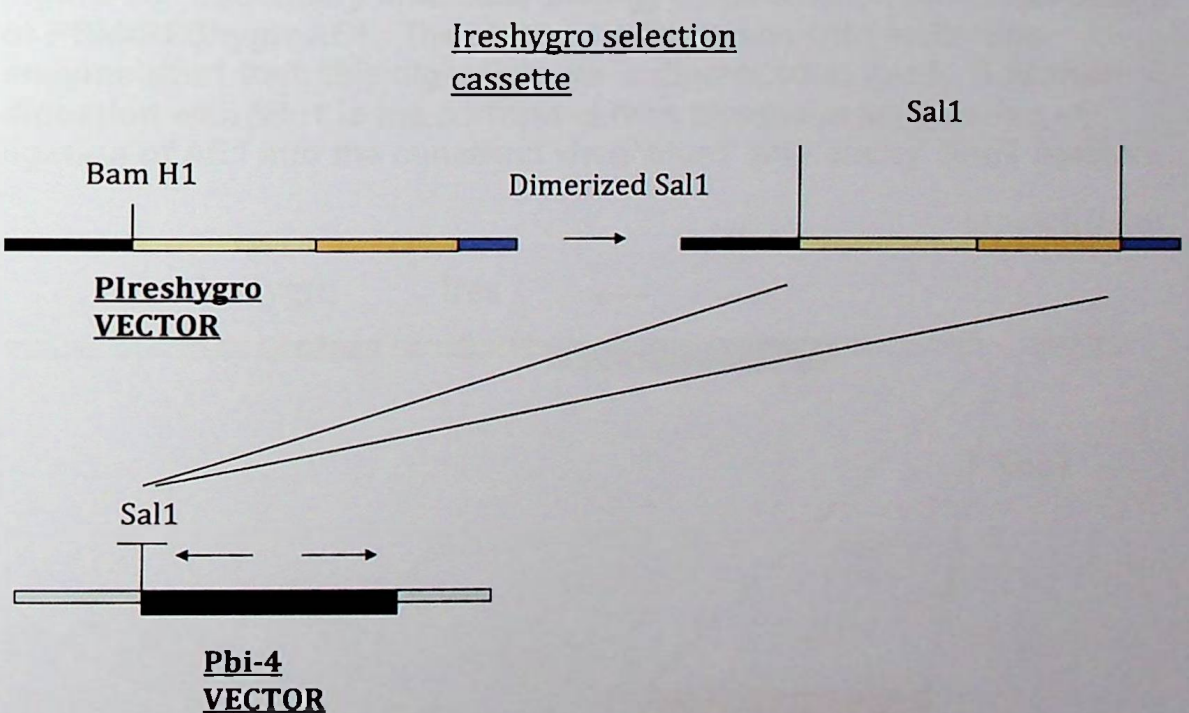

Figure 24. Initial molecular biology steps in construction of PBI4IREShygroAE1. The selection cassette is extracted from the plasmid PIREShygro via Bam H1 digestion, dimerisation to Sal1 then digestion of both ends of the cassette with Sal1. PBI4 was then digested with Sal1 at the multiple cloning site downstream of the bidirectional promoter. Ligation of the insert into the Sal1 site was then performed.

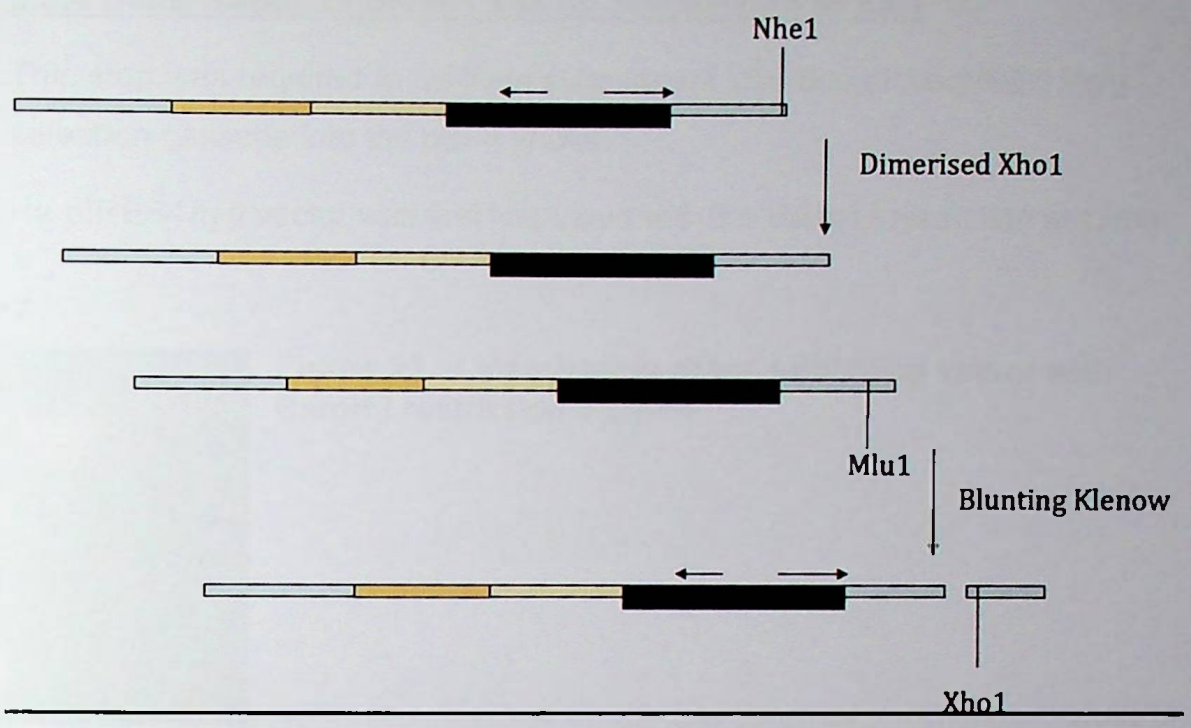

Figure 25. Secondary molecular biology steps taken in the construction of PBI4IREShygroAE1. The plasmid is linearised with restriction enzyme Nhe1 then this digestion site is dimerised to Xho1. A further digestion with Mlu1 is the performed then blunted in preparation of ligation of AE1 into the construct via a 'blunt' and 'sticky' Xho1 ligation.

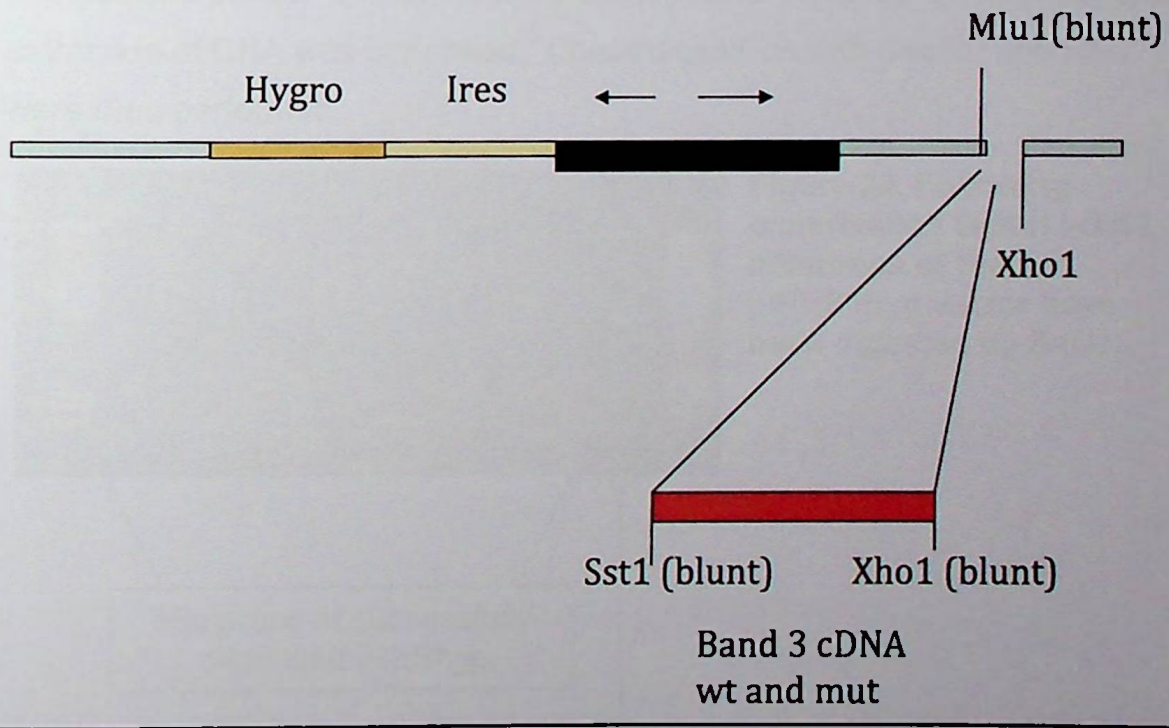

Figure 26. Final molecular biology steps taken in the construction of PBI4IREShygroAE1. AE1 is ligated into the plasmid downstream of the bi-directional promoter.

3.3.4 Dimerisation of BamH1 site on pIRESHygro to Sal I

This step was required to facilitate subsequent insertion of the pIRES1*hyg* selection cassette into the pBI-4 vector.

He pIRES1*hyg* vector was first linearised with the BamH I restriction enzyme.

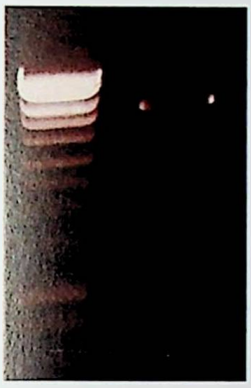

Figure 27. Linearization of the pIRES1hg vector with BamH I restriction enzyme

This digest was then precipitated. A dimerisation reaction (BamH I-Sal I) was then performed and incubated at 16 C overnight. This was then transformed in *e coli* and plated. 8 colonies were selected and "Miniprep" propagation and extraction of DNA was performed. Check digestions with BamH I and Sal I were then performed

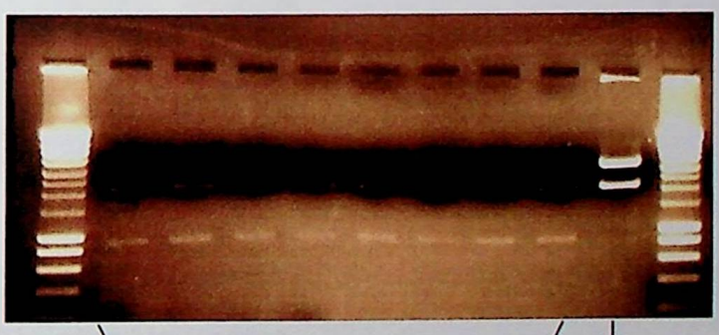

Figure 28. Following dimerisation BamH I-Sal I, minipreps of the pIRES1hyg vector have been digested by Sal I.

Minipreps of successfully dimerised IRESh*yg*

Control: digested, non-dimerised vector.

3.3.5 Preparation of pBI-4 vector

The pBI-4 vector was digested with Sal I and linearisation was confirmed with gel electrophoresis.

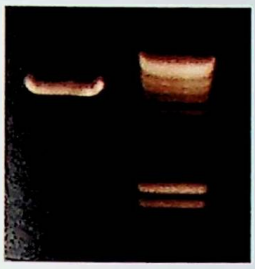

Figure 29. Agarose gel electrophoresis showing successful linearization of the pBI-4 vector with Sal I.

This digest was then precipitated, dephosphorylated, gel purified and extracted

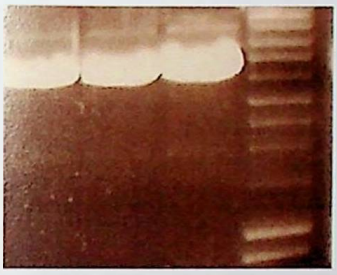

Figure 30. Agarose gel purification of linearised pBI-4

Figure 31. Linearised pBI-4 following gel purification and extraction

3.3.6 Excision of IRESHygro selection cassette from pIRESHygro bicistronic vector.

The dimerised pIRES1Hygro vector was then digested with Xho I and Sal I.

Figure 32. Dimerised pIRES1*hyg* following digestion with Xho I and Sal I

To facilitate extraction of the IRESHygro insert a further digestion with Dra I was performed. This further fragmented the vector. The digest was then gel purified and extracted

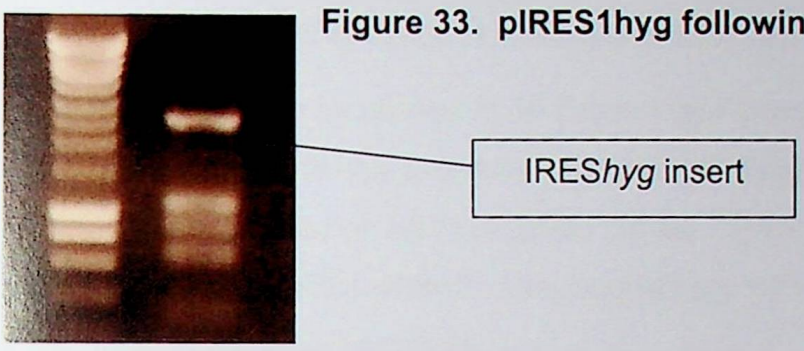

Figure 33. pIRES1hyg following digestion with Dra I.

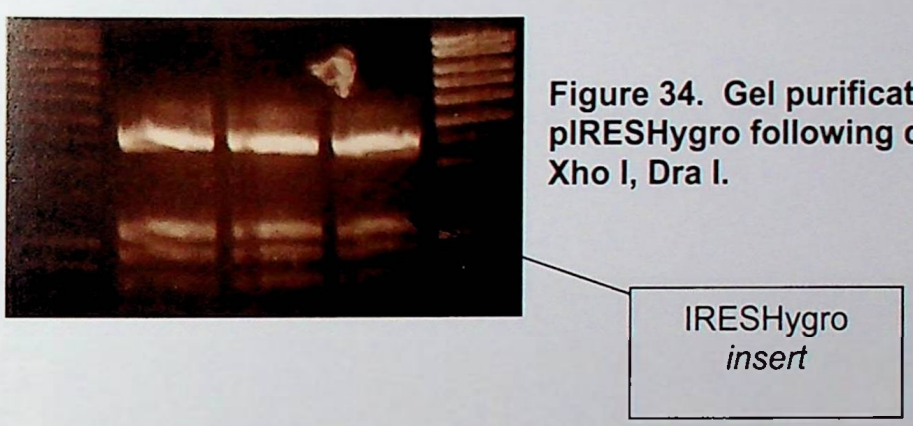

Figure 34. Gel purification of pIRESHygro following digestion Sal I, Xho I, Dra I.

3.3.7 Ligation of IRESHygro selection cassette into pBI-4 vector

A quantitative gel analysis of the prepared pBI-4 vector and IRESHygro insert was then performed.

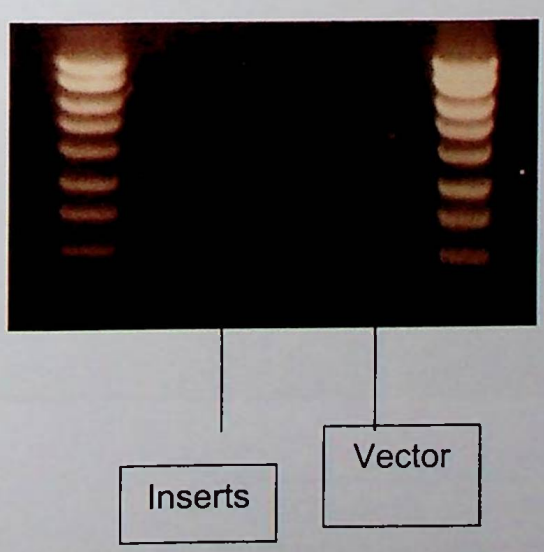

Figure 35. Quantitative agarose gel analysis of inserts and vector preparations.

Ligation reactions were then performed with the following relative amounts.

Insert: vector

Insert 3:vector 1

Insert 6: vector 1

Insert 6: vector 0.5

Insert and vector only ligations were also performed as controls.

The ligations were incubated at 16 C overnight then transformed in E.*coli*, plated on culture dishes and incubated at 37 C overnight. Good numbers of colonies were noted on all the ligation plates. There were a number of colonies on the vector control plate, suggesting some autoligation of vector, but none in the insert controls.

12 colonies were selected from the ligation plates and the DNA propagated with the *Qiagen* miniprep protocol.

A diagnostic digestion was then performed with Xba1 to check ligation and orientation.

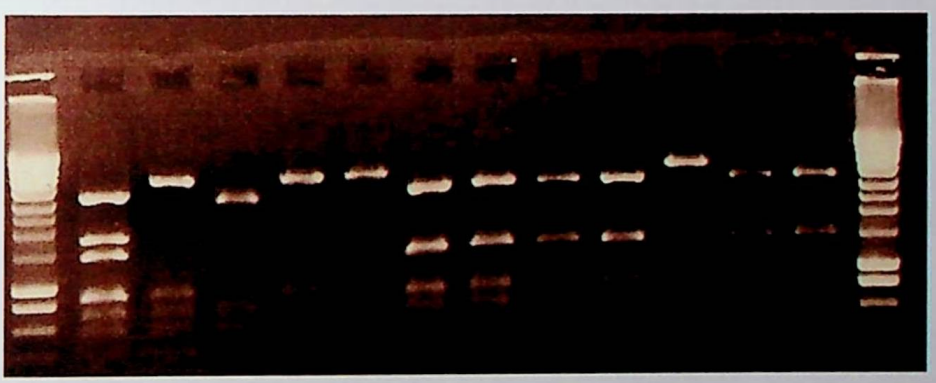

Figure 36. Ligations of IREShyg and pBI-4, ECOR1 digest

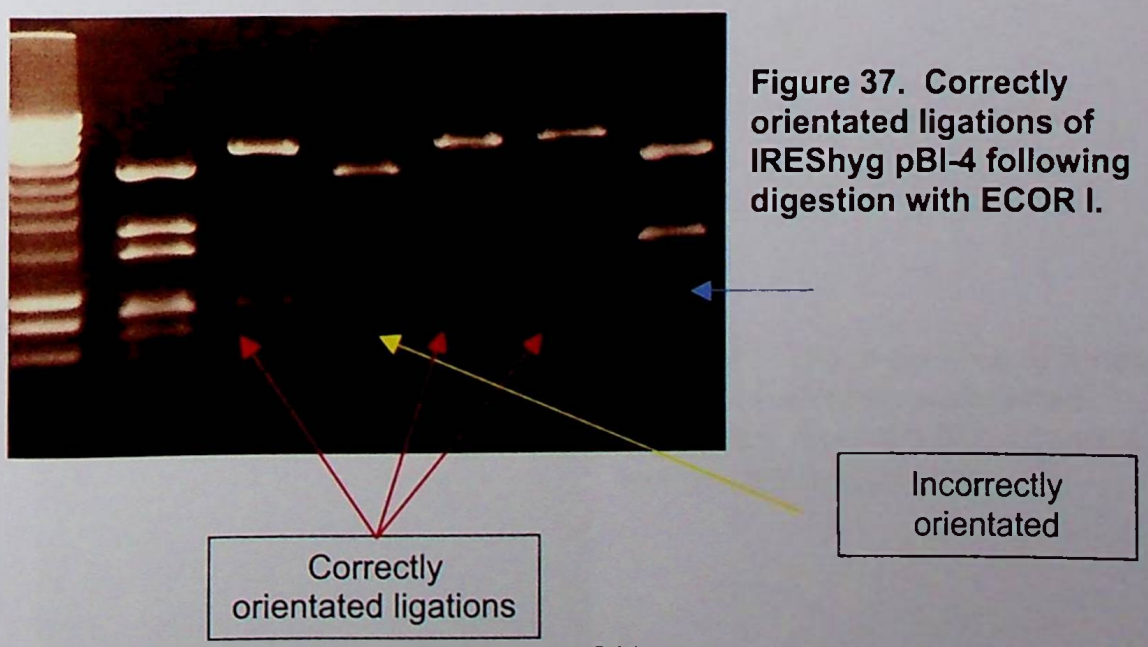

Figure 37. Correctly orientated ligations of IREShyg pBI-4 following digestion with ECOR I.

3.3.8 Abolition of residual Xho1 site at distal end of IRESHygro in pBI-4IRESHygro construct

The strategy for cloning the AE1 genes into this construct was to dimerise an NHE1 site in the 2nd multiple cloning site of the pBI-4 construct to an Xho1 site. To do this required abolition of a pre-existing Xho 1 site at the distal end of the IRESHygro selection cassette. The pBI-4/IRESHygro construct was first digested with Xho I.

Figure 38. pBI-4IRESHygro construct following linearization with Xho I.

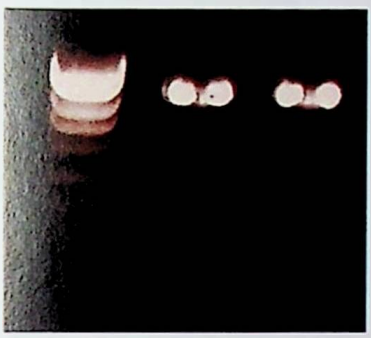

This linearised construct was then "blunted" with Klenow and DNTPs to abolish the Xho1 site. He construct was then autoligated via a blunt ligation reaction. This was incubated at 16 C overnight, transformed in *E.coli*, plated on culture dishes then incubated overnight at 37 C. 16 colonies were then selected, propagated and the DNA extracted via the QIAGEN miniprep method. The minipreps were then digested with Xho I.

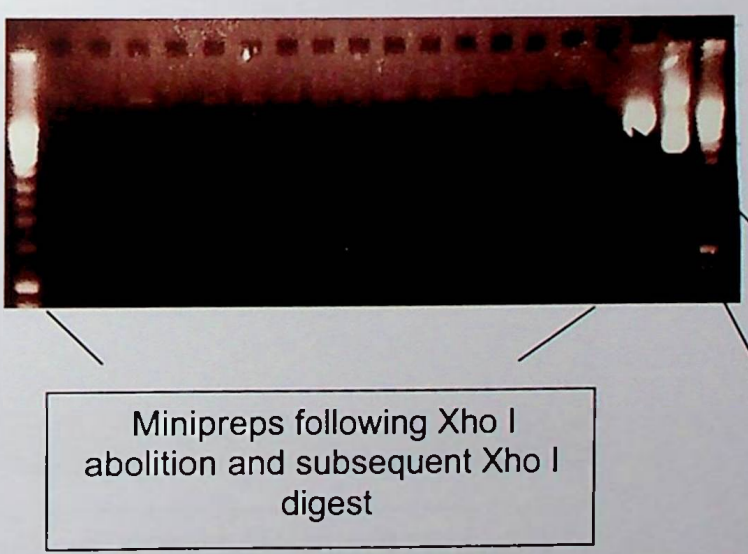

Figure 39. Digestion of 16 minipreps following abolition of Xho I site.

Figure 40. Close-up view of figure 15, demonstrating undigested minipreps, digested Xho I control and undigested control.

3.3.9 Dimerisation of NHE I to Xho I in pBI-4IRESHygrp construct

This step was undertaken to facilitate the cloning of the AE1 genes into the 2nd multiple cloning site of the pBI-4 vector. Initially the pBI-4/IRESHygro construct was linearised with NHE1.

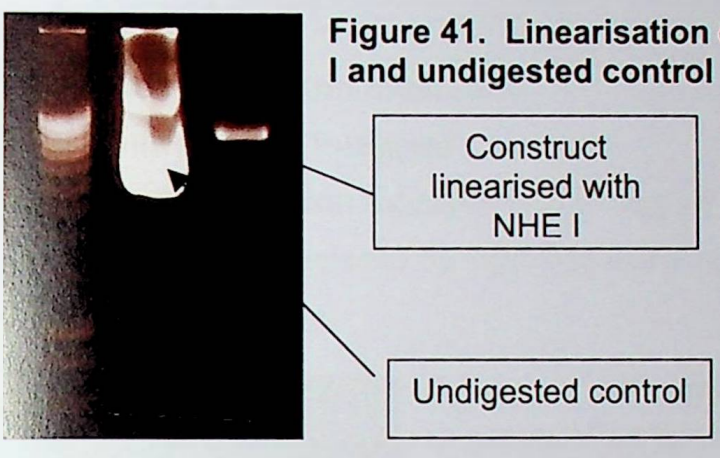

Figure 41. Linearisation of pBI-4IRESHygro with NHE I and undigested control

This digest was then precipitated and an NHE I-Xho I dimerisation reaction was undertaken. This was incubated at 16 C overnight. The dimerisation was then transformed in *E.coli,* plated and incubated at 37 C on culture medium. Numerous colonies were present. 16 were selected, propagated and the DNA extracted according to the *Qiagen* "minipep" method.

Figure 42. pBI-4/IREShyg following dimerisation of NHE I to Xho I and subsequent Xho I digestion.

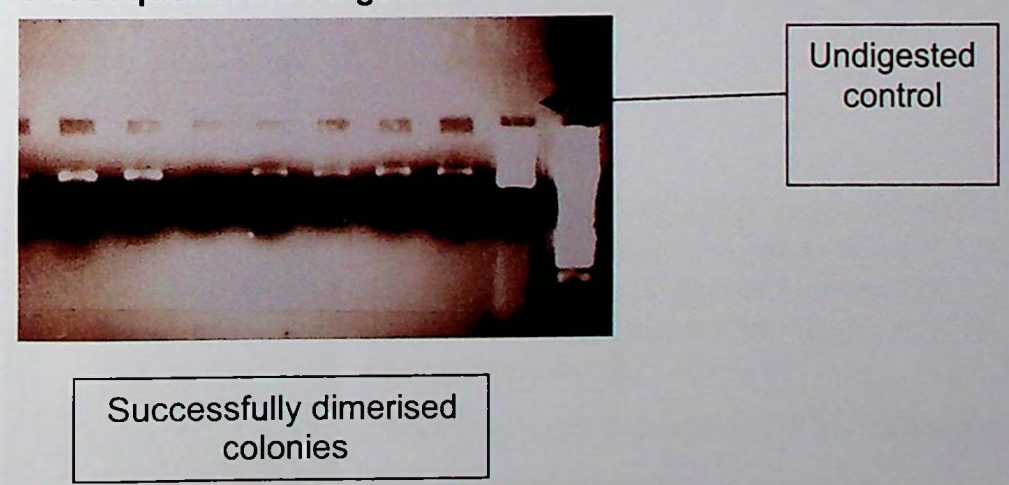

A "maxiprep" DNA propagation was then performed on two of the successfully dimerised pBI-4IREShygro plasmids according to the QIAGEN protocol previously described.

3.3.10 Cloning of AE1 cDNA into pBI-4IRESHygro vector for inducible expression

As for the pCDNA3 transient transfection vector I planned to clone the following AE1 genes into this construction.

AE1 wild type

AE1 mutant (Walton mutation)

AE1 wild type GFP-tagged

AE1 mutant (Walton mutation) GFP-tagged

The vector was prepared by digesting at the Mlu I site on the second pBI-4 multiple cloning site.

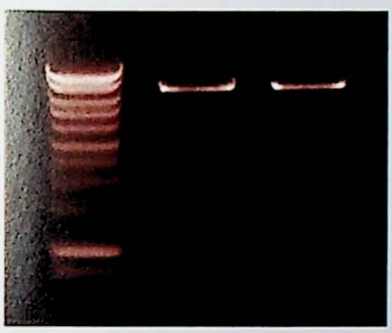

Figure 43. pBI-4IRESHygro digested with MLU I in preparation for KB3 cloning. The proximal end of the AE1 cDNA will be ligated at this site.

This digest was precipitated, blunted with Klenow and DNTPs, gel purified and the DNA extracted. A digestion was then performed at the Xho I site (dimerised from NHE I previously) on the second pBI-4 multiple cloning site. Gel analysis confirmed a single Xho I digestion, and prior abolition of the second Xho I site.

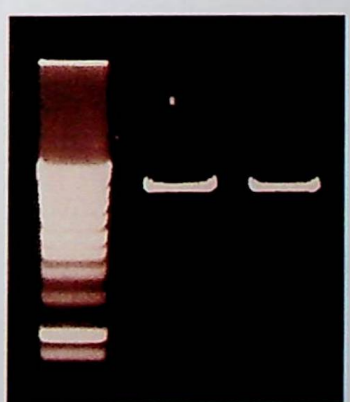

Figure 44. pBI-4IRESHygro vector following digestion with Xho I in preparation for AE1 cloning. This confirms abolition of second Xho I site. A single site remains; for the ligation of the distal end of the AE1 cDNA.

This digest was then gel purified, dephosphorylated and then gel purified again.

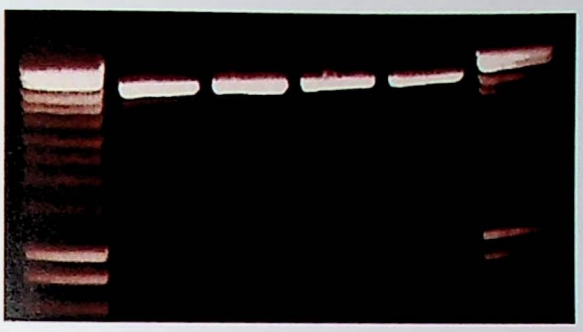

Figure 45. Gel purification of pBI-4IRESHygro following digestion Mlu I, blunting, digestion Xho I and dephosphorylation

The preparation of the AE1 cDNA inserts has been described previously in the section on the formation of the $pCDNA_3AE1$ constructs. These cDNA inserts consisted of a blunted 5' end. The 3' end of the WT and MUT AE1 cDNAs had been digested with Xho I. The 3' ends of the WT-GFP and MUT-GFP AE1 cDNAs had been digested with Sal1, which can be cloned into an Xho I site. A quantitative gel analysis of the prepared pBI-4IRESHygro vector and the AE1 inserts was then performed.

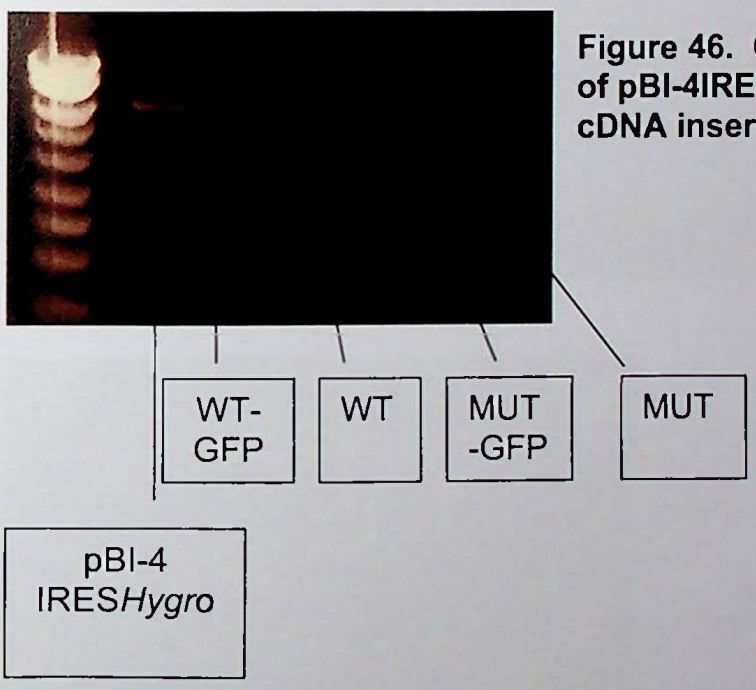

Figure 46. Quantitative gel analysis of pBI-4IRESHygro vector and AE1 cDNA inserts.

Ligations were then performed. The following ligation mixes were used.

Insert 3:vector1

Insert 6:vector 1

Vector and Insert only ligations were also performed as controls

The ligations were incubated at 16 C overnight, transformed in *E.coli*, plated on culture plates. This demonstrated good numbers of colonies on ligation culture plates, with some colonies in both insert and vector controls. 18

colonies of each of the ligations were then selected. These were then propagated and the plasmids DNA extracted using the QIAGEN miniprep protocol.

Following selection of correctly orientated construct clones for WT and MUT pBI-4IRESHygro further check digestions were performed with HPA I, ECOR I, ECORV and Xba I.

18 minpreps of both WT and MUT pBI-4IRESHygro construction after digestion ECOR1

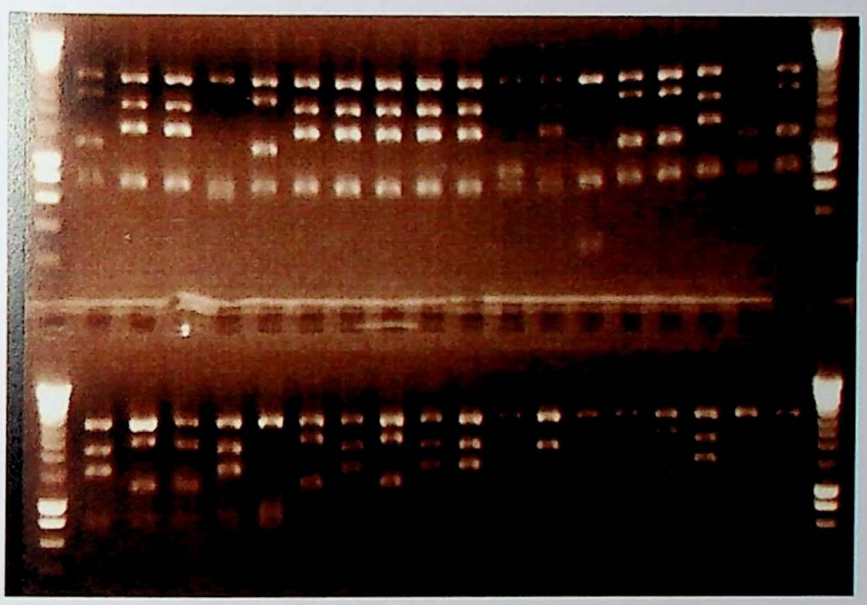

Figure 47.

18 minpreps of both WT and MUT pBI-4IRESHygro construction following digestion

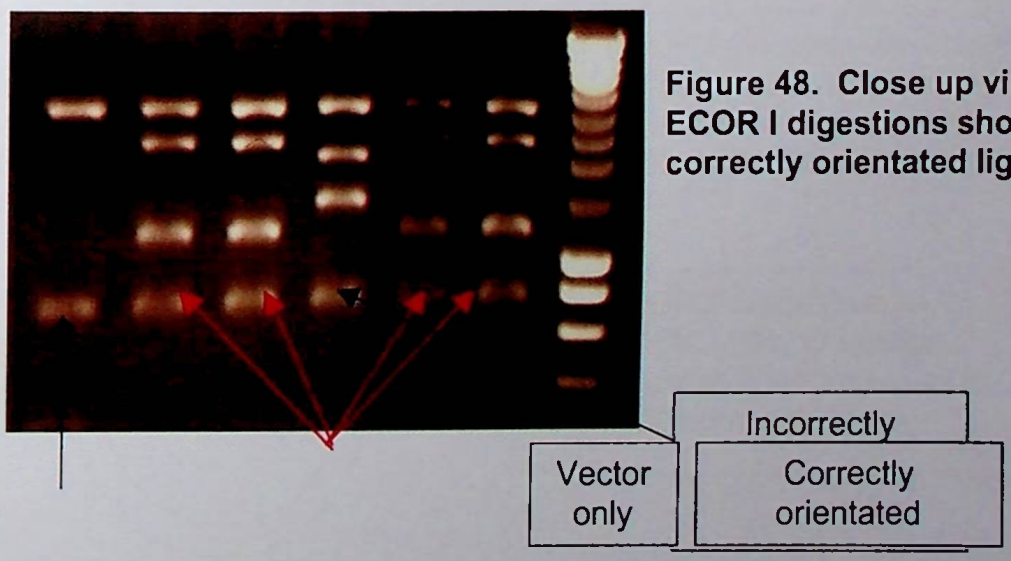

Figure 48. Close up view of ECOR I digestions showing correctly orientated ligations.

Following selection of correctly orientated construct clones for WT and MUT pBI-4IRESHygro further check digestions were performed with HPA I, ECOR I, ECORV and Xba I.

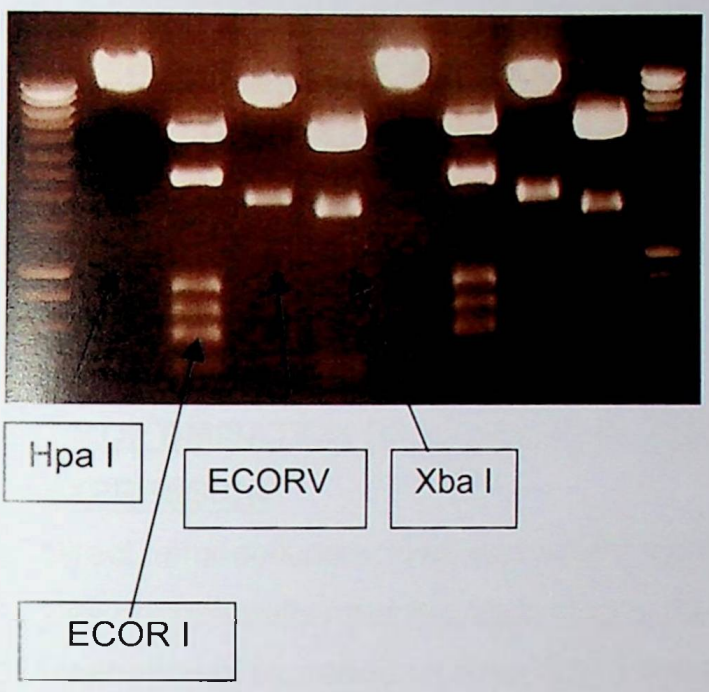

Figure 49. Further diagnostic digestions

WT pBI-4IRESHygro

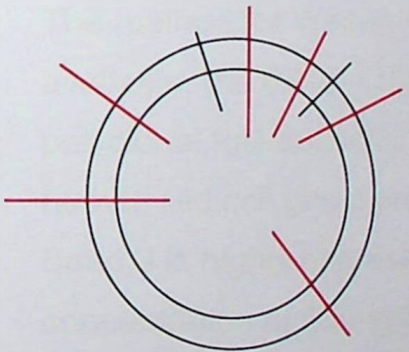

ECOR I digestion sites on pBI-4IRESHygro. Digestion results in 6 visible bands at 4419, 2400, 857, 700, 563 and 372

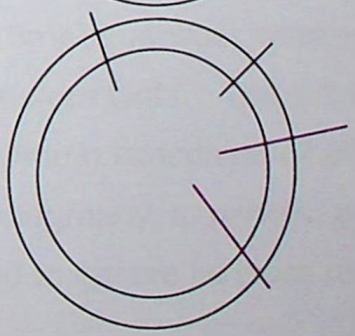

ECORV digestion sites on pBI-4IRESHygro. Digestion results in 2 visible bands at 7700 bp and 1700 bp.

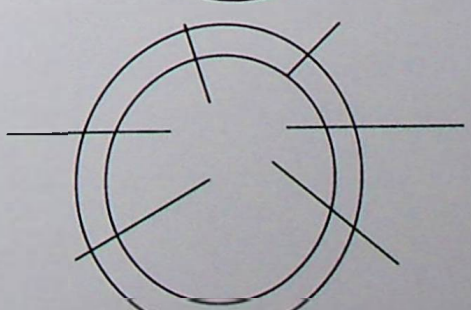

Xba I digestion sites on pBI-4IRESHygro. This results in 3 visible bands at of 4059, 3697 and 341 bp

The WT and MUT-GFP ligations were also checked with similar digestions.

3.4 SEQUENCING OF INSERT SITES FOR pBI-4IRESHygroAE1MUT AND pBI-4IRESHygroAE1WT

The ligation sites of the IREShygro selection cassette and the WT and MUT AE1 cDNA inserts were all checked with direct sequencing, following design of appropriate primers.

3.5 OPTIMISATION OF WESTERN BLOTTING FOR SCREENING FOR AE1 EXPRESSION

Direct immunofluorescence was a fairly limited resource in the laboratory and was not generally used to screen clones. Its use was usually limited to further evaluation of expression models where there was some evidence of expression through alternative screening methods such as Western Blotting. INSERM U478 had not previously studied AE1, while Professor Tanner's laboratory in Bristol used immunofluorescence for screening rather than Western blotting. As such it was necessary to optimise conditions for the Western blot.

The method for Western blotting is described earlier. Two antibodies were available, the BRIC-170, a mouse monoclonal antibody and a rabbit polyclonal IgG antibody against the cytosolic domain of AE1 at 43KDa. A human red cell ghost preparation was used as a positive control, given that Band 3 is highly expressed in the red cell membrane. This was prepared at a concentration of 0.5mg/L. 0.25mL (0.125mg), 0.5mL (0.25mg) and 1mL (0.5mg) quantities were tried as positive controls for initial optimisation Western blots. The aim in optimisation Western blotting was to determine the optimum concentration of primary antibody, the optimum exposure times for radiography, to perform a comparison of the performance of both antibodies and to ensure no cross reactivity from secondary antibody.

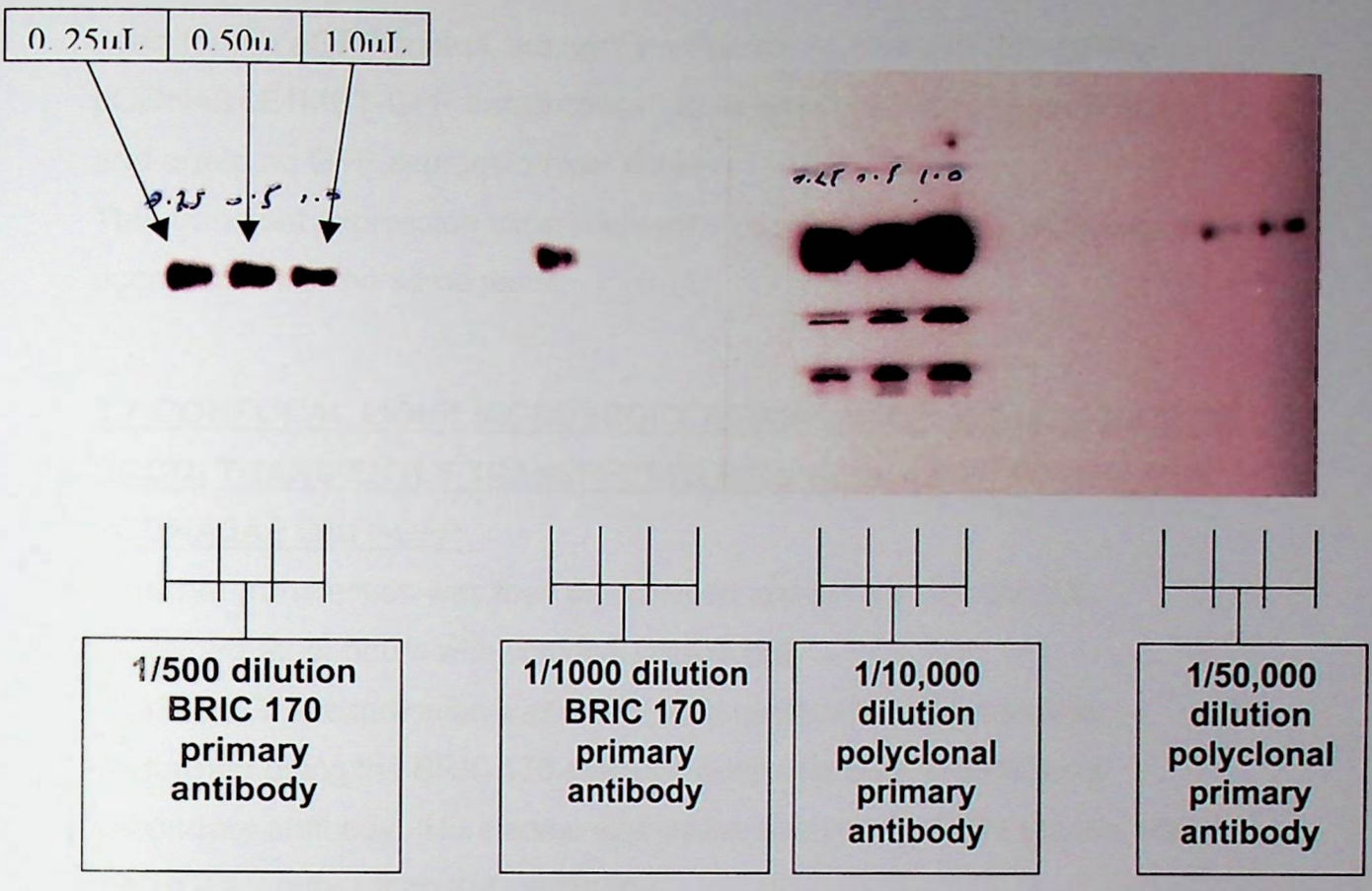

Figure 50. Western blot of red cell ghosts. 3 concentrations of red cell ghosts were used. BRIC 170 and a polyclonal Band 3 antibody were used at two different concentrations as shown. This was a 1-minute exposure.

Clearly I was able to successfully demonstrate Band 3 on western blotting. On the basis of this experiment the BRIC 170 antibody was selected and used at 1/500 dilution.

3.6 TRANSIENT TRANSFECTION AND FLUORESCENT LIGHT MICROSCOPY OF $RCCD_1$ WITH pCDNA3AE1WT-GFP AND PCDNA3AE1MUT-GFP

Firstly the pCDNA3WT-GFP and pCDNA3MUT-GFP plasmids were transfected into $RCCD_1$ according to the transient transfection method described in Chapter 2. An e-GFP control was used. This is a vector with a strong CMV promoter and the GFP gene in isolation.

Cells were inspected 24 hours after transfection. There was good confluence of healthy $RCCD_1$ in transfection wells. The cells were then inspected under fluorescent light microscopy in darkness. Strong fluorescence of GFP was

seen for the eGFP control, but not for either the pCDNA3AE1WT-GFP or pCDNA3AE1MUT-GFP transfections. Cells were inspected again on day 2 and again no GFP expression was noted.

This transient expression experiment was repeated again on a subsequent 2 occasions with the same result.

3.7 CONFOCAL LIGHT MICROSCOPY AND IMMUNOFLUORESCENCE OF $RCCD_1$ TRANSIENTLY TRANSFECTED WITH pCDNA3AE1WT-GFP AND PCDNA3AE1MUT-GFP

A further transfection was then transformed and the transfected cells examined at 24 hours with confocal microscopy.

Again no GFP expression was noted. Immunofluorescence was then performed using the BRIC 170 antibody used neat prior to addition of secondary antibody. Here some expression was noted of AE1 but this was in the $RCCD_1$ rather than the membrane.

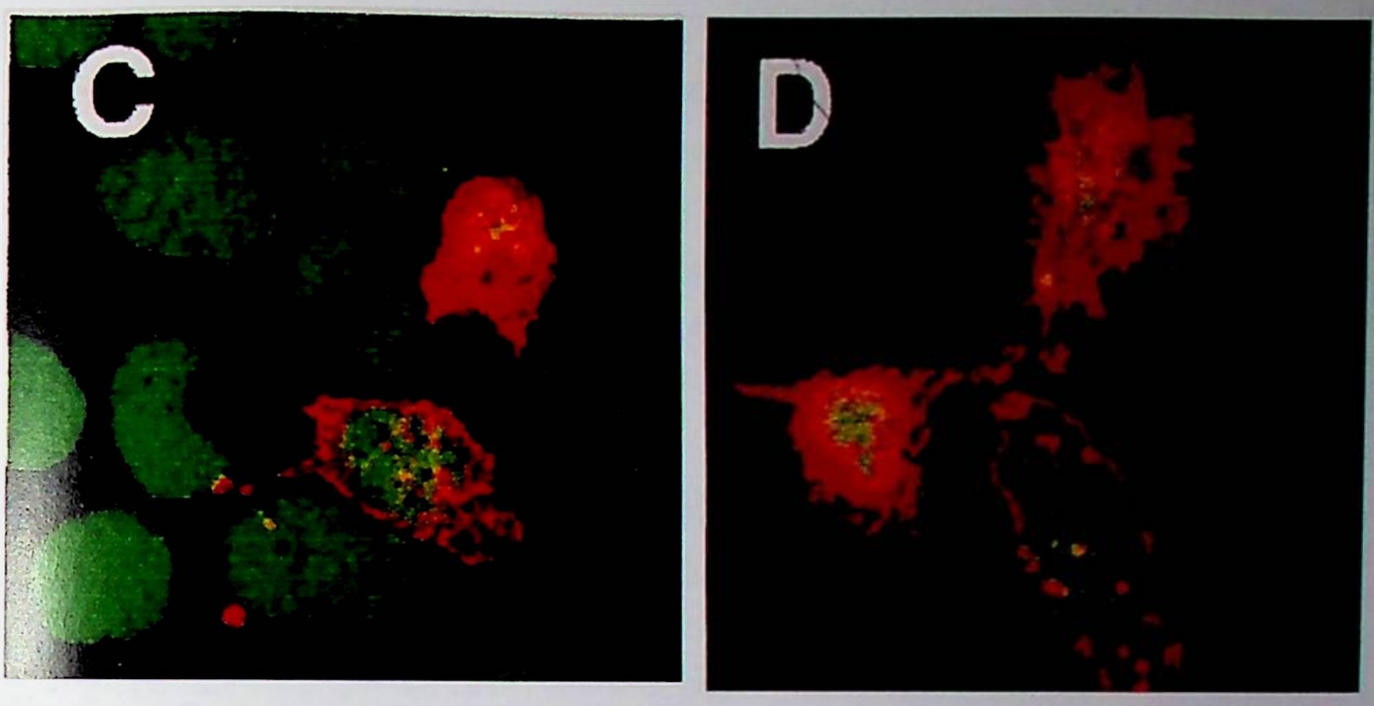

Figure 51. $RCCD_1$ following Transient transfection with pCDNA3AE1WT-GFP and following immunofluorescence with BRIC 170 monoclonal antibody. There is diffuse cytoplasmic expression of WTAE1, but no membrane expression. GFP fluorescence was not seen.

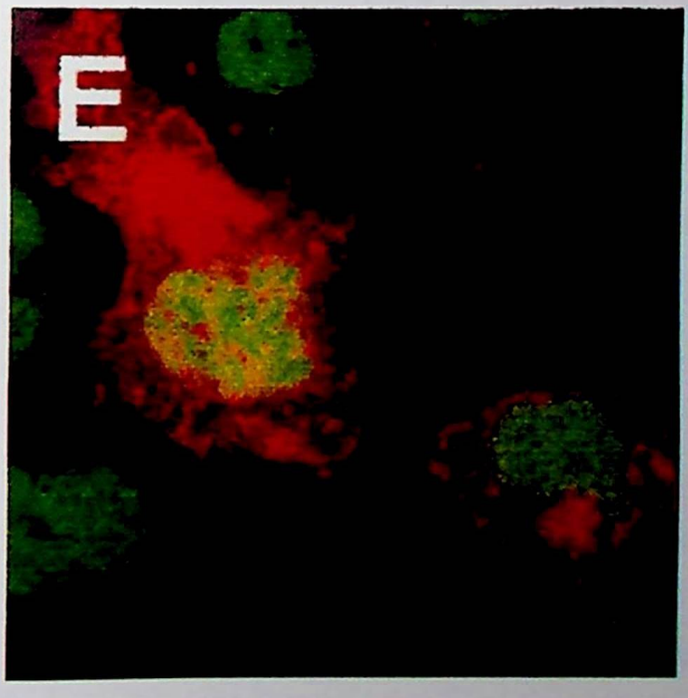

Figure 52. Confocal microscopy $RCCD_1$ following transient transfection with pCDNA3AE1MUT-GFP and following immunofluorescence with BRIC 170 monoclonal antibody. Again there is diffuse cytoplasmic expression of AE1-Walton but no membrane expression. Again GFP fluorescence was not seen.

3.8 TRANSIENT TRANSFECTION OF $RCCD_1$ WITH pCDNA3AE1WT AND pCDNA3AE1MUT

Non GFP-tagged AE1 constructs were also cloned into the pCDNA3 transient transfection vector as described in the previous chapter.

Transient transfections were performed as outlined previously. Again the eGFP plasmid was used as a control for the transfection technique. Cells were inspected at 24 hours and found to be in good health with good expression of the eGFP control.

3.9 CONFOCAL LIGHT MICROSCOPY AND IMMUNOFLUORESCENCE OF $RCCD_1$ TRANSFECTED WITH pCDNA3AE1WT AND pCDNA3AE1MUT

The cells were examined with confocal microscopy following immunofluorescence with BRIC 170 antibody.

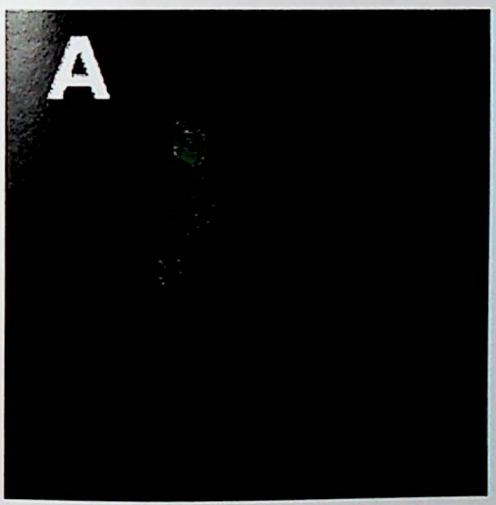

Figure 53. Confocal microscopy $RCCD_1$ following transient transfection with pCDNA3AE1WT (A) and pCDNA3AE1MUT (B) following immunofluorescence with BRIC-170 antibody. There is no AE1 WT or MUT expression seen.

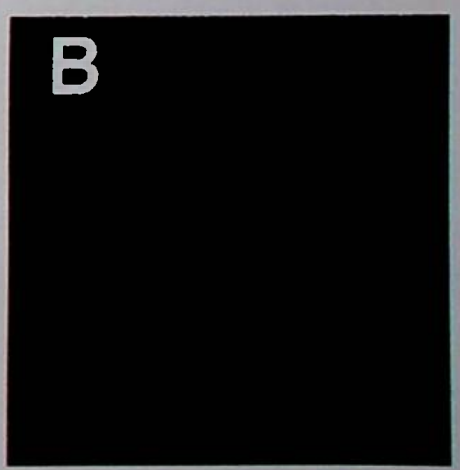

3.10 WESTERN BLOTTING OF RCCD1 FOLLOWING TRANSFECTIONS WITH pCDNA3AE1WT-GFP, pCDNA3AE1MUT-GFP, pCDNA3AE1WT and pCDNA3AE1MUT

Further transfections were then performed and, at 24 hours post-transfection, cells were then lysed for protein preparation by the previously described method. Western blotting was then performed with the Bric 170 antibody, optimised as previously described. The red cell ghost preparation was used as a positive control for Band 3 expression and untransfected $RCCD_1$ cells were also blotted. Cell preparations were quantified by the Lowry method. 50mg of $RCCD_1$ cell protein were deposited in each well, 0.25mg of red cell ghost for positive control.

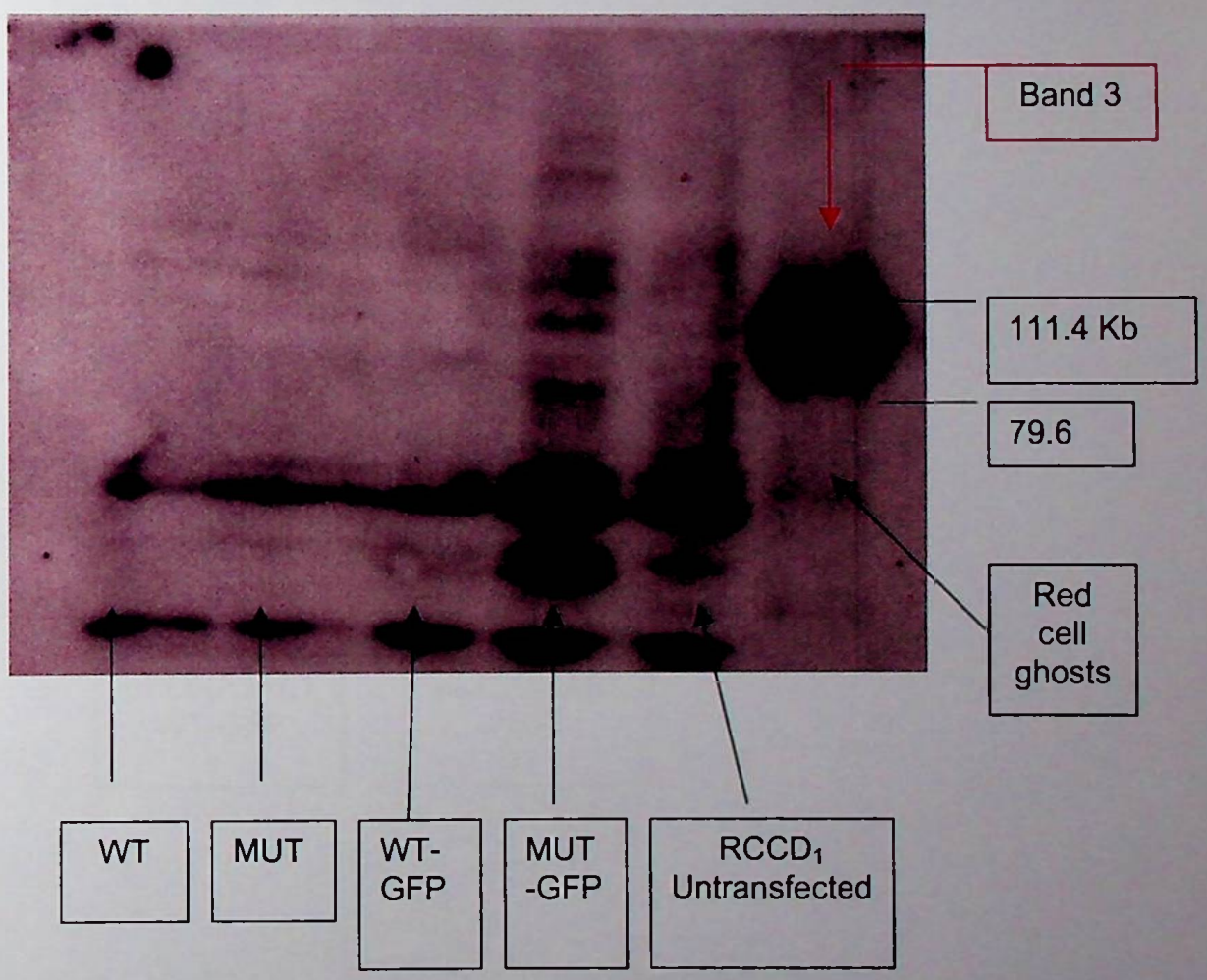

Figure 54. Western blot of $RCCD_1$ cells transiently transfected with the 4 pCDNA3 AE1 constructs with untransfected $RCCD_1$ and red cell ghosts as controls. There is strong immunodetection of AE1 in red cell ghosts, but not in native $RCCD_1$ or in any of transfected cells.

3.11 IN VITRO TRANSLATION OF AE1WT, AE1MUT, AE1WT-GFP and AE1MUT-GFP VIA pCDNA3 VECTOR.

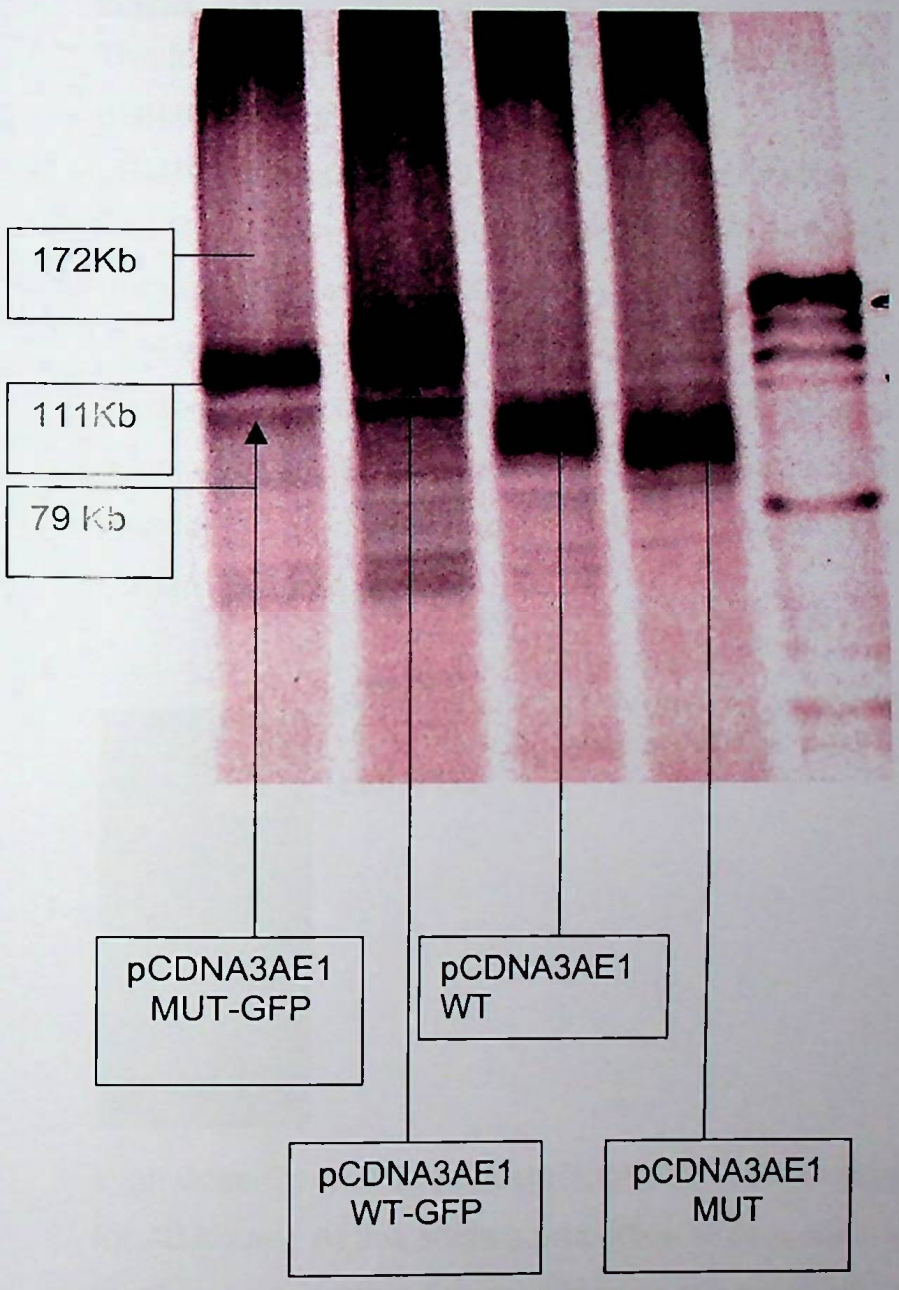

Figure 55. In vitro translation of pCDNA3AE1 constructs with pCDNA3MR receptor control. Gene transcription has been demonstrated.

3.12 TRANSFECTION, SELECTION AND PROPAGATION OF $RCCD_1$ CLONES WITH THE pBI-4IRESHygroAE1MUT AND pBI-4IRESHygroAE1WT CONSTRUCTIONS

3.12.1 Transfection

The following responder constructs were transfected

pBI4IRESHygroAE1WT (Wild-type AE1)

pBI4IRESHygroAE1MUT (AE1, Walton mutation)

The B5 $RCCD_1$ rtTA clone was defrosted and propagated in cell culture dishes until adequate cells were present for transfection experiments. These cells were then split with collagenase, counted and seeded into 6 well clusters. The constructs were linearised with the Hpa1 restriction enzyme. 12 hours after splitting the cells were in good condition with 50% confluence. A standard lipofectamine transfection was then performed with the linearised constructs (1mg per well)

Figure 56. Hpa1 linearisation of pBI-4IRESHygroAE1WT responder construct prior to transfection in $RCCD_1$-rtTA clone B5.

High dose Doxycycline (Dox) (5mg/ml) was then added to the culture medium for 48 hours. At this stage a proportion of cells were lysed for Western blotting (to ascertain if there had been any successful Band 3 expression following transient transfection).

3.12.2 Selection

The remainder of the cells appeared healthy and were split and transferred to large culture dishes with 5mg/ml Dox and high dose (400mg/ml) Hygromycin (Hygro) for selection. Clones with adequate, Dox-inducible expression of Hygro-resistance should hopefully have inducible KB3 under the same, bi-directional promoter in tandem with the rtTA transactivator construct.

3.12.3 Clone isolation

Following selection there were 13 surviving wild-type colonies and 2 surviving mutant colonies. These colonies were subsequently isolated and transferred to large (10ml) culture dishes for propagation.

3.12.4 Clone propagation and tet-dependant Hygromycin resistance

Rates of propagation were dependent on the clone, with some growing much more rapidly. Transgene expression was maintained by continuing (following recovery after cell splitting) selection pressure with Dox 5ml/ml then (after 48 hours) low dose Hygromycin at 200mg/ml). There was clearly Dox-dependant Hygromycin resistance and this was further demonstrated by selecting for Hygromycin with and without Dox-induction for each clone. Without Dox induction all cells were lysed, while following Dox induction a variable, but smaller proportion of cells were lost.

Clones were propagated, under selection pressure, until sufficient numbers were present for freezing, protein preparation for western blotting and ongoing culture. This, from the point of transfection, took several weeks.

3.13 WESTERN BLOTTING OF THE RCCD$_1$ pBI-4IRESHygroAE1MUT/pBI-4IRESHygroAE1WT CLONES

Cell lysis of clones was performed after two days of Doxycycline 5mg/ml induction of gene transcription. Western blotting was the performed using the previously described method, utilising the BRIC170 antibody, with the red cell ghost preparation as a positive control. The results for several Western blots for clones that had exhibited Dox-dependant Hygromycin resistance are shown in Figures 57 and 57. Unfortunately no AE1 expression could be demonstrated for clones transfected with either wild type or mutant AE1.

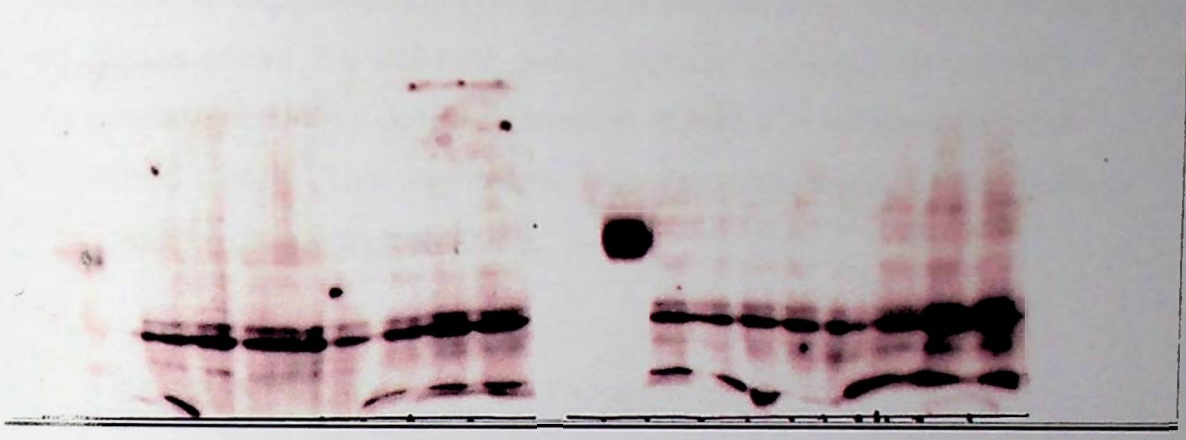

Figure 57. Two Western blots examining Dox-inducible AE1 expression in stably transfected $RCCD_1$ cells. AE1 red cell ghost prep has been loaded in the wells on the extreme left as a positive control. BRIC 170 antibody was used at a concentration of 1/500, as per previously described optimisation. Protein preps from 8 clones are shown with and without Dox stimulation. No expression of AE1 has been detected in these clones.

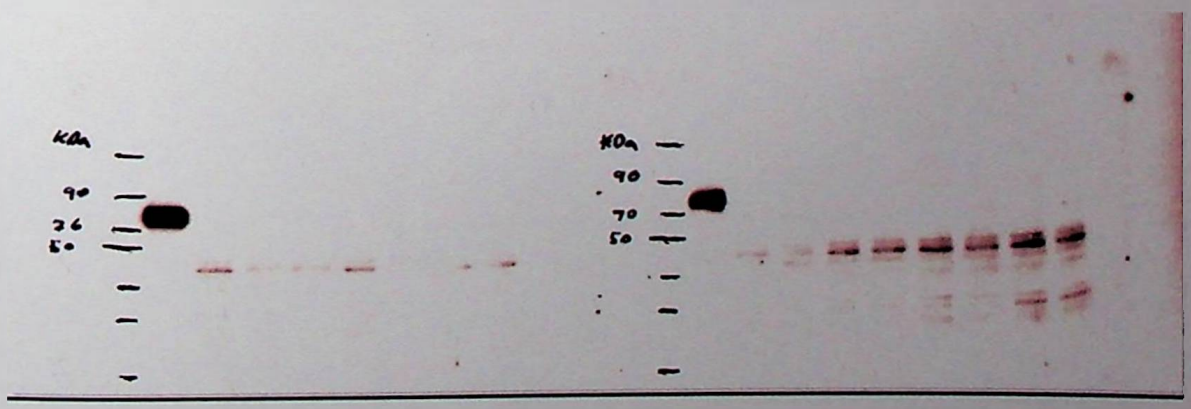

Figure 58. These Western blots have been used to screen further clones with and without Dox stimulation. BRIC 170 antibody was used at a concentration of 1/500, as per previously described optimisation. Again no AE1 expression is detected. All clones had demonstrable inducible Hygromycin resistance, suggesting that the responder construct had been successfully incorporated into the rtTA $RCCD_1$ cells.

3.14 CONFOCAL LIGHT MICROSCOPY AND IMMUNOFLUORESCENCE OF RCCD$_1$ pBI-4IRESHygroAE1MUT and pBI-4IRESHygroAE1WT CLONES

Induction of expression with Doxycycline 5mg/ml was performed for two days on clones grown in 6 well petri dishes. Bric170 antibody was used to immunostain. Unfortunately expression of AE1 was not detected in all screened clones. This was in spite of these clones having demonstrable inducible Hygromycin resistance.

3.15 SCREENING FOR AE1 MUTATIONS IN dRTA PATIENTS

Mutation screening with SSCP and sequencing demonstrated heterozygosity of the R589H mutation in 1 Dutch RTA patient with an apparently dominant inheritance. Heterozygosity for the R589H was also demonstrated in a sporadic case of dRTA.

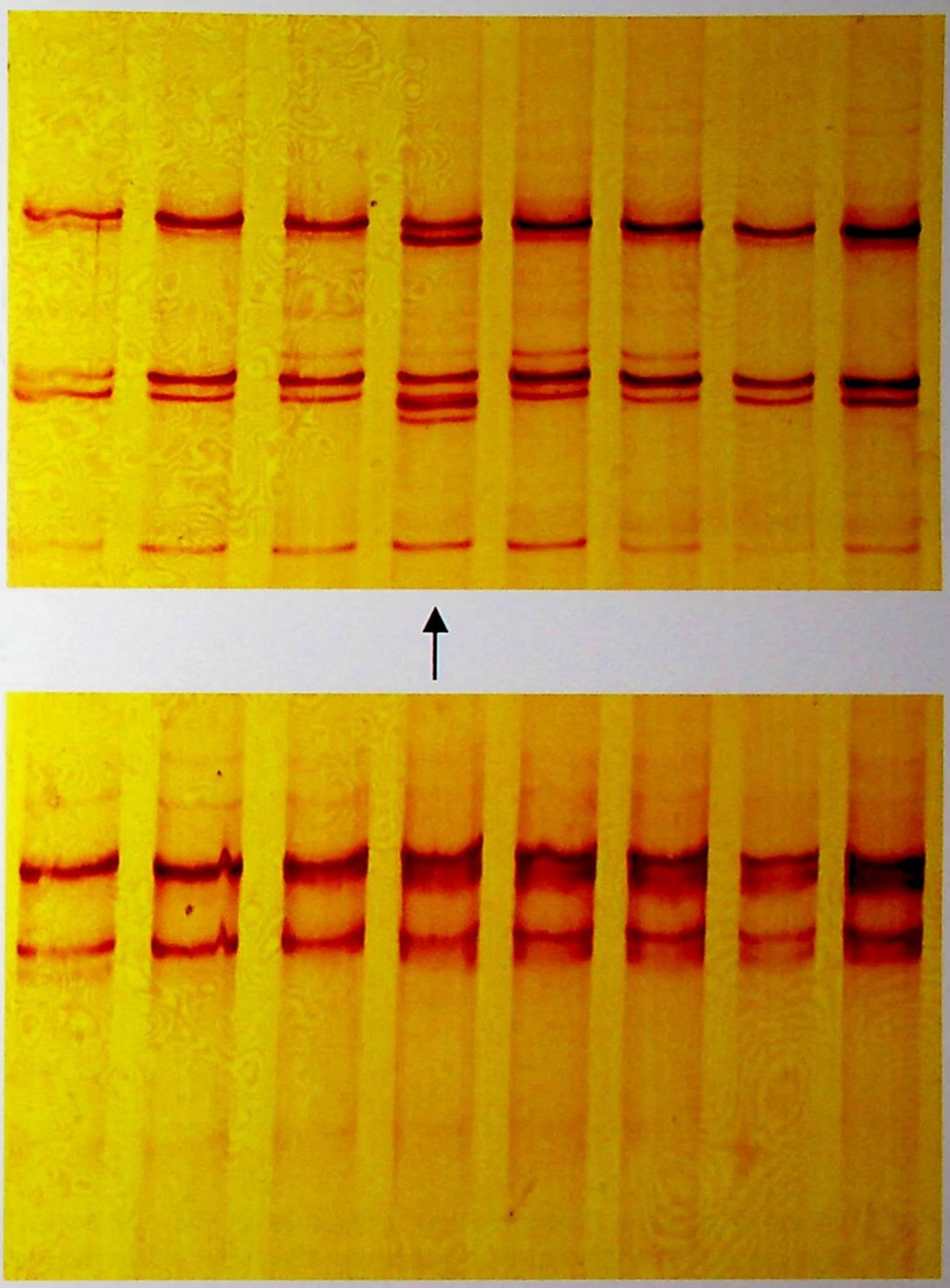

Figure 59. SSCP exon 11 – new RTA sporadic case shows variation at room temperature (upper image - arrow). This is less apparent at 4C (lower image). Sequencing showed this to be a non-mutation causing variation

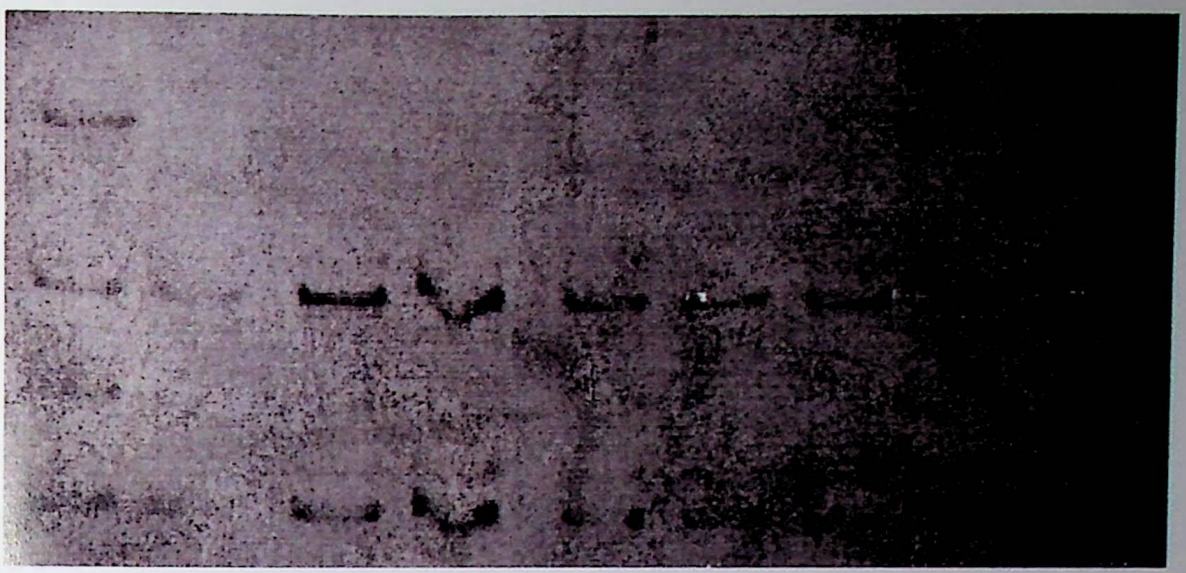

Figure 60. SSCP showing conformation change in exon 14 at room temperature in a new, autosomal dominant dRTA patient. Subsequent sequencing showed this to be the R589H mutation originally described by Bruce *et al.* The conformation of a member of this original index family is also shown.

SECTION IV - CHAPTER 4

CONCLUSIONS

4.1 TRANSIENT AND CONSTITUTIVE TRANSFECTION OF AE1 IN THE $RCCD_1$ CELL LINE

I was unsuccessful in my aim of achieving AE1 expression in the $RCCD_1$ cell line in THE transient expression model.

I successfully cloned WT and MUT AE1 into the $PCDNA_{3\ expression}$ vector. I was able to transfect $RCCD_1$ with $PCDNA_3$ with an eGFP insert as a control and demonstrated fluorescence. The cell culture and transfection techniques were therefore verified. I was, however, unable to demonstrate GFP fluorescence in GFP-tagged WT and MUT AE1 following transient transfection with these genes cloned into $PCDNA_3$. Similarly, transient transfection of $RCCD_1$ with the non-GFP-tagged AE1 cloned into $PCDNA_3$ did not result in demonstrable AE1 expression. In this case expression was tested initially using western blotting. My technique (and the immunostaining) was validated by successful western blotting of AE1 using a control 'red cell ghost' preparation, derived from human red cell membrane. The detection method I used was, therefore, robust. I Subsequently performed immunofluorescence of RCCD1 with a specific AE1 antibody using confocal microscopy for detection. There was no membrane expression of AE1 noted with this technique either.

I performed in-vitro translation using this construct and found that it did indeed yield in-vitro AE1 production, detected as appropriately sized proteins on western blotting. This suggests the AE1 constructs (provided by A. Toye) did result in AE1 translation in an in-vitro situation.

The integrity of the PCDNA3-AE1 constructs was checked for correct orientation with enzymatic digestion as shown. I also arranged for commercial sequencing across the ligation sites and the DNA sequence did show successful ligation, correct orientation and integrity of the AE1 sequence at the ligation sites. The sequencing extended across the promoter and stop codon for the AE1 inserts.

$PCDNA_3$ has a strong CMV promoter, and the failure of expression in $RCCD_1$ this promoter does suggest a fundamental problem with this model. Unfortunately I was unable to get sufficient data from northern blotting to determine whether RNA transcription was occurring. From the available

evidence I was able to accrue it would seem likely that AE1 was unstable in $RCCD_1$ was removed by $RCCD_1$ cell sorting mechanisms or resulted in $RCCD_1$ lethality. The latter is certainly conceivable as $RCCD_1$ is certainly not of the stable α–intercalated cell type and has considerable plasticity. Furthermore, I was not able to detect rat AE1 in any $RCCD_1$ during western blotting. This may be because I was using a human AE1 antibody, with human red-cell ghosts as a control. There is however, considerable homology between rat and human AE1 and it is perhaps unlikely that BRIC 170 would not immunostain rat AE1. This would imply that $RCCD_1$ does not express native rat AE1, which makes a deleterious effect of expressing a WT or MUT human form more conceivable. A rat AE1 antibody control (which I did not have) would have helped resolve the issue of whether there is native rat AE1 in these cells.

As regards the constitutive, inducible expression model I was able to successfully construct the PBI4IRESHygro vector. As described, the intention was to provide tet-dependent expression from a bi-directional promoter, with one direction driving Hygromycin resistance, the other AE1 expression. I successful in developing this vector and was then able to successfully clone WT and MUT AE1 into this construct.

I arranged for commercial sequencing of the ligation sites of the construct prior to transfection and these were as intact, with the AE1 insert correctly orientated. I also performed multiple diagnostic digestions of the construct at its various stages of completion, with several diagnostic digests of the completed construct. These results (shown in the previous chapter) confirmed the construct had been built as planned.

Having built the PBI4IRESHygroAE1 constructs I successfully transfected them into $RCCD_1$. Using antibiotic selection I was able to select out clones expressing the PBI4IRESHygro construct as immortalised cell lines and propagate these cell lines in culture. By separating colonies of the same clone and inducing Hygromycin resistance with tet in one colony (but not the other) and then adding the antibiotic I was able to demonstrate tet-dependent inducible Hygromycin resistance in these colonies. While sufficient cells were being grown for downstream experiments (western blotting) I intermittently

performed tet-induced Hygromycin selection to maintain the integrity of the clones. There was clear, sustained, tet-dependent Hygromycin resistance, suggesting that the PBI4IRESHygro construct, with inducible Hygromycin resistance, was operational in these cells. It is worth noting that colonies immortalised with PBI4IRESHygroAE1MUT (i.e. those with the mutant AE1 insert) appeared to thrive less than those transfected with the PBI4IRESHygroAE1WT. There was also considerable variation in propagation rates of different clones, particularly under Hygromycin selection.

Having propagated sufficient quantities of the $RCCD_1$ colonies for protein preparation I was unable to find significant expression of AE1 on western blotting. This was in spite of optimising the condition of the western blot and being able to successfully detect $RCCD_1$ in a human red cell ghost preparation. I then repeated the process of transfection, selection and propagation and screened several new colonies. The results were similar. With this second batch of clones I screened for expression with immunofluorescence and confocal microscopy. Again no significant AE1 expression was detected.

As per transient transfection with AE1 using the PCDNA3 vector, my efforts to constitutively express AE1 in the $RCCD_1$ cell line were unsuccessful. This was particularly disappointing given the efforts made to build the inducible construct, transfect the cells and propagate colonies under tet-dependent selection. The latter represented many months of work. Propagating clones for northern blotting was attempted, however this too was extremely time-consuming and took several weeks to propagate significant amounts of cells (under periodic antibiotic selection) to perform these experiments. Unfortunately I was unable to get adequate data from northern blotting to determine whether AE1 translation was occurring, as I did not have sufficient time available to gain full competence in this difficult method.

In retrospect using confocal microscopy as a standard method for screening of clones (rather than western blotting) would have greatly reduced the time spent on this process. The propagation of sufficient numbers of cells for lysis and protein preparation was very time consuming as the cells did not propapagate rapidly, particularly under repeated tet-induced Hygromycin

selection. Unfortunately access to the confocal microscope was limited in the laboratory and this was generally used as a tool for characterising expression, rather than for screening clones.

I can say that the preparation of the inducible constructs was successful, and that these were successfully transfected into $RCCD_1$ resulting in immortalised $RCCD_1$ clones. I am also able to say that I had Dox-dependent expression of Hygromycin resistance in these cells, and that the bi-directional promoter appeared to be operational. What is not clear is why this promoter was not also driving AE1 expression. I am unable to say whether RNA translation was present, as my northern blot results were not adequate. I can say that the same AE1 gene inserts were able to drive in-vitro translation under the PCDNA3 CMV promoter (as described previously). One might conclude from this, and the transient transfection data, that AE1 may cause $RCCD_1$ toxicity. This would mean that only clones with no or weak AE1 expression survived the tet-induction and selection process. An alternative explanation is that levels of expression were simply too low for detection with the BRIC170 antibody. This antibody has, however, been used successfully to detect AE1 expression in MDCK cells (Ashley Toye).

4.2 RENAL AE1 EXPRESSION STUDIES UNDERTAKEN BY OTHER GROUPS

Though my efforts to express mutant and wild-type AE1 in the $RCCD_1$ cell line were unsuccessful the hypothesis on which the project has been based has been proved correct. Initial studies on non-polarised MDCK cells (54) and HEK293 cells (55,56) suggested that dominant AE1 mutations cause aberrant targeting of kAE1 in the a-IC and that these mutations exert a dominant negative effect on cell surface expression of wild type kAE1 by hetero-oligomer formation (54-56). However, a significant drawback of these experiments was that they were done in non-polarised cells. Using transient transfection in polarised MDCK cells, Devonald *et al* were the first to report mistargeting of the C-terminally truncated kAE1 Walton mutation (see earlier) to both the apical and basolateral cell membranes (57). In contrast, using

stably transfected polarised MDCK cells, Toye *et al* were able to show expression of this mutant exclusively at the apical membrane and normal targeting of the wild type kAE1 to the basolateral membrane (58). A potential explanation for the exclusive apical localisation observed in stably transfected cells might be that transient over-expression of kAE1 saturates the cellular sorting machinery, allowing some mutant AE1 to reside at the (default) basolateral membrane. The disturbed targeting of kAE1 Walton in non-polarised and polarised renal cells suggested the existence of an important targeting motif in the C-terminal portion of AE1, which was shown to involve the Y904 residue of AE1. Toye and colleagues have also expressed the R589H and S613F kAE1 mutant in their polarised MDCK cell system and found that they do not reach the plasma membrane. In addition, Rungroi *et al*, again using transient transfection in their MDCK cell system, reported that the G609R mutation, which is close to the S613F mutation, resulted in non-polarised targeting, similar to their finding with kAE1 Walton (59). Interestingly, immunostaining of renal tissue from a patient with dRTA due to the S613F mutation shows both cytosolic retention and mistargeting of kAE1 to the apical membrane of a-IC (60).

REFERENCES

SECTION I: THE ENAMEL-RENAL SYNDROME

1. MacGibbon, D. Generalized enamel hypoplasia and renal dysfunction. Aust Dent J 17, 61-63 (1972).

2. Lubinsky, M., Angle, C., Marsh, P. W. & Witkop, C. J. Syndrome of amelogenesis imperfecta, nephrocalcinosis, impaired renal concentration, and possible abnormality of calcium metabolism. Am J Med Genet 20, 233-243 (1985).

3. Phakey, P., Palamara, J., Hall, R. K. & McCredie, D. A. Ultrastructural study of tooth enamel with amelogenesis imperfecta in AI-nephrocalcinosis syndrome. Connect Tissue Res 32, 253-259 (1995).

4. Hall, R. K., Phakey, P., Palamara, J. & McCredie, D. A. Amelogenesis imperfecta and nephrocalcinosis syndrome. Case studies of clinical features and ultrastructure of tooth enamel in two siblings. Oral Surg Oral Med Oral Pathol Oral Radiol Endod 79, 583-592 (1995).

5. Dellow, E. L., Harley, K. E., Unwin, R. J., Wrong, O., et al. Amelogenesis imperfecta, nephrocalcinosis, and hypocalciuria syndrome in two siblings from a large family with consanguineous parents. Nephrol Dial Transplant 13, 3193-3196 (1998).

6. Normand de la Tranchade, I., Bonarek, H., Marteau, J. M., Boileau, M. J. & Nancy, J. Amelogenesis imperfecta and nephrocalcinosis: a new case of this rare syndrome. J Clin Pediatr Dent 27, 171-175 (2003).

7. Paula, L. M., Melo, N. S., Silva Guerra, E. N., Mestrinho, D. H. & Acevedo, A. C. Case report of a rare syndrome associating amelogenesis imperfecta and nephrocalcinosis in a consanguineous family. Arch Oral Biol 50, 237-242 (2005).

8. Fu, X.J., Nozu K., Goji K., Ikeda K., Kamioka I., Fujita T., Kaito H., Nishio H., Lijima K., Matsuo M. Enamel-renal syndrome associated with hypokalaemic metabolic alkalosis and impaired renal concentration: a novel syndrome? Nephrol Dial Transplant 10, 2959-2962 (2006).

9. Hunter, L., Addy, L. D., Knox, J. & Drage, N. Is amelogenesis imperfecta an indication for renal examination? Int J Paediatr Dent 17, 62-65 (2007).

10. Hu, J. C., Chun, Y. H., Al Hazzazzi, T. & Simmer, J. P. Enamel formation and amelogenesis imperfecta. Cells Tissues Organs 186, 78-85 (2007).

11. Simmer, J. P. & Fincham, A. G. Molecular mechanisms of dental enamel formation. Crit Rev Oral Biol Med 6, 84-108 (1995).

12. Wright, J. T., Hall, K. & Yamauchi, M. The protein composition of normal and developmentally defective enamel. Ciba Found Symp 205, 85-99; discussion 99-106 (1997).

13. Goose, D. H. The importance of hereditary factors in dental surgery. Br Dent J 136, 15-19 (1974).

14. Winter, G. B. & Brook, A. H. Enamel hypoplasia and anomalies of the enamel. Dent Clin North Am 19, 3-24 (1975).

15. Shokeir, M. H. Hereditary enamel hypoplasia. Clin Genet 2, 387-391 (1971).

16. Bäckman, B. Inherited enamel defects. Ciba Found Symp 205, 175-82; discussion 183-6 (1997).

17. Rao, S. & Witkop, C. J. Inherited defects in tooth structure. Birth Defects Orig Artic Ser 7, 153-184 (1971).

18. Witkop, C. J. Hereditary defects in enamel and dentin. Acta Genet Stat Med 7, 236-239 (1957).

19. Bäckman, B. & Holmgren, G. Amelogenesis imperfecta: a genetic study. Hum Hered 38, 189-206 (1988).

20. Sundell, S. & Valentin, J. Hereditary aspects and classification of hereditary amelogenesis imperfecta. Community Dent Oral Epidemiol 14, 211-216 (1986).

21. Fischman, S. L. & Fischman, B. C. Hypoplastic amelogenesis imperfecta: report of case. J Am Dent Assoc 75, 929-931 (1967).

22. Giansanti, J. S. A kindred showing hypocalcified amelogenesis imperfecta: report of case. J Am Dent Assoc 86, 675-678 (1973).

23. McLarty, E. L., Giansanti, J. S. & Hibbard, E. D. X-linked hypomaturation type of amelogenesis imperfecta exhibiting lyonization in affected females. Oral Surg Oral Med Oral Pathol 36, 678-685 (1973).

24. Gertzman, G. B., Gaston, G. & Quinn, I. Amelogenesis imperfecta: local hypoplastic type with pulpal calcification. J Am Dent Assoc 99, 637-639 (1979).

28, 61-66 (1973).

25. Witkop, C. J., Kuhlmann, W. & Sauk, J. Autosomal recessive pigmented hypomaturation amelogenesis imperfecta. Report of a kindred. Oral Surg Oral Med Oral Pathol 36, 367-382 (1973).

26. Burzynski, N. J., Gonzalez, W. E. & Snawder, K. D. Autosomal dominant smooth hypoplastic amelogenesis imperfecta. Report of a case. Oral Surg Oral Med Oral Pathol 36, 818-823 (1973).

27. Escobar, V. H., Goldblatt, L. I. & Bixler, D. A clinical, genetic, and ultrastructural study of snow-capped teeth: amelogenesis imperfecta, hypomaturation type. Oral Surg Oral Med Oral Pathol 52, 607-614 (1981).

28. Witkop, C. J. Amelogenesis imperfecta, dentinogenesis imperfecta and dentin dysplasia revisited: problems in classification. J Oral Pathol 17, 547-553 (1988).

29. Aldred, M. J., Savarirayan, R. & Crawford, P. J. Amelogenesis imperfecta: a classification and catalogue for the 21st century. Oral Dis 9, 19-23 (2003).

30. Salido, E. C., Yen, P. H., Koprivnikar, K., Yu, L. C. & Shapiro, L. J. The human enamel protein gene amelogenin is expressed from both the X and the Y chromosomes. Am J Hum Genet 50, 303-316 (1992).

31. DenBesten, P. K. & Li, R. S. Characterization of amelogenin mRNA from secretory- and maturation-stage rat incisor enamel. Arch Oral Biol 37, 1097-1100 (1992).

32. Brookes, S. J., Robinson, C., Kirkham, J. & Bonass, W. A. Biochemistry and molecular biology of amelogenin proteins of developing dental enamel. Arch Oral Biol 40, 1-14 (1995).

33. Hu, J. C., Yamakoshi, Y., Yamakoshi, F., Krebsbach, P. H. & Simmer, J. P. Proteomics and genetics of dental enamel. Cells Tissues Organs 181, 219-231 (2005).

34. Lee, S. K., Krebsbach, P. H., Matsuki, Y., Nanci, A., et al. Ameloblastin expression in rat incisors and human tooth germs. Int J Dev Biol 40, 1141-1150 (1996).

35. Paine, M. L., Krebsbach, P. H., Chen, L. S., Paine, C. T., et al. Protein-to-protein interactions: criteria defining the assembly of the enamel organic matrix. J Dent Res 77, 496-502 (1998).

36. Fukumoto, S., Kiba, T., Hall, B., Iehara, N., et al. Ameloblastin is a cell adhesion molecule required for maintaining the differentiation state of ameloblasts. J Cell Biol 167, 973-983 (2004).

37. Krebsbach, P. H., Lee, S. K., Matsuki, Y., Kozak, C. A., et al. Full-length sequence, localization, and chromosomal mapping of ameloblastin. A novel tooth-specific gene. J Biol Chem 271, 4431-4435 (1996).

38. Simmons, D., Gu, T. T., Krebsbach, P. H., Yamada, Y. & MacDougall, M. Identification and characterization of a cDNA for mouse ameloblastin. Connect Tissue Res 39, 3-12; discussion 63-7 (1998).

39. MacDougall, M., Simmons, D., Gu, T. T., Forsman-Semb, K., et al. Cloning, characterization and immunolocalization of human ameloblastin. Eur J Oral Sci 108, 303-310 (2000).

40. Deutsch, D., Dafni, L., Palmon, A., Hekmati, M., et al. Tuftelin: enamel mineralization and amelogenesis imperfecta. Ciba Found Symp 205, 135-47; discussion 147-155 (1997).

41. Deutsch, D., Palmon, A., Dafni, L., Mao, Z., et al. Tuftelin--aspects of protein and gene structure. Eur J Oral Sci 106 Suppl 1, 315-323 (1998).

42. Deutsch, D., Palmon, A., Fisher, L. W., Kolodny, N., et al. Sequencing of bovine enamelin ("tuftelin") a novel acidic enamel protein. J Biol Chem 266, 16021-16028 (1991).

43. Deutsch, D., Palmon, A., Young, M. F., Selig, S., et al. Mapping of the human tuftelin (TUFT1) gene to chromosome 1 by fluorescence in situ hybridization. Mamm Genome 5, 461-462 (1994).

44. Bashir, M. M., Abrams, W. R., Tucker, T., Sellinger, B., et al. Molecular cloning and characterization of the bovine and human tuftelin genes. Connect Tissue Res 39, 13-24; discussion 63-7 (1998).

45. Aldred, M. J., Crawford, P. J., Roberts, E., Gillespie, C. M., et al. Genetic heterogeneity in X-linked amelogenesis imperfecta. Genomics 14, 567-573 (1992).

46. Aldred, M. J., Crawford, P. J., Roberts, E. & Thomas, N. S. Identification of a nonsense mutation in the amelogenin gene (AMELX) in a family with X-linked amelogenesis imperfecta (AIH1). Hum Genet 90, 413-416 (1992).

47. Lagerström-Fermér, M., Pettersson, U. & Landegren, U. Molecular basis and consequences of a deletion in the amelogenin gene, analyzed by capture PCR. Genomics 17, 89-92 (1993).

48. Lench, N. J., Brook, A. H. & Winter, G. B. SSCP detection of a nonsense mutation in exon 5 of the amelogenin gene (AMGX) causing X-linked amelogenesis imperfecta (AIH1). Hum Mol Genet 3, 827-828 (1994).

49. Lagerström-Fermér, M. & Landegren, U. Understanding enamel formation from mutations causing X-linked amelogenesis imperfecta. Connect Tissue Res 32, 241-246 (1995).

50. Lagerström-Fermér, M., Nilsson, M., Bäckman, B., Salido, E., et al. Amelogenin signal peptide mutation: correlation between mutations in the amelogenin gene (AMGX) and manifestations of X-linked amelogenesis imperfecta. Genomics 26, 159-162 (1995).

51. Lench, N. J. & Winter, G. B. Characterisation of molecular defects in X-linked amelogenesis imperfecta (AIH1). Hum Mutat 5, 251-259 (1995).

52. Hart, P. S., Hart, T. C., Simmer, J. P. & Wright, J. T. A nomenclature for X-linked amelogenesis imperfecta. Arch Oral Biol 47, 255-260 (2002).

53. Hart, P. S., Aldred, M. J., Crawford, P. J., Wright, N. J., et al. Amelogenesis imperfecta phenotype-genotype correlations with two amelogenin gene mutations. Arch Oral Biol 47, 261-265 (2002).

54. Greene, S. R., Yuan, Z. A., Wright, J. T., Amjad, H., et al. A new frameshift mutation encoding a truncated amelogenin leads to X-linked amelogenesis imperfecta. Arch Oral Biol 47, 211-217 (2002).

55. Wright, J. T., Hart, P. S., Aldred, M. J., Seow, K., et al. Relationship of phenotype and genotype in X-linked amelogenesis imperfecta. Connect Tissue Res 44 Suppl 1, 72-78 (2003).

56. Forsman, K., Lind, L., Bäckman, B., Westermark, E. & Holmgren, G. Localization of a gene for autosomal dominant amelogenesis imperfecta (ADAI) to chromosome 4q. Hum Mol Genet 3, 1621-1625 (1994).

57. Kärrman, C., Bäckman, B., Dixon, M., Holmgren, G. & Forsman, K. Mapping of the locus for autosomal dominant amelogenesis imperfecta (AIH2) to a 4-Mb YAC contig on chromosome 4q11-q21. Genomics 39, 164-170 (1997).

58. MacDougall, M., DuPont, B. R., Simmons, D., Reus, B., et al. Ameloblastin gene (AMBN) maps within the critical region for autosomal dominant amelogenesis imperfecta at chromosome 4q21. Genomics 41, 115-118 (1997).

59. Feest, T.G., Wrong O.M. Nephrocalcinosis. Book chapter. Oxford Textbook of Nephrology.

60. Vervaet, B. A., Verhulst, A., D'Haese, P. C. & De Broe, M. E. Nephrocalcinosis: new insights into mechanisms and consequences. Nephrol Dial Transplant 24, 2030-2035 (2009).

61. Ammenti, A., Pelizzoni, A., Cecconi, M., Molinari, P. P. & Montini, G. Nephrocalcinosis in children: a retrospective multi-centre study. Acta Paediatr 98, 1628-1631 (2009).

62. Karlowicz, M. G. & Adelman, R. D. What are the possible causes of neonatal nephrocalcinosis? Semin Nephrol 18, 364-367 (1998).

63. Alon, U. S. Nephrocalcinosis. Curr Opin Pediatr 9, 160-165 (1997).

64. Eaton, D. G. & Hewitt, C. A. Renal function in hyperparathyroidism with complicating nephrocalcinosis. Acta Paediatr 82, 111-112 (1993).

65. Jaeger, P., Jones, W., Kashgarian, M., Segre, G. V. & Hayslett, J. P. Mechanism of nephrocalcinosis in primary hyperparathyroidism. Adv Exp Med Biol 208, 379-382 (1986).

66. Vazquez, A. M. Nephrocalcinosis and hypertension in juvenile primary hyperparathyroidism. Am J Dis Child 125, 104-106 (1973).

67. Vezzoli, G., Soldati, L. & Gambaro, G. Hypercalciuria revisited: one or many conditions? Pediatr Nephrol 23, 503-506 (2008).

68. Laing, C. M., Toye, A. M., Capasso, G. & Unwin, R. J. Renal tubular acidosis: developments in our understanding of the molecular basis. Int J Biochem Cell Biol 37, 1151-1161 (2005).

69. Laing, C. M. & Unwin, R. J. Renal tubular acidosis. J Nephrol 19 Suppl 9, S46-S52 (2006).

69. Cho, H. Y., Lee, B. H., Kang, J. H., Ha, I. S., et al. A clinical and molecular genetic study of hypophosphatemic rickets in children. Pediatr Res 58, 329-333 (2005).

70. Ono, T. & Seino, Y. Medical management and complications of X-linked hypophosphatemic vitamin D resistant rickets. Acta Paediatr Jpn 39, 503-507 (1997).

71. Eddy, M. C., McAlister, W. H. & Whyte, M. P. X-linked hypophosphatemia: normal renal function despite medullary nephrocalcinosis 25 years after transient vitamin D2-induced renal azotemia. Bone 21, 515-520 (1997).

72. Gambaro, G., Vezzoli, G., Casari, G., Rampoldi, L., et al. Genetics of hypercalciuria and calcium nephrolithiasis: from the rare monogenic to the common polygenic forms. Am J Kidney Dis 44, 963-986 (2004).

73. Eggert, P., Müller, D. & Schröter, T. Nephrocalcinosis in three siblings with idiopathic hypercalciuria. Pediatr Nephrol 12, 144-146 (1998).

74. Pook, M. A., Wrong, O., Wooding, C., Norden, A. G., et al. Dent's disease, a renal Fanconi syndrome with nephrocalcinosis and kidney stones, is associated with a microdeletion involving DXS255 and maps to Xp11.22. Hum Mol Genet 2, 2129-2134 (1993).

75. Fisher, S. E., Black, G. C., Lloyd, S. E., Hatchwell, E., et al. Isolation and partial characterization of a chloride channel gene which is expressed in kidney and is a candidate for Dent's disease (an X-linked hereditary nephrolithiasis). Hum Mol Genet 3, 2053-2059 (1994).

76. Wrong, O. M., Norden, A. G. & Feest, T. G. Dent's disease; a familial proximal renal tubular syndrome with low-molecular-weight proteinuria, hypercalciuria, nephrocalcinosis, metabolic bone disease, progressive renal failure and a marked male predominance. QJM 87, 473-493 (1994).

77. Igarashi, T., Hayakawa, H., Shiraga, H., Kawato, H., et al. Hypercalciuria and nephrocalcinosis in patients with idiopathic low-molecular-weight proteinuria in Japan: is the disease identical to Dent's disease in United Kingdom? Nephron 69, 242-247 (1995).

78. Lloyd, S. E., Pearce, S. H., Fisher, S. E., Steinmeyer, K., et al. A common molecular basis for three inherited kidney stone diseases. Nature 379, 445-449 (1996).

79. Nakazato, H., Hattori, S., Furuse, A., Kawano, T., et al. Mutations in the CLCN5 gene in Japanese patients with familial idiopathic low-molecular-weight proteinuria. Kidney Int 52, 895-900 (1997).

80. Thakker, R. V. The role of renal chloride channel mutations in kidney stone disease and nephrocalcinosis. Curr Opin Nephrol Hypertens 7, 385-388 (1998).

81. Thakker, R. V. Pathogenesis of Dent's disease and related syndromes of X-linked nephrolithiasis. Kidney Int 57, 787-793 (2000).

82. Piwon, N., Günther, W., Schwake, M., Bösl, M. R. & Jentsch, T. J. ClC-5 Cl--channel disruption impairs endocytosis in a mouse model for Dent's disease. Nature 408, 369-373 (2000).

10TJ Jentsch, Chloride transport in the kidney: lessons from human disease and knockout mice., in J Am Soc Nephrol

83. Neild, G. H., Thakker, R. V., Unwin, R. J. & Wrong, O. M. Dent's disease. Nephrol Dial Transplant 20, 2284-2285 (2005).

84. Broyer, M., Jouvet, P., Niaudet, P., Daudon, M. & Revillon, Y. Management of oxalosis. *Kidney Int Suppl* 53, S93-S98 (1996).

85. Kemper, M. J., Conrad, S. & Müller-Wiefel, D. E. Primary hyperoxaluria type 2. *Eur J Pediatr* 156, 509-512 (1997).

86. van Woerden, C. S., Groothoff, J. W., Wanders, R. J., Davin, J. C. & Wijburg, F. A. Primary hyperoxaluria type 1 in The Netherlands: prevalence and

outcome. *Nephrol Dial Transplant* 18, 273-279 (2003).

87. Milliner, D. S. The primary hyperoxalurias: an algorithm for diagnosis. *Am J Nephrol* 25, 154-160 (2005).

88. Jungers, P., Joly, D., Blanchard, A., Courbebaisse, M., *et al.* [Inherited monogenic kidney stone diseases: recent diagnostic and therapeutic advances]. *Nephrol Ther* 4, 231-255 (2008).

89. Bobrowski, A. E. & Langman, C. B. The primary hyperoxalurias. *Semin Nephrol* 28, 152-162 (2008).

90. Hoppe, B., Beck, B. B. & Milliner, D. S. The primary hyperoxalurias. *Kidney Int* 75, 1264-1271 (2009).

91. Harris, R. E., Fuchs, E. F. & Kaempf, M. J. Medullary sponge kidney and congenital hemihypertrophy: case report and literature review. *J Urol* 126, 676-678 (1981).

92. Fick, G. M. & Gabow, P. A. Hereditary and acquired cystic disease of the kidney. *Kidney Int* 46, 951-964 (1994).

93. Jaeger, P. Genetic versus environmental factors in renal stone disease. Curr Opin Nephrol Hypertens 5, 342-346 (1996).

94. Indridason, O. S., Thomas, L. & Berkoben, M. Medullary sponge kidney associated with congenital hemihypertrophy. J Am Soc Nephrol 7, 1123-1130 (1996).

95. Gambaro, G., Feltrin, G. P., Lupo, A., Bonfante, L. et al. Medullary sponge kidney (Lenarduzzi-Cacchi-Ricci disease): a Padua Medical School discovery in the 1930s. Kidney Int 69, 663-670 (2006).

96. Konrad, M. & Weber, S. Recent advances in molecular genetics of hereditary magnesium-losing disorders. J Am Soc Nephrol 14, 249-260 (2003).

97. Karlowicz, M. G. & Adelman, R. D. What are the possible causes of neonatal nephrocalcinosis? Semin Nephrol 18, 364-367 (1998).

98. Makhoul, I. R., Soudack, M., Smolkin, T., Sujov, P., et al. Neonatal transient renal failure with renal medullary hyperechogenicity: clinical and laboratory features. Pediatr Nephrol 20, 904-909 (2005).

99. Ammenti, A., Pelizzoni, A., Cecconi, M., Molinari, P. P. & Montini, G. Nephrocalcinosis in children: a retrospective multi-centre study. Acta Paediatr 98, 1628-1631 (2009).

100. Kim, J. J. & Amin, S. Does nephrocalcinosis in ex-premature babies cause long-term renal problems? Arch Dis Child 94, 991-992 (2009).

101. Haffner, D., Weinfurth, A., Manz, F., Schmidt, H., et al. Long-term outcome of paediatric patients with hereditary tubular disorders. Nephron 83, 250-260 (1999).

102. Cochat, P., Pichault, V., Bacchetta, J., Dubourg, L., et al. Nephrolithiasis related to inborn metabolic diseases. Pediatr Nephrol 25, 415-424 (2010).

103. Coe, F. L., Parks, J.H., Evan, A., Worcester, E. Pathogenesis and treatment of nephrolithiasis. Book chapter. Seldin and Geibisch's The kidney. Forth edition.

104. Rodriguez, M., Nemeth, E. & Martin, D. The calcium-sensing receptor: a key factor in the pathogenesis of secondary hyperparathyroidism. *Am J Physiol Renal Physiol* 288, F253-F264 (2005).

105. Dusso, A. S., Brown, A. J. & Slatopolsky, E. Vitamin D. *Am J Physiol Renal Physiol* 289, F8-28 (2005).

106. Van de Graaf, S. F., Hoenderop, J. G. & Bindels, R. J. Regulation of TRPV5 and TRPV6 by associated proteins. *Am J Physiol Renal Physiol* 290, F1295-F1302 (2006).

107. Friedman, P.A. Renal calcium metabolism. Book chapter. Seldin and Geibisch's The Kidney. Fourth edition.

108. Coe, F. L. & Bushinsky, D. A. Pathophysiology of hypercalciuria. *Am J Physiol* 247, F1-13 (1984).

109. Friedman, P. A. & Gesek, F. A. Calcium transport in renal epithelial cells. *Am J Physiol* 264, F181-F198 (1993).

110. Kawasaki, K. & Weiss, K. M. SCPP gene evolution and the dental mineralization continuum. *J Dent Res* 87, 520-531 (2008).

111. Huq, N. L., Cross, K. J., Ung, M. & Reynolds, E. C. A review of protein structure and gene organisation for proteins associated with mineralised tissue and calcium phosphate stabilisation encoded on human chromosome 4. *Arch Oral Biol* 50, 599-609 (2005).

112. Butler, W. T. The nature and significance of osteopontin. *Connect Tissue Res* 23, 123-136 (1989).

113. Müller, G. A. & Strutz, F. M. Renal fibroblast heterogeneity. *Kidney Int Suppl* 50, S33-S36 (1995).

114. Rovin, B. H. & Phan, L. T. Chemotactic factors and renal inflammation. *Am J Kidney Dis* 31, 1065-1084 (1998).

115. Wüthrich, R. P. The complex role of osteopontin in renal disease. *Nephrol Dial Transplant* 13, 2448-2450 (1998).

116. Diamond, J. R., Ricardo, S. D. & Klahr, S. Mechanisms of interstitial fibrosis in obstructive nephropathy. *Semin Nephrol* 18, 594-602 (1998).

117. Gerstenfeld, L. C. Osteopontin in skeletal tissue homeostasis: An emerging picture of the autocrine/paracrine functions of the extracellular matrix. *J Bone Miner Res* 14, 850-855 (1999).

118. Gravallese, E. M. Osteopontin: a bridge between bone and the immune system. *J Clin Invest* 112, 147-149 (2003).

119. Kleinman, J. G., Wesson, J. A. & Hughes, J. Osteopontin and calcium stone formation. *Nephron Physiol* 98, p43-p47 (2004).

120. Narayanan, K., Gajjeraman, S., Ramachandran, A., Hao, J. & George, A. Dentin matrix protein 1 regulates dentin sialophosphoprotein gene transcription during early odontoblast differentiation. *J Biol Chem* 281, 19064-19071 (2006).

121. Butler, W. T. Dentin matrix proteins and dentinogenesis. *Connect Tissue Res* 33, 59-65 (1995).

122. Strom, T. M. & Jüppner, H. PHEX, FGF23, DMP1 and beyond. *Curr Opin Nephrol Hypertens* 17, 357-362 (2008).

123. Pettifor, J. M. What's new in hypophosphataemic rickets? *Eur J Pediatr* 167, 493-499 (2008).

124. Qin, C., D'Souza, R. & Feng, J. Q. Dentin matrix protein 1 (DMP1): new and important roles for biomineralization and phosphate homeostasis. *J Dent Res* 86, 1134-1141 (2007).

125. Kim, J. W. & Simmer, J. P. Hereditary dentin defects. *J Dent Res* 86, 392-399 (2007).

126. Raymond, M. H., Schutte, B. C., Torner, J. C., Burns, T. L. & Willing, M. C. Osteocalcin: genetic and physical mapping of the human gene BGLAP and its potential role in postmenopausal osteoporosis. *Genomics* 60, 210-217 (1999).

127. Gallop, P. M., Lian, J. B. & Hauschka, P. V. Carboxylated calcium-binding proteins and vitamin K. *N Engl J Med* **302,** 1460-1466 (1980).

128. Kumar, R. Vitamin D metabolism and mechanisms of calcium transport. J Am Soc Nephrol 1, 30-42 (1990).

129. Shearer, M. J. Vitamin K. Lancet 345, 229-234 (1995).

130. Christenson, R. H. Biochemical markers of bone metabolism: an overview. Clin Biochem 30, 573-593 (1997).

131. Hart, S. M. & Eastell, R. Biochemical markers of bone turnover. Curr Opin Nephrol Hypertens 8, 421-427 (1999).

132. Wada, S., Fukawa, T. & Kamiya, S. [Osteocalcin and bone]. Clin Calcium 17, 1673-1677 (2007).

133. Yasui, T., Yamada, M. & Irahara, M. [Clinical application of undercarboxylated osteocalcin]. Clin Calcium 17, 1709-1716 (2007).

134. Johnson, T. L., Sakaguchi, A. Y., Lalley, P. A. & Leach, R. J. Chromosomal assignment in mouse of matrix Gla protein and bone Gla protein genes. *Genomics* 11, 770-772 (1991).

135. Glowacki, J., Rey, C., Cox, K. & Lian, J. Effects of bone matrix components on osteoclast differentiation. Connect Tissue Res 20, 121-129 (1989).

136. Hauschka, P. V., Lian, J. B., Cole, D. E. & Gundberg, C. M. Osteocalcin and matrix Gla protein: vitamin K-dependent proteins in bone. Physiol Rev 69, 990-1047 (1989).

137. Cancela, L., Hsieh, C.L., Francke, U., Price, P.A.. Molecular structure, chromosome, and promoter organization of the human matrix la protein gene. J

Biol Chem. 265, 15040-15048 (1990).

138. 7. Munroe, P. B.; Olgunturk, R. O.; Fryns, J.-P.; Van Maldergem, L.; Ziereisen, F.; Yuksel, B.; Gardiner, R. M.; Chung, E. :Mutations in the gene encoding the human matrix Gla protein cause Keutel syndrome. Nature Genet. 21: 142-144 (1999).

139. Laize, V.; Martel, P.; Viegas, C. S. B.; Price, P. A.; Cancela, M. L. : Evolution of matrix and bone gamma-carboxyglutamic acid proteins in vertebrates. J. Biol. Chem. 280: 26659-26668 (2005).

140. Chang, Q.; Hoefs, S.; van der Kemp, A. W.; Topala, C. N.; Bindels, R. J.; Hoenderop, J. G. The beta-glucuronidase klotho hydrolyzes and activates the TRPV5 channel. Science 310: 490-493, 2005.

141. Muller, D.; Hoenderop, J. G. J.; Merkx, G. F. M.; van Os, C. H.; Bindels, R. J. M.. Gene structure and chromosomal mapping of human epithelial calcium channel. Biochem. Biophys. Res. Commun. 275: 47-52, 2000.

142. Müller, D., Hoenderop, J. G., van Os, C. H. & J M Bindels, R. The epithelial calcium channel, ECaC1: molecular details of a novel player in renal calcium handling. Nephrol Dial Transplant 16, 1329-1335 (2001).

143. Bouillon, R., Van Cromphaut, S. & Carmeliet, G. Intestinal calcium absorption: Molecular vitamin D mediated mechanisms. J Cell Biochem 88, 332-339 (2003).

144. Van de Graaf, S. F., Boullart, I., Hoenderop, J. G. & Bindels, R. J. Regulation of the epithelial Ca2+ channels TRPV5 and TRPV6 by 1alpha,25-dihydroxy Vitamin D3 and dietary Ca2+. J Steroid Biochem Mol Biol 89-90, 303-308 (2004).

145. Ensrud, K. E., Stone, K., Cauley, J. A., White, C., et al. Vitamin D receptor gene polymorphisms and the risk of fractures in older women. For the Study of Osteoporotic Fractures Research Group. J Bone Miner Res 14, 1637-1645 (1999).

146. Vanholder, R. & Glorieux, G. Molecular mechanisms of vitamin D hyporesponsiveness in renal failure. Nephrol Dial Transplant 14, 16-19 (1999).

147. Bover, J. & Bosch, R. J. Vitamin D receptor polymorphisms as a determinant of bone mass and PTH secretion: from facts to controversies. Nephrol Dial Transplant 14, 1066-1068 (1999).

148. Langman, C. B. New developments in calcium and vitamin D metabolism. Curr Opin Pediatr 12, 135-139 (2000).

149. Rachez, C. & Freedman, L. P. Mechanisms of gene regulation by vitamin D(3) receptor: a network of coactivator interactions. Gene 246, 9-21 (2000).

150. Bouillon, R., Van Cromphaut, S. & Carmeliet, G. Intestinal calcium absorption: Molecular vitamin D mediated mechanisms. J Cell Biochem 88, 332-339 (2003).

151. Dusso, A. S. Vitamin D receptor: mechanisms for vitamin D resistance in renal failure. Kidney Int Suppl S6-S9 (2003).

152. Dusso, A. S., Thadhani, R. & Slatopolsky, E. Vitamin D receptor and analogs. Semin Nephrol 24, 10-16 (2004).

153. Pörsti, I. H. Expanding targets of vitamin D receptor activation: downregulation of several RAS components in the kidney. Kidney Int 74, 1371-1373 (2008).

154. Gross, M. & Kumar, R. Physiology and biochemistry of vitamin D-dependent calcium binding proteins. Am J Physiol 259, F195-F209 (1990).

155. Johnson, J. A. & Kumar, R. Vitamin D and renal calcium transport. Curr Opin Nephrol Hypertens 3, 424-429 (1994).

156. Friedman, P. A. Calcium transport in the kidney. Curr Opin Nephrol Hypertens 8, 589-595 (1999).

157. Sooy, K., Kohut, J. & Christakos, S. The role of calbindin and 1,25dihydroxyvitamin D3 in the kidney. Curr Opin Nephrol Hypertens 9, 341-347 (2000).

158. Christakos, S., Barletta, F., Huening, M., Dhawan, P., et al. Vitamin D target proteins: function and regulation. J Cell Biochem 88, 238-244 (2003).

159. Lambers, T. T., Bindels, R. J. & Hoenderop, J. G. Coordinated control of renal Ca2+ handling. Kidney Int 69, 650-654 (2006).

160. Giunta, J. L. Dental changes in hypervitaminosis D. Oral Surg Oral Med Oral Pathol Oral Radiol Endod 85, 410-413 (1998).

161. Hu, C. C., Hart, T. C., Dupont, B. R., Chen, J. J., et al. Cloning human enamelin cDNA, chromosomal localization, and analysis of expression during tooth development. J Dent Res 79, 912-919 (2000).

162. Mårdh, C. K., Bäckman, B., Holmgren, G., Hu, J. C., et al. A nonsense mutation in the enamelin gene causes local hypoplastic autosomal dominant amelogenesis imperfecta (AIH2). Hum Mol Genet 11, 1069-1074 (2002).

163. Kida, M., Ariga, T., Shirakawa, T., Oguchi, H. & Sakiyama, Y. Autosomal-dominant hypoplastic form of amelogenesis imperfecta caused by an enamelin gene mutation at the exon-intron boundary. J Dent Res 81, 738-742 (2002).

164. Hart, P. S., Michalec, M. D., Seow, W. K., Hart, T. C. & Wright, J. T. Identification of the enamelin (g.8344delG) mutation in a new kindred and presentation of a standardized ENAM nomenclature. Arch Oral Biol 48, 589-596 (2003).

165. Hart, P. S., Wright, J. T., Savage, M., Kang, G., et al. Exclusion of candidate genes in two families with autosomal dominant hypocalcified amelogenesis imperfecta. Eur J Oral Sci 111, 326-331 (2003).

166. Hart, T. C., Hart, P. S., Gorry, M. C., Michalec, M. D., et al. Novel ENAM mutation responsible for autosomal recessive amelogenesis imperfecta and localised enamel defects. J Med Genet 40, 900-906 (2003).

167. Kim, J. W., Seymen, F., Lin, B. P., Kiziltan, B., et al. ENAM mutations in autosomal-dominant amelogenesis imperfecta. J Dent Res 84, 278-282 (2005).

168. Ozdemir, D., Hart, P. S., Firatli, E., Aren, G., et al. Phenotype of ENAM mutations is dosage-dependent. J Dent Res 84, 1036-1041 (2005).

169. MacDougall, M. Dental structural diseases mapping to human chromosome 4q21. Connect Tissue Res 44 Suppl 1, 285-291 (2003).

170. Hu, J. C. & Yamakoshi, Y. Enamelin and autosomal-dominant amelogenesis imperfecta. Crit Rev Oral Biol Med 14, 387-398 (2003).

171. Gopinath, V. K., Yoong, T. P., Yean, C. Y. & Ravichandran, M. Identifying polymorphism in enamelin gene in amelogenesis imperfecta (AI). Arch Oral Biol 53, 937-940 (2008).

172. Masuya, H., Shimizu, K., Sezutsu, H., Sakuraba, Y., et al. Enamelin (Enam) is essential for amelogenesis: ENU-induced mouse mutants as models for different clinical subtypes of human amelogenesis imperfecta (AI). Hum Mol Genet 14, 575-583 (2005).

173. Caterina, J. J., Skobe, Z., Shi, J., Ding, Y., et al. Enamelysin (matrix metalloproteinase 20)-deficient mice display an amelogenesis imperfecta phenotype. J Biol Chem 277, 49598-49604 (2002).

174. Paine, M. L., Luo, W., Wang, H. J., Bringas, P., et al. Dentin sialoprotein and dentin phosphoprotein overexpression during amelogenesis. J Biol Chem 280, 31991-31998 (2005).

175. Ozdemir, D., Hart, P. S., Ryu, O. H., Choi, S. J., et al. MMP20 active-site mutation in hypomaturation amelogenesis imperfecta. J Dent Res 84, 1031-1035 (2005).

176. Stephanopoulos, G., Garefalaki, M. E. & Lyroudia, K. Genes and related proteins involved in amelogenesis imperfecta. J Dent Res 84, 1117-1126 (2005).

177. JW Kim, JP Simmer, TC Hart, PS Hart, MD Ramaswami, JD Bartlett, JC Hu, MMP-20 mutation in autosomal recessive pigmented hypomaturation amelogenesis imperfecta., in J Med Genet

178. Kim, J. W., Simmer, J. P., Lin, B. P., Seymen, F., et al. Mutational analysis of candidate genes in 24 amelogenesis imperfecta families. Eur J Oral Sci 114 Suppl 1, 3-12; discussion 39-41, 379 (2006).

179. Wright, J. T., Daly, B., Simmons, D., Hong, S., et al. Human enamel phenotype associated with amelogenesis imperfecta and a kallikrein-4 (g.2142G>A) proteinase mutation. Eur J Oral Sci 114 Suppl 1, 13-7; discussion 39-41, 379 (2006).

180. Hart P.S., TC Hart, MD Michalec, OH Ryu, D Simmons, S Hong, JT Wright, Mutation in kallikrein 4 causes autosomal recessive hypomaturation amelogenesis imperfecta., in J Med Genet

181. Papagerakis, P., Lin, H. K., Lee, K. Y., Hu, Y., et al. Premature stop codon in MMP20 causing amelogenesis imperfecta. J Dent Res 87, 56-59 (2008).

182. PS Hart, S Becerik, D Cogulu, G Emingil, D Ozdemir-Ozenen, ST Han, PP Sulima, E Firatli, TC Hart, Novel FAM83H mutations in Turkish families with autosomal dominant hypocalcified amelogenesis imperfecta., in Clin Genet

183. Mendoza, G., Pemberton, T. J., Lee, K., Scarel-Caminaga, R., et al. A new locus for autosomal dominant amelogenesis imperfecta on chromosome 8q24.3. Hum Genet 120, 653-662 (2007).

184. Kim, J. W., Lee, S. K., Lee, Z. H., Park, J. C., et al. FAM83H mutations in families with autosomal-dominant hypocalcified amelogenesis imperfecta. Am J Hum Genet 82, 489-494 (2008).

185. Wright, J. T., Frazier-Bowers, S., Simmons, D., Alexander, K., et al. Phenotypic variation in FAM83H-associated amelogenesis imperfecta. J Dent Res 88, 356-360 (2009).

186. Ding, Y., Estrella, M. R., Hu, Y. Y., Chan, H. L., et al. Fam83h is associated with intracellular vesicles and ADHCAI. J Dent Res 88, 991-996 (2009).

SECTION II: AUTOSOMAL DOMINANT DIABETES INSIPIDUS

1. Schrier, R. W., Berl, T. & Anderson, R. J. Osmotic and nonosmotic control of vasopressin release. Am J Physiol 236, F321-F332 (1979).

2. Hamlyn, J. M. & Blaustein, M. P. Sodium chloride, extracellular fluid volume, and blood pressure regulation. Am J Physiol 251, F563-F575 (1986).

3. Baylis, P. H. Osmoregulation and control of vasopressin secretion in healthy humans. Am J Physiol 253, R671-R678 (1987).

4. Richter, D. Molecular events in expression of vasopressin and oxytocin and their cognate receptors. Am J Physiol 255, F207-F219 (1988).

5. Lindheimer, M. D., Barron, W. M. & Davison, J. M. Osmoregulation of thirst and vasopressin release in pregnancy. Am J Physiol 257, F159-F169 (1989).

6. Gellai, M. Modulation of vasopressin antidiuretic action by renal alpha 2-adrenoceptors. Am J Physiol 259, F1-F8 (1990).

7. Knepper, M. A. Molecular physiology of urinary concentrating mechanism: regulation of aquaporin water channels by vasopressin. Am J Physiol 272, F3-12 (1997).

8. Fushimi, K. & Marumo, F. Water channels. Curr Opin Nephrol Hypertens 4, 392-397 (1995).

9. van Lieburg, A. F., Knoers, N. V. & Deen, P. M. Discovery of aquaporins: a breakthrough in research on renal water transport. Pediatr Nephrol 9, 228-234 (1995).

10. Knoers, N., Van Lieburg, A. F., Monnens, L. A., Van Oost, B. A., et al. Aquaporins: from physiology to nephrogenic diabetes insipidus. Adv Nephrol Necker Hosp 25, 257-273 (1996).

11. Nielsen, S. Aquaporin water channels in the kidney: localization and regulation. Perit Dial Int 16 Suppl 1, S25-S27 (1996).

12. Knepper, M. A., Verbalis, J. G. & Nielsen, S. Role of aquaporins in water balance disorders. Curr Opin Nephrol Hypertens 6, 367-371 (1997).

13. Nielsen, S., Frør, J. & Knepper, M. A. Renal aquaporins: key roles in water balance and water balance disorders. Curr Opin Nephrol Hypertens 7, 509-516 (1998).

14. Yamamoto, T. & Sasaki, S. Aquaporins in the kidney: emerging new aspects. Kidney Int 54, 1041-1051 (1998).

15. Martin, P. Y. & Schrier, R. W. Role of aquaporin-2 water channels in urinary concentration and dilution defects. Kidney Int Suppl 65, S57-S62 (1998).

16. Ishikawa, S., Sasaki, S. & Saito, T. Urinary excretion of aquaporin-2 in disorders of water metabolism. Nephrol Dial Transplant 13, 1615-1616 (1998).

17. Van Os, C. H. & Deen, P. M. Role of aquaporins in renal water handling:

physiology and pathophysiology. Nephrol Dial Transplant 13, 1645-1651 (1998).

18. Zeidel, M. L. Recent advances in water transport. Semin Nephrol 18, 167-177 (1998).

19. Marples, D., Frøkiaer, J. & Nielsen, S. Long-term regulation of aquaporins in the kidney. Am J Physiol 276, F331-F339 (1999).

20. Lohmeier, T. E. Neurohypophysial hormones. Am J Physiol Regul Integr Comp Physiol 285, R715-R717 (2003).

21. De Keyzer, Y., René, P., Lenne, F., Auzan, C., et al. V3 vasopressin receptor and corticotropic phenotype in pituitary and nonpituitary tumors. Horm Res 47, 259-262 (1997).

22. Thibonnier, M., Berti-Mattera, L. N., Dulin, N., Conarty, D. M. & Mattera, R. Signal transduction pathways of the human V1-vascular, V2-renal, V3-pituitary vasopressin and oxytocin receptors. Prog Brain Res 119, 147-161 (1998).

23. Chan, W. Y., Wo, N. C., Stoev, S. T., Cheng, L. L. & Manning, M. Discovery and design of novel and selective vasopressin and oxytocin agonists and antagonists: the role of bioassays. Exp Physiol 85 Spec No, 7S-18S (2000).

24. Thibonnier, M., Coles, P., Thibonnier, A. & Shoham, M. The basic and clinical pharmacology of nonpeptide vasopressin receptor antagonists. Annu Rev Pharmacol Toxicol 41, 175-202 (2001).

25. Holmes, C. L., Landry, D. W. & Granton, J. T. Science review: Vasopressin and the cardiovascular system part 1--receptor physiology. Crit Care 7, 427-434 (2003).

26. Treschan, T. A. & Peters, J. The vasopressin system: physiology and clinical strategies. Anesthesiology 105, 599-612; quiz 639-40 (2006).

27. Baldasso, E., Ramos Garcia, P. C., Piva, J. P. & Einloft, P. R. Hemodynamic and metabolic effects of vasopressin infusion in children with shock. J Pediatr (Rio J) 83, S137-S145 (2007).

28. Bie, P. Osmoreceptors, vasopressin, and control of renal water excretion. Physiol Rev 60, 961-1048 (1980).

29. Bourque, C. W. & Oliet, S. H. Osmoreceptors in the central nervous system. Annu Rev Physiol 59, 601-619 (1997).

30. McKinley, M. J., Mathai, M. L., McAllen, R. M., McClear, R. C., et al. Vasopressin secretion: osmotic and hormonal regulation by the lamina terminalis. J Neuroendocrinol 16, 340-347 (2004).

31. Robertson, G.L. Thirst and vasopressin. Book chapter. Seldin and Giebisch's The Kidney.

32. Share, L. Role of cardiovascular receptors in the control of ADH release. Cardiology 61 suppl 1, 51-64 (1976).

33. Baylis, P. H. Osmoregulation and control of vasopressin secretion in healthy humans. Am J Physiol 253, R671-R678 (1987).

34. Hirsch, A. T., Dzau, V. J. & Creager, M. A. Baroreceptor function in congestive heart failure: effect on neurohumoral activation and regional vascular resistance. Circulation 75, IV36-IV48 (1987).

35. Forfar, J. C. Neuroendocrine activation in congestive heart failure. Am J Cardiol 67, 3C-5C (1991).

36. Brooks, V. L. & Osborn, J. W. Hormonal-sympathetic interactions in long-term regulation of arterial pressure: an hypothesis. Am J Physiol 268, R1343-R1358 (1995).

37. Hasser, E. M., Bishop, V. S. & Hay, M. Interactions between vasopressin and baroreflex control of the sympathetic nervous system. Clin Exp Pharmacol Physiol 24, 102-108 (1997).

38. Martin, P. Y. & Schrier, R. W. Sodium and water retention in heart failure: pathogenesis and treatment. Kidney Int Suppl 59, S57-S61 (1997).

39. Antunes-Rodrigues, J., de Castro, M., Elias, L. L., Valença, M. M. & McCann, S. M. Neuroendocrine control of body fluid metabolism. Physiol Rev 84, 169-208 (2004).

40. Schrier, R. W. Water and sodium retention in edematous disorders: role of vasopressin and aldosterone. Am J Med 119, S47-S53 (2006).

41. De Leon, J., Dadvand, M., Canuso, C., Odom-White, A., et al. Polydipsia and water intoxication in a long-term psychiatric hospital. Biol Psychiatry 40, 28-34 (1996).

42. Hayfron-Benjamin, J., Peters, C. A. & Woodhouse, R. A. Screening patients with mental retardation for polydipsia. Can J Psychiatry 41, 523-527 (1996).

43. Buckley, P. F. & Schulz, S. C. Clozapine and risperidone: refining and extending their use. Harv Rev Psychiatry 4, 184-199 (1996).

44. Hsu, Y. J., Chiu, J. S., Lu, K. C., Chau, T. & Lin, S. H. Biochemical and etiological characteristics of acute hyponatremia in the emergency department. J Emerg Med 29, 369-374 (2005).

45. Lee, Y. J., Huang, F. Y., Shen, E. Y., Kao, H. A., et al. Neurogenic diabetes insipidus in children with hypoxic encephalopathy: six new cases and a review of the literature. Eur J Pediatr 155, 245-248 (1996).

46. Pogacar, P. R., Mahnke, S. & Rivkees, S. A. Management of central diabetes insipidus in infancy with low renal solute load formula and chlorothiazide. Curr Opin Pediatr 12, 405-411 (2000).

47. Arafah, B. M. & Nasrallah, M. P. Pituitary tumors: pathophysiology, clinical manifestations and management. Endocr Relat Cancer 8, 287-305 (2001).

48. Nishimura, K., Takao, T., Mimoto, T., Matsumori, A., et al. A case of anterior hypopituitarism showing recurrent pituitary mass associated with central diabetes insipidus. Endocr J 50, 825-829 (2003).

49. Yang, M. H., Chuang, H., Jung, S. M., Van, Y. H. & Lo, F. S. Pituitary

apoplexy due to prolactinoma in a Taiwanese boy: patient report and review of the literature. J Pediatr Endocrinol Metab 16, 1301-1305 (2003).

50. Moritz, M. L. & Ayus, J. C. Dysnatremias in the critical care setting. Contrib Nephrol 144, 132-157 (2004).

51. Kim, R. J., Malattia, C., Allen, M., Moshang, T. & Maghnie, M. Vasopressin and desmopressin in central diabetes insipidus: adverse effects and clinical considerations. Pediatr Endocrinol Rev 2 Suppl 1, 115-123 (2004).

52. Bohn, D., Davids, M. R., Friedman, O. & Halperin, M. L. Acute and fatal hyponatraemia after resection of a craniopharyngioma: a preventable tragedy. QJM 98, 691-703 (2005).

53. Kengne, F. G., Fabrice, G. K., Decaux, G. & Gay, D. Inappropriate secretion of ADH and central diabetes insipidus are related to antiphospholipid antibodies in SLE--case report and review of the literature. Nephrol Dial Transplant 21, 3311-3315 (2006).

54. Christensen, J. H. & Rittig, S. Familial neurohypophyseal diabetes insipidus--an update. Semin Nephrol 26, 209-223 (2006).

55. Jung, J. W., Noh, G. Y., Lee, T. H., Lee, Y. Y., et al. Polyuria and polydipsia in a patient with non-small-cell lung cancer. Clin Lung Cancer 8, 565-567 (2007).

56. Ghirardello, S., Garrè, M. L., Rossi, A. & Maghnie, M. The diagnosis of children with central diabetes insipidus. J Pediatr Endocrinol Metab 20, 359-375 (2007).

57. Rutishauser, J., Böni-Schnetzler, M., Böni, J., Wichmann, W., et al. A novel point mutation in the translation initiation codon of the pre-pro-vasopressin-neurophysin II gene: cosegregation with morphological abnormalities and clinical symptoms in autosomal dominant neurohypophyseal diabetes insipidus. J Clin Endocrinol Metab 81, 192-198 (1996).

58. Ueta, Y., Taniguchi, S., Yoshida, A., Murakami, I., et al. A new type of familial central diabetes insipidus caused by a single base substitution in the neurophysin II coding region of the vasopressin gene. J Clin Endocrinol Metab 81, 1787-1790 (1996).

59. Repaske, D. R., Summar, M. L., Krishnamani, M. R., Gültekin, E. K., et al. Recurrent mutations in the vasopressin-neurophysin II gene cause autosomal dominant neurohypophyseal diabetes insipidus. J Clin Endocrinol Metab 81, 2328-2334 (1996).

60. Repaske, D. R., Medlej, R., Gültekin, E. K., Krishnamani, M. R., et al. Heterogeneity in clinical manifestation of autosomal dominant neurohypophyseal diabetes insipidus caused by a mutation encoding Ala-1-->Val in the signal peptide of the arginine vasopressin/neurophysin II/copeptin precursor. J Clin Endocrinol Metab 82, 51-56 (1997).

61. Gagliardi, P. C., Bernasconi, S. & Repaske, D. R. Autosomal dominant neurohypophyseal diabetes insipidus associated with a missense mutation

encoding Gly23-->Val in neurophysin II. J Clin Endocrinol Metab 82, 3643-3646 (1997).

62. Calvo, B., Bilbao, J. R., Urrutia, I., Eizaguirre, J., et al. Identification of a novel nonsense mutation and a missense substitution in the vasopressin-neurophysin II gene in two Spanish kindreds with familial neurohypophyseal diabetes insipidus. J Clin Endocrinol Metab 83, 995-997 (1998).

63. Baglioni, S., Corona, G., Maggi, M., Serio, M. & Peri, A. Identification of a novel mutation in the arginine vasopressin-neurophysin II gene affecting the sixth intrachain disulfide bridge of the neurophysin II moiety. Eur J Endocrinol 151, 605-611 (2004).

64. Christensen, J. H., Siggaard, C., Corydon, T. J., deSanctis, L., et al. Six novel mutations in the arginine vasopressin gene in 15 kindreds with autosomal dominant familial neurohypophyseal diabetes insipidus give further insight into the pathogenesis. Eur J Hum Genet 12, 44-51 (2004).

65. Wahlstrom, J. T., Fowler, M. J., Nicholson, W. E. & Kovacs, W. J. A novel mutation in the preprovasopressin gene identified in a kindred with autosomal dominant neurohypophyseal diabetes insipidus. J Clin Endocrinol Metab 89, 1963-1968 (2004).

66. Tae, H. J., Baek, K. H., Shim, S. M., Yoo, S. J., et al. A novel splice site mutation of the arginine vasopressin-neurophysin II gene identified in a kindred with autosomal dominant familial neurohypophyseal diabetes insipidus. Mol Genet Metab 86, 307-313 (2005).

67. Ito, M. & Jameson, J. L. Molecular basis of autosomal dominant neurohypophyseal diabetes insipidus. Cellular toxicity caused by the accumulation of mutant vasopressin precursors within the endoplasmic reticulum. J Clin Invest 99, 1897-1905 (1997).

68. Maldonado, P., Pino, S. & Norero, C. [Nephrogenic diabetes insipidus: report of 3 cases. Brief review of the theme]. Rev Chil Pediatr 51, 61-67 (1980).

69. Bichet, D. G. Nephrogenic diabetes insipidus. Semin Nephrol 14, 349-356 (1994).

70. Garofeanu, C. G., Weir, M., Rosas-Arellano, M. P., Henson, G., et al. Causes of reversible nephrogenic diabetes insipidus: a systematic review. Am J Kidney Dis 45, 626-637 (2005).

71. Khanna, A. Acquired nephrogenic diabetes insipidus. Semin Nephrol 26, 244-248 (2006).

72. Dürr, J. A. Diabetes insipidus in pregnancy. Am J Kidney Dis 9, 276-283 (1987).

73. Ramsey, T. A. & Cox, M. Lithium and the kidney: a review. Am J Psychiatry 139, 443-449 (1982).

74. Boton, R., Gaviria, M. & Batlle, D. C. Prevalence, pathogenesis, and treatment of renal dysfunction associated with chronic lithium therapy. Am J

Kidney Dis 10, 329-345 (1987).

75. Simard, M., Gumbiner, B., Lee, A., Lewis, H. & Norman, D. Lithium carbonate intoxication. A case report and review of the literature. Arch Intern Med 149, 36-46 (1989).

76. Walker, R. G. Lithium nephrotoxicity. Kidney Int Suppl 42, S93-S98 (1993).

77. Izzedine, H., Launay-Vacher, V. & Deray, G. Antiviral drug-induced nephrotoxicity. Am J Kidney Dis 45, 804-817 (2005).

78. Muther, R. S., McCarron, D. A. & Bennett, W. M. Granulomatous sarcoid nephritis: a cause of multiple renal tubular abnormalities. Clin Nephrol 14, 190-197 (1980).

79. Cannon, J. F. Diabetes insipidus; clinical and experimental studies with consideration of genetic relationships. AMA Arch Intern Med 96, 215-272 (1955).

80. Bell, N. H., Clark, C. M., Avery, S., Sinha, T., et al. Demonstration of a defect in the formation of adenosine 3',5'-monophosphate in vasopressin-resistant diabetes insipidus. Pediatr Res 8, 223-230 (1974).

81. Knoers, N., van der Heyden, H., van Oost, B. A., Ropers, H. H., et al. Nephrogenic diabetes insipidus: close linkage with markers from the distal long arm of the human X chromosome. Hum Genet 80, 31-38 (1988).

82. Knoers, N., van der Heyden, H., van Oost, B. A., Monnens, L., et al. Three-point linkage analysis using multiple DNA polymorphic markers in families with X-linked nephrogenic diabetes insipidus. Genomics 4, 434-437 (1989).

83. Van den Ouweland, A. M., Knoop, M. T., Knoers, V. V., Markslag, P. W., et al. Colocalization of the gene for nephrogenic diabetes insipidus (DIR) and the vasopressin type 2 receptor gene (AVPR2) in the Xq28 region. Genomics 13, 1350-1352 (1992).

84. Rosenthal, W., Seibold, A., Antaramian, A., Lonergan, M., et al. Molecular identification of the gene responsible for congenital nephrogenic diabetes insipidus. Nature 359, 233-235 (1992).

85. van den Ouweland, A. M., Dreesen, J. C., Verdijk, M., Knoers, N. V., et al. Mutations in the vasopressin type 2 receptor gene (AVPR2) associated with nephrogenic diabetes insipidus. Nat Genet 2, 99-102 (1992).

86. Knoers, N., van den Ouweland, A., Dreesen, J., Verdijk, M., et al. Nephrogenic diabetes insipidus: identification of the genetic defect. Pediatr Nephrol 7, 685-688 (1993).

87. Fujiwara, T. M., Morgan, K. & Bichet, D. G. Molecular biology of diabetes insipidus. Annu Rev Med 46, 331-343 (1995).

88. Bichet, D. G. Vasopressin receptor mutations in nephrogenic diabetes insipidus. Semin Nephrol 28, 245-251 (2008).

89. Bichet, D. G., Oksche, A. & Rosenthal, W. Congenital nephrogenic diabetes insipidus. J Am Soc Nephrol 8, 1951-1958 (1997).

90. Bichet, D. G. Nephrogenic diabetes insipidus. Am J Med 105, 431-442 (1998).

91. Knoers, N. V. & van Os, C. H. Molecular and cellular defects in nephrogenic diabetes insipidus. Curr Opin Nephrol Hypertens 5, 353-358 (1996).

92. Van't Hoff, W. G. Biology and genetics of inherited renal tubular disorders. Exp Nephrol 4, 253-262 (1996).

93. Robben, J. H., Knoers, N. V. & Deen, P. M. Cell biological aspects of the vasopressin type-2 receptor and aquaporin 2 water channel in nephrogenic diabetes insipidus. Am J Physiol Renal Physiol 291, F257-F270 (2006).

94. Fujiwara, T. M. & Bichet, D. G. Molecular biology of hereditary diabetes insipidus. J Am Soc Nephrol 16, 2836-2846 (2005).

95. Bichet, D. G. Vasopressin receptors in health and disease. Kidney Int 49, 1706-1711 (1996).

96. Zimmerman, D.; Green, O. C. Nephrogenic diabetes insipidus type II: defect distal to the adenylate cyclase step. Pediat. Res. 9: 381 only (1975).

97. Deen, P. M. T.; Verdijk, M. A. J.; Knoers, N. V. A. M.; Wieringa, B.; Monnens, L. A. H.; van Os, C. H.; van Oost, B. A. Requirement of human renal water channel aquaporin-2 for vasopressin-dependent concentration of urine. Science 264, 92-94 (1994).

98. Knoers, N., Van Lieburg, A. F., Monnens, L. A., Van Oost, B. A., et al. Aquaporins: from physiology to nephrogenic diabetes insipidus. Adv Nephrol Necker Hosp 25, 257-273 (1996).

99. King, L. S. & Agre, P. Pathophysiology of the aquaporin water channels. Annu Rev Physiol 58, 619-648 (1996).

100. Knepper, M. A., Verbalis, J. G. & Nielsen, S. Role of aquaporins in water balance disorders. Curr Opin Nephrol Hypertens 6, 367-371 (1997).

101. Frøkiaer, J., Marples, D., Knepper, M. A. & Nielsen, S. Pathophysiology of aquaporin-2 in water balance disorders. Am J Med Sci 316, 291-299 (1998).

102. Deen, P. M. & Knoers, N. V. Vasopressin type-2 receptor and aquaporin-2 water channel mutants in nephrogenic diabetes insipidus. Am J Med Sci 316, 300-309 (1998).

103. Verkman, A. S. Role of aquaporin water channels in kidney and lung. Am J Med Sci 316, 310-320 (1998).

104. Knoers, N. V. & Deen, P. M. Aquaporin molecular biology and clinical abnormalities of the water transport channels. Curr Opin Pediatr 10, 428-434 (1998).

105. Berl, T. Water channels in health and disease. Kidney Int 53, 1417-1418 (1998).

106. Martin, P. Y. & Schrier, R. W. Role of aquaporin-2 water channels in

urinary concentration and dilution defects. Kidney Int Suppl 65, S57-S62 (1998).

107. Van Os, C. H. & Deen, P. M. Role of aquaporins in renal water handling: physiology and pathophysiology. Nephrol Dial Transplant 13, 1645-1651 (1998).

108. Knoers, N. V. & Monnens, L. L. Nephrogenic diabetes insipidus. Semin Nephrol 19, 344-352 (1999).

109. Nielsen, S., Kwon, T. H., Christensen, B. M., Promeneur, D., et al. Physiology and pathophysiology of renal aquaporins. J Am Soc Nephrol 10, 647-663 (1999).

110. Knoers, N. V. & Deen, P. M. Molecular and cellular defects in nephrogenic diabetes insipidus. Pediatr Nephrol 16, 1146-1152 (2001).

111. Noda, Y., Sohara, E., Ohta, E. & Sasaki, S. Aquaporins in kidney pathophysiology. Nat Rev Nephrol 6, 168-178 (2010).

112. Frasier, S. D., Kutnik, L. A., Schmidt, R. T. & Smith, F. G. A water deprivation test for the diagnosis of diabetes insipidus in children. Am J Dis Child 114, 157-160 (1967).

113. Hendricks, S. A., Lippe, B., Kaplan, S. A. & Lee, W. N. Differential diagnosis of diabetes insipidus: use of DDAVP to terminate the seven-hour water deprivation test. J Pediatr 98, 244-246 (1981).

114. Adam, P. Evaluation and management of diabetes insipidus. Am Fam Physician 55, 2146-2153 (1997).

115. Mohn, A., Acerini, C. L., Cheetham, T. D., Lightman, S. L. & Dunger, D. B. Hypertonic saline test for the investigation of posterior pituitary function. Arch Dis Child 79, 431-434 (1998).

116. Matsumura, Y., Uchida, S., Kondo, Y., Miyazaki, H., et al. Overt nephrogenic diabetes insipidus in mice lacking the CLC-K1 chloride channel. Nat Genet 21, 95-98 (1999).

117. Uchida, S. In vivo role of CLC chloride channels in the kidney. Am J Physiol Renal Physiol 279, F802-F808 (2000).

118. Ozata, M., Tayfun, C., Kurtaran, K., Yetkin, I., et al. Magnetic resonance imaging of posterior pituitary for evaluation of the neurohypophyseal function in idiopathic and autosomal dominant neurohypophyseal diabetes insipidus. Eur Radiol 7, 1098-1102 (1997).

119. Tien, R., Kucharczyk, J. & Kucharczyk, W. MR imaging of the brain in patients with diabetes insipidus. AJNR Am J Neuroradiol 12, 533-542 (1991).

120. Shalev, H., Romanovsky, I., Knoers, N. V., Lupa, S. & Landau, D. Bladder function impairment in aquaporin-2 defective nephrogenic diabetes insipidus. Nephrol Dial Transplant 19, 608-613 (2004).

121 Ulinski, C Grapin, V Forin, R Vargas-Poussou, G Deschênes, A Bensman, Severe bladder dysfunction in a family with ADH receptor gene mutation responsible for X-linked nephrogenic diabetes insipidus., in Nephrol Dial

Transplant .

122. Zender, H. O., Ruedin, P., Moser, F., Bolle, J. F. & Leski, M. Traumatic rupture of the urinary tract in a patient presenting nephrogenic diabetes insipidus associated with hydronephrosis and chronic renal failure: case report and review of the literature. Clin Nephrol 38, 196-202 (1992).

123. Uribarri, J. & Kaskas, M. Hereditary nephrogenic diabetes insipidus and bilateral nonobstructive hydronephrosis. Nephron 65, 346-349 (199354)

124. Seckl, J. R. & Dunger, D. B. Diabetes insipidus. Current treatment recommendations. Drugs 44, 216-224 (1992).

125. Knoers, N. & Monnens, L. A. Nephrogenic diabetes insipidus: clinical symptoms, pathogenesis, genetics and treatment. Pediatr Nephrol 6, 476-482 (1992).

126. Bichet, D. G. Polyuria and diabetes insipidus. Book chapter. Seldin and Geibisch's The Kidney.

127. Land, H., Schütz, G., Schmale, H. & Richter, D. Nucleotide sequence of cloned cDNA encoding bovine arginine vasopressin-neurophysin II precursor. Nature 295, 299-303 (1982).

128. Furutani, Y., Morimoto, Y., Shibahara, S., Noda, M., et al. Cloning and sequence analysis of cDNA for ovine corticotropin-releasing factor precursor. Nature 301, 537-540 (1983).

129. Ivell, R., Schmale, H. & Richter, D. Vasopressin and oxytocin precursors as model preprohormones. Neuroendocrinology 37, 235-240 (1983).

130. Richter, D. & Schmale, H. The structure of the precursor to arginine-vasopressin: a model preprohormone. Prog Brain Res 60, 227-233 (1983).

131. Ruppert, S., Scherer, G. & Schütz, G. Recent gene conversion involving bovine vasopressin and oxytocin precursor genes suggested by nucleotide sequence. Nature 308, 554-557 (1984).

132. Hough, C. J. & Chaiken, I. M. Characterization of the size and 5' cap of messenger RNA encoding neurophysin precursors. Nucleic Acids Res 12, 4397-4410 (1984).

133. Ivell, R. & Richter, D. Structure and comparison of the oxytocin and vasopressin genes from rat. Proc Natl Acad Sci U S A 81, 2006-2010 (1984).

134. Ando, S., McPhie, P. & Chaiken, I. M. Sequence redesign and the assembly mechanism of the oxytocin/bovine neurophysin I biosynthetic precursor. J Biol Chem 262, 12962-12969 (1987).

135. Brakch, N., Boussetta, H., Rholam, M. & Cohen, P. Processing endoprotease recognizes a structural feature at the cleavage site of peptide prohormones. The pro-ocytocin/neurophysin model. J Biol Chem 264, 15912-15916 (1989).

136. Siggaard, C., Rittig, S., Corydon, T. J., Andreasen, P. H., et al. Clinical and

molecular evidence of abnormal processing and trafficking of the vasopressin preprohormone in a large kindred with familial neurohypophyseal diabetes insipidus due to a signal peptide mutation. J Clin Endocrinol Metab 84, 2933-2941 (1999).

137. Rutishauser, J., Kopp, P., Gaskill, M. B., Kotlar, T. J. & Robertson, G. L. Clinical and molecular analysis of three families with autosomal dominant neurohypophyseal diabetes insipidus associated with a novel and recurrent mutations in the vasopressin-neurophysin II gene. Eur J Endocrinol 146, 649-656 (2002).

138. Davies, J. H., Penney, M., Abbes, A. P., Engel, H. & Gregory, J. W. Clinical features, diagnosis and molecular studies of familial central diabetes insipidus. Horm Res 64, 231-237 (2005).

139. Ito, M.; Mori, Y.; Oiso, Y.; Saito, H. A single base substitution in the coding region for neurophysin II associated with familial central diabetes insipidus. J. Clin. Invest. 87: 725-728 (1991).

140. Rittig, S., Robertson, G. L., Siggaard, C., Kovács, L., et al. Identification of 13 new mutations in the vasopressin-neurophysin II gene in 17 kindreds with familial autosomal dominant neurohypophyseal diabetes insipidus. Am J Hum Genet 58, 107-117 (1996).

141. Miyakoshi, M., Kamoi, K., Murase, T., Sugimura, Y. & Oiso, Y. Novel mutant vasopressin-neurophysin II gene associated with familial neurohypophyseal diabetes insipidus. Endocr J 51, 551-556 (2004).

142. Vutskits, L., Bartanusz, V., Schulz, M. F. & Kiss, J. Z. Magnocellular vasopressinergic neurons in explant cultures are rescued from cell death by ciliary neurotrophic factor and leukemia inhibiting factor. Neuroscience 87, 571-582 (1998).

143. Willcutts, M. D., Felner, E. & White, P. C. Autosomal recessive familial neurohypophyseal diabetes insipidus with continued secretion of mutant weakly active vasopressin. Hum Mol Genet 8, 1303-1307 (1999).

144. Ito, M., Yu, R. N. & Jameson, J. L. Mutant vasopressin precursors that cause autosomal dominant neurohypophyseal diabetes insipidus retain dimerization and impair the secretion of wild-type proteins. J Biol Chem 274, 9029-9037 (1999).

145. Beuret, N., Rutishauser, J., Bider, M. D. & Spiess, M. Mechanism of endoplasmic reticulum retention of mutant vasopressin precursor caused by a signal peptide truncation associated with diabetes insipidus. J Biol Chem 274, 18965-18972 (1999).

146. Siggaard, C., Rittig, S., Corydon, T. J., Andreasen, P. H., et al. Clinical and molecular evidence of abnormal processing and trafficking of the vasopressin preprohormone in a large kindred with familial neurohypophyseal diabetes insipidus due to a signal peptide mutation. J Clin Endocrinol Metab 84, 2933-

2941 (1999).

147. Calvo, B., Bilbao, J. R., Rodríguez, A., Rodríguez-Arnao, M. D. & Castaño, L. Molecular analysis in familial neurohypophyseal diabetes insipidus: early diagnosis of an asymptomatic carrier. J Clin Endocrinol Metab 84, 3351-3354 (1999).

148. Phillips, J. A. Dominant-negative diabetes insipidus and other endocrinopathies. J Clin Invest 112, 1641-1643 (2003).

149. Russell, T. A., Ito, M., Ito, M., Yu, R. N., et al. A murine model of autosomal dominant neurohypophyseal diabetes insipidus reveals progressive loss of vasopressin-producing neurons. J Clin Invest 112, 1697-1706 (2003).

150. Christensen, J. H., Siggaard, C., Corydon, T. J., Robertson, G. L., et al. Differential cellular handling of defective arginine vasopressin (AVP) prohormones in cells expressing mutations of the AVP gene associated with autosomal dominant and recessive familial neurohypophyseal diabetes insipidus. J Clin Endocrinol Metab 89, 4521-4531 (2004).

SECTION III: AUTOSOMAL DOMINANT RENAL FANCONI SYNDROME

1. Engle, R. L. & Wallis, L. A. The adult Fanconi syndrome. II. Review of eighteen cases. Am J Med 22, 13-23 (1957).

2. Worthen, H. G. & Good, R. A. The de Toni-Fanconi syndrome with cystinosis; clinical and metabolic study of two cases in a family and a critical review on the nature of the syndrome. AMA J Dis Child 95, 653-688 (1958).

3. Gatti, R. [Considerations on the De Toni-Debré-Fanconi syndrome]. Minerva Pediatr 19, 719-723 (1967).

4. Perkoff, G. T. The hereditary renal diseases. N Engl J Med 277, 129-38 concl (1967).

5. Morris, R. C. Renal tubular acidosis. Mechanisms, classification and implications. N Engl J Med 281, 1405-1413 (1969).

6. Brodehl, J. & Bickel, H. Aminoaciduria and hyperaminoaciduria in childhood. Clin Nephrol 1, 149-168 (1973).

13. Caskey, C. T. Inherited biochemical defects affecting the kidney. Perspect Nephrol Hypertens 3, 255-274 (1976).

14. McSherry, E. Renal tubular acidosis in childhood. Kidney Int 20, 799-809 (1981).

7. Quigley, R. Proximal renal tubular acidosis. J Nephrol 19 Suppl 9, S41-S45 (2006).

8. Hall, A. M. & Unwin, R. J. The not so 'mighty chondrion': emergence of renal diseases due to mitochondrial dysfunction. Nephron Physiol 105, p1-10 (2007).

9. Devuyst, O., Jouret, F., Auzanneau, C. & Courtoy, P. J. Chloride channels and endocytosis: new insights from Dent's disease and ClC-5 knockout mice. Nephron Physiol 99, p69-p73 (2005).

10. Ganapathy, V. & Leibach, F. H. Carrier-mediated reabsorption of small peptides in renal proximal tubule. Am J Physiol 251, F945-F953 (1986).

11. Silverman, M. Comparison of glucose transport mechanisms at opposing surfaces of the renal proximal tubular cell. Biochem Cell Biol 64, 1092-1098 (1986).

12. Scherberich, J. E. Urinary proteins of tubular origin: basic immunochemical and clinical aspects. Am J Nephrol 10 Suppl 1, 43-51 (1990).

13. Silverman, M. Glucose reabsorption in the kidney: glucosuria: molecular mechanism of Na/glucose cotransport. Book chapter. Seldin and Giebisch's The Kidney.

14. Silbernagi, S., Gekle, M. Amino acids, oligopeptides and hyperaminoaciduria. Book chater. Seldin and Giebisch's The Kidney.

15. DuBose, T. D., Good, D. W., Hamm, L. L. & Wall, S. M. Ammonium

transport in the kidney: new physiological concepts and their clinical implications. J Am Soc Nephrol 1, 1193-1203 (1991).

16. Karim, Z., Szutkowska, M., Vernimmen, C. & Bichara, M. Recent concepts concerning the renal handling of NH3/NH4+. J Nephrol 19 Suppl 9, S27-S32 (2006).

17. Karim, Z., Szutkowska, M., Vernimmen, C. & Bichara, M. Renal handling of NH3/NH4+: recent concepts. Nephron Physiol 101, p77-p81 (2005).

18. Parker, M., D., Boron, W.,F. Sodium-coupled bicarbonate transporters. Book chapter. Seldin and Giebisch's The Kidney.

19. Curthoys, N., M. Renal ammonium ion production and excretion. Book chapter. Seldin and Giebisch's The Kidney.

20. Hamm, L., L., Alpern, R.,J., Preisig, P.,A. Cellular mechanisms of renal tubular acidification. Book chapter. Seldin and Giebisch's The Kidney.

21. DiBona, G. F. Neurogenic regulation of renal tubular sodium reabsorption. Am J Physiol 233, F73-F81 (1977).

22. Moss, N. G. Renal function and renal afferent and efferent nerve activity. Am J Physiol 243, F425-F433 (1982).

23. Spitzer, A. The role of the kidney in sodium homeostasis during maturation. Kidney Int 21, 539-545 (1982).

24. Beyenbach, K. W. Secretory NaCl and volume flow in renal tubules. Am J Physiol 250, R753-R763 (1986).

25. Hall, J. E. Control of sodium excretion by angiotensin II: intrarenal mechanisms and blood pressure regulation. Am J Physiol 250, R960-R972 (1986).

26. Sonnenberg, H. Renal regulation of salt balance: a primer for non-purists. Pediatr Nephrol 4, 354-357 (1990).

27. Wang, X., Armando, I., Upadhyay, K., Pascua, A. & Jose, P. A. The regulation of proximal tubular salt transport in hypertension: an update. Curr Opin Nephrol Hypertens 18, 412-420 (2009).

28. Andreoli, T. E. An overview of salt absorption by the nephron. J Nephrol 12 Suppl 2, S3-15 (1999).

29. Weinstein, M. Sodium and chloride transport: Proximal tubule. Book chapter. Seldin and Giebisch's The Kidney.

30. Suki, W. N. Disposition and regulation of body potassium: an overview. Am J Med Sci 272, 31-41 (1976).

31. Hammerman, M. R. Phosphate transport across renal proximal tubular cell membranes. Am J Physiol 251, F385-F398 (1986).

32. Murer, H. & Biber, J. Control of proximal tubular apical Na/Pi cotransport. Exp Nephrol 4, 201-204 (1996).

33. Biber, J. Cellular aspects of proximal tubular phosphate reabsorption. Kidney Int 36, 360-369 (1989).

34. Murer, H., Forster, I., Hernando, N., Biber, J. Proximal tubular handling of phosphate: Na/Pi-cotransporters and their regulation. Book chapter. Seldin and Giebisch's The Kidney.

35. Malnic, G., Muto, S., Giebisch, G. Regulation of potassium excretion. Book chapter. Seldin and Giebisch's The Kidney.

36. Brodehl, J. & Bickel, H. Aminoaciduria and hyperaminoaciduria in childhood. Clin Nephrol 1, 149-168 (1973).

38. Cogan, M. G. Disorders of proximal nephron function. Am J Med 72, 275-288 (1982).

39. Schulman, J. D. & Schneider, J. A. Cystinosis and the Fanconi syndrome. Pediatr Clin North Am 23, 779-793 (1976).

40. Foreman, J. W. & Roth, K. S. Human renal Fanconi syndrome--then and now. Nephron 51, 301-306 (1989).

41. Bickel, H. & Manz, F. Hereditary tubular disorders of the Fanconi type and the idiopathic Fanconi syndrome. Prog Clin Biol Res 305, 111-135 (1989).

42. Gregory, M. J. & Schwartz, G. J. Diagnosis and treatment of renal tubular disorders. Semin Nephrol 18, 317-329 (1998).

43 Foreman, J., W. Fanconi syndrome and other proximal tubular disorders. Book chapter. Comprehensive Clinical Nephrology (Feehally, J., Floege, J., Johnson, R.J. editors).

44. Laing, C. M. & Unwin, R. J. Renal tubular acidosis. J Nephrol 19 Suppl 9, S46-S52 (2006).

45. Chadha, V. & Alon, U. S. Hereditary renal tubular disorders. Semin Nephrol 29, 399-411 (2009).

46. Thakker, R. V. Pathogenesis of Dent's disease and related syndromes of X-linked nephrolithiasis. Kidney Int 57, 787-793 (2000).

47. Yu, A. S. Role of ClC-5 in the pathogenesis of hypercalciuria: recent insights from transgenic mouse models. Curr Opin Nephrol Hypertens 10, 415-420 (2001).

48. Chen, Y. T. Type I glycogen storage disease: kidney involvement, pathogenesis and its treatment. Pediatr Nephrol 5, 71-76 (1991).

49. Sessa, A., Meroni, M., Battini, G., Maglio, A., et al. Renal pathological changes in Fabry disease. J Inherit Metab Dis 24 Suppl 2, 66-70; discussion 65 (2001).

50. Santer, R., Steinmann, B. & Schaub, J. Fanconi-Bickel syndrome--a congenital defect of facilitative glucose transport. Curr Mol Med 2, 213-227 (2002).

51. Morgan, H. G., Stewart, W. K., Lowe, K. G., Stowers, J. M. & Johnstone, J.

H. Wilson's disease and the Fanconi syndrome. Q J Med 31, 361-384 (1962).

52. Redfield, V. A., Mimouni, F., Strife, F. C. & Tsang, R. C. Severe rickets in Lowe syndrome: treatment with continuous nasogastric infusion. Pediatr Nephrol 5, 696-699 (1991).

53. Lin, T., Orrison, B. M., Leahey, A. M., Suchy, S. F., et al. Spectrum of mutations in the OCRL1 gene in the Lowe oculocerebrorenal syndrome. Am J Hum Genet 60, 1384-1388 (1997).

54. Bockenhauer, D., Bokenkamp, A., van't Hoff, W., Levtchenko, E., et al. Renal phenotype in Lowe Syndrome: a selective proximal tubular dysfunction. Clin J Am Soc Nephrol 3, 1430-1436 (2008).

55. Adamson, M. D., Andersson, H. C. & Gahl, W. A. Cystinosis. Semin Nephrol 9, 147-161 (1989).

56. Gahl, W. A., Thoene, J. G., Schneider, J. A., O'Regan, S., et al. NIH conference. Cystinosis: progress in a prototypic disease. Ann Intern Med 109, 557-569 (1988).

57. Niaudet, P. & Rötig, A. Renal involvement in mitochondrial cytopathies. Pediatr Nephrol 10, 368-373 (1996).

58. Walker, U. A. Update on mitochondrial toxicity: where are we now? J HIV Ther 8, 32-35 (2003).

59. Rötig, A. Renal disease and mitochondrial genetics. J Nephrol 16, 286-292 (2003).

60. Wang, L. C., Lee, W. T., Tsai, W. Y., Tsau, Y. K. & Shen, Y. Z. Mitochondrial cytopathy combined with Fanconi's syndrome. Pediatr Neurol 22, 403-406 (2000).

61. Hsiao, P. J., Wang, S. C., Wen, M. C., Diang, L. K. & Lin, S. H. Fanconi syndrome and CKD in a patient with paroxysmal nocturnal hemoglobinuria and hemosiderosis. Am J Kidney Dis 55, e1-e5 (2010).

62. Chisolm, J. J. The use of chelating agents in the treatment of acute and chronic lead intoxication in childhood. J Pediatr 73, 1-38 (1968).

63. Izzedine, H., Launay-Vacher, V., Isnard-Bagnis, C. & Deray, G. Drug-induced Fanconi's syndrome. Am J Kidney Dis 41, 292-309 (2003).

64. Kintzel, P. E. Anticancer drug-induced kidney disorders. Drug Saf 24, 19-38 (2001).

65. Melnick, J. Z., Baum, M. & Thompson, J. R. Aminoglycoside-induced Fanconi's syndrome. Am J Kidney Dis 23, 118-122 (1994).

66. Isnard Bagnis, C., Deray, G., Baumelou, A., Le Quintrec, M. & Vanherweghem, J. L. Herbs and the kidney. Am J Kidney Dis 44, 1-11 (2004).

67. Quimby, D. & Brito, M. O. Fanconi syndrome associated with use of tenofovir in HIV-infected patients: a case report and review of the literature. AIDS Read 15, 357-364 (2005).

68. Fine, D. M. Editorial comment: tenofovir nephrotoxicity--vigilance required. AIDS Read 15, 362-363 (2005).

69. Szeto, C. C. & Chow, K. M. Nephrotoxicity related to new therapeutic compounds. Ren Fail 27, 329-333 (2005).

70. Barbier, O., Jacquillet, G., Tauc, M., Cougnon, M. & Poujeol, P. Effect of heavy metals on, and handling by, the kidney. Nephron Physiol 99, p105-p110 (2005).

71. Zimmermann, A. E., Pizzoferrato, T., Bedford, J., Morris, A., et al. Tenofovir-associated acute and chronic kidney disease: a case of multiple drug interactions. Clin Infect Dis 42, 283-290 (2006).

72. Choudhury, D. & Ahmed, Z. Drug-associated renal dysfunction and injury. Nat Clin Pract Nephrol 2, 80-91 (2006).

73. Tsimihodimos, V., Psychogios, N., Kakaidi, V., Bairaktari, E. & Elisaf, M. Salicylate-induced proximal tubular dysfunction. Am J Kidney Dis 50, 463-467 (2007).

74. D'Ythurbide, G., Goujard, C., Méchaï, F., Blanc, A., et al. Fanconi syndrome and nephrogenic diabetes insipidus associated with didanosine therapy in HIV infection: a case report and literature review. Nephrol Dial Transplant 22, 3656-3659 (2007).

75. Woodward, C. L., Hall, A. M., Williams, I. G., Madge, S., et al. Tenofovir-associated renal and bone toxicity. HIV Med 10, 482-487 (2009).

76. Lino, M., Binaut, R., Noël, L. H., Patey, N., et al. Tubulointerstitial nephritis and Fanconi syndrome in primary biliary cirrhosis. Am J Kidney Dis 46, e41-e46 (2005).

77. Koike, K., Lida, S., Usui, M., Matsumoto, Y., et al. Adult-onset acute tubulointerstitial nephritis and uveitis with Fanconi syndrome. Case report and review of the literature. Clin Nephrol 67, 255-259 (2007).

78. Maldonado, J. E., Velosa, J. A., Kyle, R. A., Wagoner, R. D., et al. Fanconi syndrome in adults. A manifestation of a latent form of myeloma. Am J Med 58, 354-364 (1975).

79. Fang, L. S. Light-chain nephropathy. Kidney Int 27, 582-592 (1985).

80. Said, S. M., Assaad, A. M., Cerda, J. & Nasr, S. H. Light chain tubulopathy without Fanconi syndrome. Nephrol Dial Transplant 21, 3589-3590 (2006).

81. Merlini, G. & Pozzi, C. Mechanisms of renal damage in plasma cell dyscrasias: an overview. Contrib Nephrol 153, 66-86 (2007).

82. Batuman, V. Proximal tubular injury in myeloma. Contrib Nephrol 153, 87-104 (2007).

83. Lacy, M. Q. & Gertz, M. A. Acquired Fanconi's syndrome associated with monoclonal gammopathies. Hematol Oncol Clin North Am 13, 1273-1280 (1999).

84. Messiaen, T., Deret, S., Mougenot, B., Bridoux, F., et al. Adult Fanconi

syndrome secondary to light chain gammopathy. Clinicopathologic heterogeneity and unusual features in 11 patients. Medicine (Baltimore) 79, 135-154 (2000).

85. Maldonado, J. E., Velosa, J. A., Kyle, R. A., Wagoner, R. D., et al. Fanconi syndrome in adults. A manifestation of a latent form of myeloma. Am J Med 58, 354-364 (1975).

86. Kobayashi, T., Muto, S., Nemoto, J., Miyata, Y., et al. Fanconi's syndrome and distal (type 1) renal tubular acidosis in a patient with primary Sjögren's syndrome with monoclonal gammopathy of undetermined significance. Clin Nephrol 65, 427-432 (2006).

87. Dent, C.,E., Harris H. The genetics of cystinuria. Ann. Eugen 16, 60-87 ((1951).

88. Brenton, D. P., Isenberg, D. A., Cusworth, D. C., Garrod, P., et al. The adult presenting idiopathic Fanconi syndrome. J Inherit Metab Dis 4, 211-215 (1981).

89. Luder, J., Sheldon, W. A familial tubular absorption defect of glucose and amino acids. *Arch* Dis Child 30, 160-164 (1955).

90. 1. Patrick, A., Cameron, J. S. & Ogg, C. S. A family with a dominant form of idiopathic Fanconi syndrome leading to renal failure in adult life. Clin Nephrol 16, 289-292 (1981).

91. Smith, R., Lindenbaum, R. H. & Walton, R. J. Hypophosphataemic osteomalacia and Fanconi syndrome of adult onset with dominant inheritance. Possible relationship with diabetes mellitus. Q J Med 45, 387-400 (1976).

92. Harrison, N. A., Bateman, J. M., Ledingham, J. G. & Smith, R. Renal failure in adult onset hypophosphatemic osteomalacia with Fanconi syndrome: a family study and review of the literature. Clin Nephrol 35, 148-150 (1991).

93. Lichter-Konecki, U., Broman, K. W., Blau, E. B. & Konecki, D. S. Genetic and physical mapping of the locus for autosomal dominant renal Fanconi syndrome, on chromosome 15q15.3. Am J Hum Genet 68, 264-268 (2001).

94. Long, W. S., Seashore, M. R., Siegel, N. J. & Bia, M. J. Idiopathic Fanconi syndrome with progressive renal failure: a case report and discussion. Yale J Biol Med 63, 15-28 (1990).

95. Wen, S. F., Friedman, A. L. & Oberley, T. D. Two case studies from a family with primary Fanconi syndrome. Am J Kidney Dis 13, 240-246 (1989).

96. Tolaymat, A., Sakarcan, A. & Neiberger, R. Idiopathic Fanconi syndrome in a family. Part I. Clinical aspects. J Am Soc Nephrol 2, 1310-1317 (1992).

97. Hunt, D. D., Stearns, G., Froning, E. C., McKinley, J. B., et al. Long term study of a family with the Fanconi syndrome and cystinuria. Surg Forum 16, 462-464 (1965).

98. Lee, D. B., Drinkard, J. P., Rosen, V. J. & Gonick, H. C. The adult Fanconi syndrome: observations on etiology, morphology, renal function and mineral metabolism in three patients. Medicine (Baltimore) 51, 107-138 (1972).

99. Lindor, N. M., Petersen, G. M., Hadley, D. W., Kinney, A. Y., et al. Recommendations for the care of individuals with an inherited predisposition to Lynch syndrome: a systematic review. JAMA 296, 1507-1517 (2006).

100. Lynch, H. T., Boland, C. R., Rodriguez-Bigas, M. A., Amos, C., et al. Who should be sent for genetic testing in hereditary colorectal cancer syndromes? J Clin Oncol 25, 3534-3542 (2007).

101. Evans, D. G., Walsh, S., Hill, J. & McMahon, R. T. Strategies for identifying hereditary nonpolyposis colon cancer. Semin Oncol 34, 411-417 (2007).

102. Dionigi, G., Bianchi, V., Rovera, F., Boni, L., et al. Genetic alteration in hereditary colorectal cancer. Surg Oncol 16 Suppl 1, S11-S15 (2007).

103. Lynch, H. T., Lynch, P. M., Lanspa, S. J., Snyder, C. L., et al. Review of the Lynch syndrome: history, molecular genetics, screening, differential diagnosis, and medicolegal ramifications. Clin Genet 76, 1-18 (2009).

104. Lynch, H. T., Lynch, J. F. & Attard, T. A. Diagnosis and management of hereditary colorectal cancer syndromes: Lynch syndrome as a model. CMAJ 181, 273-280 (2009).

105. Garg, K. & Soslow, R. A. Lynch syndrome (hereditary non-polyposis colorectal cancer) and endometrial carcinoma. J Clin Pathol 62, 679-684 (2009).

106. Koornstra, J. J., Mourits, M. J., Sijmons, R. H., Leliveld, A. M., et al. Management of extracolonic tumours in patients with Lynch syndrome. Lancet Oncol 10, 400-408 (2009).

107. Jaeger, E. E., Woodford-Richens, K. L., Lockett, M., Rowan, A. J., et al. An ancestral Ashkenazi haplotype at the HMPS/CRAC1 locus on 15q13-q14 is associated with hereditary mixed polyposis syndrome. Am J Hum Genet 72, 1261-1267 (2003).

108. Park, W. S., Park, J. Y., Oh, R. R., Yoo, N. J., et al. A distinct tumor suppressor gene locus on chromosome 15q21.1 in sporadic form of colorectal cancer. Cancer Res 60, 70-73 (2000).

109. Daley, D., Lewis, S., Platzer, P., MacMillen, M., et al. Identification of susceptibility genes for cancer in a genome-wide scan: results from the colon neoplasia sibling study. Am J Hum Genet 82, 723-736 (2008).

110. Haas, R. C. & Strauss, A. W. Separate nuclear genes encode sarcomere-specific and ubiquitous human mitochondrial creatine kinase isoenzymes. J Biol Chem 265, 6921-6927 (1990).

111. Steeghs, K., Merkx, G. & Wieringa, B. The ubiquitous mitochondrial creatine kinase gene maps to a conserved region on human chromosome 15q15 and mouse chromosome 2 bands F1-F3. Genomics 24, 193-195 (1994).

112. Qin, W., Khuchua, Z., Cheng, J., Boero, J., et al. Molecular characterization of the creatine kinases and some historical perspectives. Mol Cell Biochem 184, 153-167 (1998).

113. Schlattner, U. & Wallimann, T. Octamers of mitochondrial creatine kinase

isoenzymes differ in stability and membrane binding. J Biol Chem 275, 17314-17320 (2000).

114. Schlattner, U., Dolder, M., Wallimann, T. & Tokarska-Schlattner, M. Mitochondrial creatine kinase and mitochondrial outer membrane porin show a direct interaction that is modulated by calcium. J Biol Chem 276, 48027-48030 (2001).

115. Onda, T., Uzawa, K., Endo, Y., Bukawa, H., et al. Ubiquitous mitochondrial creatine kinase downregulated in oral squamous cell carcinoma. Br J Cancer 94, 698-709 (2006).

116. Bürklen, T. S., Hirschy, A. & Wallimann, T. Brain-type creatine kinase BB-CK interacts with the Golgi Matrix Protein GM130 in early prophase. Mol Cell Biochem 297, 53-64 (2007).

117. Lenz, H., Schmidt, M., Welge, V., Kueper, T., et al. Inhibition of cytosolic and mitochondrial creatine kinase by siRNA in HaCaT- and HeLaS3-cells affects cell viability and mitochondrial morphology. Mol Cell Biochem 306, 153-162 (2007).

SECTION IV: AUTOSOMAL DOMINANT RENAL TUBULAR ACIDOSIS

1. Hamm, L. H., Alpern, R. J., Preisig, P. A. Cellular mechanisms of renal tubular acidification. Book chapter. Seldin and Geibisch's The Kidney Physiology and Pathophysiology.

2. Unwin, R. J., Shirley, D. G. & Capasso, G. Urinary acidification and distal renal tubular acidosis. J Nephrol 15 Suppl 5, S142-S150 (2002).

3. Unwin, R. J. & Capasso, G. The renal tubular acidoses. J R Soc Med 94, 221-225 (2001).

4. Alper, S. L. Genetic diseases of acid-base transporters. Annu Rev Physiol 64, 899-923 (2002).

4. Tanner, M. J. The structure and function of band 3 (AE1): recent developments (review). Mol Membr Biol 14, 155-165 (1997).

5. Alper, S. L. The band 3-related anion exchanger (AE) gene family. Annu Rev Physiol 53, 549-564 (1991).

6. Romero, M. F., Fulton, C. M. & Boron, W. F. The SLC4 family of HCO 3 - transporters. Pflugers Arch 447, 495-509 (2004).

7. Chambers, E. J., Bloomberg, G. B., Ring, S. M. & Tanner, M. J. Structural studies on the effects of the deletion in the red cell anion exchanger (band 3, AE1) associated with South East Asian ovalocytosis. J Mol Biol 285, 1289-1307 (1999).

8. Kuma, H., Abe, Y., Askin, D., Bruce, L. J., et al. Molecular basis and functional consequences of the dominant effects of the mutant band 3 on the structure of normal band 3 in Southeast Asian ovalocytosis. Biochemistry 41, 3311-3320 (2002).

9. Bruce, L. J., Cope, D. L., Jones, G. K., Schofield, A. E., et al. Familial distal renal tubular acidosis is associated with mutations in the red cell anion exchanger (Band 3, AE1) gene. J Clin Invest 100, 1693-1707 (1997).

10. Bruce, L. J., Unwin, R. J., Wrong, O. & Tanner, M. J. The association between familial distal renal tubular acidosis and mutations in the red cell anion exchanger (band 3, AE1) gene. Biochem Cell Biol 76, 723-728 (1998).

11. Jarolim, P., Shayakul, C., Prabakaran, D., Jiang, L., et al. Autosomal dominant distal renal tubular acidosis is associated in three families with heterozygosity for the R589H mutation in the AE1 (band 3) Cl-/HCO3- exchanger. J Biol Chem 273, 6380-6388 (1998).

12. Karet, F. E., Gainza, F. J., Györy, A. Z., Unwin, R. J., et al. Mutations in the chloride-bicarbonate exchanger gene AE1 cause autosomal dominant but not autosomal recessive distal renal tubular acidosis. Proc Natl Acad Sci U S A 95, 6337-6342 (1998).

13. Sritippayawan, S., Kirdpon, S., Vasuvattakul, S., Wasanawatana, S., et al. A de novo R589C mutation of anion exchanger 1 causing distal renal tubular acidosis. Pediatr Nephrol 18, 644-648 (2003).

14. Toye, A. M., Bruce, L. J., Unwin, R. J., Wrong, O. & Tanner, M. J. Band 3 Walton, a C-terminal deletion associated with distal renal tubular acidosis, is expressed in the red cell membrane but retained internally in kidney cells. Blood 99, 342-347 (2002).

15. Tanphaichitr, V. S., Sumboonnanonda, A., Ideguchi, H., Shayakul, C., et al. Novel AE1 mutations in recessive distal renal tubular acidosis. Loss-of-function is rescued by glycophorin A. J Clin Invest 102, 2173-2179 (1998).

16. Yenchitsomanus, P. T., Vasuvattakul, S., Kirdpon, S., Wasanawatana, S., et al. Autosomal recessive distal renal tubular acidosis caused by G701D mutation of anion exchanger 1 gene. Am J Kidney Dis 40, 21-29 (2002).

17. Vasuvattakul, S., Yenchitsomanus, P. T., Vachuanichsanong, P., Thuwajit, P., et al. Autosomal recessive distal renal tubular acidosis associated with Southeast Asian ovalocytosis. Kidney Int 56, 1674-1682 (1999).

18. Bruce, L. J., Wrong, O., Toye, A. M., Young, M. T., et al. Band 3 mutations, renal tubular acidosis and South-East Asian ovalocytosis in Malaysia and Papua New Guinea: loss of up to 95% band 3 transport in red cells. Biochem J 350 Pt 1, 41-51 (2000).

19. Wrong, O., Bruce, L. J., Unwin, R. J., Toye, A. M. & Tanner, M. J. Band 3 mutations, distal renal tubular acidosis, and Southeast Asian ovalocytosis. Kidney Int 62, 10-19 (2002).

20. Ribeiro, M. L., Alloisio, N., Almeida, H., Gomes, C., et al. Severe hereditary spherocytosis and distal renal tubular acidosis associated with the total absence of band 3. Blood 96, 1602-1604 (2000).

21. Wagner, C. A., Finberg, K. E., Breton, S., Marshansky, V., et al. Renal vacuolar H+-ATPase. Physiol Rev 84, 1263-1314 (2004).

22. DeFranco, P. E., Haragsim, L., Schmitz, P. G. & Bastani, B. Absence of vacuolar H(+)-ATPase pump in the collecting duct of a patient with hypokalemic distal renal tubular acidosis and Sjögren's syndrome. J Am Soc Nephrol 6, 295-301 (1995).

23. Stanković, K. M., Brown, D., Alper, S. L. & Adams, J. C. Localization of pH regulating proteins H+ATPase and Cl-/HCO3- exchanger in the guinea pig inner ear. Hear Res 114, 21-34 (1997).

24. Karet, F. E., Finberg, K. E., Nayir, A., Bakkaloglu, A., et al. Localization of a gene for autosomal recessive distal renal tubular acidosis with normal hearing (rdRTA2) to 7q33-34. Am J Hum Genet 65, 1656-1665 (1999).

25. Karet, F. E., Finberg, K. E., Nelson, R. D., Nayir, A., et al. Mutations in the gene encoding B1 subunit of H+-ATPase cause renal tubular acidosis with sensorineural deafness. Nat Genet 21, 84-90 (1999).

26. Smith, A. N., Finberg, K. E., Wagner, C. A., Lifton, R. P., et al. Molecular cloning and characterization of Atp6n1b: a novel fourth murine vacuolar H+-ATPase a-subunit gene. J Biol Chem 276, 42382-42388 (2001).

27. Smith, A. N., Skaug, J., Choate, K. A., Nayir, A., et al. Mutations in ATP6N1B, encoding a new kidney vacuolar proton pump 116-kD subunit, cause recessive distal renal tubular acidosis with preserved hearing. Nat Genet 26, 71-75 (2000).

28. Hahn, H., Kang, H. G., Ha, I. S., Cheong, H. I. & Choi, Y. ATP6B1 gene mutations associated with distal renal tubular acidosis and deafness in a child. Am J Kidney Dis 41, 238-243 (2003).

29. Ruf, R., Rensing, C., Topaloglu, R., Guay-Woodford, L., et al. Confirmation of the ATP6B1 gene as responsible for distal renal tubular acidosis. Pediatr Nephrol 18, 105-109 (2003).

30. Stover, E. H., Borthwick, K. J., Bavalia, C., Eady, N., et al. Novel ATP6V1B1 and ATP6V0A4 mutations in autosomal recessive distal renal tubular acidosis with new evidence for hearing loss. J Med Genet 39, 796-803 (2002).

31. Stehberger, P. A., Schulz, N., Finberg, K. E., Karet, F. E., et al. Localization and regulation of the ATP6V0A4 (a4) vacuolar H+-ATPase subunit defective in an inherited form of distal renal tubular acidosis. J Am Soc Nephrol 14, 3027-3038 (2003).

32. Igarashi, T., Sekine, T., Inatomi, J. & Seki, G. Unraveling the molecular pathogenesis of isolated proximal renal tubular acidosis. J Am Soc Nephrol 13, 2171-2177 (2002).

33. T Igarashi, J Inatomi, T Sekine, SH Cha, Y Kanai, M Kunimi, K Tsukamoto, H Satoh, M Shimadzu, F Tozawa, T Mori, M Shiobara, G Seki, H Endou, Mutations in SLC4A4 cause permanent isolated proximal renal tubular acidosis with ocular abnormalities. Nat Genet 23, 264-266 (1999).

34. Igarashi, T., Inatomi, J., Sekine, T., Seki, G., et al. Novel nonsense mutation in the Na+/HCO3- cotransporter gene (SLC4A4) in a patient with permanent isolated proximal renal tubular acidosis and bilateral glaucoma. J Am Soc Nephrol 12, 713-718 (2001).

35. Dinour, D., Chang, M. H., Satoh, J., Smith, B. L., et al. A novel missense mutation in the sodium bicarbonate cotransporter (NBCe1/SLC4A4) causes proximal tubular acidosis and glaucoma through ion transport defects. J Biol Chem 279, 52238-52246 (2004).

36. Usui, T., Hara, M., Satoh, H., Moriyama, N., et al. Molecular basis of ocular abnormalities associated with proximal renal tubular acidosis. J Clin Invest 108, 107-115 (2001).

37. Bok, D., Schibler, M. J., Pushkin, A., Sassani, P., et al. Immunolocalization of electrogenic sodium-bicarbonate cotransporters pNBC1 and kNBC1 in the rat eye. Am J Physiol Renal Physiol 281, F920-F935 (2001).

38. Satoh, H., Moriyama, N., Hara, C., Yamada, H., et al. Localization of Na+-HCO-3 cotransporter (NBC-1) variants in rat and human pancreas. Am J Physiol Cell Physiol 284, C729-C737 (2003).

39. Lemann, J., Adams, N. D., Wilz, D. R. & Brenes, L. G. Acid and mineral balances and bone in familial proximal renal tubular acidosis. Kidney Int 58, 1267-1277 (2000).

40. Sly, W. S., Hewett-Emmett, D., Whyte, M. P., Yu, Y. S. & Tashian, R. E. Carbonic anhydrase II deficiency identified as the primary defect in the autosomal recessive syndrome of osteopetrosis with renal tubular acidosis and cerebral calcification. Proc Natl Acad Sci U S A 80, 2752-2756 (1983).

41. Sly, W. S., Whyte, M. P., Sundaram, V., Tashian, R. E., et al. Carbonic anhydrase II deficiency in 12 families with the autosomal recessive syndrome of osteopetrosis with renal tubular acidosis and cerebral calcification. N Engl J Med 313, 139-145 (1985).

42. Venta, P. J., Welty, R. J., Johnson, T. M., Sly, W. S. & Tashian, R. E. Carbonic anhydrase II deficiency syndrome in a Belgian family is caused by a point mutation at an invariant histidine residue (107 His----Tyr): complete structure of the normal human CA II gene. Am J Hum Genet 49, 1082-1090 (1991).

43. Roth, D. E., Venta, P. J., Tashian, R. E. & Sly, W. S. Molecular basis of human carbonic anhydrase II deficiency. Proc Natl Acad Sci U S A 89, 1804-1808 (1992).

44. Hu, P. Y., Ernst, A. R., Sly, W. S., Venta, P. J., et al. Carbonic anhydrase II deficiency: single-base deletion in exon 7 is the predominant mutation in Caribbean Hispanic patients. Am J Hum Genet 54, 602-608 (1994).

45. Shah, G. N., Bonapace, G., Hu, P. Y., Strisciuglio, P. & Sly, W. S. Carbonic anhydrase II deficiency syndrome (osteopetrosis with renal tubular acidosis and brain calcification): novel mutations in CA2 identified by direct sequencing expand the opportunity for genotype-phenotype correlation. Hum Mutat 24, 272 (2004).

46. Fathallah, D. M., Bejaoui, M., Sly, W. S., Lakhoua, R. & Dellagi, K. A unique mutation underlying carbonic anhydrase II deficiency syndrome in patients of Arab descent. Hum Genet 94, 581-582 (1994).

47. Lai, L. W., Chan, D. M., Erickson, R. P., Hsu, S. J. & Lien, Y. H. Correction of renal tubular acidosis in carbonic anhydrase II-deficient mice with gene therapy. J Clin Invest 101, 1320-1325 (1998).

48. Boettger, T., Hübner, C. A., Maier, H., Rust, M. B., et al. Deafness and renal tubular acidosis in mice lacking the K-Cl co-transporter Kcc4. Nature 416, 874-878 (2002).

49. Weger, M., Deutschmann, H., Weger, W., Kotanko, P. & Skrabal, F. Incomplete renal tubular acidosis in 'primary' osteoporosis. Osteoporos Int 10, 325-329 (1999).

50. Weger, W., Kotanko, P., Weger, M., Deutschmann, H. & Skrabal, F. Prevalence and characterization of renal tubular acidosis in patients with osteopenia and osteoporosis and in non-porotic controls. Nephrol Dial Transplant 15, 975-980 (2000).

51. Deutschmann, H. A., Weger, M., Weger, W., Kotanko, P., et al. Search for occult secondary osteoporosis: impact of identified possible risk factors on bone mineral density. J Intern Med 252, 389-397 (2002).

52. Blot-Chabaud, M., Laplace, M., Cluzeaud, F., Capurro, C., *et al.* Characteristics of a rat cortical collecting duct cell line that maintains high transepithelial resistance. *Kidney Int* 50, 367-376 (1996).

53. Puttini, S., Beggah, A. T., Ouvrard-Pascaud, A., Legris, C., et al. Tetracycline-inducible gene expression in cultured rat renal CD cells and in intact CD from transgenic mice. Am J Physiol Renal Physiol 281, F1164-F1172 (2001).

54. Toye, A. M., Bruce, L. J., Unwin, R. J., Wrong, O. & Tanner, M. J. Band 3 Walton, a C-terminal deletion associated with distal renal tubular acidosis, is expressed in the red cell membrane but retained internally in kidney cells. Blood 99, 342-347 (2002).

55. Quilty, J. A., Li, J. & Reithmeier, R. A. Impaired trafficking of distal renal tubular acidosis mutants of the human kidney anion exchanger kAE1. Am J Physiol Renal Physiol 282, F810-F820 (2002).

56. Quilty, J. A., Cordat, E. & Reithmeier, R. A. Impaired trafficking of human kidney anion exchanger (kAE1) caused by hetero-oligomer formation with a truncated mutant associated with distal renal tubular acidosis. Biochem J 368, 895-903 (2002).

57. Devonald, M. A., Smith, A. N., Poon, J. P., Ihrke, G. & Karet, F. E. Non-polarized targeting of AE1 causes autosomal dominant distal renal tubular acidosis. Nat Genet 33, 125-127 (2003).

58. Toye, A. M., Banting, G. & Tanner, M. J. Regions of human kidney anion exchanger 1 (kAE1) required for basolateral targeting of kAE1 in polarised kidney cells: mis-targeting explains dominant renal tubular acidosis (dRTA). J Cell Sci 117, 1399-1410 (2004).

59 Rungroj, N., Devonald, M. A., Cuthbert, A. W., Reimann, F., et al. A novel missense mutation in AE1 causing autosomal dominant distal renal tubular acidosis retains normal transport function but is mistargeted in polarized epithelial cells. J Biol Chem 279, 13833-13838 (2004).

60. Shayakul, C. & Alper, S. L. Defects in processing and trafficking of the AE1 Cl-/HCO3- exchanger associated with inherited distal renal tubular acidosis. Clin Exp Nephrol 8, 1-11 (2004).